

# THE MINOR PLANET BULLETIN

BULLETIN OF THE MINOR PLANETS SECTION OF THE ASSOCIATION OF LUNAR AND PLANETARY OBSERVERS

VOLUME 47, NUMBER 4, A.D. 2020 OCTOBER-DECEMBER

265.

## SECTION NEWS: RETIREMENT OF MPB PRODUCER ROBERT WERNER

Frederick Pilcher  
Minor Planets Section Recorder  
fpilcher35@gmail.com

As announced in issue 47-1, this edition of *The Minor Planet Bulletin* is the last produced under the guidance of Robert Werner who has dedicated his volunteer service to the *MPB* since 1985. Pedro Valdés Sada of the Universidad de Monterrey (México), who has spent the past year in an apprentice role, now takes on the full responsibilities and title as the *MPB* Producer.

In 1985, as the *MPB* was continuing its transition from its founder Richard Hodgson, each issue rarely exceeded ten pages. Such was the case when Werner “answered the call” for production assistance and began his service with *MPB* issue 12-3. (See Werner’s 2003 retrospective in *MPB* 40, page 52.) Who knew that the day would come when a typical issue would exceed 100 pages? Through 35 years and more than 5000 pages, the quality of each page reflects Bob’s intrepid rise to meet the challenge and his meticulous dedication toward displaying the science of our field. The Minor Planets Section is pleased to convey its gratitude by announcing that Bob has received a Meritorious Service Award in recognition of his work in bringing forward the *Minor Planet Bulletin* to where it is today. Please join me in thanking Bob Werner for his tireless service to the minor planet community.

## SWAN SONG

Bob Werner, Producer, *Minor Planet Bulletin*

After more than 35 years (half my life so far), I am retiring from producing the *Minor Planet Bulletin*.

*MPB* is in good hands. Pedro Valdés Sada has taken the reins of my old job. Melissa Hayes-Gehrke distributes the printed copies, having taken over from Derald Nye. Frederick Pilcher remains steadfast as Recorder. Richard Binzel continues as Editor, assisted by Brian Warner and David Polishook.

Closing the dome now. Pedro, here are the keys.

--Bob (3891) Werner

## ROTATION PERIOD DETERMINATION FOR ASTEROIDS 992 SWASEY AND 3096 BEZRUC

Alessandro Marchini, Massimo Conti, Claudio Vallerani  
Astronomical Observatory, DSFTA - University of Siena (K54)  
Via Roma 56, 53100 - Siena, ITALY  
marchini@unisi.it

Riccardo Papini, Fabio Salvaggio  
Wild Boar Remote Observatory (K49)  
San Casciano in Val di Pesa (FI), ITALY

(Received: 2020 July 25 Revised: 2020 August 9)

Photometric observations of two main-belt asteroids were conducted from the Astronomical Observatory of the University of Siena, in Italy, in order to determine their synodic rotation periods. For 992 Swasey we found:  $P = 13.305 \pm 0.007$  h,  $A = 0.16 \pm 0.02$  mag; and for 3096 Bezzuc we found  $P = 27.350 \pm 0.004$  h,  $A = 0.62 \pm 0.03$  mag.

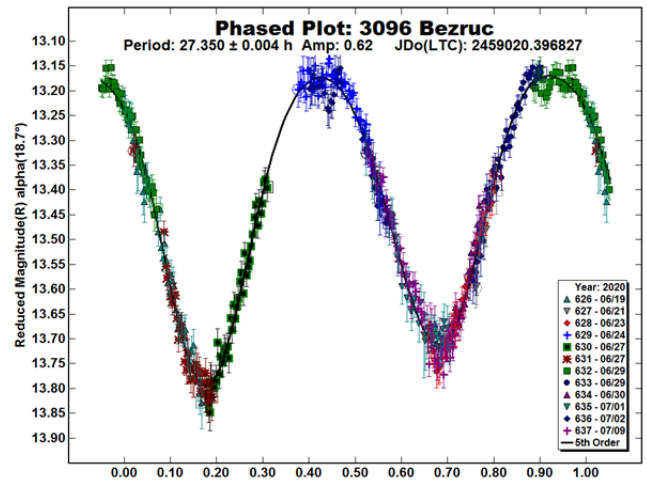
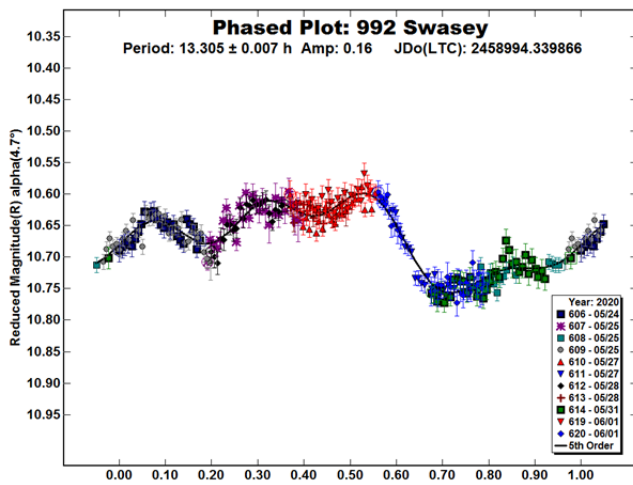
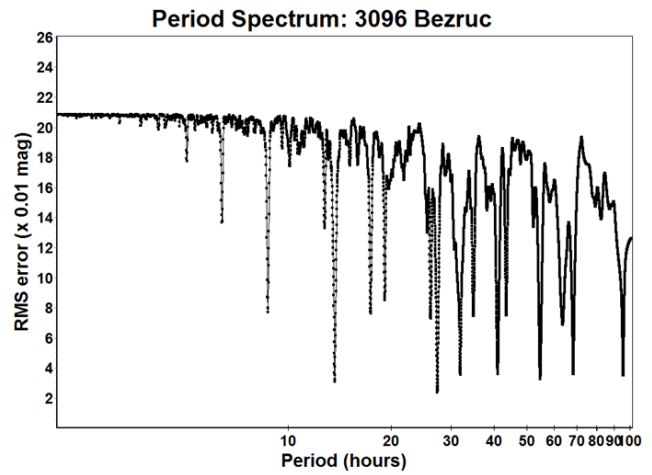
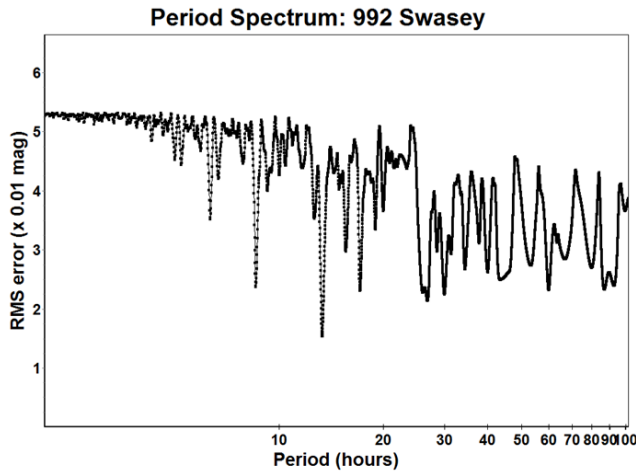
CCD photometric observations of two main-belt asteroids were carried out in 2020 May - July at the Astronomical Observatory of the University of Siena (K54), a facility inside the Department of Physical Sciences, Earth and Environment (DSFTA, 2020). We used a 0.30-m  $f/5.6$  Maksutov-Cassegrain telescope, SBIG STL-6303E NABG CCD camera, and clear filter; the pixel scale was 2.30 arcsec when binned at  $2 \times 2$  pixels. All exposures were 300 seconds.

Data processing and analysis were done with *MPO Canopus* (Warner, 2018). All images were calibrated with dark and flat-field frames and the instrumental magnitudes converted to R magnitudes using solar-colored field stars from a version of the CMC-15 catalogue distributed with *MPO Canopus*. Table I shows the observing circumstances and results.

992 Swasey (1969 TA4, A922 VD) was discovered on 1922 November 14 by O. Struve at Williams Bay and named after Ambrose Swasey of the Warner & Swasey Company, which built the 82-inch telescope named after Struve at McDonald Observatory. It is a main-belt asteroid with a semi-major axis of 3.028 AU, eccentricity 0.085, inclination 10.843 deg, and an orbital period of 5.27 years. Its absolute magnitude is  $H = 10.6$  (JPL, 2020) while its spectral class is C (Bus and Binzel, 2002; Xu et al., 1995). The WISE/NEOWISE satellite infrared radiometry survey (Masiero et al., 2014) found a diameter  $D = 27.585 \pm 0.376$  km using an absolute magnitude  $H = 10.8$ .

Observations were conducted over six nights and collected 285 data points. The period analysis shows a solution for the rotational period of  $P = 13.305 \pm 0.007$  h with an amplitude  $A = 0.16 \pm 0.02$  mag, suggested by the strongest peak in the period spectrum that confirms the result known from literature (Behrend, 2004) of  $P = 13.308$  h.

Observations over twelve nights collected 447 data points. The period analysis shows a bimodal solution for the rotational period of  $P = 27.350 \pm 0.004$  h with an amplitude  $A = 0.62 \pm 0.03$  mag, which agrees with the previously determined sidereal rotational period of 27.366 h (Durech, 2018).



**3096 Bezruc** (1981 QC1) was discovered on 1981 August 28 at Klet by Z. Vavrova and named in honor of Petr Bezruc (1867-1958), popular Silesian poet [Ref: Minor Planet Circ. 21607]. It is a main-belt asteroid with a semi-major axis of 2.668 AU, eccentricity 0.195, inclination 12.148 deg, and an orbital period of 4.36 years. Its absolute magnitude is  $H = 12.7$  (JPL, 2020). The WISE/NEOWISE satellite infrared radiometry survey (Masiero et al., 2011) found a diameter  $D = 17.122 \pm 0.170$  km using an absolute magnitude  $H = 12.6$ .

Acknowledgements

Minor Planet Circulars (MPCs) are published by the International Astronomical Union's Minor Planet Center. [https://www.minorplanetcenter.net/iau/ECS/MPCArchive/MPCArchive\\_TBL.html](https://www.minorplanetcenter.net/iau/ECS/MPCArchive/MPCArchive_TBL.html)

References

Behrend, R. (2004). Observatoire de Geneve web site. [http://obswww.unige.ch/~behrend/page\\_cou.html](http://obswww.unige.ch/~behrend/page_cou.html)

Number	Name	2020/mm/dd	Phase	$L_{PAB}$	$B_{PAB}$	Period(h)	P.E.	Amp	A.E.	Grp
992	Swasey	05/24-06/02	4.6, 7.9	235	6	13.305	0.007	0.16	0.02	MB
3096	Bezruc	06/19-07/09	18.8, 12.0	303	13	27.350	0.004	0.62	0.03	MB

Table I. Observing circumstances and results. The first line gives the results for the primary of a binary system. The phase angle is given for the first and last date. If preceded by an asterisk, the phase angle reached an extrema during the period.  $L_{PAB}$  and  $B_{PAB}$  are the approximate phase angle bisector longitude/latitude at mid-date range (see Harris et al., 1984). Grp is the asteroid family/group (Warner et al., 2009).

Bus, S.J.; Binzel, R.P. (2002). “Phase II of the small main-belt asteroid spectroscopic survey: A feature-based taxonomy.” *Icarus* **158**, 146-177.

DSFTA (2020). Dipartimento di Scienze Fisiche, della Terra e dell'Ambiente – Astronomical Observatory. <https://www.dsfta.unisi.it/en/research/labs-eng/astronomicalobservatory>

Durech, J.; Hanus, J.; Ali-Lagoa, V. (2018). “Asteroid model reconstructed from the Lowell Photometric Database and WISE data.” *Astron. Astrophys.* **617**, A57.

Harris, A.W.; Young, J.W.; Scaltriti, F.; Zappala, V. (1984). “Lightcurves and phase relations of the asteroids 82 Alkeme and 444 Gypsis.” *Icarus* **57**, 251-258.

JPL (2020). Small-Body Database Browser. <http://ssd.jpl.nasa.gov/sbdb.cgi#top>

Masiero, J.R.; Mainzer, A.K.; Grav, T.; Bauer, J.M.; Cutri, R.M.; Dailey, J.; Eisenhardt, P.R.M.; McMillan, R.S.; Spahr, T.B.; Skrutskie, M.F.; Tholen, D.; Walker, R.G.; Wright, E.L.; DeBaun, E.; Elsbury, D.; Gautier, T. IV; Gomillion, S.; Wilkins, A. (2011). “Main Belt Asteroids with WISE/NEOWISE. I. Preliminary Albedos and Diameters.” *Astrophys. J.* **741**, A68.

Masiero, J.R.; Grav, T.; Mainzer, A.K.; Nugent, C.R.; Bauer, J.M.; Stevenson, R.; Sonnett, S. (2014). “Main-belt Asteroids with WISE/NEOWISE: Near-infrared Albedos.” *Astrophys. J.* **791**, 121.

Warner, B.D.; Harris, A.W.; Pravec, P. (2009). “The Asteroid Lightcurve Database.” *Icarus* **202**, 134-146. Updated 2019 Aug. <http://www.minorplanet.info/lightcurvedatabase.html>

Warner, B.D. (2018). MPO Software, MPO Canopus v10.7.7.0. Bdw Publishing. <http://minorplanetobserver.com>

Xu, S.; Binzel, R.P.; Burbine, T.H.; Bus, S.J. (1995). “Small main-belt asteroid spectroscopic survey: Initial Results.” *Icarus* **115**, 1-35.

## PRELIMINARY SPIN-SHAPE MODEL FOR 755 QUINTILLA

Lorenzo Franco  
Balzaretto Observatory (A81), Rome, ITALY  
lor\_franco@libero.it

Robert K. Buchheim  
Altimira Observatory (G76)  
18 Altimira, Coto de Caza, CA 92679

Donald Pray  
Sugarloaf Mountain Observatory  
South Deerfield, MA USA

Michael Fauerbach  
Florida Gulf Coast University  
10501 FGCU Blvd.  
Ft. Myers, FL33965-6565

Fabio Mortari  
Hypatia Observatory (L62), Rimini, ITALY

Giovanni Battista Casalnuovo, Benedetto Chinaglia  
Filzi School Observatory (D12), Laives, ITALY

Giulio Scarfi  
Iota Scorpis Observatory (K78), La Spezia, ITALY

Riccardo Papini, Fabio Salvaggio  
Wild Boar Remote Observatory (K49)  
San Casciano in Val di Pesa (FI), ITALY

(Received: 2020 July 8)

We present a preliminary shape and spin axis model for main-belt asteroid 755 Quintilla. The model was derived using lightcurve inversion that combined dense photometric data acquired from three apparitions between 2004 and 2020 and sparse data from USNO Flagstaff. Analysis of the resulting data found a sidereal period  $P = 4.55204 \pm 0.00001$  h and two mirrored pole solutions at  $(\lambda, \beta) = (109^\circ, -12^\circ)$  and  $(288^\circ, -3^\circ)$  with an uncertainty of  $\pm 20^\circ$ .

The minor planet 755 Quintilla was observed by the authors during three oppositions from 2004 to 2020. In order to cover several apparition geometries, we used sparse data from the USNO Flagstaff Station (MPC Code 689) that were downloaded from the Asteroids Dynamic Site (AstDyS-2, 2020).

The observational details of the dense data are in Table I with the mid-date, number of lightcurves used, and the longitude and latitude of the phase angle bisector ( $LPAB$ ,  $BPAB$ ).

Reference	Mid date	# LC	$LPAB^\circ$	$BPAB^\circ$
Buchheim, Pray (2005)	2004-04-16	3	207	2
Fauerbach (2019)	2018-11-02	2	54	-3
Franco et al. (2020)	2020-01-28	6	116	-3

Table I. Observational details for the data used in the lightcurve inversion process for 755 Quintilla.

Lightcurve inversion was performed using *MPO LCInvert* v.11.8.2.0 (BDW Publishing, 2016). For a description of the modeling process see *LCInvert Operating Instructions Manual*, Durech et al. (2010, and references therein).

Figure 1 shows the PAB longitude/latitude distribution for the dense/sparse data. Figure 2 (top panel) shows the sparse photometric data distribution (intensity vs JD) and (bottom panel) the corresponding phase curve (reduced magnitudes vs phase angle).

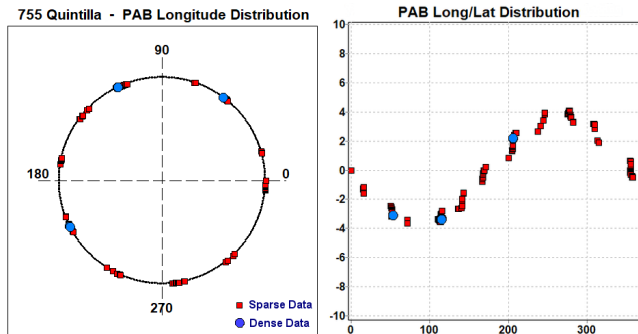


Figure 1: PAB longitude and latitude distribution of the data used for the lightcurve inversion model.

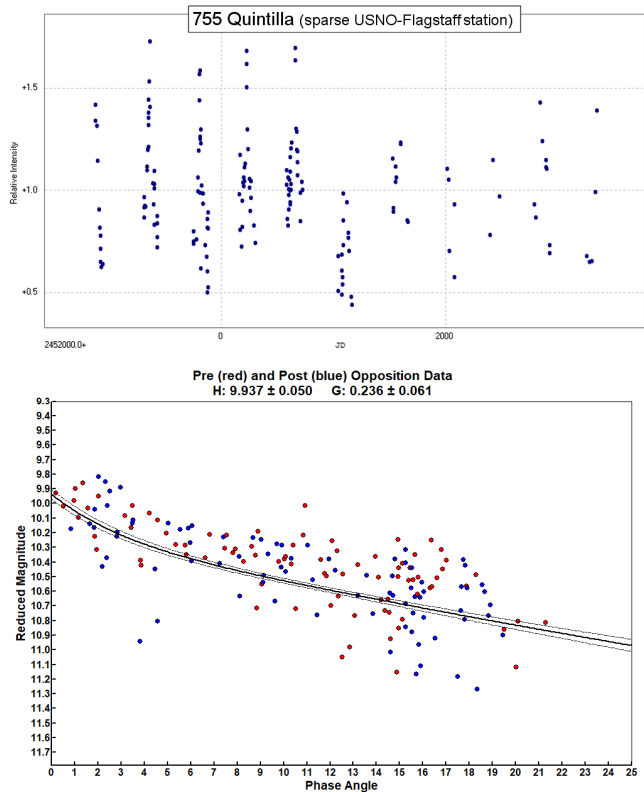


Figure 2: Top: sparse photometric data point distribution from (689) USNO Flagstaff station (relative intensity vs Julian Day). Bottom: phase curve obtained from sparse data (reduced magnitude vs phase angle).

In the analysis, the processing weighting factor was set to 1.0 for dense and 0.3 for sparse data. The “dark facet” weighting factor was set to 0.5 to keep the dark facet area below 1% of total area and the number of iterations was set to 50.

The sidereal period search was started around the average of the synodic periods found in the asteroid lightcurve database (LCDB; Warner et al., 2009). We found a group of five sidereal periods with Chi-Sq values within 10% of the lowest value, one of them more isolated and with the lowest Chi-Sq (Figure 3).

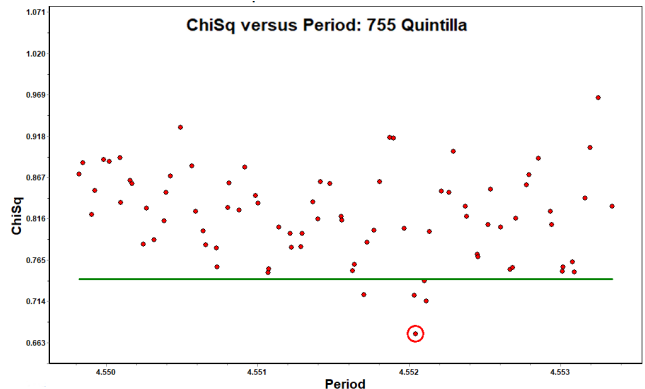


Figure 3: The period search for 755 Quintilla shows five sidereal periods with Chi-Sq values within 10% of the lowest value. The circled period was used in the initial pole search.

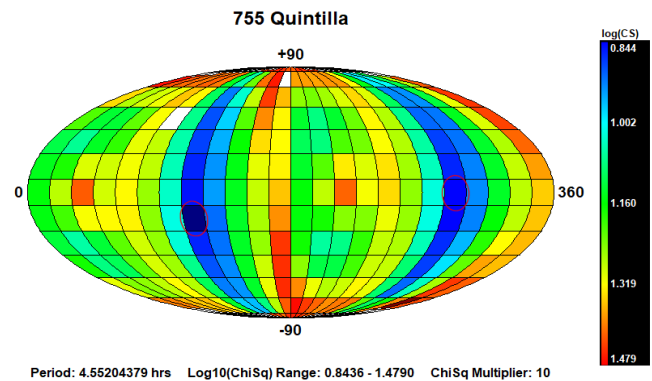


Figure 1: Pole search distribution. The dark blue region indicates the smallest Chi-Sq value while the dark red region indicates the largest.

The pole search was started using the “medium” search option (312 fixed pole positions with 15° longitude-latitude steps) and the sidereal period with the lowest Chi-Sq set to “float”. From this step we found two roughly mirrored lower Chi-Sq solutions (Figure 4) separated by about 180° in longitude at ecliptic longitude-latitude pairs  $(\lambda, \beta) = (105^\circ, -15^\circ)$  and  $(285^\circ, -3^\circ)$ .

$\lambda^\circ$	$\beta^\circ$	Sidereal Period (hours)	Chi-Sq	RMS
109	-12	$4.55204 \pm 0.00001$	0.67488	0.0274
288	-3		0.67616	0.0274

Table II. The two spin axis solutions for 755 Quintilla (ecliptic coordinates) with an uncertainty of  $\pm 20$  degrees. The sidereal period is the average of the two solutions found in the pole search.

The two best solutions (lower Chi-Sq) are reported in Table II. The sidereal period was obtained by averaging the two solutions found in the pole search. Typical errors in the pole solution are  $\pm 20^\circ$  and the uncertainty in sidereal period has been evaluated as a rotational error of  $40^\circ$  over the total time span of the data set. Figure 5 shows the shape model (first solution with a lower Chi-Sq) while Figure 6 shows the fit between the model (black line) and some observed lightcurves (red points).

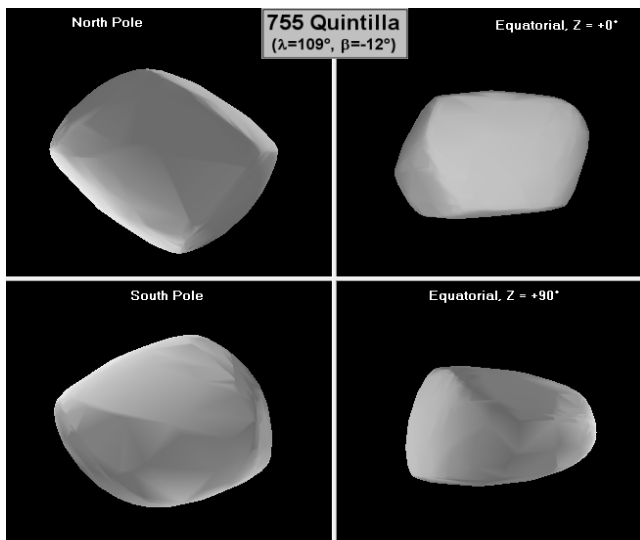


Figure 5: The shape model for 755 Quintilla ( $\lambda = 109^\circ$ ,  $\beta = -12^\circ$ ).

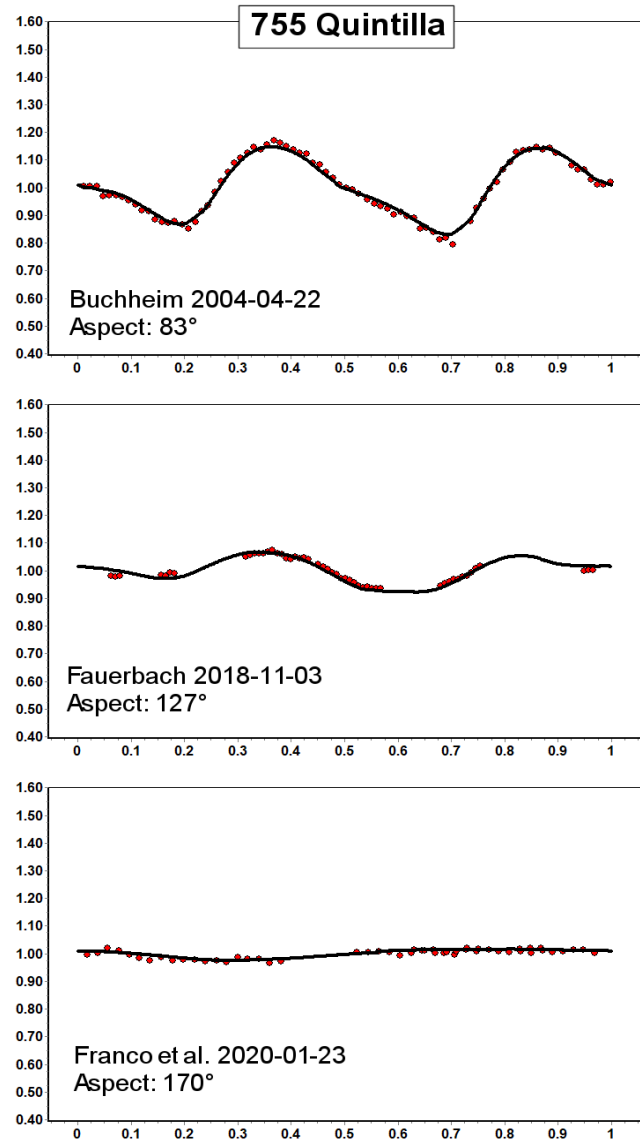


Figure 6: Model fit (black line) versus observed lightcurves (red points) for ( $\lambda = 109^\circ$ ,  $\beta = -12^\circ$ ) solution.

The analysis did not identify a unique solution (Durech et al., 2009), so we consider this to be a preliminary solution. Indeed, the pole search distribution is poorly constrained, especially along the ecliptic latitude. However, a check of the other four probable sidereal periods produced similar solutions with higher Chi-Sq and RMS values. We invite more observations of 755 Quintilla during the future oppositions, especially at large phase angles, in order to find a more robust solution.

## References

- AstDyS-2 (2020), Asteroids - Dynamic Site.  
<https://newton.spacedys.com/astdys/>
- BDW Publishing (2016).  
<http://www.minorplanetobserver.com/MPOSoftware/MPOLCInvert.htm>
- Buchheim, R.K.; Pray, D. (2005), "Lightcurve of 755 Quintilla." *Minor Planet Bulletin* **32**, 1.
- Durech, J.; Kaasalainen, M.; Warner, B.D.; Fauerbach, M.; Marks, S.A.; Fauvaud, S.; Fauvaud, M.; Vugnon, J.-M.; Pilcher, F.; Bernasconi, L.; Behrend, R. (2009), "Asteroid models from combined sparse and dense photometric data." *Astron. Astrophys.*, **493**, 291-297.
- Durech, J.; Sidorin, V.; Kaasalainen, M. (2010). "DAMIT: a database of asteroid models." *Astron. Astrophys.* **513**, A46.
- Fauerbach, M.; Fauerbach, M. (2019). "Rotational Period Determination for Asteroids 755 Quintilla, 1830 Pogson, 5076 Lebedev-Kumach, and (29153) 1998 SY2." *Minor Planet Bulletin* **46**, 138-139.
- Franco, L.; Marchini, A.; Saya, L.-F.; Galli, G.; Baj, G.; Ruocco, N.; Tinelli, L.; Scarfi, G.; Aceti, P.; Banfi, M.; Bacci, P.; Maestriperieri, M.; Papini, R.; Salvaggio, F.; Mortari, F.; Bachini, M.; Casalnuovo, G.B.; Chinaglia, B. (2020). "Collaborative Asteroid Photometry from UAI: 2020 January - March." *Minor Planet Bulletin* **47**, 242-246.
- Warner, B.D.; Harris, A.W.; Pravec, P. (2009). "The asteroid lightcurve database." *Icarus* **202**, 134-146. Updated 2020 March.  
<http://www.minorplanet.info/lightcurvedatabase.html>

## CORRIGENDUM

Franco, L.; Marchini, A.; Saya, L.-F.; Galli, G.; Baj, G.; Ruocco, N.; Mannucci, M.; Montigiani, N.; Tinelli, L.; Scarfi, G.; Aceti, P.; Banfi, M.; Bacci, P.; Maestriperieri, M.; Papini, R.; Salvaggio F.; Mortari, F.; Bachini, M.; Casalnuovo, G.B.; Chinaglia, B. (2020). "Collaborative Asteroid Photometry from UAI: 2020 January - March." *Minor Planet Bulletin* **47**, 242-246.

Incorrect values were given for the lower limit of the secondary-to-primary mean diameter ratio  $D_s/D_p$  for the asteroids 1052 Belgica and 7132 Casulli. The correct values are: 1052 Belgica,  $0.39 \pm 0.02$ ; 7132 Casulli,  $0.33 \pm 0.02$ .

## COLLABORATIVE ASTEROID PHOTOMETRY FROM UAI: 2020 APRIL-JUNE

Lorenzo Franco  
Balzaretto Observatory (A81), Rome, ITALY  
lor\_franco@libero.it

Alessandro Marchini  
Astronomical Observatory, DSFTA - University of Siena (K54)  
Via Roma 56, 53100 - Siena, ITALY

Giulio Scarfi  
Iota Scorpis Observatory (K78), La Spezia, ITALY

Riccardo Papini, Fabio Salvaggio  
Wild Boar Remote Observatory (K49)  
San Casciano in Val di Pesa (FI), ITALY

Giorgio Baj  
M57 Observatory (K38), Saltrio, ITALY

Gianni Galli  
GiaGa Observatory (203), Pogliano Milanese, ITALY

Paolo Bacci, Martina Maestriperi  
GAMP - San Marcello Pistoiese (104), Pistoia, ITALY

Luciano Tinelli  
GAV (Gruppo Astrofili Villasanta), Villasanta, ITALY

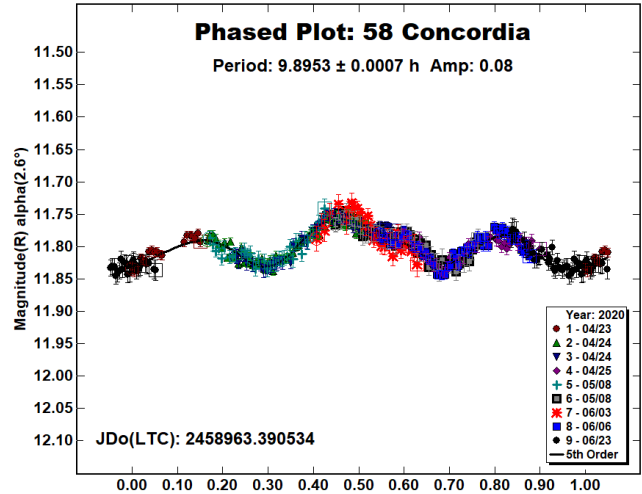
(Received: 2020 July 10)

Photometric observations of five asteroids were made in order to acquire lightcurves for shape/spin axis modeling. The synodic period and lightcurve amplitude were found for 58 Concordia:  $9.8953 \pm 0.0007$  h, 0.08 mag; 781 Kartvelia:  $19.050 \pm 0.005$  h, 0.22 mag; 913 Otila:  $4.8717 \pm 0.0007$  h, 0.18 mag; 3317 Paris:  $7.0812 \pm 0.0004$  h, 0.10 mag; and 3800 Karayusuf:  $2.2319 \pm 0.0001$  h, 0.15 mag.

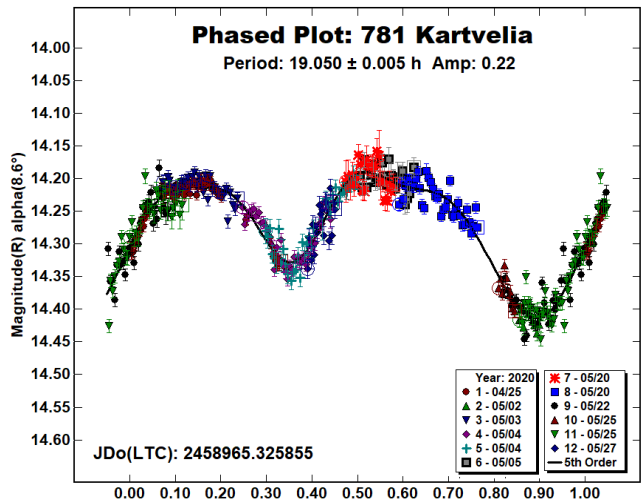
Collaborative asteroid photometry was done inside the Italian Amateur Astronomers Union (UAI; 2020) group. The targets were selected mainly in order to acquire lightcurves for shape/spin axis modeling. Table I shows the observing circumstances and results.

The CCD observations were made in 2020 April-June using the instrumentation described in the Table II. Lightcurve analysis was performed at the Balzaretto Observatory with *MPO Canopus* (Warner, 2016). All the images were calibrated with dark and flat frames and converted to R magnitudes using solar-colored field stars from the CMC15 catalogue as distributed with *MPO Canopus*.

58 Concordia is a Ch-type (Bus & Binzel, 2002) middle main-belt asteroid discovered on 1860 March 24 by R. Luther at Dusseldorf. Collaborative observations were made over six nights. The period analysis shows a synodic period of  $P = 9.8953 \pm 0.0007$  h with an amplitude  $A = 0.08 \pm 0.02$  mag. The period is close to the previously published results in the asteroid lightcurve database (LCDB; Warner et al., 2009).



781 Kartvelia is an Xc-type (Bus & Binzel, 2002) outer main-belt asteroid discovered on 1914 January 25 by G. Neujmin at Simeis. Collaborative observations were made over eight nights. We found a synodic period of  $P = 19.050 \pm 0.005$  h and amplitude  $A = 0.22 \pm 0.03$  mag. The period is close to the previously published results in the LCDB (Warner et al., 2009).



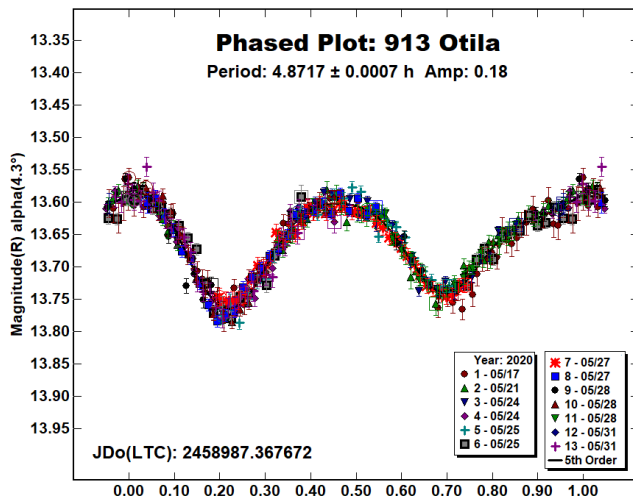
Number	Name	2020 mm/dd	Phase	$L_{PAB}$	$B_{PAB}$	Period(h)	P.E.	Amp	A.E.	Grp
58	Concordia	04/23-06/23	2.5, 20.8	213	5	9.8953	0.0007	0.08	0.02	MB-M
781	Kartvelia	04/25-05/27	8.6, 13.0	216	23	19.050	0.005	0.22	0.03	MB-O
913	Otila	05/17-05/31	4.1, 10.3	236	5	4.8717	0.0007	0.18	0.03	FLOR
3317	Paris	04/25-06/14	*6.8, 9.8	222	31	7.0812	0.0004	0.10	0.04	TR-J
3800	Karayusuf	04/24-06/12	*27.8, 23.4	237	19	2.2319	0.0001	0.15	0.05	MC

Table I. Observing circumstances and results. The first line gives the results for the primary of a binary system. The second line gives the orbital period of the satellite and the maximum attenuation. The phase angle is given for the first and last date. If preceded by an asterisk, the phase angle reached an extrema during the period.  $L_{PAB}$  and  $B_{PAB}$  are the approximate phase angle bisector longitude/latitude at mid-date range (see Harris et al., 1984). Grp is the asteroid family/group (Warner et al., 2009).

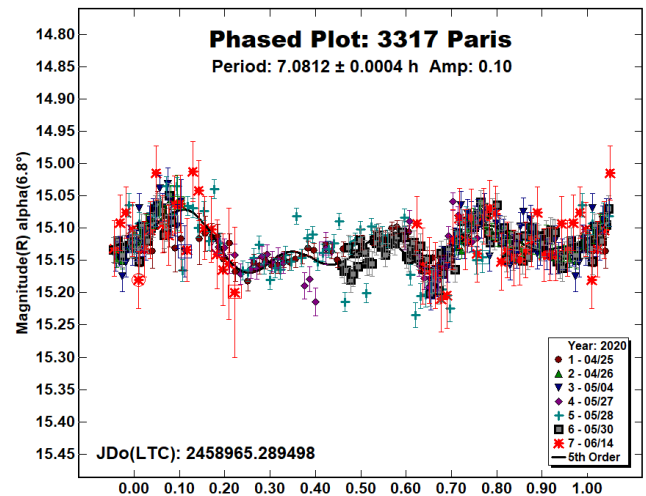
Observatory (MPC code)	Telescope	CCD	Filter	Observed Asteroids (#Sessions)
Astronomical Observatory of the University of Siena (K54)	0.30-m MCT $f/5.6$	SBIG STL-6303e (bin 2x2)	R <sub>c</sub>	58 (5), 781 (3), 913 (4), 3317 (2), 3800 (2)
Iota Scorpii (K78)	0.40-m RCT $f/8.0$	SBIG STXL-6303e (bin 2x2)	R <sub>c</sub>	781 (1), 913 (2), 3317 (2), 3800 (1)
WBRO (K49)	0.235-m SCT $f/10$	SBIG ST8-XME	C	781 (3), 3800 (3)
M57 (K38)	0.30-m RCT $f/5.5$	SBIG STT-1603	C	58 (1), 3317 (2)
GiaGa Observatory (203)	0.36-m SCT $f/5.8$	Moravian G2-3200	R <sub>c</sub>	913 (2)
GAMP (104)	0.60-m NRT $f/4.0$	Apogee Alta	C	3800 (1)
GAV	0.20-m SCT $f/6.3$	SXV-H9	R <sub>c</sub>	781 (1)

Table II. Instrumentation. MCT: Maksutov-Cassegrain, NRT: Newtonian Reflector, RCT: Ritchey-Chretien, SCT: Schmidt-Cassegrain.

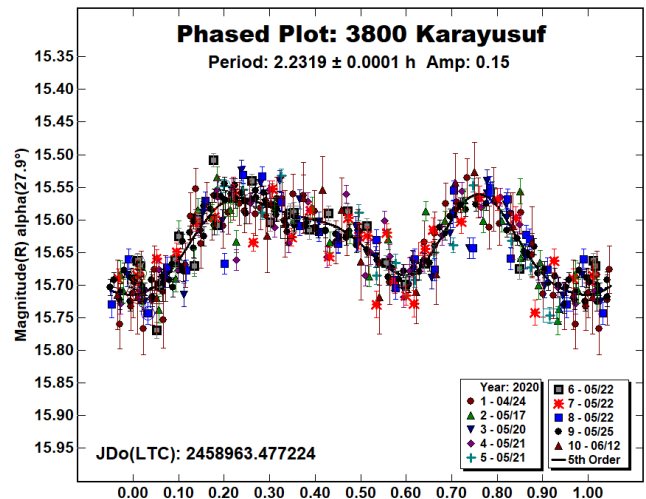
913 Otila is an Sa-type (Bus & Binzel, 2002) member of the Flora group/family; it was discovered on 1919 May 19 by K. Reinmuth at Heidelberg. Collaborative observations were made over seven nights. We found a synodic period of  $P = 4.8717 \pm 0.0007$  h with an amplitude  $A = 0.18 \pm 0.03$  mag. The period is close to the previously published results in the LCDB (Warner et al., 2009).



3317 Paris is a T-type (Bus & Binzel, 2002) Jupiter Trojan that was discovered on 1984 May 26 by C. Shoemaker and E. Shoemaker at Palomar. Collaborative observations were made over six nights. We found a synodic period of  $P = 7.0812 \pm 0.0004$  h with low amplitude  $A = 0.10 \pm 0.04$  mag. The period is close to the previously published results in the LCDB (Warner et al., 2009).



3800 Karayusuf is an S-type (Bus & Binzel, 2002) Mars-crosser asteroid discovered on 1984 January 4 by E.F. Helin at Palomar. Collaborative observations were made over seven nights. We found a synodic period of  $P = 2.2319 \pm 0.0001$  h with an amplitude  $A = 0.15 \pm 0.05$  mag. The period is close to the previously published results in the LCDB (Warner et al., 2009).



## Acknowledgements

The authors want to thank a group of high school students from Liceo “Galilei” in Erba (Como) involved in an interesting vocational guidance project about astronomy. Despite the health emergency for Covid-19, they attended some online observing sessions of 58 Concordia and participated remotely in data analysis: M. Canzi, W. Cigardi, M. Colombo, M. Creatini, L. Falato, P. Fava, A. Frigerio, C. Iezzi, V. La Bella, J. Marzullo, N. Paredi, E. Pirovano, S. Ronchetti, S. Jamil, L. Tomba.

## References

- Bus, S.J.; Binzel, R.P. (2002). “Phase II of the Small Main-Belt Asteroid Spectroscopic Survey - A Feature-Based Taxonomy.” *Icarus* **158**, 146-177.
- DSFTA (2020). Dipartimento di Scienze Fisiche, della Terra e dell'Ambiente – Astronomical Observatory, University of Siena. <https://www.dsfta.unisi.it/en/research/labs-eng/astronomicalobservatory>
- Harris, A.W.; Young, J.W.; Scaltriti, F.; Zappala, V. (1984). “Lightcurves and phase relations of the asteroids 82 Alkmene and 444 Gypsis.” *Icarus* **57**, 251-258.
- UAI (2020). “Unione Astrofili Italiani” web site. <https://www.uai.it>
- Warner, B.D.; Harris, A.W.; Pravec, P. (2009) “The asteroid lightcurve database.” *Icarus* **202**, 134-146. Updated 2020 March. <http://www.minorplanet.info/lightcurvedatabase.html>
- Warner, B.D. (2016). MPO Software, *MPO Canopus* v10.8.1.1. Bdw Publishing. <http://minorplanetobserver.com>

## SPIN-SHAPE MODEL FOR 50 VIRGINIA

Lorenzo Franco  
Balzaretto Observatory (A81), Rome, ITALY  
lor\_franco@libero.it

Frederick Pilcher  
4438 Organ Mesa Loop  
Organ Mesa Observatory (G50)  
Las Cruces, NM 88011 USA

(Received: 2020 June 29)

We present a shape and spin axis model for main-belt asteroid 50 Virginia. The model was achieved with the lightcurve inversion process, using combined dense photometric data acquired from seven apparitions between 1995-2020 and sparse data from USNO Flagstaff. Analysis of the resulting data found a sidereal period  $P = 14.31233 \pm 0.00005$  h and two mirrored pole solutions (ecliptic coordinates) at  $(\lambda, \beta) = (112^\circ, 41^\circ)$  and  $(295^\circ, 47^\circ)$  with an uncertainty of  $\pm 10$  degrees.

The minor planet 50 Virginia was observed for seven oppositions from 1995 to 2020, mainly by co-author Pilcher at Organ Mesa Observatory. The 1995 legacy data was downloaded a few years ago from the Standard Asteroid Photometric Catalogue by Piironen et al. (2001), hosted at the University of Helsinki but no longer available online. Moreover, we used sparse data from the USNO Flagstaff Station (MPC Code 689), downloaded from the Asteroids Dynamic Site (AstDyS-2, 2020).

The observational details of the dense data sets are reported in Table I with the mid-date, number of the lightcurves used for the inversion process, and longitude and latitude of the phase angle bisector ( $LPAB$ ,  $BPAB$ ).

Reference	Mid date	# LC	$LPAB^\circ$	$BPAB^\circ$
Shevchenko (1997)	1995-09-20	8	352	0
Pilcher (2009)	2008-09-25	9	7	-1
Pilcher (2011) (*)	2011-03-30	1	212	2
Pilcher (2016)	2016-06-16	7	259	4
Pilcher (2018)	2018-01-13	8	90	-4
Pilcher (2019)	2019-04-23	6	175	0
Pilcher (2020)	2020-05-15	5	234	3

Table I. Observational details for the data used in the lightcurve inversion process for 50 Virginia.\* Published on [alcdcf.org](http://alcdcf.org) web site.

Lightcurve inversion was performed using *MPO LCInvert* v.11.8.2.0 (BDW Publishing, 2016). For a description of the modeling process, see *LCInvert Operating Instructions Manual*, Durech et al. (2010 and references therein). In order to reduce the overall processing time, Pilcher’s dense data were binned at a time interval of 5 minutes.

Figure 1 shows the PAB longitude/latitude distribution for the dense and sparse data used in the lightcurve inversion process. Figure 2 (top panel) shows the sparse photometric data distribution (intensity vs JD) and (bottom panel) the corresponding phase curve (reduced magnitudes vs phase angle).

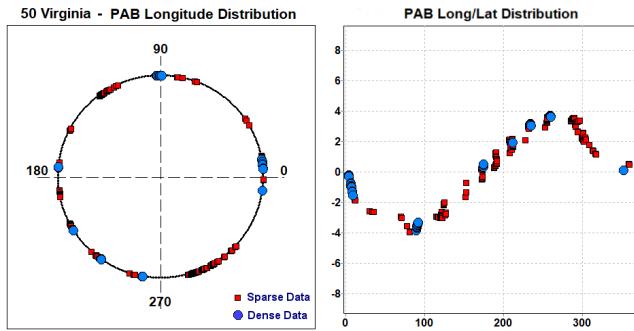


Figure 2: PAB longitude and latitude distribution of the data used for the lightcurve inversion model.

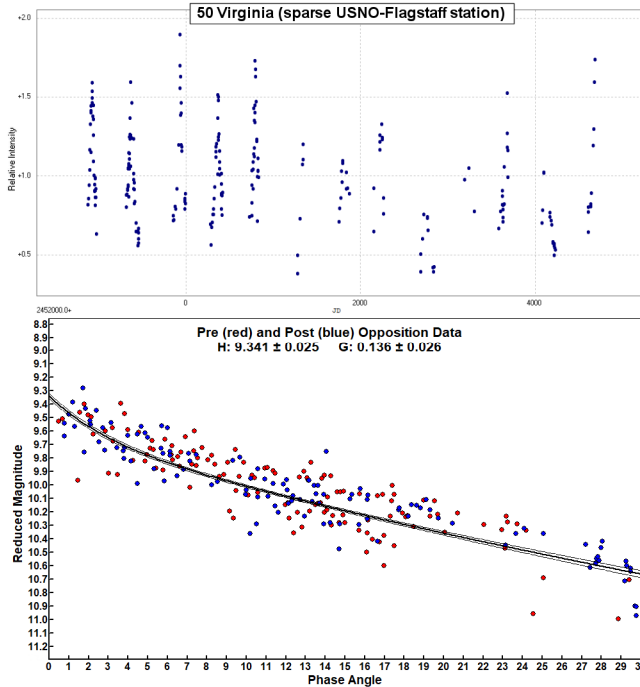


Figure 3: Top: sparse photometric data point distribution from (689) USNO Flagstaff station (relative intensity vs Julian Day). Bottom: phase curve obtained from sparse data (reduced magnitude vs phase angle).

In the analysis, the processing weighting factor was set to 1.0, 0.7 and 0.3, respectively, for Pilcher’s data, Shevchenko’s data, and the sparse data. The “dark facet” weighting factor was set to 0.5 to keep the dark facet area below 1% of total area and the number of iterations was set to 50.

The sidereal period search was started around the average of the synodic periods found in the asteroid lightcurve database (LCDB; Warner et al., 2009). We found one isolated sidereal period with a Chi-Sq value within 10% of the lowest Chi-Sq (Figure 3).

The pole search was started using the “medium” search option (312 fixed pole positions with 15° longitude-latitude steps) and the previously found sidereal period set to “float”. From this step we found two roughly mirrored lower Chi-Sq solutions (Figure 4) separated by about 180° in longitude at ecliptic longitude-latitude pairs (105°, 45°) and (300°, 45°).

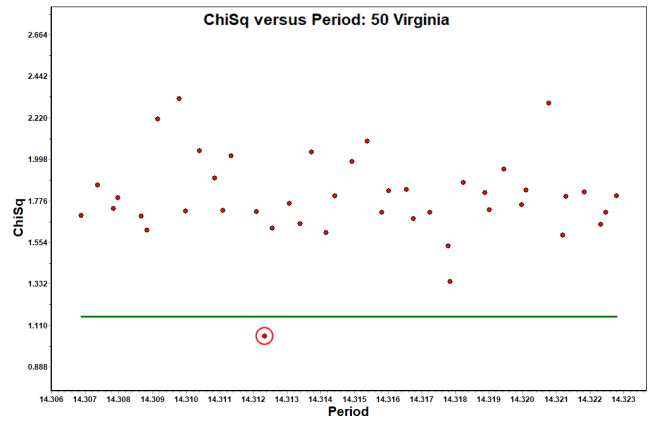


Figure 4: The period search for 50 Virginia shows one isolated sidereal period with Chi-Sq values within 10% of the lowest value.

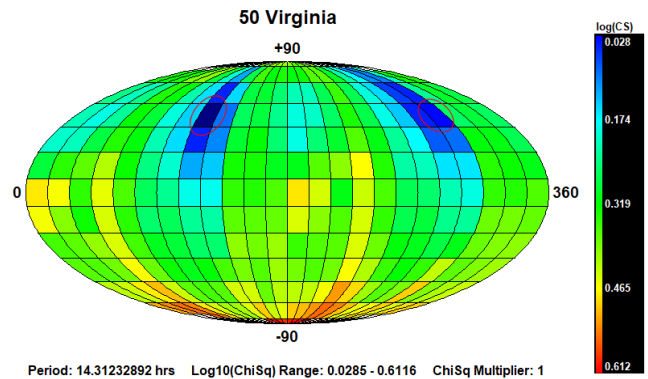


Figure 5: Pole search distribution. The dark blue region indicates the smallest Chi-Sq value while the dark red region indicates the largest.

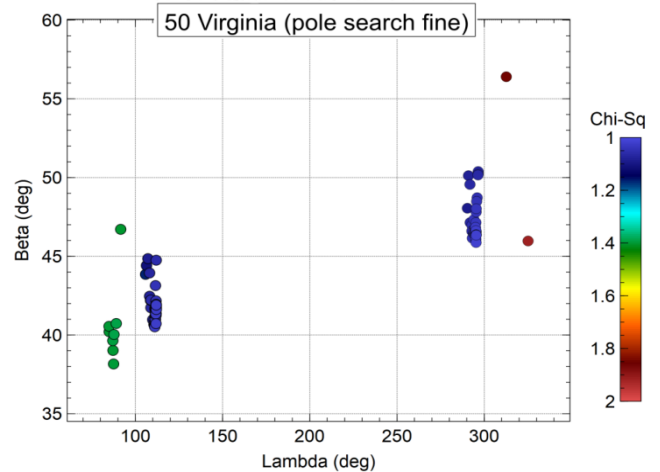


Figure 6: The “fine” pole search shows two clustered solutions centered at the ecliptic longitude/latitude (111°, 42°) and (295°, 47°) with radius approximately of 10° and Chi-Sq values within 10% of the lowest value.

The subsequent “fine” search option (49 fixed pole steps with 10° longitude-latitude pairs set to “float”) allowed us to refine the position of the pole (Figure 5). The analysis shows two sets of clustered solutions within 10° of radius that had Chi-Sq values within 10% of the lowest value, centered at ecliptic longitude-latitude (111°, 42°) and (295°, 47°).

$\lambda$ °	$\beta$ °	Sidereal Period (hours)	Chi-Sq	RMS
111	42	14.31233 ± 0.00005	1.02055	0.0181
295	47		1.01863	0.0181

Table II. The two spin axis solutions for 50 Virginia (ecliptic coordinates) with an uncertainty of  $\pm 10$  degrees. The sidereal period is the average of the two solutions found in the pole search.

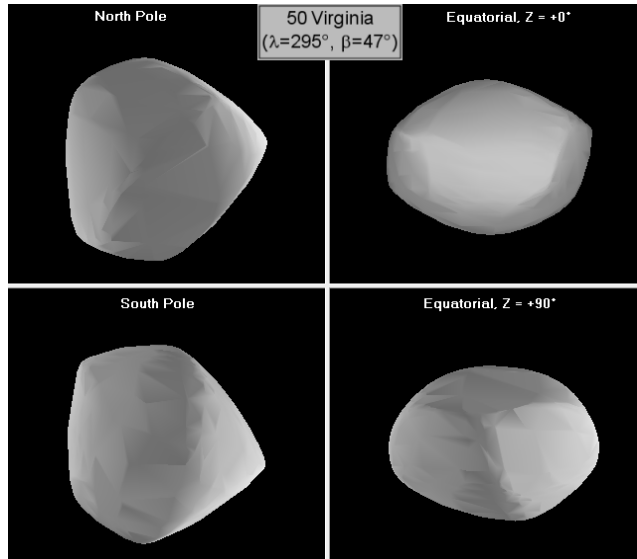


Figure 7: The shape model for 50 Virginia ( $\lambda = 295^\circ$ ,  $\beta = 47^\circ$ ).

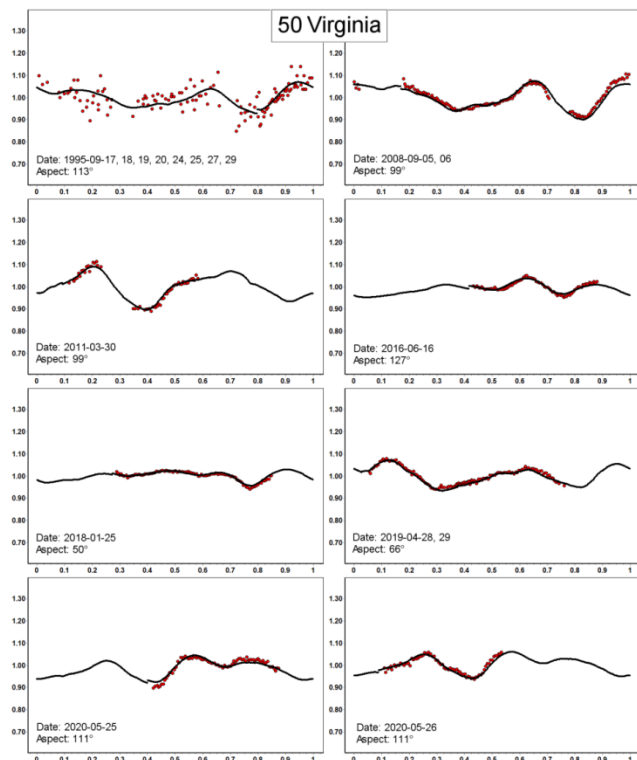


Figure 8: Model fit (black line) versus observed lightcurves (red points) for ( $\lambda = 295^\circ$ ,  $\beta = 47^\circ$ ) solution.

The two best solutions (lower Chi-Sq) are reported in Table II. The sidereal period was obtained by averaging the two solutions found in the pole search process. Typical errors in the pole solution are  $\pm 10^\circ$  and the uncertainty in sidereal period has been evaluated as a rotational error of  $20^\circ$  over the total time span of the dense data set. Figure 6 shows the shape model (second solution with lower Chi-Sq) while Figure 7 shows the fit between the model (black line) and some observed lightcurves (red points).

## References

- AstDyS-2 (2020). Asteroids - Dynamic Site. <https://newton.spacedys.com/astdys/>
- BDW Publishing. (2016). <http://www.minorplanetobserver.com/MPOSoftware/MPOLCInvert.htm>
- Durech, J.; Sidorin, V.; Kaasalainen, M. (2010). "DAMIT: a database of asteroid models." *Astron. Astrophys.* **513**, A46.
- Piironen, J.; Lagerkvist, C.-I.; Torppa, J.; Kaasalainen, M.; Warner, B. (2001). "Standard Asteroid Photometric Catalogue." *Bulletin of the American Astronomical Society* **33**, 1562.
- Pilcher, F. (2009). "Period Determinations for 33 Polyhymnia, 38 Leda, 50 Virginia, 189 Phthia, and 290 Bruna." *Minor Planet Bulletin* **36**, 25-27.
- Pilcher, F. (2016). "Rotation Determinations for 50 Virginia, 58 Concordia, 307 Nike, and 339 Dorothea." *Minor Planet Bulletin* **43**, 304-306.
- Pilcher, F. (2018). "Rotation Period Determinations for 50 Virginia, 142 Polana, and 597 Bandusia." *Minor Planet Bulletin* **45**, 246-247.
- Pilcher, F. (2019). "New Lightcurves of 50 Virginia, 57 Mnemosyne, 59 Elpis, 194 Prokne, 444 Gypsis, and 997 Priska." *Minor Planet Bulletin* **46**, 445-448.
- Pilcher, F. (2020). "Lightcurves and rotation periods of 50 Virginia, 57 Mnemosyne, 58 Concordia, 59 Elpis, 78 Diana, and 529 Preziosa." *Minor Planet Bulletin* **47**, 344-346.
- Shevchenko, V.G.; Belskaya, I.N.; Chiorny, V.G.; Piironen, J.; Erikson, A.; Neukum, G.; Mohamed, R. (1997). "Asteroid observations at low phase angles. I. 50 Virginia, 91 Aegina and 102 Miriam." *Planetary and Space Science* **45**, 1615-1623.
- Warner, B.D.; Harris, A.W.; Pravec, P. (2009). "The asteroid lightcurve database." *Icarus* **202**, 134-146. Updated 2020 March. <http://www.minorplanet.info/lightcurvedatabase.html>

## MAIN-BELT ASTEROIDS OBSERVED FROM CS3: 2020 APRIL TO JUNE

Robert D. Stephens

Center for Solar System Studies (CS3) / MoreData!  
11355 Mount Johnson Ct., Rancho Cucamonga, CA 91737 USA  
rstephens@foxandstephens.com

Brian D. Warner

Center for Solar System Studies (CS3) / MoreData!  
Eaton, CO

(Received: 2020 July 13)

CCD photometric observations of 18 main-belt asteroids were obtained at the Center for Solar System Studies (CS3) from 2020 April to June.

The Center for Solar System Studies (CS3) has seven telescopes which are normally used in program asteroid family studies. The focus is on near-Earth asteroids, but when suitable targets are not available, Jovian Trojans and Hildas are observed. When a nearly full moon is too close to the family targets being studied, targets of opportunity amongst the main-belt families were selected.

Table I lists the telescopes and CCD cameras that were used to make the observations. Images were unbinned with no filter and had master flats and darks applied. The exposures depended upon various factors including magnitude of the target, sky motion, and Moon illumination.

Telescope	Camera
0.30-m f/6.3 Schmidt-Cass	FLI Microline 1001E
0.35-m f/9.1 Schmidt-Cass	FLI Microline 1001E
0.35-m f/9.1 Schmidt-Cass	FLI Microline 1001E
0.35-m f/9.1 Schmidt-Cass	FLI Microline 1001E
0.35-m f/11 Schmidt-Cass	FLI Microline 1001E
0.40-m f/10 Schmidt-Cass	FLI Proline 1001E
0.50-m F8.1 R-C	FLI Proline 1001E

Table I: List of CS3 telescope/CCD camera combinations.

Image processing, measurement, and period analysis were done using *MPO Canopus* (Bdw Publishing), which incorporates the Fourier analysis algorithm (FALC) developed by Harris (Harris et al., 1989). The Comp Star Selector feature in *MPO Canopus* was used to limit the comparison stars to near solar color. Night-to-night calibration was done using field stars from the ATLAS catalog (Tonry et al., 2018), which has Sloan *griz* magnitudes that were derived from the GAIA and Pan-STARR catalogs and are “native” magnitudes of the catalog.

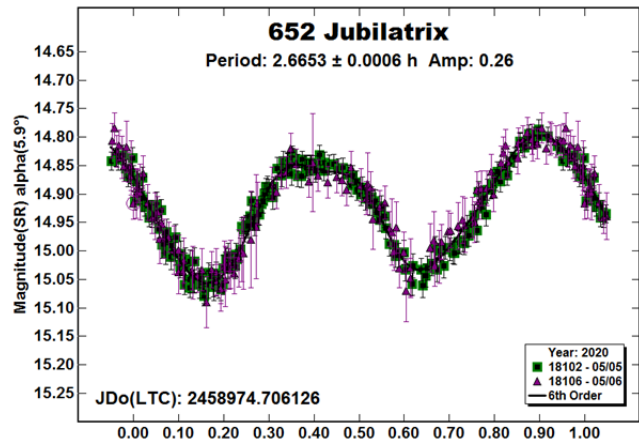
We used the ATLAS  $r'$  (SR) magnitudes. Those adjustments are mostly  $\leq 0.03$  mag. The occasions where larger corrections were required may have been related in part to using unfiltered observations, poor centroiding of the reference stars, and not correcting for second-order extinction terms.

The magnitudes were normalized to the comparison stars used in the earliest session and to the phase angle given in parentheses using  $G = 0.15$ . In other words, the data were made to seem that they were all obtained at the same time using the same comparison stars. The X-axis rotational phase ranges from  $-0.05$  to  $1.05$ .

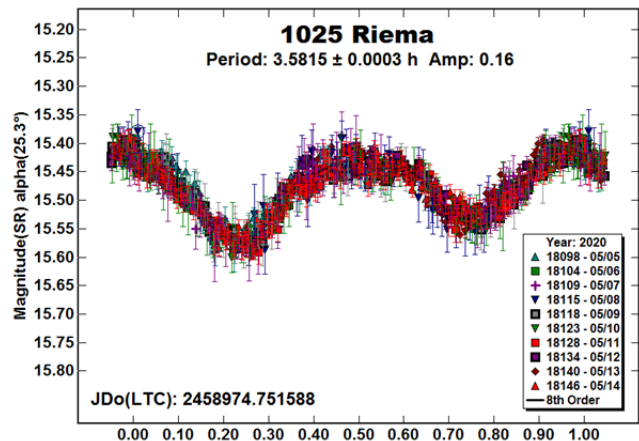
The amplitude indicated in the plots (e.g. Amp. 0.23) is the amplitude of the Fourier model curve and not necessarily the adopted amplitude of the lightcurve.

For brevity, only some of the previously reported rotational periods may be referenced. A complete list is available at the asteroid lightcurve database (LCDB; Warner et al., 2009).

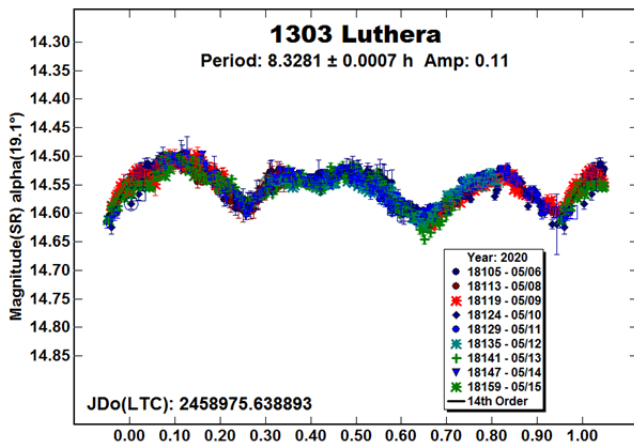
**652 Jubilatrix.** This member of the Eunomia group or family was undertaken as a ‘Full moon’ project to keep the telescopes observing when dimmer targets could not be observed. It was previously observed by Pilcher (2010) and Behrend (2015web, 2020web) who reported periods near 2.66 h. Kim et al. (2014) reported a spin axis model with  $(\lambda, \beta) = (143^\circ, 34^\circ)$  or  $(321^\circ, 27^\circ)$  and a sidereal period of 2.6626693 h.



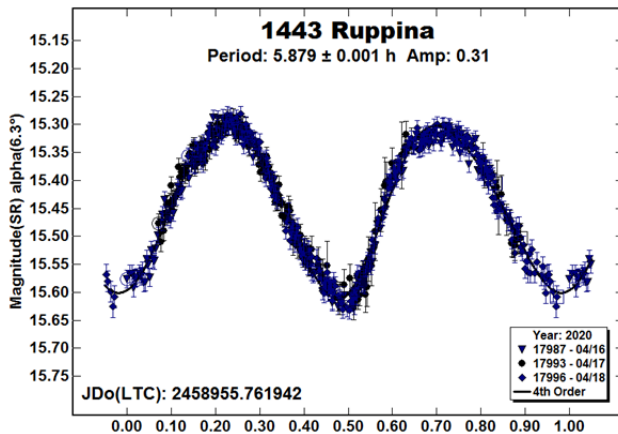
**1025 Riema.** We observed this Hungaria family or group member six times in the past (Warner, 2017 and references therein), each time finding a rotational period near 3.58 h. In the 2020 data we found evidence of a weak second period near 42 h. The mutual events, if real, were no more than 0.06 mag. deep. To verify the existence of a second period warrants high-quality observations by a collaboration of observers at different longitudes at future apparitions.



**1303 Luthera.** This outer main-belt asteroid has been observed several times in the past with a range of results. Sada (2008) found 5.878 h while Behrend (2009web, 2020web) found 7.92 h and 8.3246 h respectively. The 2020 Behrend observations were obtained five weeks prior to ours with essentially the same result.



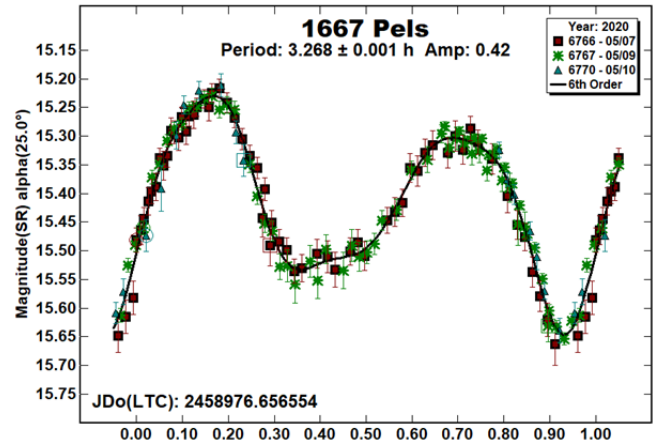
**1443 Ruppina.** This outer main-belt asteroid was observed many times in the past. Using sparse data from the Palomar Transient Factory Survey, Chang et al. (2015) and Waszczk et al. (2015) both found periods near 5.9 h. We found a period from our 2017 data near 5.88 h (Stephens, 2018). All of these periods are in good agreement with this year's result.



Because of the availability of the Chang and Waszczk data in the Asteroid Lightcurve Data Exchange Format database (ALCDEF, 2020), sparse data at the Asteroids – Dynamic web site (AstDyS-2, 2020), and our dense data from two apparitions, we attempted to solve for the sidereal period and pole position and create a shape model. This data was combined using *MPO LCInvert* (Bdw Publishing). This Windows-based program incorporates the algorithms developed by Kaasalainen and Torppa (2001) and Kaasalainen et al (2001) and converted by Josef Āurech from the original FORTRAN to C. A period search was made over a sufficiently wide range to assure finding a global minimum in  $\chi^2$  values.

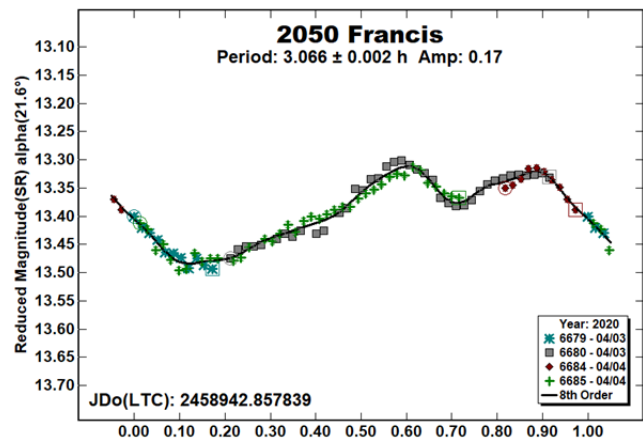
As is often the case, the pole model showed a number of possible solutions with two probable solutions  $180^\circ$  apart;  $(\lambda, \beta, P) = (120^\circ, -15^\circ, 5.879288$  h) and  $(295^\circ, -22^\circ, 5.879290$  h). Our preferred solution is  $(120^\circ, -15^\circ)$ .

**1667 Pels.** This inner main-belt asteroid has been observed several times in the past (Behrend, 2020web; Kryszczyńska, 2012; Stephens and Warner, 2019b) each time finding a period near 3.26 h. This year's result is in good agreement with those prior findings.



Because of the availability of sparse data and our dense data from two oppositions, we attempted a pole/shape model. A sidereal period of 3.268280 h stood out above all other possibilities. Since all of the possible pole solutions are in the southern hemisphere, the object is clearly rotating retrograde. Two probable pole positions are  $(\lambda, \beta, P) = (182^\circ, -53^\circ, 3.268280$  h) and  $(16^\circ, -63^\circ, 3.268280$  h), which are about  $180^\circ$  apart. Our preferred solution is  $(182^\circ, -53^\circ)$ .

**2050 Francis.** This member of the Phocaea family/group was observed by Franco et al. (2013), who found a rotational period of 3.069 h. Behrend (2020web) reported a period of 6.136 h with four extrema and twice the period reported by Franco et al. Our data in 2020, obtained a week after the Behrend data, resulted in a period which is a good fit with the Franco result.



# SPIN/SHAPE MODEL FOR 1443 Ruppina

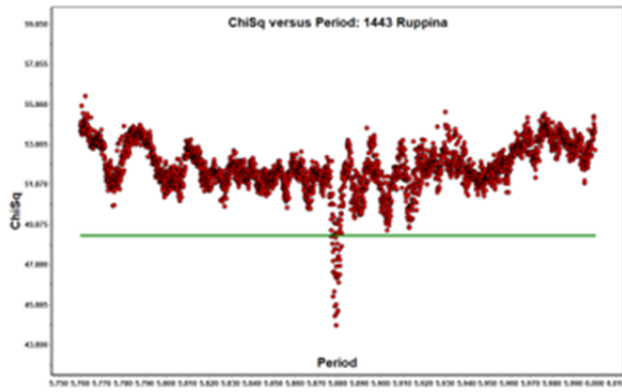


Figure 1. The initial period search results.

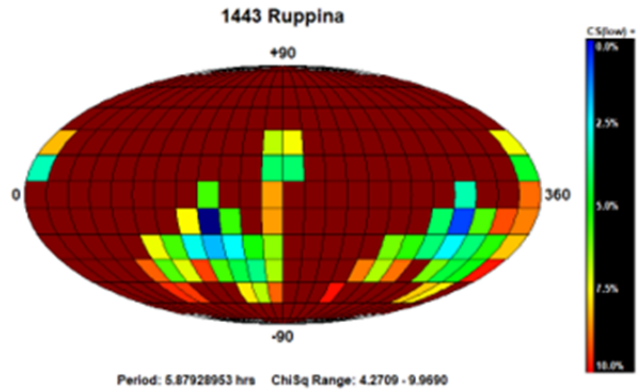


Figure 2. In this pole plot, dark red represents a solution that is more than 10% above the lowest  $\chi^2$  value. The pole search found two probable solutions.

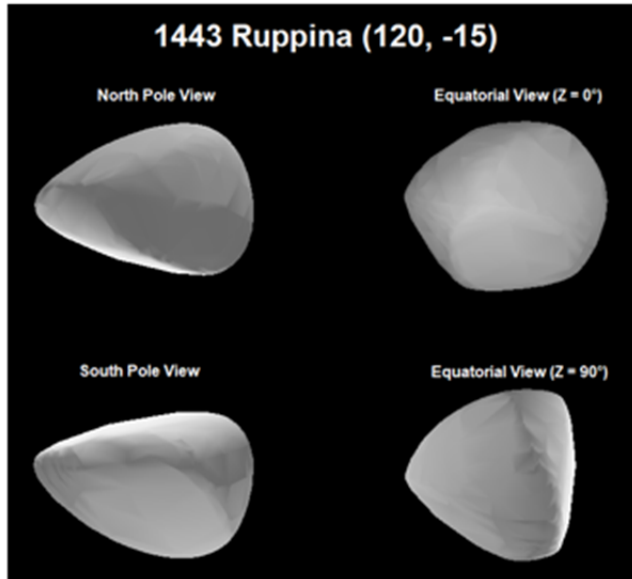


Figure 3. The shape of the asteroid based on the preferred solution.

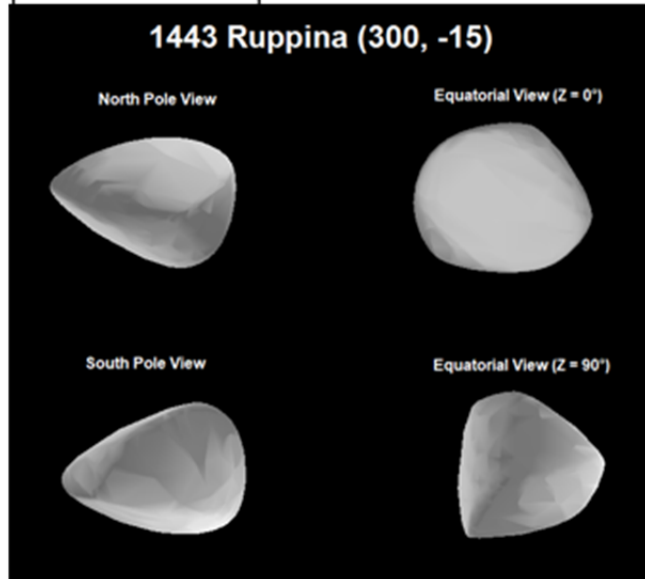


Figure 4. The shape of the asteroid based on the secondary solution.

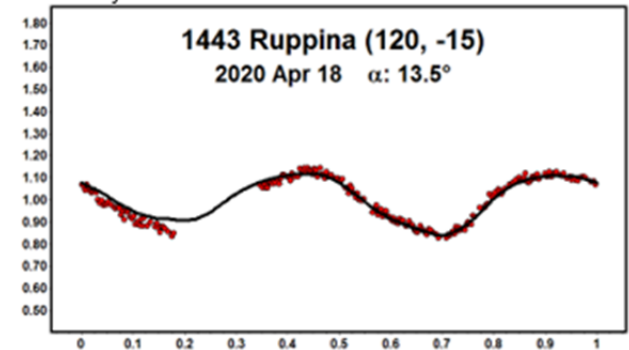
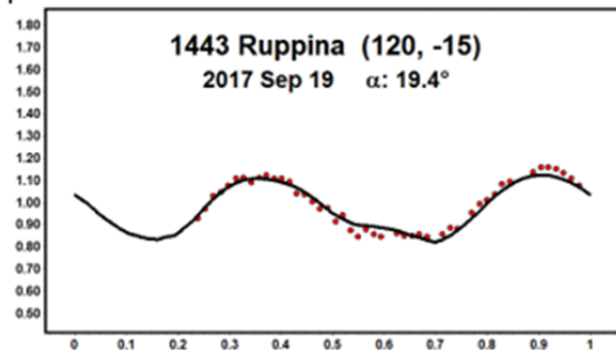


Figure 5/6. The comparison plots against the preferred pole solution for the 2017 and 2020 data. The red dots indicate the data used for modeling while the black line is the smoothed lightcurve for generated by the shape at the time of the observations. The match is very close on all occasions, which gives confidence in the shape/spin axis model.

# SPIN/SHAPE MODEL FOR 1667 PELS

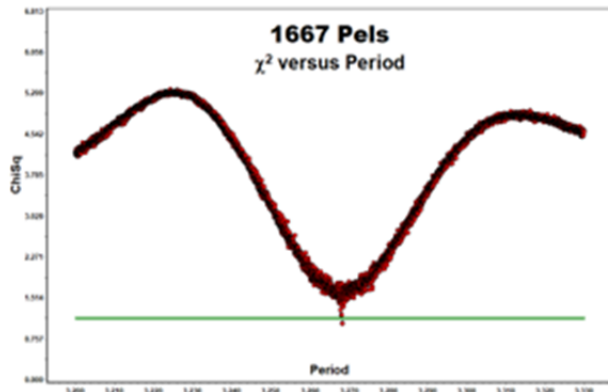


Figure 1. The initial period search results.

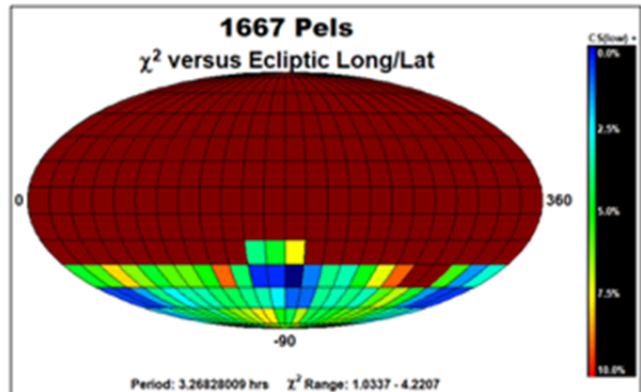


Figure 2. The pole search found two probable solutions.

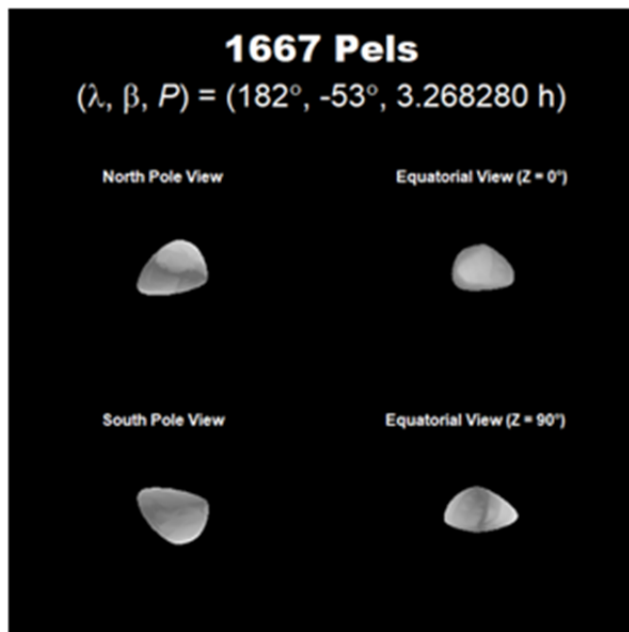


Figure 3. The shape of the asteroid based on the preferred solution.

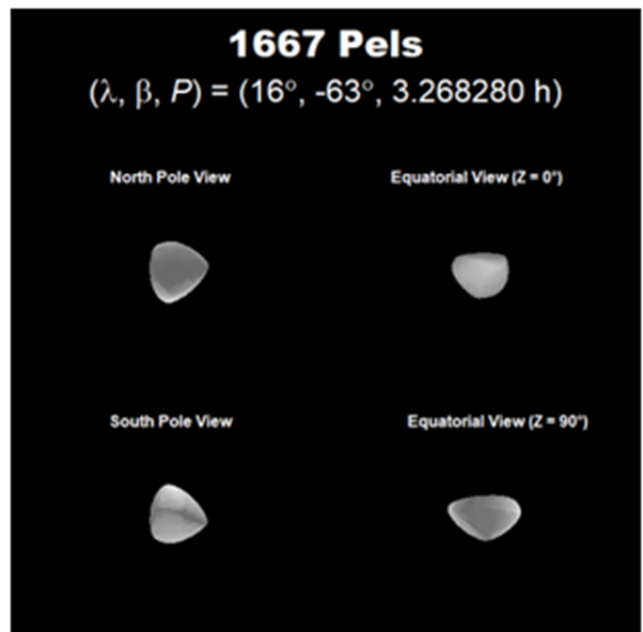


Figure 4. The shape of the asteroid based upon the secondary solution.

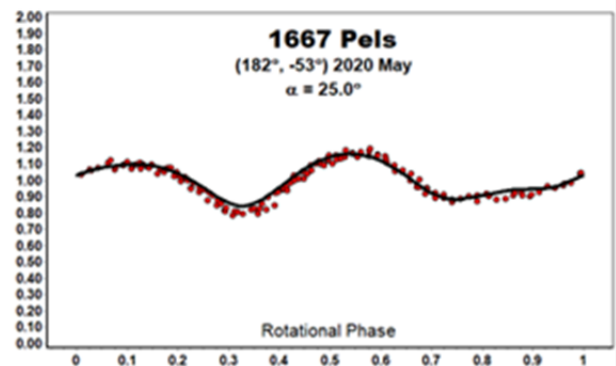
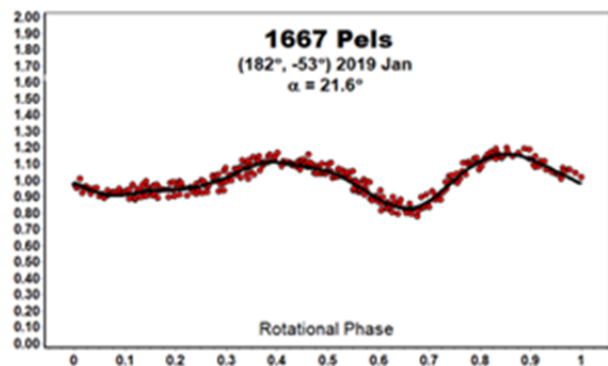
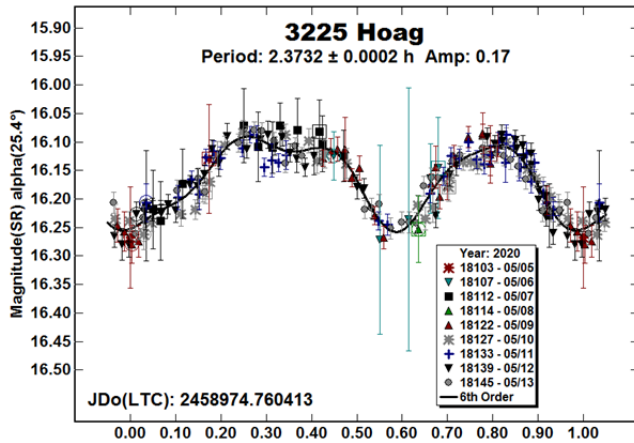
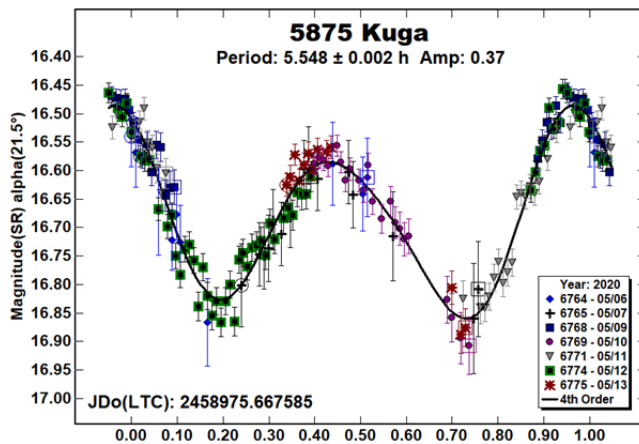


Figure 5/6. The comparison plots are against the preferred pole solution. The red dots indicate the data used for modeling while the black line is the smoothed lightcurve for generated by the shape at the time of the observations. The match is very close on both occasions, which gives confidence in the shape/spin axis model.

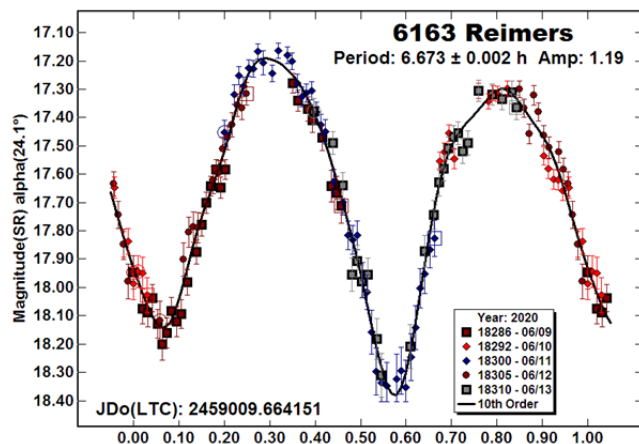
**3225 Hoag.** We have observed this member of the Hungaria family/group many times in the past (Stephens and Warner, 2019a and references therein), each time finding a rotational period near 2.37 h. We undertook observations this year to improve upon a preliminary pole solution.



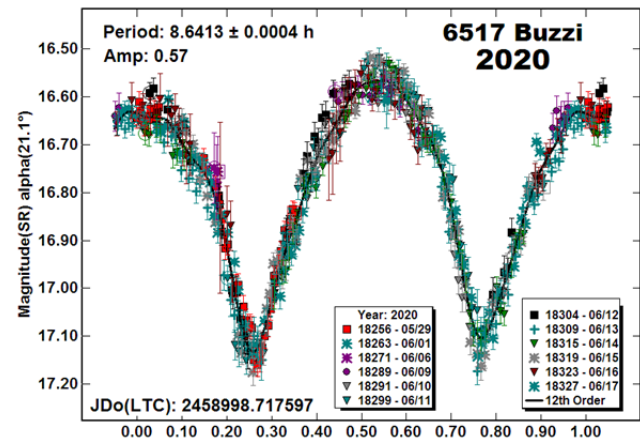
**5875 Kuga.** Carbo et al. (2009) observed this 9-km Vestoid finding a rotational period of 5.551 h. Using data from 2015 and 2016, Oszkiewicz et al. (2017) found rotational periods near 5.55 h. Our result from this year is in good agreement.



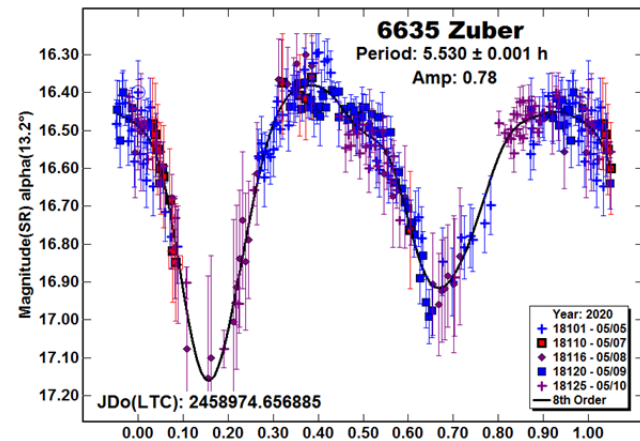
**6163 Reimers.** There are two reported periods in the LCDB for this member of the Hungaria family/group (Warner, 2011, 6.68 h; Waszczak et al., 2015, 6.686 h). The analysis of our data in 2020 is in good agreement with those previous results.



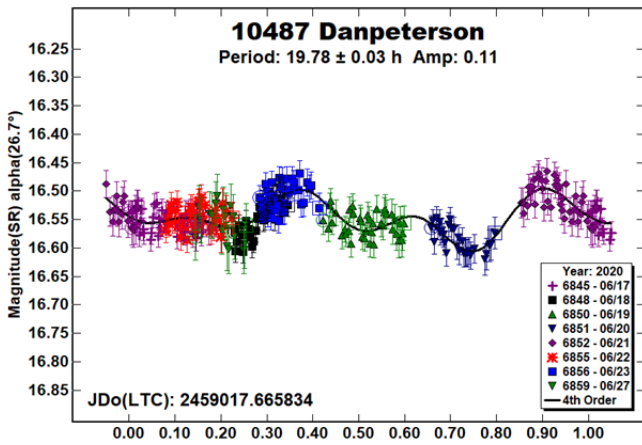
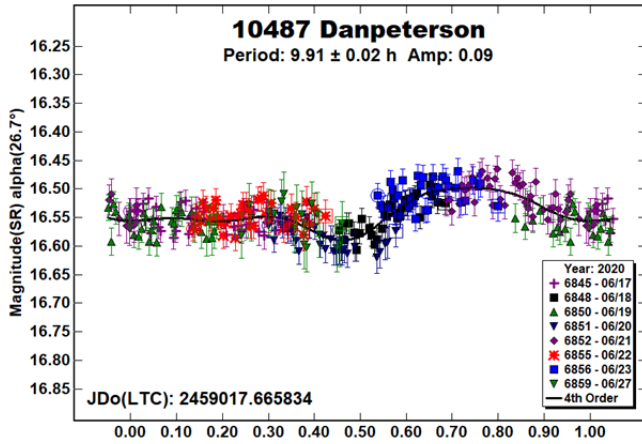
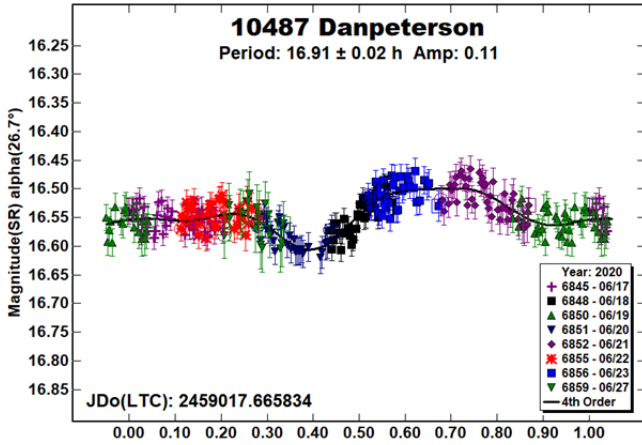
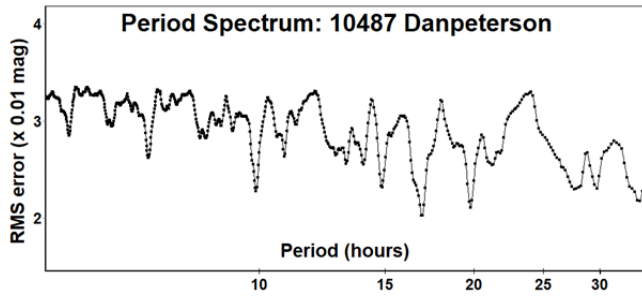
**6517 Buzzi.** We observed this member of the Hungaria family/group four times in the past (Warner 2014 and references therein) each time finding periods near 8.64 h. This year's result is in good agreement with those prior findings and provides additional data for a pole solution. Hanuš et al. (2016) found a pole solution  $(\lambda, \beta, P) = (227^\circ, -75^\circ, 8.64468 \text{ h})$ .



**6635 Zuber.** We have also observed this member of the Hungaria family/group four times in the past (Warner 2015 and references therein), each time finding periods near 5.53 h. Using thermal infrared data acquired by the NASA's Wide-field Infrared Survey Explorer (WISE), Hanuš et al. (2018) found a pole solution  $(\lambda, \beta, P) = (262^\circ, -77^\circ, 5.53564 \text{ h})$ .

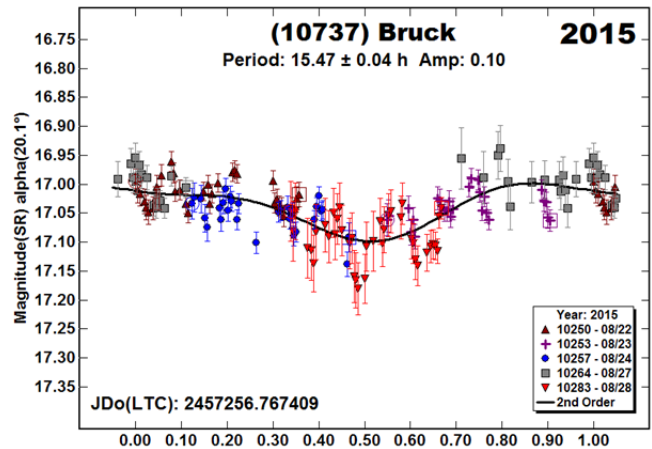
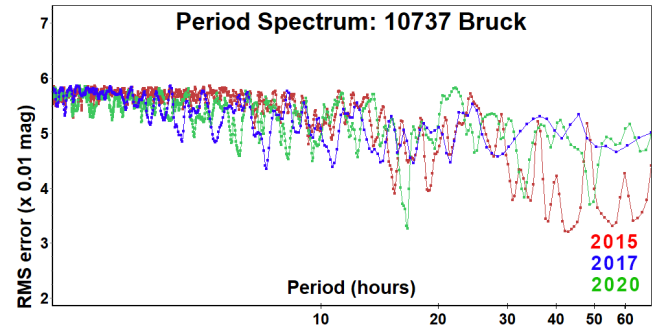
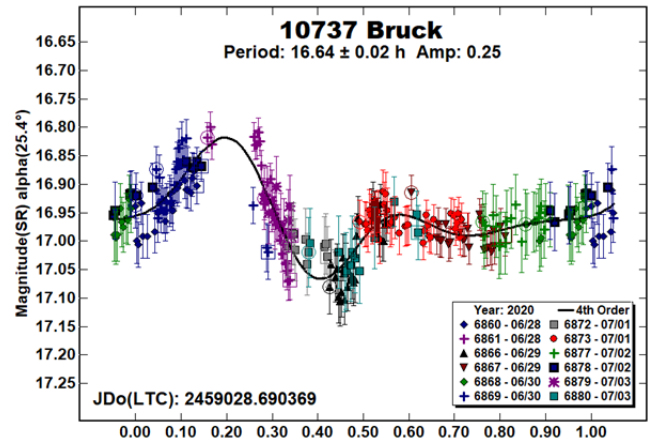


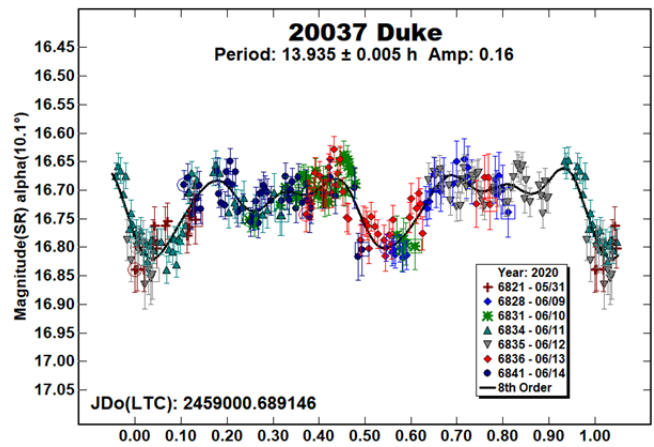
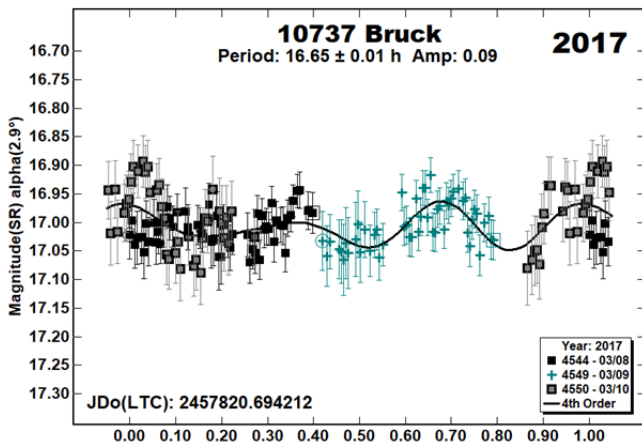
**10487 Danpeterson.** We found no reported lightcurves for this member of the Phocaea family/group in the LCDB. The period spectrum shows three possible solutions. Those at 16.91 h and 9.91 h are low amplitude, bimodal lightcurves and are 5:3 aliases of each other. The 19.78 h solution is a *fit by exclusion*, which is where the Fourier analysis finds a local RMS minimum by minimizing the number of overlapping data points. We have adopted the 16.91 h solution for this paper because of the slightly higher amplitude.



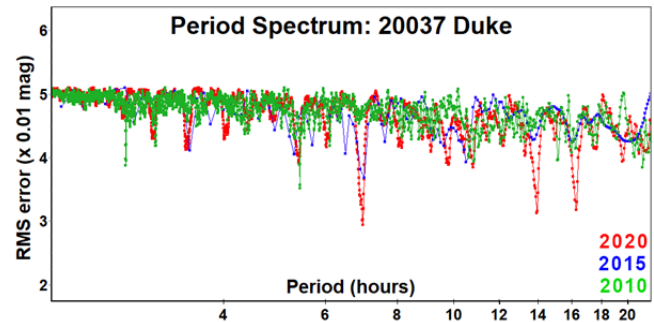
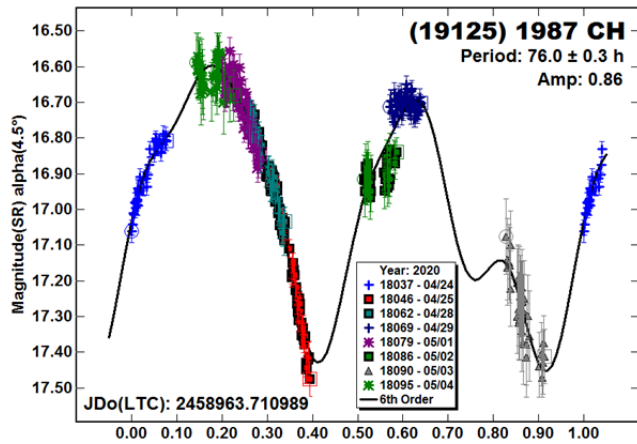
10737 Bruck. We have studied this Hungaria twice in the past (Warner 2016, 3.22 h; 2011; Stephens 2017, 7.29 h). However, the data obtained in 2020 would not fit either of those two periods. We converted the comp star magnitudes used in the 2015 and 2017 lightcurves to ATLAS SR magnitudes and reprocessed the lightcurves. The results were still not definitive. We then stacked all three period spectra on top of each other to assist in finding a dominate solution and excluding solutions not present in all three datasets.

We discounted any solutions longer than 30 h because they were all a *fit by exclusion*. The best remaining solutions were near 16.7 h, but they were not convincing. In particular, the 2015 and 2017 datasets were too sparse to be definitive for a longer period, as well as low amplitude and somewhat noisy. The next good opposition for the northern hemisphere is in 2023 October.

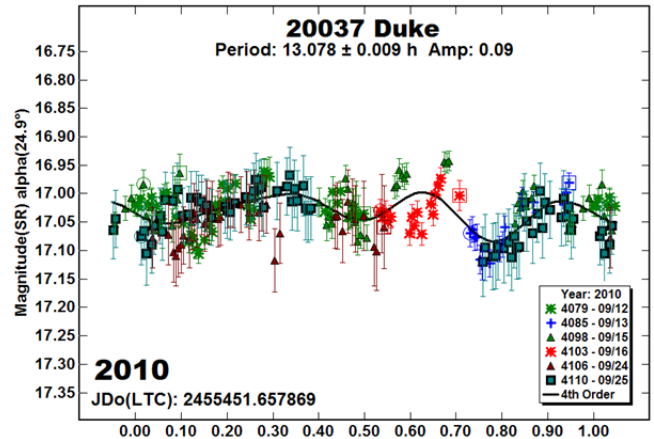




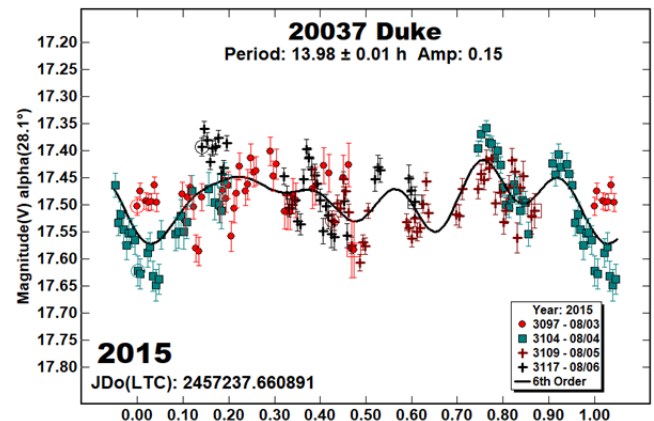
(19125) 1987 CH. Using data from the Transiting Exoplanet Survey Satellite (TESS), Pál et al. (2020) reported a rotational period of 75.8 h for this member of the Flora family/group. Our result is in good agreement.

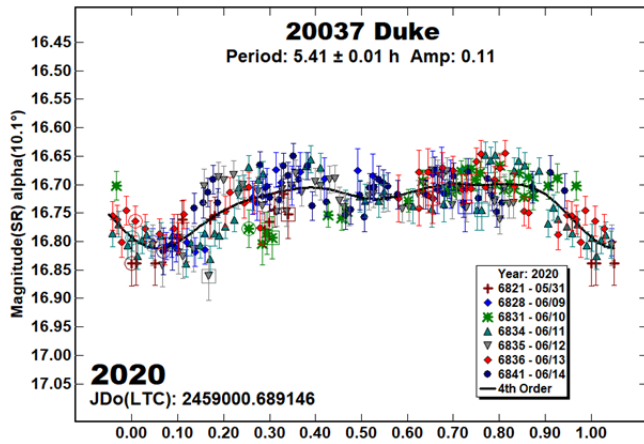
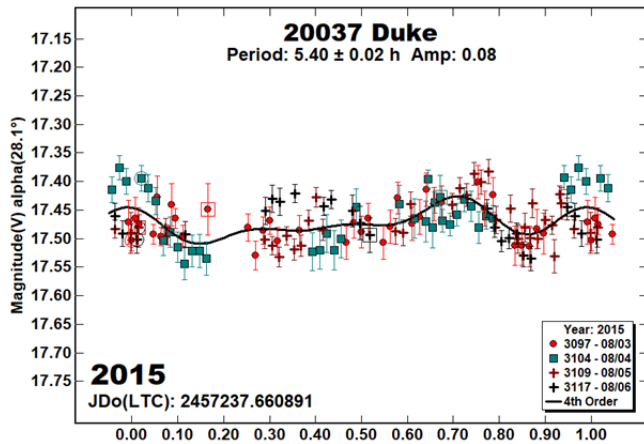
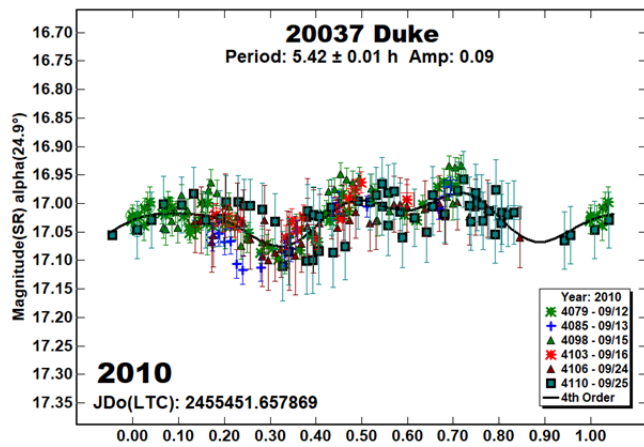


20037 Duke. Duke is another problematic low amplitude member of the Hungaria family/group. We observed this 2-km object twice in the past (Warner 2011, 5.428 h; Stephens 2016, 5.29 h). Using data from the Transiting Exoplanet Survey Satellite (TESS), Pál et al. (2020) reported a rotational period of 13.8267 h. The period spectrum showed several possible aliases; 5.4 h, 7 h, and 13.9 h.

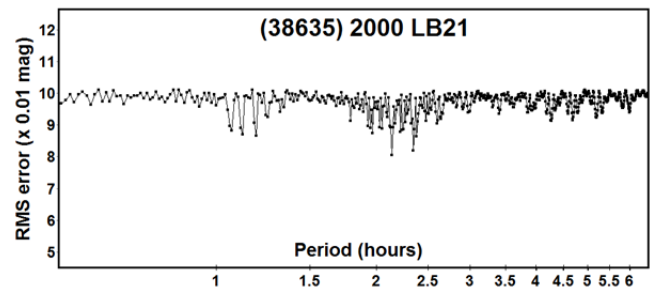
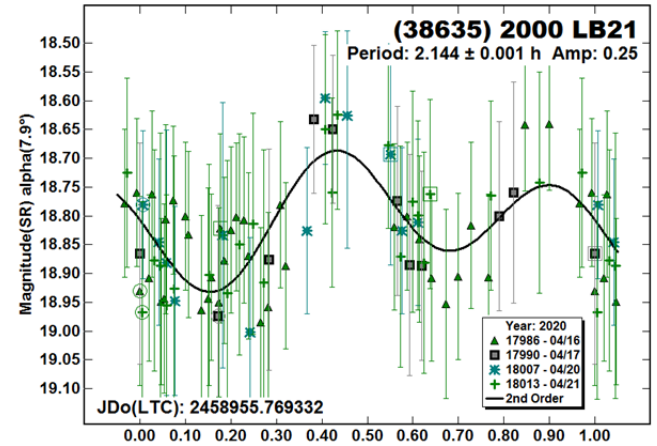


We again tried stacking the period spectra for all three datasets to look for a common period. A weak 5.4-h period was present for 2010, 2015, and 2020. The most dominant period was near 7 h, but only for 2015 and 2020. The 2020 data had a dominant 13.9-h period with a four extrema lightcurve, which matched the Pál et al. result. However, the results using the 2010 and 2015 data would not produce a good match to that period. For this paper, we are adopting the 13.935 h period with an alternate period of 5.41 h, which are a 2:5 aliases of each other.

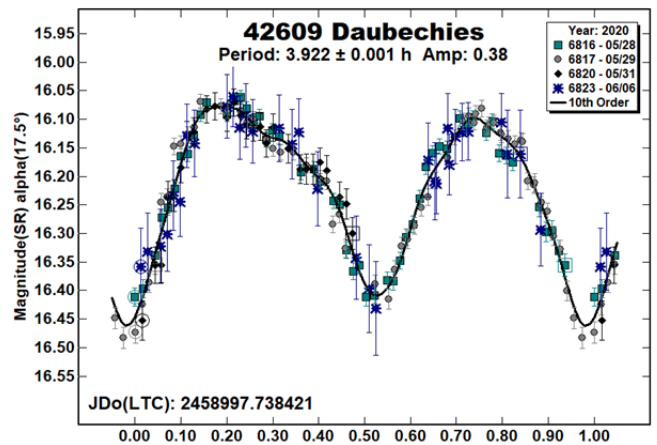




(38635) 2000 LB21. There were no previous lightcurve entries in the LCDB for this 2-km member of the Flora family/group. This was a target of opportunity using 60 second exposures on a target that was  $V \sim 18.8$  mag. To be able to measure the resulting low SNR, we used the Stack/Sum - Multi processing feature in *MPO Canopus*. Images were in groups of 3 with no more than 3 minutes between any successive images in a group. There were 79 stacked-images used in the analysis.



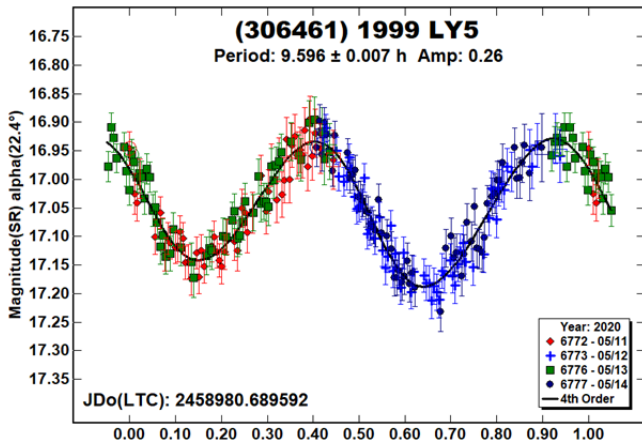
42609 Daubechies. There were no previous lightcurve entries in the LCDB for this estimated 3-km Mars-crosser.



Number	Name	2020 mm/dd	Phase	L <sub>PAB</sub>	B <sub>PAB</sub>	Period(h)	P.E.	Amp	A.E.	Grp
652	Jubilatrix	05/05-05/06	5.9,5.7	230	12	2.6653	0.0006	0.26	0.02	EUN
1025	Riema	05/05-05/14	25.3,24.3	253	37	3.5815	0.0003	0.16	0.01	H
1303	Luthera	05/06-05/15	19.1,19.9	169	21	8.3281	0.0007	0.11	0.01	MB-O
1443	Ruppina	04/16-04/18	6.4,5.6	223	2	5.879	0.001	0.31	0.02	MB-O
	Pole ( $\lambda$ , $\beta$ , P)	<b>(120°, -15°, 5.879288 h)</b>		(295°, -22°, 5.879290 h)			<b>a/b: 1.291</b>	<b>a/c: 1.210</b>		
1667	Pels	05/07-05/10	25.0,25.7	177	5	3.268	0.001	0.42	0.02	FLOR
	Pole ( $\lambda$ , $\beta$ , P)	<b>(182°, -53°, 3.268280 h)</b>		(16°, -63°, 3.268280 h)			<b>a/b: 1.247</b>	<b>a/c: 1.135</b>		
2050	Francis	04/03-04/04	21.6,21.5	201	33	3.066	0.002	0.17	0.01	PHO
3225	Hoag	05/05-05/13	25.4,27.8	183	4	2.3732	0.0002	0.17	0.02	H
5875	Kuga	05/06-05/13	21.5,22.7	177	-8	5.548	0.002	0.37	0.03	V
6163	Reimers	06/09-06/13	24.2,25.4	233	9	6.673	0.002	1.19	0.04	H
6517	Buzzi	05/29-06/17	*21.1,21.1	252	29	8.6413	0.0004	0.57	0.03	H
6635	Zuber	05/05-05/10	13.2,14.4	221	20	5.530	0.001	0.78	0.05	H
10487	Danpeterson	06/17-06/27	26.7,27.2	201	25	16.91	0.02	0.11	0.02	PHO
						<sup>A</sup> 9.91	0.02	0.09	0.02	
10737	Bruck	06/28-07/03	25.5,25.6	274	31	16.64	0.02	0.25	0.05	H
19125	1987 CH	04/24-05/04	*4.5,6.4	216	7	76.0	0.3	0.86	0.05	FLOR
20037	Duke	05/31-06/14	10.1,17.3	246	15	13.935	0.005	0.16	0.02	H
						<sup>A</sup> 5.41	0.01	0.11	0.02	
38635	2000 LB21	04/16-04/21	8.0,5.6	222	2	2.144	0.001	0.20	0.05	FLOR
42609	Daubechies	05/28-06/06	17.5,22.0	229	8	3.922	0.001	0.38	0.02	MC
306461	1999 LY5	05/11-05/14	22.5,23.7	201	5	9.596	0.007	0.26	0.03	MC

Table III. Observing circumstances and results. <sup>A</sup>The alternate period of an ambiguous solution. The phase angle is given for the first and last date. If preceded by an asterisk, the phase angle reached an extrema during the period. L<sub>PAB</sub> and B<sub>PAB</sub> are the approximate phase angle bisector longitude/latitude at mid-date range (see Harris et al., 1984). Grp is the asteroid family/group (Warner et al., 2009). For 1443 and 1667, the second line gives the spin axis/shape modeling results. The pole solution in bold is the preferred one.

(306461) 1999 LY5. We could not find any entries in the LCDB for this Mars-crosser, estimated to be 6 km in size.



Acknowledgements

Observations at CS3 and continued support of the asteroid lightcurve database (LCDB; Warner et al., 2009) are supported by NASA grant 80NSSC18K0851.

This work includes data from the Asteroid Terrestrial-impact Last Alert System (ATLAS) project. ATLAS is primarily funded to search for near earth asteroids through NASA grants NN12AR55G, 80NSSC18K0284, and 80NSSC18K1575; byproducts of the NEO search include images and catalogs from the survey area. The ATLAS science products have been made possible through the contributions of the University of Hawaii Institute for Astronomy, the Queen's University Belfast, the Space Telescope Science Institute, and the South African Astronomical Observatory.

The authors gratefully acknowledge Shoemaker NEO Grants from the Planetary Society (2007, 2013). These were used to purchase some of the telescopes and CCD cameras used in this research.

References

ALCDEF (2020). Asteroid Lightcurve Data Exchange Format database. <http://www.alcdef.org/>

AstDys-2 (2020). Asteroids - Dynamic web site. <https://newton.spacedys.com/astdys/>

Behrend, R. (2009web, 2015web, 2020web). Observatoire de Geneve web site. [http://obswww.unige.ch/~behrend/page\\_cou.html](http://obswww.unige.ch/~behrend/page_cou.html)

Carbo, L.; Green, D.; Kragh, K.; Krotz, J.; Meiers, A.; Patino, B.; Pligge, Z.; Shaffer, N.; Ditton, R. (2009). "Asteroid Lightcurve Analysis at the Oakley Southern Sky Observatory: 2008 October thru 2009 March." *Minor Planet Bull.* **36**, 152.

Chang, C.-K.; Ip, W.-H.; Lin, H.-W.; Cheng, Y.-C.; Ngeow, C.-C.; Yang, T.-C.; Waszczak, A.; Kulkarni, S.R.; Levitan, D.; Sesar, B.; Laher, R.; Surace, J.; Prince, T.A. (2015). "Asteroid Spin-rate Study Using the Intermediate Palomar Transient Factory." *Ap. J. Suppl. Ser.* **219**, A27.

Franco, L.; Tomassini, A.; Scardella, M. (2013). "Rotational Period of Asteroid Francis." *Minor Planet Bull.* **40**, 197.

Hanuš, J.; Ďurech, J.; Oszkiewicz, D.A.; Behrend, R.; Carry, B.; Delbo, M.; Adam, O.; Afonina, V.; Anquetin, R.; Antonini, P.; Arnold, L.; Audejean, M.; Aurard, P.; Bachschmidt, M.; Baduel, B.; Barbotin, E.; Barroy, P.; Baudouin, P.; Berard, L.; Berger, N.; and 150 others (2016). "New and updated convex shape models of asteroids based on optical data from a large collaboration network." *Astron. Astrophys.* **586**, A108.

- Hanuš, J.; Delbo, M.; Ďurech, J.; Alí-Lagoa, V. (2018). "Thermophysical modeling of main-belt asteroids from WISE thermal data." *Icarus* **309**, 297-337.
- Harris, A.W.; Young, J.W.; Scaltriti, F.; Zappala, V. (1984). "Lightcurves and phase relations of the asteroids 82 Alkeme and 444 Gypsis." *Icarus* **57**, 251-258.
- Harris, A.W.; Young, J.W.; Bowell, E.; Martin, L.J.; Millis, R.L.; Poutanen, M.; Scaltriti, F.; Zappala, V.; Schober, H.J.; Debehogne, H.; Zeigler, K.W. (1989). "Photoelectric Observations of Asteroids 3, 24, 60, 261, and 863." *Icarus* **77**, 171-186.
- Kaasalainen, M.; Torppa J. (2001). "Optimization Methods for Asteroid Lightcurve Inversion. I. Shape Determination." *Icarus* **153**, 24-36.
- Kaasalainen, M.; Torppa J.; Muinonen, K. (2001). "Optimization Methods for Asteroid Lightcurve Inversion. II. The Complete Inverse Problem." *Icarus* **153**, 37-51.
- Kim, M.; Choi, Y.; Moon, H.; Byun, Y.; Brosch, N.; Kaplan, M.; Kaynar, S.; Uysal, Ö.; Güzel, E.; Behrend, R.; Yoon, J.-N.; Mottola, S.; Hellmich, S.; Hinse, T.; Eker, Z.; Park, J. (2014). "Rotational Properties of the Maria Asteroid Family." *Ap. J.* **147**, A15.
- Kryszczyńska, A.; Colas, F.; Polińska, M.; Hirsch, R.; Ivanova, V.; Apostolovska, G.; Bilkina, B.; Velichko, F.P.; Kwiatkowski, T.; Kankiewicz, P.; Vachier, F.; Umlenski, V.; Michałowski, T.; Marciniak, A.; Maury, A.; Kamiński, K.; Fagas, M.; Dimitrov, W.; Borezyk, W.; Sobkowiak, K. (2012). "Do Slivan states exist in the Flora family? I. Photometric survey of the Flora region." *Astron. Astrophys.* **546**, A72.
- Oszkiewicz, D.A.; Skiff, B.A.; Moskovitz, N.; Kankiewicz, P.; Marciniak, A.; Licandro, J.; Galiazzo, M.A.; Zeilinger, W.W. (2017). "Non-Vestoid candidate asteroids in the inner main belt." *Astron. Astrophys.* **599**, A107.
- Pál, A.; Szakáts, R.; Kiss, C.; Bódi, A.; Bognár, Z.; Kalup, C.; Kiss, L.L.; Marton, G.; Molnár, L.; Plachy, E.; Sárneczky, K.; Szabó, G.M.; Szabó, R. (2020). "Solar System Objects Observed with TESS - First Data Release: Bright Main-belt and Trojan Asteroids from the Southern Survey." *Ap. J.* **247**, A26.
- Pilcher, F. (2010). "Rotation Period Determinations for 81 Terpsichore, 419 Aurelia 452 Hamiltonia, 610 Valeska, 649 Josefa, and 652 Jubilatrix." *Minor Planet Bull.* **37**, 45-46.
- Sada, P.V. (2008). "CCD Photometry of Six Asteroids from the Universidad de Monterrey Observatory." *Minor Planet Bull.* **35** 105-107.
- Stephens, R.D. (2016). "Asteroids Observed from CS3: 2015 July - September." *Minor Planet Bull.* **43**, 52-56.
- Stephens, R.D. (2017). "Asteroids Observed from CS3: 2017 January - March." *Minor Planet Bull.* **44**, 257-258.
- Stephens, R.D. (2018). "Asteroids Observed from CS3: 2017 July - September." *Minor Planet Bull.* **45**, 50-54.
- Stephens, R.D.; Warner, B.D. (2019a). "Main-belt Asteroids Observed from CS3: 2018 October - December." *Minor Planet Bull.* **46**, 180-187.
- Stephens, R.D.; Warner, B.D. (2019b). "Main-Belt Asteroids Observed from CS3: 2019 January - March." *Minor Planet Bull.* **46**, 298-301.
- Tonry, J.L.; Denneau, L.; Flewelling, H.; Heinze, A.N.; Onken, C.A.; Smartt, S.J.; Stalder, B.; Weiland, H.J.; Wolf, C. (2018). "The ATLAS All-Sky Stellar Reference Catalog." *Ap. J.* **867**, A105.
- Warner, B.D. (2011). "Lightcurve Analysis at the Palmer Divide Observatory: 2010 June-September." *Minor Planet Bull.* **38**, 25-31.
- Warner, B.D. (2014). "Asteroid Lightcurve Analysis at CS3-Palmer Divide Station: 2014 January-March." *Minor Planet Bull.* **41**, 144-155.
- Warner, B.D. (2015). "Asteroid Lightcurve Analysis at CS3-Palmer Divide Station: 2015 March-June." *Minor Planet Bull.* **42**, 267-276.
- Warner, B.D. (2016). "Asteroid Lightcurve Analysis at CS3-Palmer Divide Station: 2015 June-September." *Minor Planet Bull.* **43**, 57-65.
- Warner, B.D. (2017). "Asteroid Lightcurve Analysis at CS3-Palmer Divide Station: 2016 December thru 2017 March." *Minor Planet Bull.* **44**, 213-219.
- Warner, B.D.; Harris, A.W.; Pravec, P. (2009). "The Asteroid Lightcurve Database." *Icarus* **202**, 134-146. Updated 2020 June. <http://www.minorplanet.info/lightcurvedatabase.html>
- Waszczak, A.; Chang, C.-K.; Ofek, E.O.; Laher, R.; Masci, F.; Levitan, D.; Surace, J.; Cheng, Y.-C.; Ip, W.-H.; Kinoshita, D.; Helou, G.; Prince, T.A.; Kulkarni, S. (2015). "Asteroid Light Curves from the Palomar Transient Factory Survey: Rotation Periods and Phase Functions from Sparse Photometry." *Astron. J.* **150**, A75.

**LIGHTCURVE ANALYSIS OF L5 TROJAN ASTEROIDS  
AT THE CENTER FOR SOLAR SYSTEM STUDIES:  
2020 APRIL TO JUNE**

Robert D. Stephens

Center for Solar System Studies (CS3) / MoreData!  
11355 Mount Johnson Ct., Rancho Cucamonga, CA 91737 USA  
rstephens@foxandstephens.com

Brian D. Warner

Center for Solar System Studies (CS3) / MoreData!  
Eaton, CO

(Received: 2020 July 13)

Lightcurves for nine L5 Jovian Trojan asteroids were obtained at the Center for Solar System Studies (CS3) from 2020 April to June.

CCD Photometric observations of nine Trojan asteroids from the L<sub>5</sub> (Trojan) Lagrange point were obtained at the Center for Solar System Studies (CS3, MPC U81). For several years, CS3 has been conducting a study of Jovian Trojan asteroids. This is another in a series of papers reporting data analysis being accumulated for family pole and shape model studies. It is anticipated that for most Jovian Trojans, two to five dense lightcurves per target at oppositions well distributed in ecliptic longitudes will be needed and can be supplemented with reliable sparse data for the brighter Trojan asteroids. For six of these targets we were able to get preliminary pole positions and create shape models from sparse data and the dense lightcurves obtained to date. These preliminary models will be improved as more data are acquired at future oppositions and will be published at a later date.

Table I lists the telescopes and CCD cameras that were used to make the observations. Images were unbinned with no filter and had master flats and darks applied. The exposures depended upon various factors including magnitude of the target, sky motion, and Moon illumination.

Telescope	Camera
0.40-m f/10 Schmidt-Cass	FLI Proline 1001E
0.40-m f/10 Schmidt-Cass	Fli Microline 1001E
0.35-m f/10 Schmidt-Cass	Fli Microline 1001E

Table I. List of telescopes and CCD cameras used at CS3.

Image processing, measurement, and period analysis were done using *MPO Canopus* (Bdw Publishing), which incorporates the Fourier analysis algorithm (FALC) developed by Harris (Harris et al., 1989). The Comp Star Selector feature in *MPO Canopus* was used to limit the comparison stars to near solar color. Night-to-night calibration was done using field stars from the ATLAS catalog (Tonry et al., 2018), which has Sloan *griz* magnitudes that were derived from the GAIA and Pan-STARR catalogs and are the “native” magnitudes of the catalog.

To reduce the number of times and amount of resetting nightly zero points, we use the ATLAS *r'* (SR) magnitudes. Those adjustments are mostly  $\leq 0.03$  mag. The occasions where larger corrections were required may have been related in part to using unfiltered observations, poor centroiding of the reference stars, and not correcting for second-order extinction terms.

Unless otherwise indicated, the Y-axis of lightcurves are ATLAS SR “sky” (catalog) magnitudes. During period analysis, the magnitudes were normalized to the phase angle given in parentheses using  $G = 0.15$ . The X-axis rotational phase ranges from  $-0.05$  to  $1.05$ .

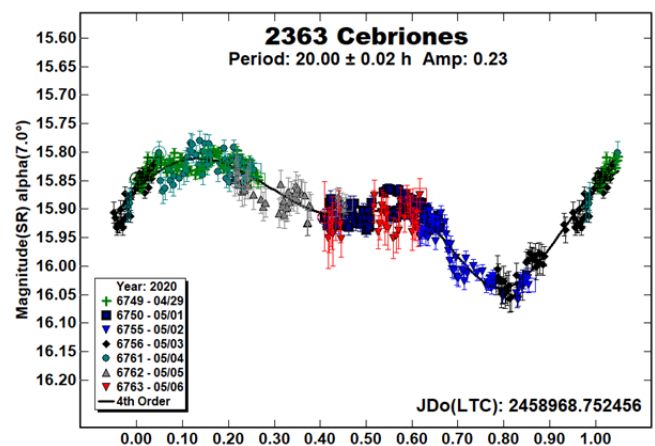
The amplitude indicated in the plots (e.g. Amp. 0.23) is the amplitude of the Fourier model curve and not necessarily the adopted amplitude of the lightcurve.

Targets were selected for this L<sub>5</sub> observing campaign were mostly based upon the availability of dense lightcurves acquired in previous years. We obtained two to four lightcurves for most of these Trojans at previous oppositions.

For brevity, only some of the previously reported rotational periods may be referenced. A complete list is available at the asteroid lightcurve database (LCDB; Warner et al., 2009).

To evaluate the quality of the data obtained and to determine how much more data might be needed, preliminary pole and shape models were created for all of these targets. Sparse data observations were obtained from the Catalina Sky Survey and USNO-Flagstaff survey using the AstDyS-2 site (2020). These sparse data were combined with our dense data as well as any other dense data found in the Asteroid Lightcurve Data Exchange Format database (ALCDEF, 2020) using *MPO LCInvert*, (Bdw Publishing). This Windows-based program incorporates the algorithms developed by Kaasalainen and Torppa (2001a) and Kaasalainen et al. (2001b) and converted by Josef Durech from the original FORTRAN to C. A period search was made over a sufficiently wide range to assure finding a global minimum in  $\chi^2$  values.

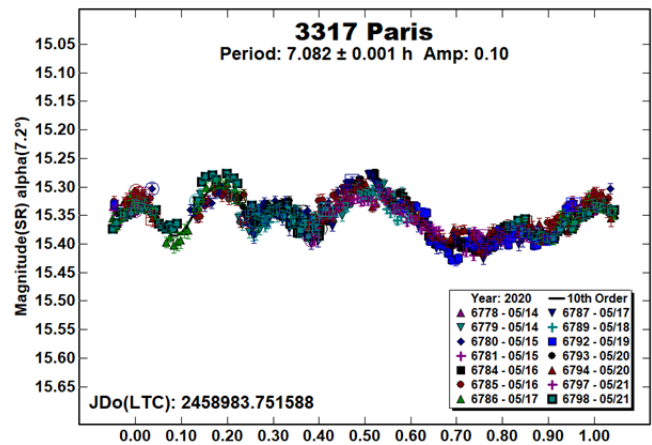
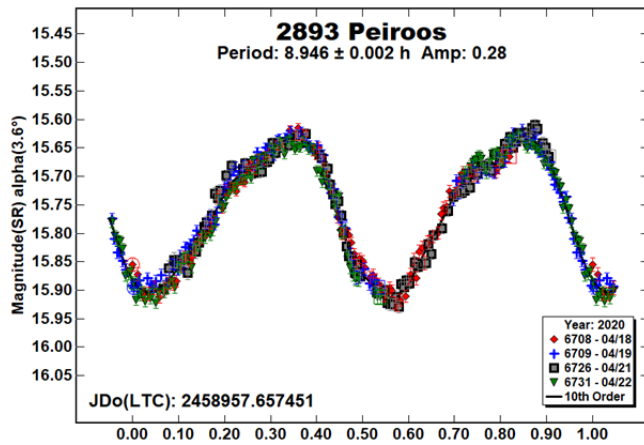
**2363 Cebiriones.** Reliable rotational rates for this Trojan were obtained four times in the past (Galad and Kornos, 2008; Mottola et al., 2011; Skiff et al., 2019; Stephens and Warner 2019b), each time finding a period near 20.1 h. The 2020 results are in good agreement. Using sparse data from the AstDys-2 (2020) and ALCDEF (2020) sites, a preliminary shape model with a sidereal rotational period of  $20.118791 \pm 0.00001$  h was created.



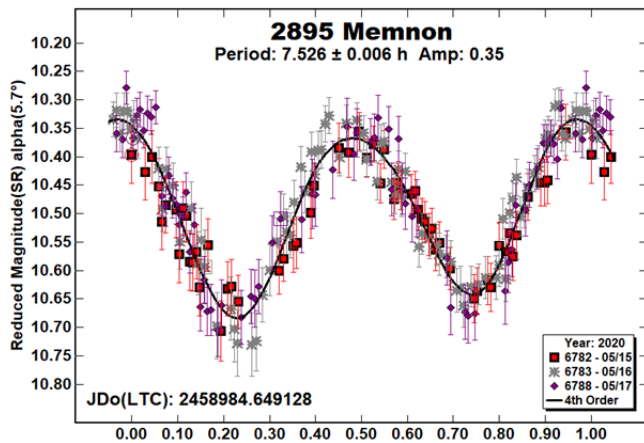
**2893 Peiroos.** We observed Peiroos four times in the past. Lightcurves were obtained in 2015, 2016, 2017 and 2019 (Stephens and Warner, 2019a and references therein). The data collected this year, when combined with our previous data and available sparse data, were used to create a preliminary shape model with a sidereal rotational period of  $8.94893 \pm 0.00001$  h.

Number	Name	2020 mm/dd	Phase	L <sub>PAB</sub>	B <sub>PAB</sub>	Period(h)	P.E.	Amp	A.E.
2363	Cebriones	04/29-05/06	7.1, 6.2	247	21	20.00	0.02	0.23	0.03
2893	Peiroos	04/18-04/22	3.6, 3.6	211	16	8.946	0.002	0.28	0.02
2895	Memnon	05/15-05/17	5.7, 5.6	237	29	7.526	0.006	0.35	0.03
3317	Paris	05/14-05/21	7.2, 7.6	222	31	7.082	0.001	0.10	0.01
3451	Mentor	04/23-04/28	8.2, 7.6	247	25	7.695	0.002	0.11	0.01
5144	Achates	04/12-04/18	4.9, 5.9	178	-6	5.959	0.001	0.21	0.02
5476	1989 TO11	05/01-05/04	2.2, 1.9	227	7	5.759	0.003	0.31	0.03
12444	Prothoon	05/22-06/10	6.1, 9.1	213	2	15.676	0.004	0.33	0.03
12929	1999 TZ1	04/19-04/29	7.6, 6.8	236	30	9.272	0.004	0.15	0.03
		2019/05/26-06/02	7.3, 8.3	208	11	9.27	0.01	0.08	0.02

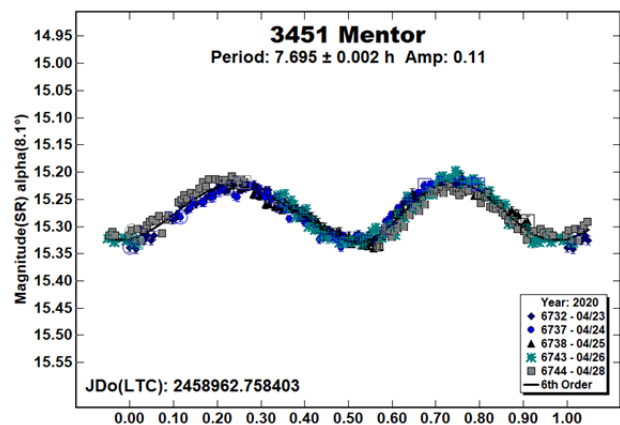
Table II. Observing circumstances and results. The phase angle is given for the first and last date. L<sub>PAB</sub> and B<sub>PAB</sub> are the approximate phase angle bisector longitude/latitude at mid-date range (see Harris et al., 1984).



2895 Memnon. The synodic period we found this year agrees with previous synodic results (Binzel and Sauter, 1992; Mottola et al., 2011; French et al., 2011; Stephens et al., 2015, 2016; Stephens and Coley, 2017; Stephens and Warner, 2018). These data were combined with available sparse data to find a preliminary shape model with a sidereal rotational period of  $7.519252 \pm 0.00001$  h.

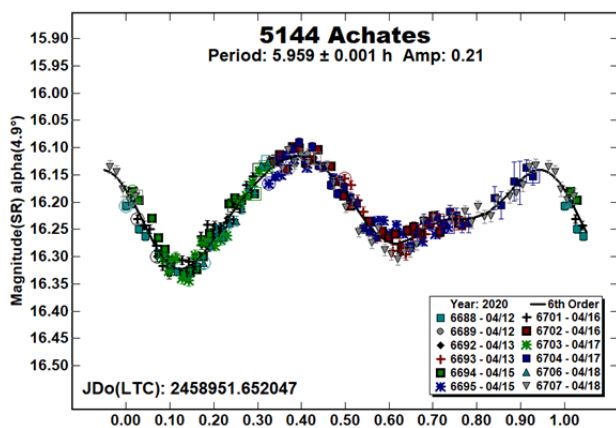


3451 Mentor. We observed this Trojan four times in the past (Stephens and Coley, 2017 and references therein), each time finding a period near 7.69 h. The 2020 data resulted in a bimodal lightcurve with a period that in good agreement with those prior results. We were able to create a preliminary shape model with a sidereal rotational period of  $7.6966367 \pm 0.000001$  h and an ecliptic longitude/latitude of  $84^\circ/10^\circ$ . In the Database of Asteroid Models from Inversion Techniques (DAMIT, 2020) website, Durech reports an ecliptic longitude/latitude of  $81^\circ/18^\circ$ , close to our preliminary model.

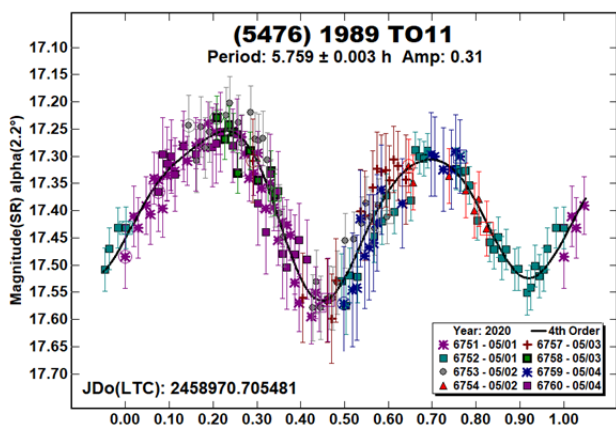


3317 Paris. The synodic period found in 2020 agrees with previous synodic results (Mottola et al., 2011; Stephens and Warner, 2019a and references therein). All of these previous periods were near 7.08 h. The results in 2020 are in good agreement and, when combined with our previous data and available sparse data, were used to create a preliminary shape model with a sidereal rotational period of  $7.08100 \pm 0.00001$  h.

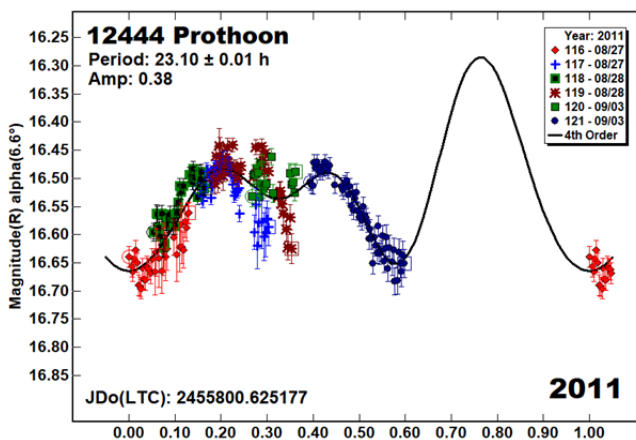
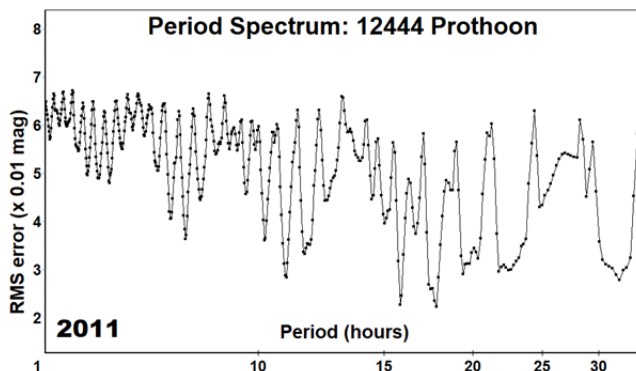
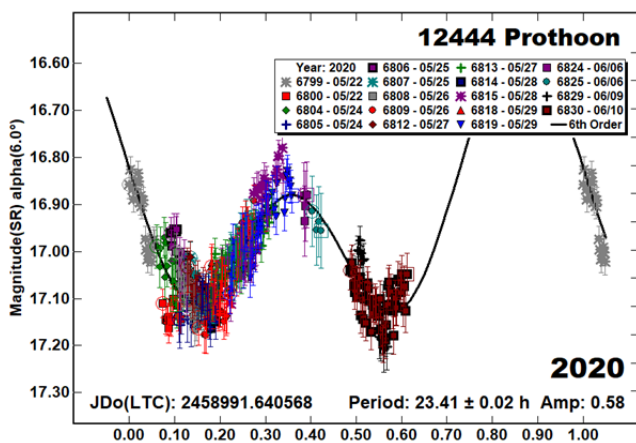
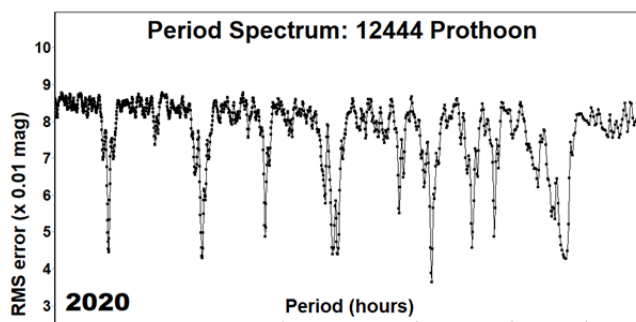
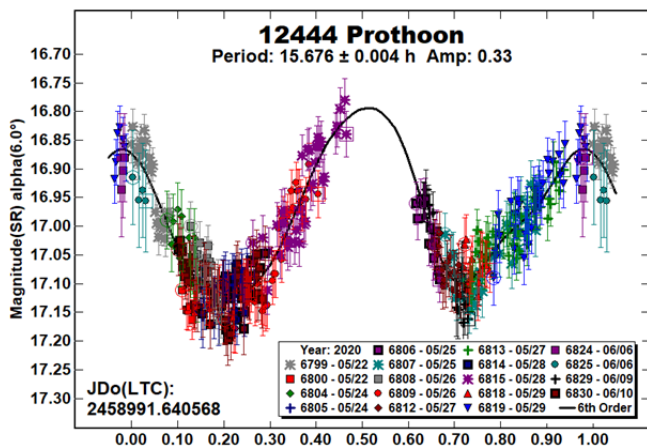
5144 Achates. This Trojan was observed five times in the past (Molnar et al., 2008; Mottola et al., 2011; Stephens et al., 2015; Stephens and Warner, 2018, 2019a), each time finding a period near 5.95 h. The 2019 results are in good agreement and were used to create a preliminary shape model with a sidereal rotational period of  $5.95392 \pm 0.00001$  h.



(5476) 1989 TO11. Only one prior rotational period is reported in the lightcurve database (LCDB; Warner et al., 2009). Mottola et al. (2011) reported a rotational period of 5.780 h from observations obtained in 1994. Our result this year of 5.759 h has a denser dataset over four consecutive nights and is in good agreement.



12444 Prothoon. From our data in 2011 (French et al., 2012) we reported a rotational period of 15.82 h. The data we collected in 2020 were a reasonable fit to that rotational period. Using data from the Transiting Exoplanet Survey Satellite (TESS), Pál et al. (2020) found a rotational period of 23.10 h, a 2:3 alias of our period. The period spectrums for both the 2011 and 2019 data show periods near 23 h. The 2011 lightcurve rephased to approximately 23 h has a bad fit and the 2020 rephased lightcurve has an unlikely shape with the extrema being only 0.3 phase apart.

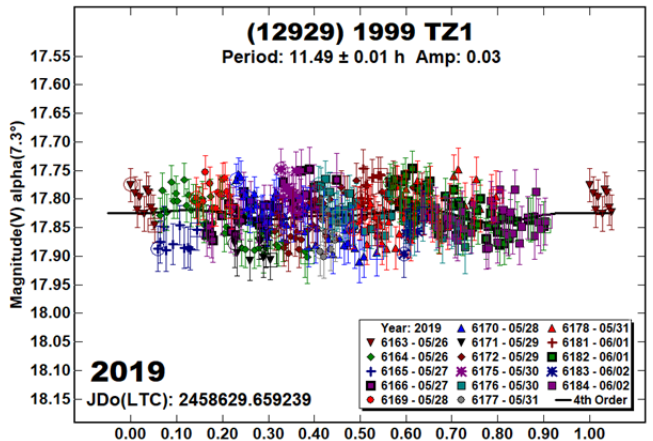
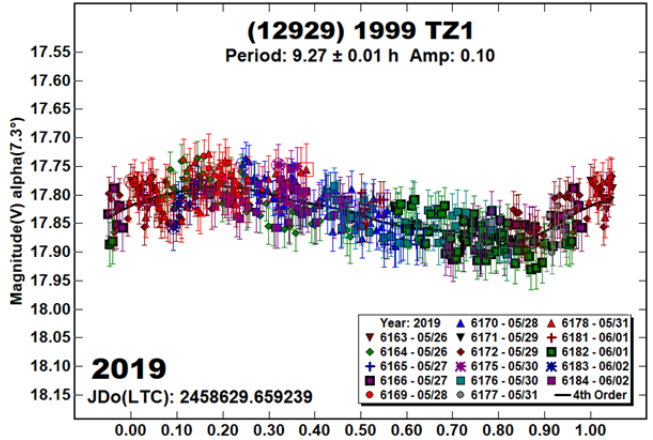
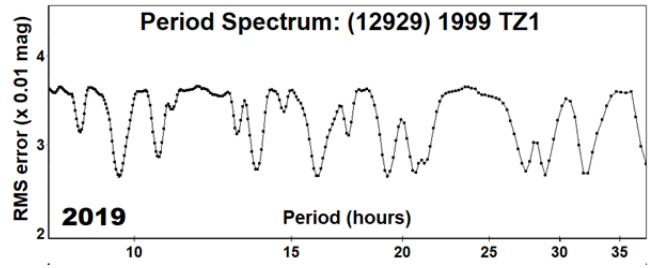
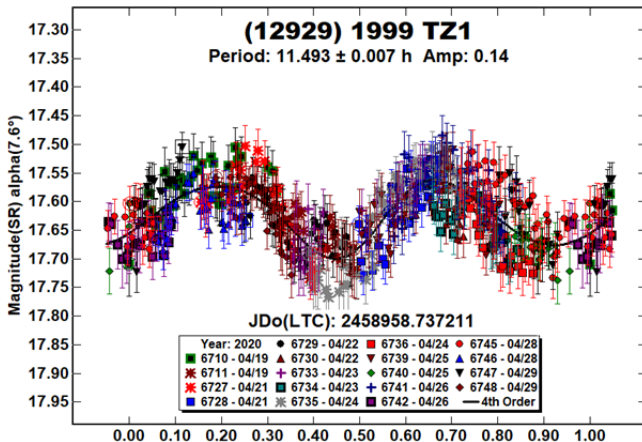
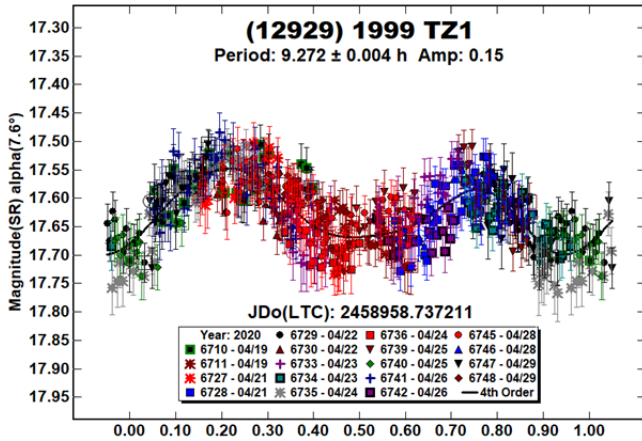
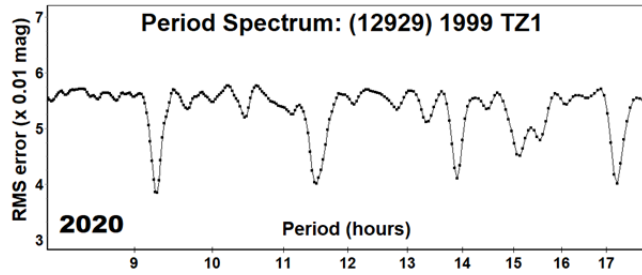


(12929) 1999 TZ1. This L<sub>5</sub> Jovian Trojan has been observed several times in the past. Moullet et al. (2008) observed it in 2007 reporting a rotational period of 10.4 h from sparse data over 12 nights. The resulting lightcurve was a poor fit. Over seven nights in 2009, Mottola et al. (2011) used sparse data and found a rotational period of 9.2749 h with a single extremum. Thirouin et

al. (2010) used sparse data over six nights in 2007 to find two ambiguous periods, a bimodal 5.211 h period and a 10.422 h period with four extrema. Both lightcurves show scatter equal to the 0.07 mag. amplitude. Our period of 13.73 h from our 2019 data (Stephens and Warner, 2019b) is based on a much denser dataset but still had an ambiguous solution.

The period spectrum for our 2020 data shows possible solutions near 9.3 h, 11.5 h, and 13.8 h. Those latter periods being 4:5 and 2:3 aliases of the 9.3 h period. Phasing the 2020 data to a 13.8 h period resulted in a noisy and improbable three extrema lightcurve. Phasing the 2020 data to either 9.27 h or 11.49 h resulted in bimodal lightcurves, with the 9.27 h solution being slightly asymmetric. To break the tie, we rephased the 2019 data to both the 9.27 h and 11.49 h periods. The 9.27 h 2019 period resulted in a single modal lightcurve. No reasonable period could be found near 11.5 h for the 2019 data.

Our preferred solution, and the one adopted for this paper, is 9.272 h for the 2020 data and 9.27 h for the 2019 data. Both are in good agreement with the Mottola result which had a 0.17 mag amplitude, per the LCDB, the highest reported for any opposition.



Acknowledgements

Observations at CS3 and continued support of the asteroid lightcurve database (LCDB; Warner et al., 2009) are supported by NASA grant 80NSSC18K0851. This work includes data from the Asteroid Terrestrial-impact Last Alert System (ATLAS) project. ATLAS is primarily funded to search for near earth asteroids through NASA grants NN12AR55G, 80NSSC18K0284, and 80NSSC18K1575; byproducts of the NEO search include images and catalogs from the survey area. The ATLAS science products have been made possible through the contributions of the University of Hawaii Institute for Astronomy, the Queen's University Belfast, the Space Telescope Science Institute, and the South African Astronomical Observatory. The purchase of a FLI-1001E CCD camera was made possible by a 2013 Gene Shoemaker NEO Grants from the Planetary Society.

## References

- AstDys-2 (2020). Asteroids – Dynamic web site.  
<https://newton.spacedys.com/astdys/>
- ALCDEF (2020). Asteroid Lightcurve Data Exchange Format database. <http://www.alcdef.org/>
- DAMIT (2020). Database of Asteroid Models from Inversion Techniques (DAMIT).  
<https://astro.troja.mff.cuni.cz/projects/damit/>
- Binzel, R.P.; Sauter, L.M. (1992). “Trojan, Hilda, and Cybele asteroids - New lightcurve observations and analysis.” *Icarus* **95**, 222-238.
- French, L.M.; Stephens, R.D.; Lederer, S.M.; Coley, D.R.; Rhol, D.A. (2011). “Preliminary Results from a Study of Trojan Asteroids.” *Minor Planet Bull.* **38**, 183-187.
- French, L.M.; Stephens, R.D.; Coley, D.R.; Megna, R.; Wasserman, L.H. (2012). “Photometry of 17 Jovian Trojan Asteroids.” *Minor Planet Bull.* **39**, 116-120.
- Galad, A.; Kornos, L. (2008). “A Collection of Lightcurves from Modra: 2007 December - 2008 June.” *Minor Planet Bull.* **35**, 114-146.
- Harris, A.W.; Young, J.W.; Scaltriti, F.; Zappala, V. (1984). “Lightcurves and phase relations of the asteroids 82 Alkmene and 444 Gytis.” *Icarus* **57**, 251-258.
- Harris, A.W.; Young, J.W.; Bowell, E.; Martin, L.J.; Millis, R.L.; Poutanen, M.; Scaltriti, F.; Zappala, V.; Schober, H.J.; Debehogne, H.; Zeigler, K.W. (1989). “Photoelectric Observations of Asteroids 3, 24, 60, 261, and 863.” *Icarus* **77**, 171-186.
- Kaasalainen, M.; Torppa, J. (2001a). “Optimization Methods for Asteroid Lightcurve Inversion. I. Shape Determination.” *Icarus* **153**, 24-36.
- Kaasalainen, M.; Torppa, J.; Muinonen, K. (2001b). “Optimization Methods for Asteroid Lightcurve Inversion. II. The Complete Inverse Problem.” *Icarus* **153**, 37-51.
- Molnar, L.A.; Jaegert, M.J.; Hoogetboom, K.M. (2008). “Lightcurve Analysis of an Unbiased Sample of Trojan Asteroids.” *Minor Planet Bull.* **35**, 82-84.
- Mottola, S.; Di Martino, M.; Erikson, A.; Gonano-Beurer, M.; Carbognani, A.; Carsenty, U.; Hahn, G.; Schober, H.; Lahulla, F.; Delbò, M.; Lagerkvist, C. (2011). “Rotational Properties of Jupiter Trojans. I. Light Curves of 80 Objects.” *Astron. J.* **141**, A170.
- Moulet, A.; Lellouch, E.; Doressoundiram, A.; Ortiz, J.L.; Duffard, R.; Morbidelli, A.; Vernazza, P.; Moreno, R. (2008). “Physical and dynamical properties of (12929) 1999 TZ1 suggest that it is a Trojan.” *Astron. and Astrophys.* **483**, L17-L20.
- Pál, A.; Szakáts, R.; Kiss, C.; Bódi, A.; Bognár, Z.; Kalup, C.; Kiss, L.; Marton, G.; Molnár, L.; Plachy, E.; Sárneczky, K.; Szabó, G.; Szabó, R. (2020). “Solar System Objects Observed with TESS - First Data Release: Bright Main-belt and Trojan Asteroids from the Southern Survey.” *Astron. J.* **247**, id 26.
- Skiff, B.A.; McLelland, K.P.; Sanborn, J.J.; Pravec, P.; Koehn, B.W. (2019). “Lowell Observatory Near-Earth Asteroid Photometric Survey (NEAPS): Paper 3.” *Minor Planet Bull.* **46**, 238-265.
- Stephens, R.D.; Coley, D.R.; French, L.M. (2015). “Dispatches from the Trojan Camp - Jovian Trojan L5 Asteroids Observed from CS3: 2014 October - 2015 January.” *Minor Planet Bull.* **42**, 216-224.
- Stephens, R.D.; Coley, D.R.; French, L.M. (2016). “A Report from the L5 Trojan Camp - Lightcurves of Jovian Trojan Asteroids from the Center for Solar System Studies.” *Minor Planet Bull.* **43**, 265-270.
- Stephens, R.D.; Coley, D.R. (2017). “Lightcurve Analysis of Trojan Asteroids at the Center for Solar System Studies 2017 January - March.” *Minor Planet Bull.* **44**, 252-257.
- Stephens, R.D.; Warner, B.D. (2018). “Lightcurve Analysis of L5 Trojan Asteroids at the Center for Solar System Studies 2018 April to May.” *Minor Planet Bull.* **45**, 343-347.
- Stephens, R.D.; Warner, B.D. (2019a). “Lightcurve Analysis of L5 Trojan Asteroids at the Center for Solar System Studies: 2019 January to March.” *Minor Planet Bull.* **46**, 315-317.
- Stephens, R.D.; Warner, B.D. (2019b). “Lightcurve Analysis of L5 Trojan Asteroids at the Center for Solar System Studies: 2019 April to June.” *Minor Planet Bull.* **46**, 389-392.
- Thirouin, A.; Ortiz, J.L.; Duffard, R.; Santos-Sanz, P.; Aceituno, F.J.; Morales, N. (2010). “Short-term variability of a sample of 29 trans-Neptunian objects and Centaurs.” *Astron. and Astrophys.* **522**, A93.
- Tonry, J.L.; Denneau, L.; Flewelling, H.; Heinze, A.N.; Onken, C.A.; Smartt, S.J.; Stalder, B.; Weiland, H.J.; Wolf, C. (2018). “The ATLAS All-Sky Stellar Reference Catalog.” *Astrophys. J.* **867**, A105.
- Warner, B.D.; Harris, A.W.; Pravec, P. (2009). “The Asteroid Lightcurve Database.” *Icarus* **202**, 134-146. Updated 2020 June.  
<http://www.minorplanet.info/lightcurvedatabase.html>

**NEAR-EARTH ASTEROID LIGHTCURVE ANALYSIS  
AT THE CENTER FOR SOLAR SYSTEM STUDIES:  
2020 APRIL - JUNE**

Brian D. Warner  
Center for Solar System Studies / MoreData!  
446 Sycamore Ave.  
Eaton, CO 80615 USA  
brian@MinorPlanetObserver.com

Robert D. Stephens  
Center for Solar System Studies / MoreData!  
Rancho Cucamonga, CA 91730

(Received: 2020 July 13)

Lightcurves for 29 near-Earth asteroids (NEAs) obtained at the Center for Solar System Studies (CS3) from 2020 April to June were analyzed for rotation period, peak-to-peak amplitude, and signs of satellites or tumbling.

CCD photometric observations of 29 near-Earth asteroids (NEAs) were made at the Center for Solar System Studies (CS3) from 2020 April to June. Table I lists the telescopes and CCD cameras that are combined to make observations.

Up to nine telescopes can be used for the campaign, although seven is more common. All the cameras use CCD chips from the KAF blue-enhanced family and so have essentially the same response. The pixel scales ranged from 1.24-1.60 arcsec/pixel.

Telescopes	Cameras
0.30-m f/6.3 Schmidt-Cass	FLI Microline 1001E
0.35-m f/9.1 Schmidt-Cass	FLI Proline 1001E
0.40-m f/10 Schmidt-Cass	SBIG STL-1001E
0.40-m f/10 Schmidt-Cass	
0.50-m f/8.1 Ritchey-Chrétien	

Table I. List of available telescopes and CCD cameras at CS3. The exact combination for each telescope/camera pair can vary due to maintenance or specific needs.

All lightcurve observations were unfiltered since a clear filter can cause a 0.1-0.3 mag loss. The exposure duration varied depending on the asteroid's brightness and sky motion. Guiding on a field star sometimes resulted in a trailed image for the asteroid.

Measurements were made using *MPO Canopus*. The Comp Star Selector utility in *MPO Canopus* found up to five comparison stars of near solar-color for differential photometry. Comp star magnitudes were taken from ATLAS catalog (Tonry et al., 2018), which has Sloan *griz* magnitudes that were derived from the GAIA and Pan-STARR catalogs, among others, and are the "native" magnitudes of the catalog.

To reduce the number of times and amount of resetting nightly zero points, we use the ATLAS *r'* (SR) magnitudes. Those adjustments are mostly  $\leq 0.03$  mag. The occasions where larger corrections were required may have been related in part to using unfiltered observations, poor centroiding of the reference stars, and not correcting for second-order extinction terms.

Unless otherwise indicated, the Y-axis of lightcurves is ATLAS SR "sky" (catalog) magnitudes. During period analysis, the magnitudes were normalized to the comparison stars used in the earliest session and to the phase angle given in parentheses using

$G = 0.15$ , unless another value is given. The X-axis shows rotational phase from  $-0.05$  to  $1.05$ . If the plot includes the amplitude, e.g., "Amp: 0.65", this is the amplitude of the Fourier model curve and *not necessarily the adopted amplitude for the lightcurve*.

Our initial search for previous results started with the asteroid lightcurve database (LCDB; Warner et al., 2009) found on-line at <http://www.minorplanet.info/lightcurvedatabase.html>. Readers are strongly encouraged to obtain, when possible, the original references listed in the LCDB. From here on, we'll use only "LCDB" to reference the paper by Warner et al. (2009).

**1685 Toro**. The estimated size of this well-studied NEA is about 4 km. Higgins (2008) reported a period of 10.1995 h based on observations in 2007. His amplitude of 0.47 mag at  $L_{PAB} = 251^\circ$  and phase angle  $\alpha = 5.8^\circ$  is the smallest reported to-date in the LCDB. The largest amplitude to-date, 1.80 mag, was found by Warner (2013a) in 2012 August with  $L_{PAB} = 29^\circ$  and  $\alpha = 96.5^\circ$ . A direct comparison of the two amplitudes at different  $L_{PAB}$  values is complicated because the phase angles are significantly different.

Zappala et al. (1990) developed Eq. 1 to determine the amplitude at  $0^\circ$  phase angle based on the amplitude at a given angle ( $\alpha$ ).

$$A(0^\circ) = A(\alpha)/(1 + m\alpha) \quad (\text{Eq. 1})$$

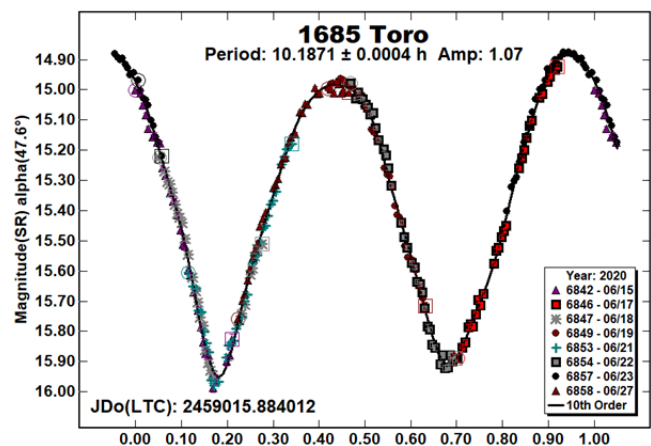
where  $m$  is a coefficient depending on approximate taxonomic class. Binzel et al. (2019) determined Toro to be a type Sq and so the Zappala et al. value of  $m = 0.030$  was used in Eq. 1 to compare the resulting  $A(0^\circ)$  values.

$$A(0^\circ) = A(5.8^\circ)/(1 + 0.030*5.8) = 0.40 \text{ mag}$$

$$A(0^\circ) = A(96.5^\circ)/(1 + 0.030*96.5) = 0.46 \text{ mag}$$

Given the uncertainties in the value for  $m$  and the amplitudes, the two results are in good agreement.

The 2020 observations at CS3 led to a period of 10.1871 h and amplitude 1.07 mag at  $\alpha = 49.5^\circ$  ( $A(0^\circ) = 0.43$  mag). These data were combined with our dense data sets from past apparitions (ALCDEF, 2020) and sparse data from the Catalina Sky Survey (CSS; 2020) downloaded from the AstDys (2020) web site to try to model the spin axis and shape. We used *MPO LCInvert* to implement the lightcurve inversion methods developed by the late Mikko Kaasalainen (Kaasalainen and Torpa, 2001; Kaasalainen et al., 2001). The results are shown in Fig 1-5 in the callout box below.



# SPIN/SHAPE MODEL FOR 1685 TORO

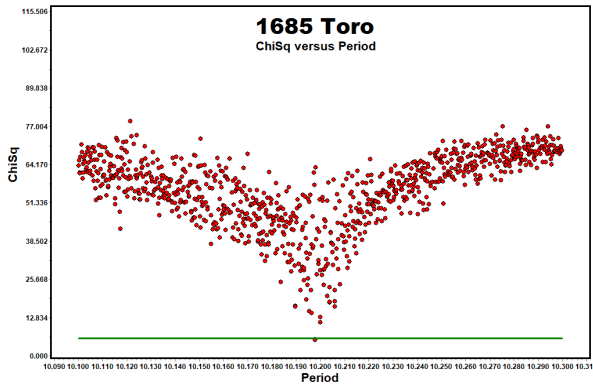


Figure 1. The initial period search results.

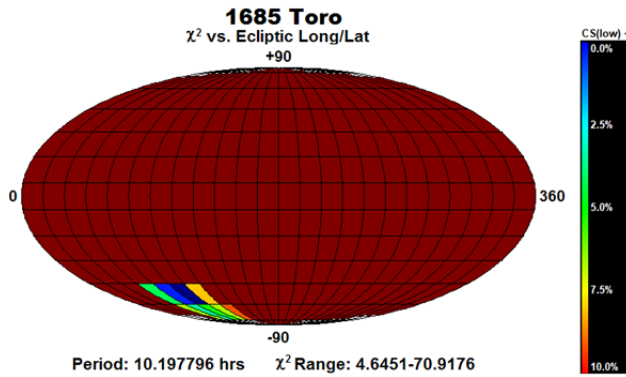


Figure 2. The pole search found two probable solutions.

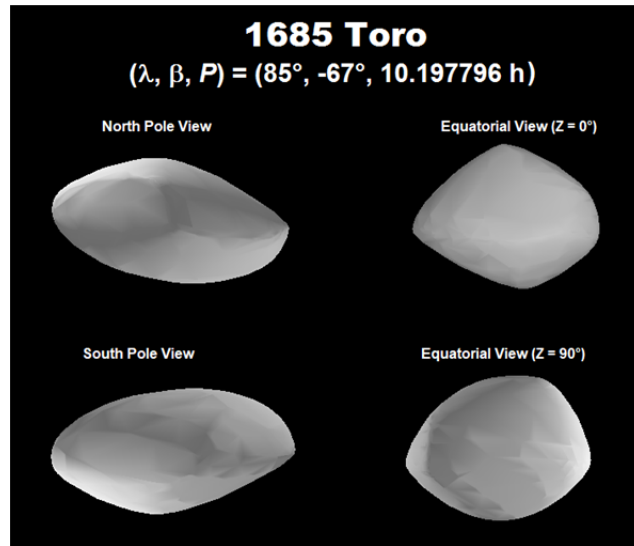


Figure 3. The shape of the asteroid based on the preferred pole solution.

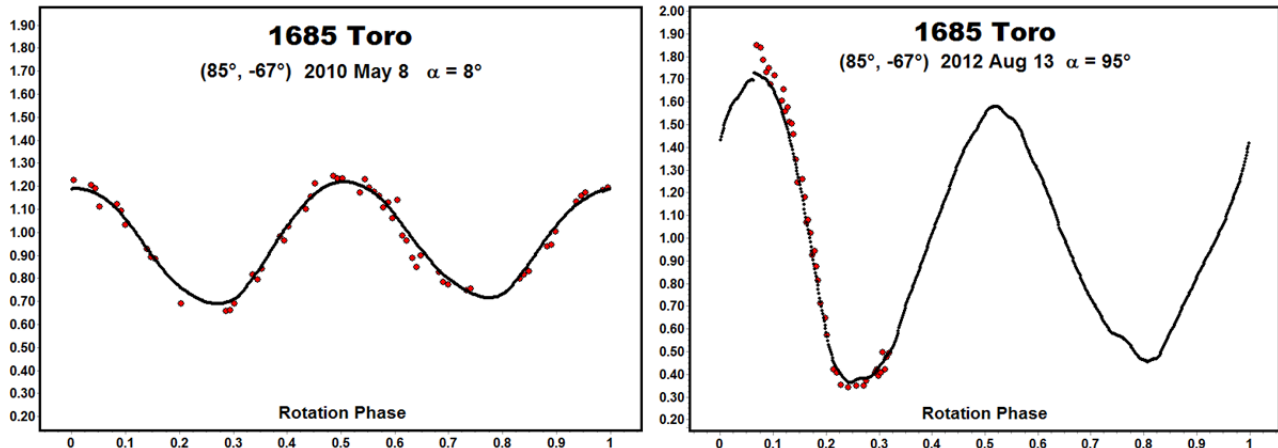


Figure 4/5. The comparison plots are against the adopted pole solution. The red dots indicate the data used for modeling while the black line is the smoothed lightcurve for generated by the shape at the time of the observations. The match is very close in 2010 but not quite so much for 2012. The fit to the 2020 data is also not ideal. Even so, when taking into account the possibility of the YORP effect changing the spin rate of the asteroid, the overall model is good.

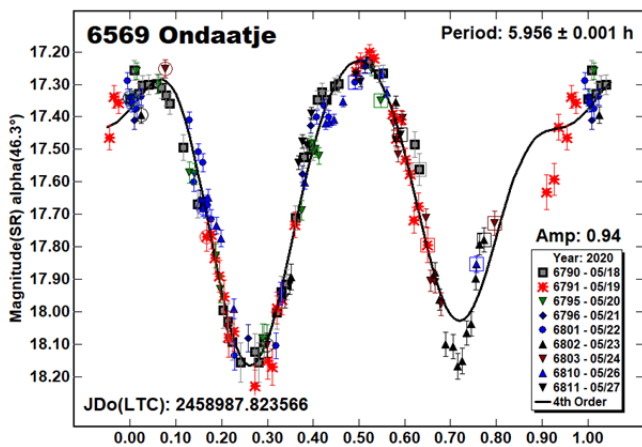
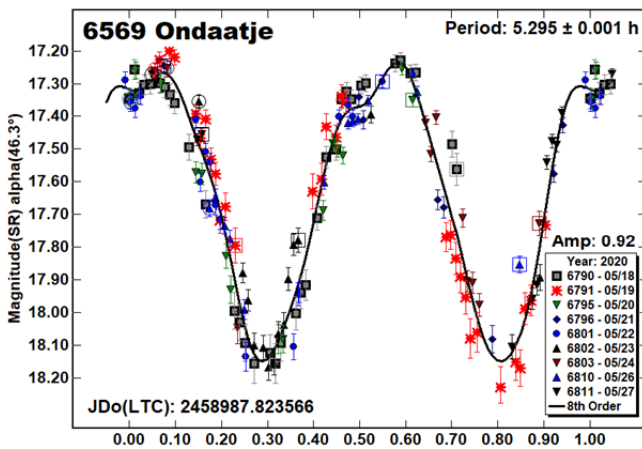
The green line in Fig. 1 represents a value that is 10% greater than the smallest  $\chi^2$  value. With only the one point below the line, the fixed period solution (see below) seemed secure, as was the pole search, which found a single solution near

$(\lambda, \beta) = (75^\circ, -60^\circ)$ . The refined search led to a final solution of  $(\lambda, \beta, P) = (85^\circ, -67^\circ, 10.197796 \text{ h})$ . This is in good agreement with Āurech et al. (2018), who found  $(\lambda, \beta, P) = (71^\circ, -69^\circ, 10.19782 \text{ h, Epoch 1972 July 8.5})$ .

Noting the epoch is important when trying to determine if the YORP effect (Rubincam, 2000) is causing the asteroid's rotation rate to change over time. Based on data through 2017, they found an inconclusive result that the spin rate was decreasing (the period increasing) such that there would be a phase shift of about 22° over the 44 years covered by their data. When removing data from 1996, the difference between a fixed period solution and one influenced by YORP became almost negligible. It's hoped that these latest data can help lead to a more certain result.

6569 Ondaatje. Pravec et al. (1996) reported a period of 5.959 h. Waszczak et al. (2015) found a similar period of 5.916 h using sparse wide-field survey data. The 2020 data set from CS3 found a similar period, but only if using a looser-fitting Fourier solution (4<sup>th</sup> order). Given the large amplitude of 0.94 mag, a higher order Fourier solution (8<sup>th</sup> order) seemed more appropriate. It found a significantly different period of 5.295 h.

We have adopted the shorter period for this paper based on 1) the longer period solution has a significant gap in the lightcurve that hints at a *fit by exclusion*, which is where the Fourier analysis finds a local minimum by minimizing the number of overlapping data points, and 2) the data from May 19 do not have a good fit to the Fourier curve. The shorter period with the higher-order solution, however, has no noteworthy gaps in coverage and more accurately follows the deep minimums.

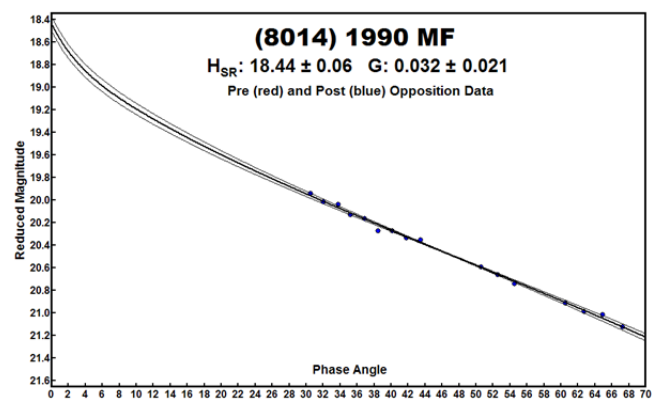
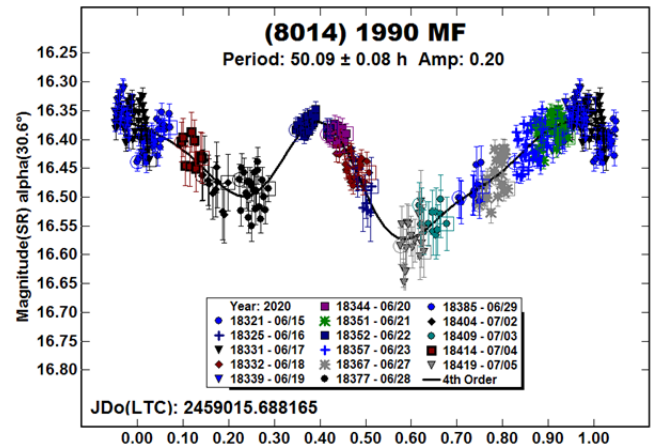


(8014) 1990 MF. There were no previous entries in the LCDB for this 500-meter NEA. The nightly runs were short in comparison to the derived period. The high-confidence in the nightly zero points using the ATLAS catalog (Tonry et al., 2018) was vital in this case. The H-G plot shows a good fit to the linear portion of the solution. When the Sloan  $r'$  (SR) magnitudes were converted to

approximate V magnitudes, the result was  $H = 18.62$ , which is close to the value of  $H = 18.7$  listed in the MPCOrb file from the Minor Planet Center (MPC; 2020).

Something to bear in mind is that the H-G system is not as well-defined at phase angles  $> \sim 50^\circ$  and so the low value for  $G$ , which would be indicative of a low albedo (dark) asteroid (Warner et al., 2009), is suspect. Also not taken into account is the well-known but often ignored phase reddening effect (Alan Harris, private communications), which causes an asteroid's color to be more red as the phase angle increases. If reddening had been taken into account, the value for  $G$  might be larger and so come closer to values typical of type S asteroids (Warner et al., 2009).

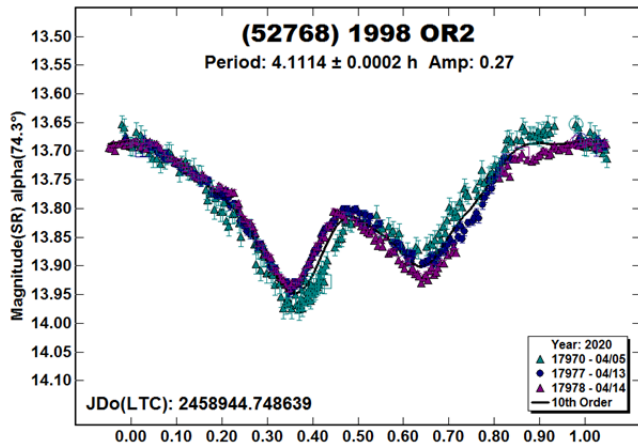
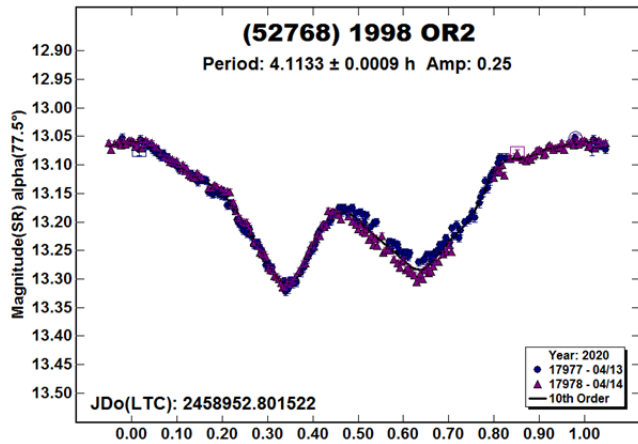
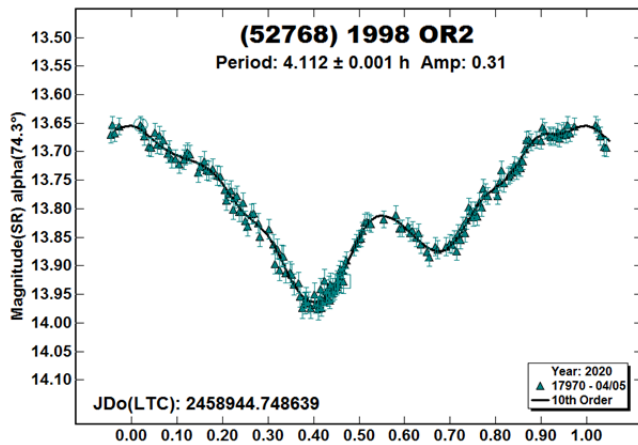
However, it is not automatic that type S asteroids have moderate albedos. The LCDB features at least seven asteroids where the measured taxonomic class is in the S-complex and the measured albedo is  $< 0.10$ , e.g., 542 Susanna ( $p_V = 0.0897$ , Tholen type S).



(52768) 1998 OR<sub>2</sub>. The estimated diameter of 1990 MF is about 2 km (Radar Team, 2020). Betzler and Novaes (2009) found a period of 3.198 h. A more likely solution of 4.112 h was reported by Koehn et al. (2014) based on observations made shortly before those by Betzler and Novaes.

Our 2020 data set showed a significant evolution of the lightcurve over just a few days. The plot for April 5 shows two “dips” with noticeably different depths and shapes. About a week later, the two were more equal in depth and the overall amplitude of the lightcurve was 0.06 mag smaller.

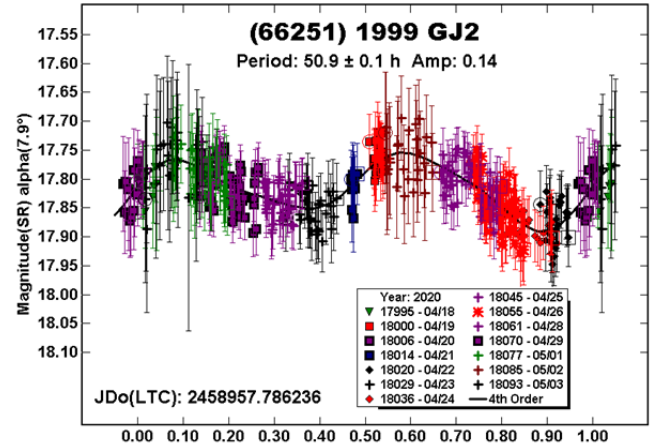
The differences are more dramatic when trying to find a period using the entire data set. Despite those differences, the combined set still allowed finding a refined synodic period of 4.1114 h.



(66251) 1999 GJ2. Pravec et al. (2005web) reported a period of 2.4621 h but their lightcurve is not available. Polishook (2012) reported a low-quality solution of 2.5 h. The 2020 data set from CS3 does not support a short period but, in fact, leads to a period of 50.9 h when setting all nightly zero points to 0.0, i.e., assuming that the ATLAS catalog magnitudes were good to 0.01-0.02 mag.

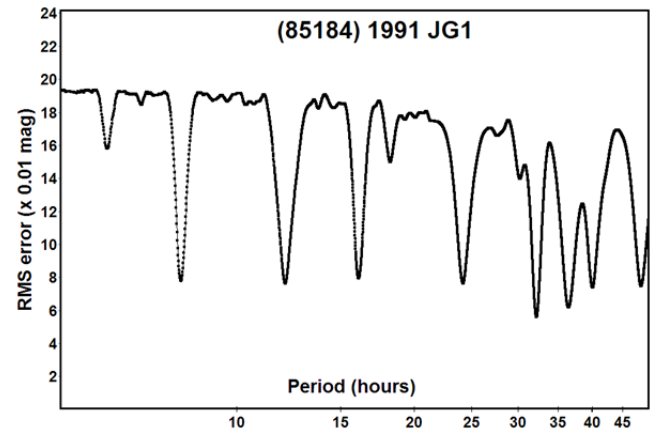
We tried forcing the solution to  $2 < P < 3$  h. The result was a noisy “flat line” with essentially no signal in the period spectrum. Our data are not the highest quality, which may taint the analysis to some degree, and it’s possible that the different viewing circumstances (Pravec et al.,  $L_{PAB} = 7^\circ$ ,  $\alpha = 40^\circ$ ; this work,  $L_{PAB} = 216^\circ$ ,  $\alpha = 6^\circ$ ) played a role as well.

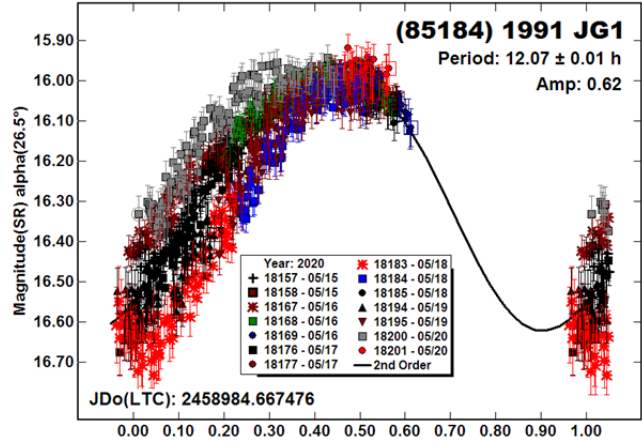
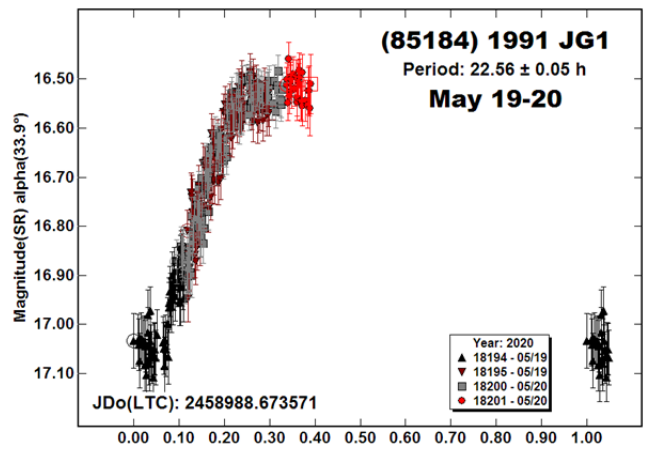
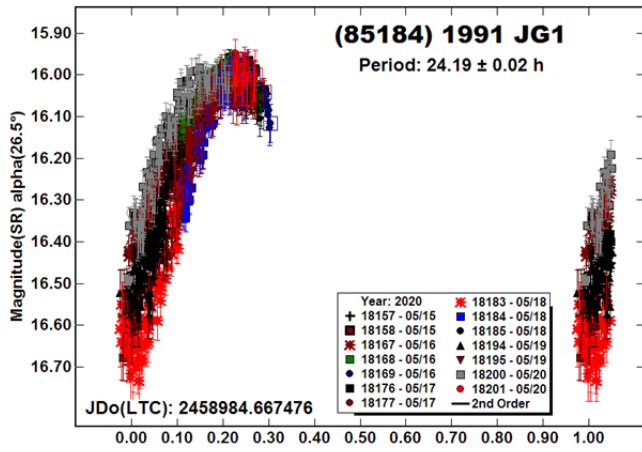
A good chance to solve the mystery comes in 2022 June ( $V \sim 17.1$ ,  $\delta \sim 8^\circ$ ) and in 2024 September ( $V \sim 15.2$ ,  $\delta \sim 13^\circ$ ).



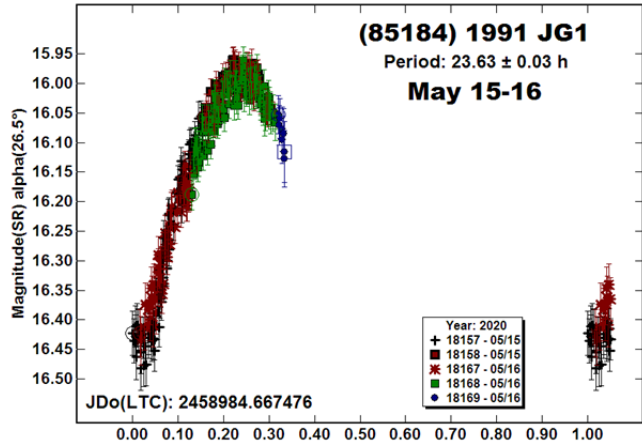
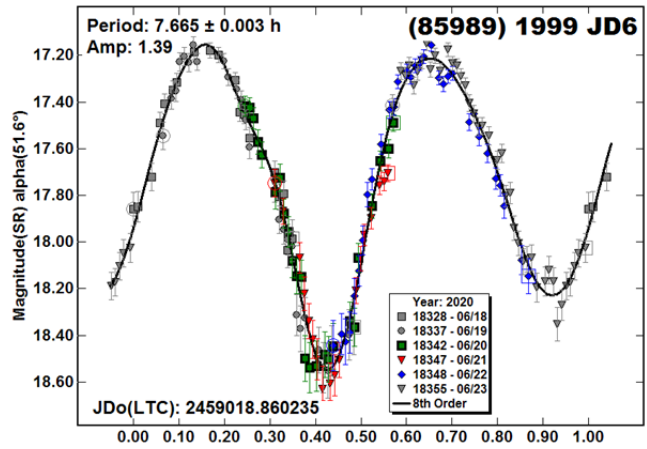
(85184) 1991 JG1. This NEA was well south of the equator in early 2020 May. By the time it was observable at CS3, it was fading and heading for high declinations. As the period spectrum shows, all the potential solutions were nearly commensurate with an Earth day, which made finding a solution nearly impossible from a single station.

Pravec et al. (2020web) reported a period of 24.02 h. This is close to what we found, with the solution changing slightly based on which subset of data that was used. Given the amplitude and not too extreme phase angle, a bimodal lightcurve was very likely (Harris et al., 2014) and so we adopted a period of 24.19 h for this work. This is based on using the entire dataset. The additional lightcurves show the apparent evolution of shape and amplitude during the apparition.

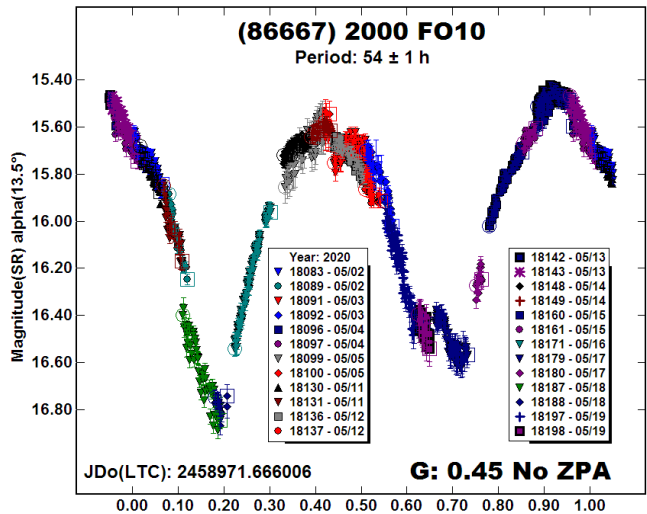
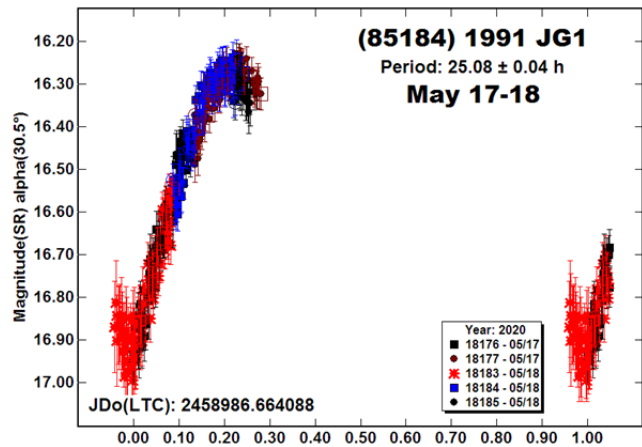


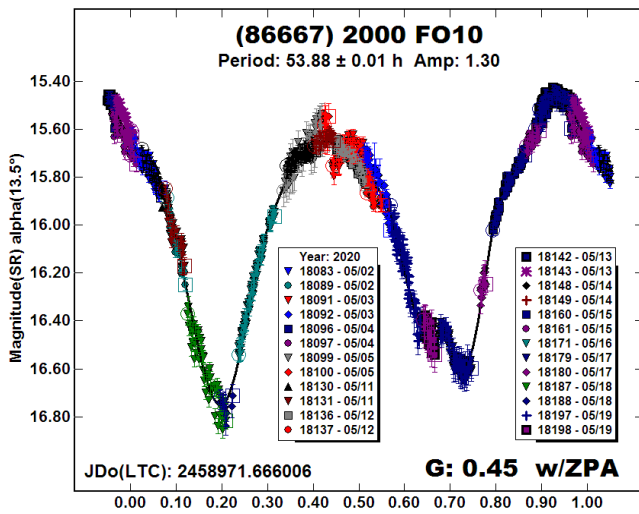


(85989) 1999 JD6. This 1.2 km NEA has been worked numerous times in the past, e.g., Pravec et al. (1999web; 7.666 h), Polishook and Brosch (2008; 7.6638 h), and Warner (2014; 7.667 h).

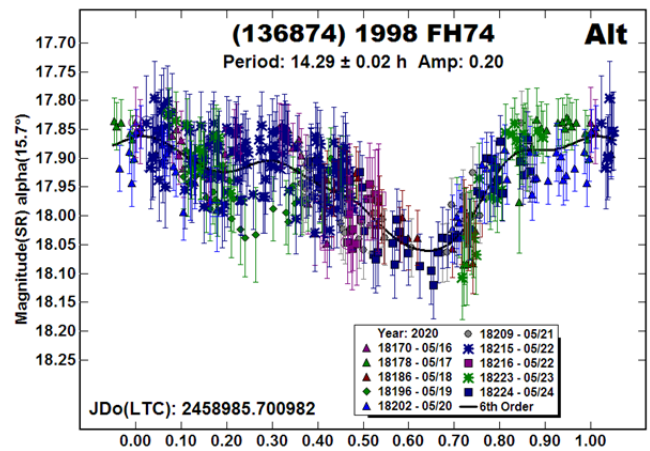
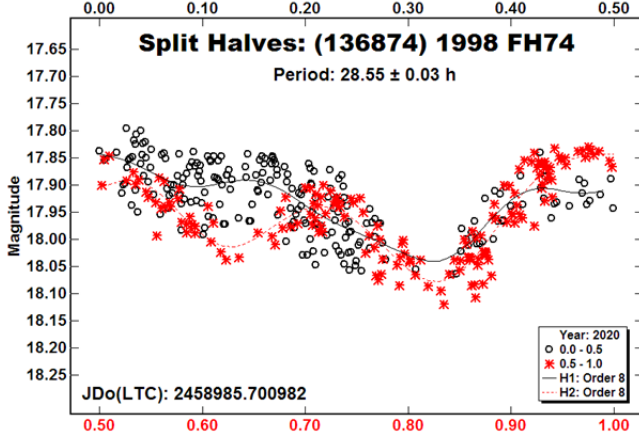
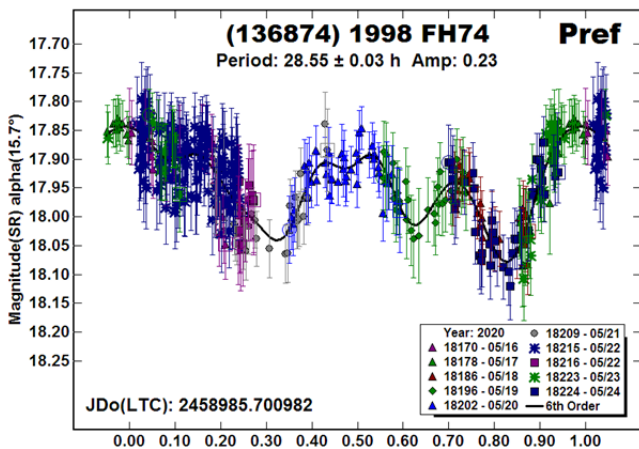


(86667) 2000 FO10. Polishook and Brosch (2008) found a low-quality solution of 26 h. Using  $G = 0.45$  gave a better fit to our data without having unusually large zero-point adjustments. With some minor adjustments (4 sessions at  $< |0.04|$  mag), the fit to the Fourier curve was even tighter.

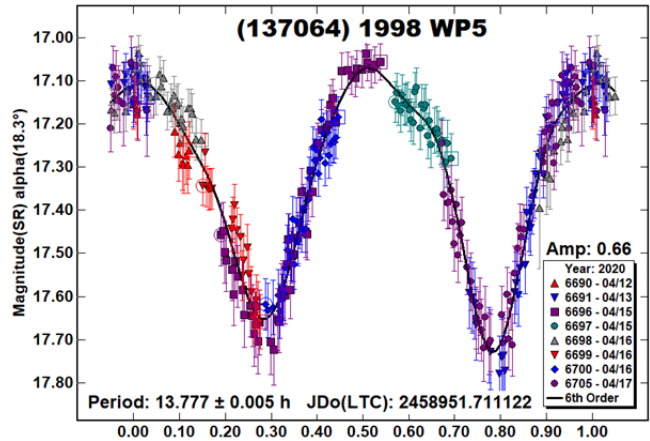




(136874) 1998 FH74. This appears to be the first reported lightcurve rotation period in the LCDB. The period spectrum shows two strong possibilities with the preferred solution being the longer one of 28.55 h. The split halves plot (see Harris et al., 2014) shows significant differences between the two halves, which helped exclude, but not quite formally, the half-period of 14.29 h.

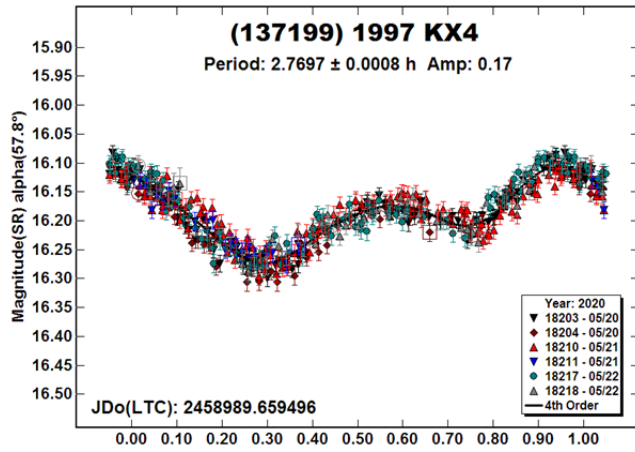


(137064) 1998 WP5. Pravec et al. (2020web) observed this 500-meter NEA about the same as we did, mid-April. There was enough difference in viewing aspects, however, to show the phase angle-amplitude relationship (Zappala et al., 1990). The phase angle for Pravec et al. was about 8.6° and amplitude 0.52 mag. Our observations were near 16° phase angle and, as expected, the amplitude was larger: 0.66 mag.



(137199) 1999 KX4. Our previous observations (Warner, 2013b) led to a period of 2.767 h, which is nearly the same as our result from the most recent observations. In contrast, data from 2019 December (Warner and Stephens, 2020) led to a period of 2.860 h, which is well outside the error bars for the two data sets.

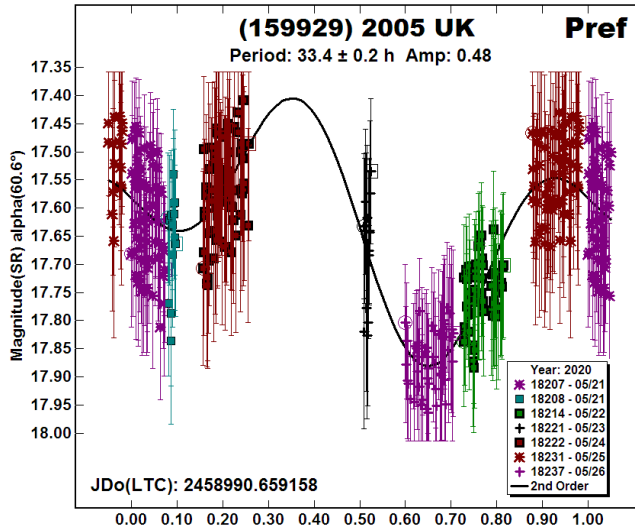
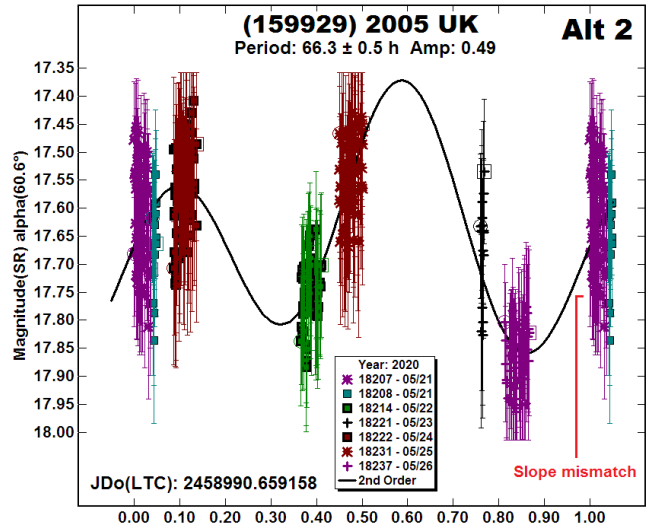
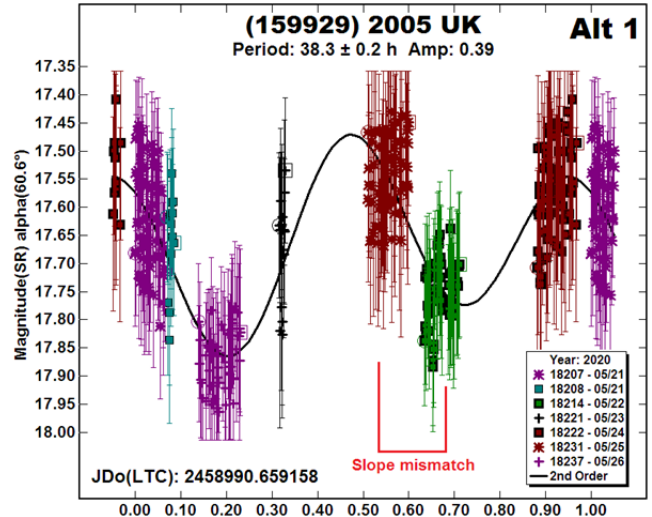
The significant difference may be due to the large change in phase angle bisector longitude ( $L_{PAB}$ ), which was 100° in 2019 December and 225° in 2020 May. In addition, the fact that the rotation period decreased as the asteroid moved away from opposition (and presumably increased as it moved towards opposition) is a likely indicator that the asteroid's spin axis rotation is retrograde.



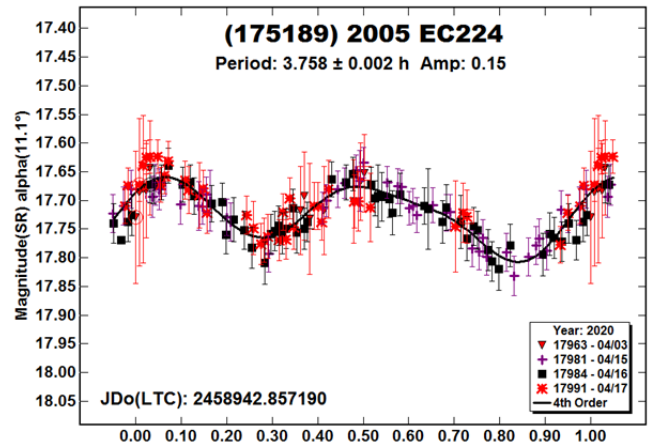
(159929) 2005 UK. There were no rotation periods previously listed in the LCDB. The period spectrum shows several possibilities, none of them overly convincing because of the low-quality data and poor coverage of the lightcurve at any of the potential periods.

We have adopted a period of 33.4 h based on the somewhat marginal evidence of how the slope of the data for each session compared to the slope of the Fourier model curve. Despite the odd shape of the lightcurve for 33.4 h, the data slopes match the Fourier slopes. The large phase angle and associated shadowing effects probably combined to make for the unusual shape.

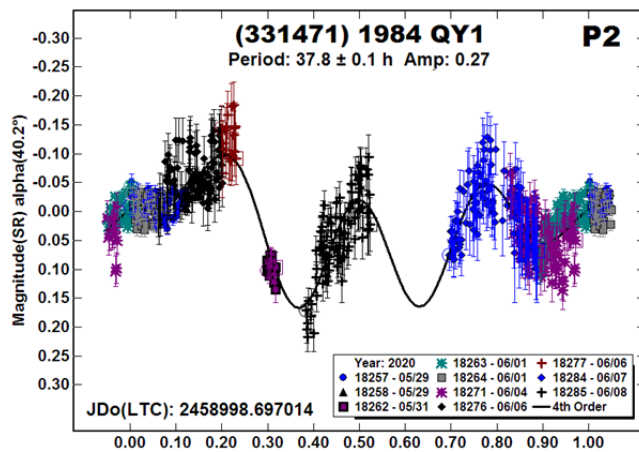
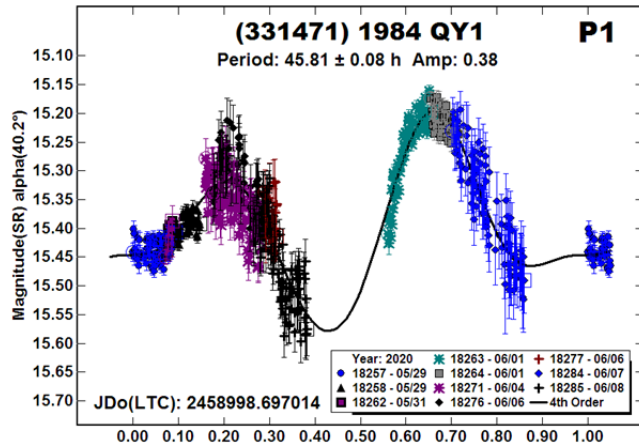
Looking at the  $P = 38.3$  h solution (“Alt1”), the slope of the two marked sessions appear to be positive while the slope of the Fourier curve at those points is negative. The opposite argument can be made for the 66-hour solution (“Alt2”). Here the evidence is much thinner and, since the lightcurve shape is more symmetrical, it’s about equally possible that the 66-hour double period might be the better choice for the preferred period. Looking ahead, the next time 2005 UK makes an appearance  $V < 19$  is 2033 May, when it passes only 0.13 au from Earth and reaches  $V \sim 13.5$  at  $\delta = -17^\circ$ .



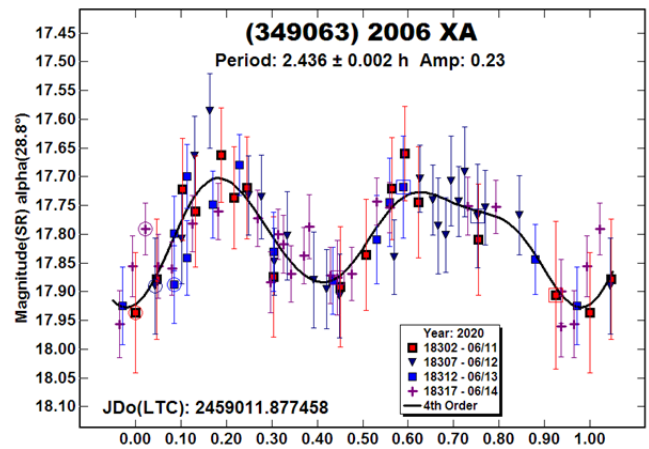
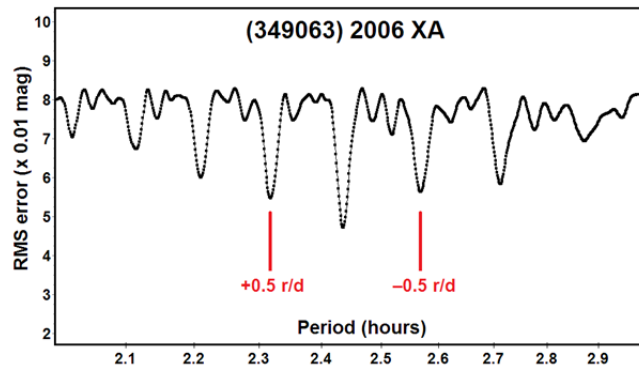
(175189) 2005 EC224. This was the first rotation period entry in the LCDB for this 650 m NEA. Fortunately, it was a relatively easy target and the solution is considered secure.



(331471) 1984 QY1. A general rule-of-thumb (Pravec et al., 2014; 2005) for the shorter of two damping times (from tumbling to non-tumbling) favors this asteroid to be in non-principal axis rotation (NPAR; tumbling). The fact that *MPO Canopus* found two dominant periods, neither one indicative of a satellite, adds credence to the argument for tumbling. *MPO Canopus* cannot directly analyze tumbling asteroids, so these two periods may or may not be the actual ones of rotation and precession, assuming the asteroid is tumbling.

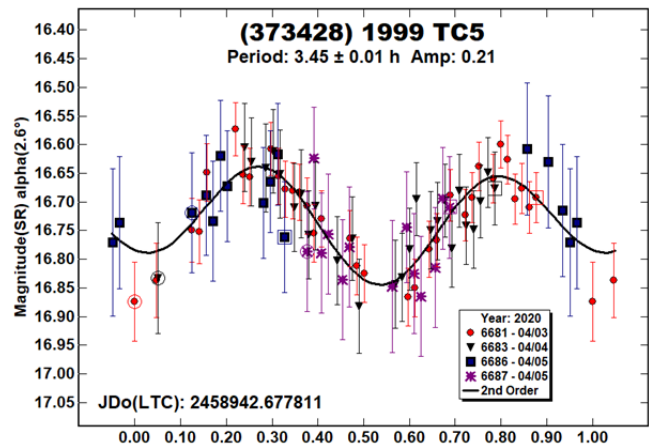
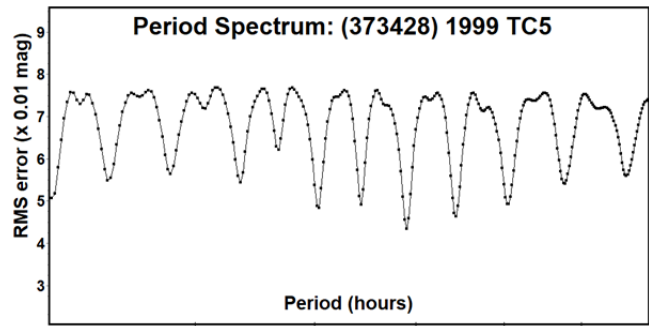


(349063) 2006 XA. The period  $P = 2.436$  h is mostly secure but two solutions that differ by one-half rotation over 24 hours cannot be formally excluded, especially since the three lightcurves differ minimally among one another. The preferred period is the result of the data better matching the slopes of the Fourier curve and placement against the two maximums.

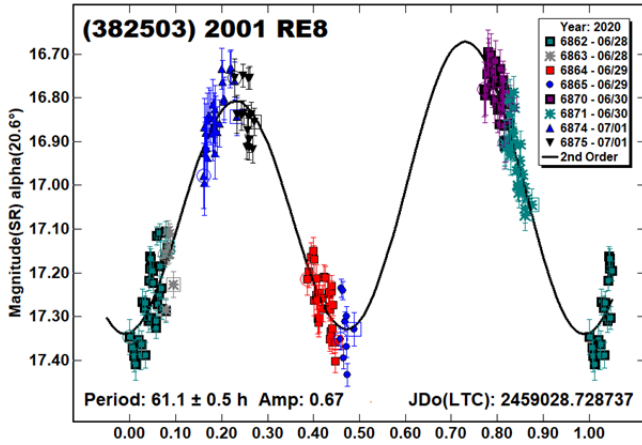


(373428) 1999 TC5. The situation for this 500-meter NEA is similar to 2006 XA above, i.e., while one period seems to be the likely choice others cannot be formally excluded. The period spectrum may not indicate it, but the adopted lightcurve has a noticeably better fit to the Fourier curve than those for nearby solutions.

Fortunately, there is corroborating evidence: Pravec et al. (2020web) found a period of 3.453 h based on observations at nearly the same time as ours.

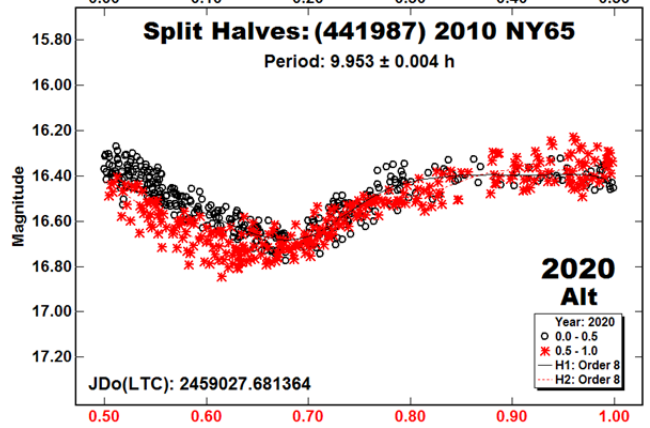
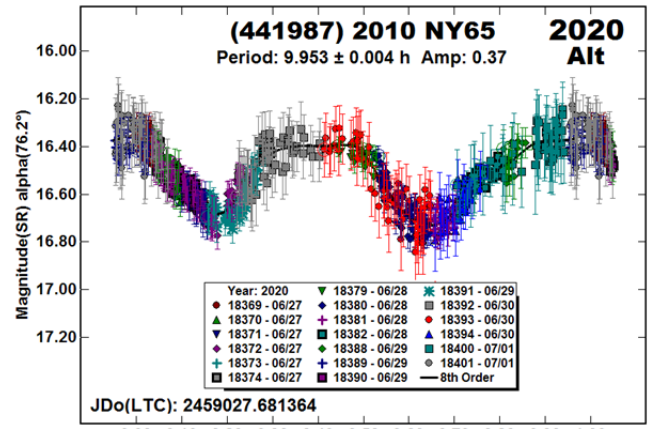
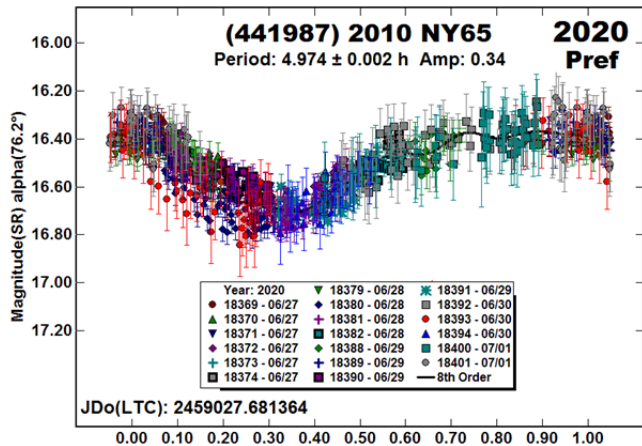
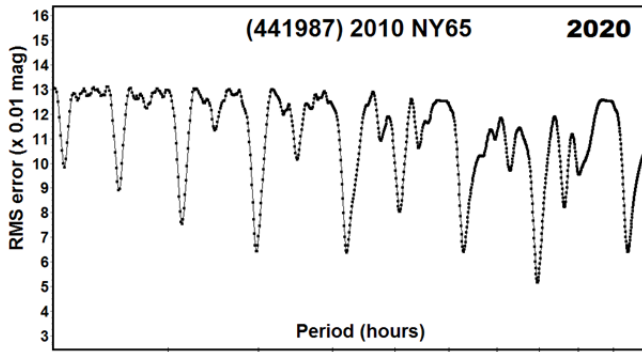


(382503) 2001 RE8. There were no previous entries in the LCDB for 2001 RE, which has an estimated diameter of 500 m. While the lightcurve has large gaps, reasonable coverage near the extrema, along with the large amplitude at a relatively low phase angle make the solution good enough for rotation statistical studies.



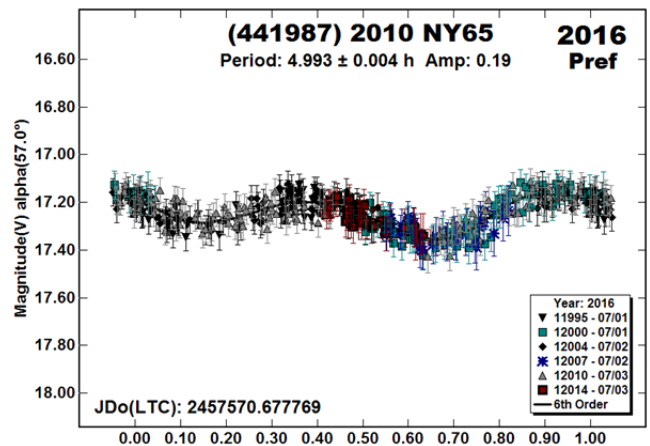
(441987) 2010 NY65. This NEA has been problematic for us over the years. The first observations (Warner 2016; 2017) found a period near 4.79 h. Data obtained in 2018 (Warner and Stephens, 2019) led to a period of 5.541 h, which is about one rotation less over 48 hours. The data from the earlier dates could be fit to a period near 5.55 h and so the 5.541 h period was adopted.

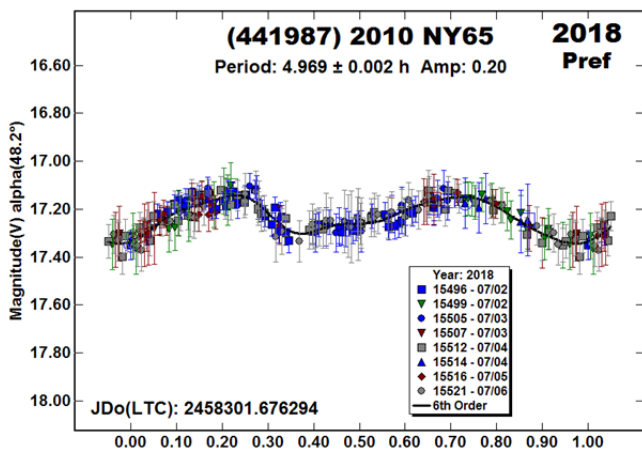
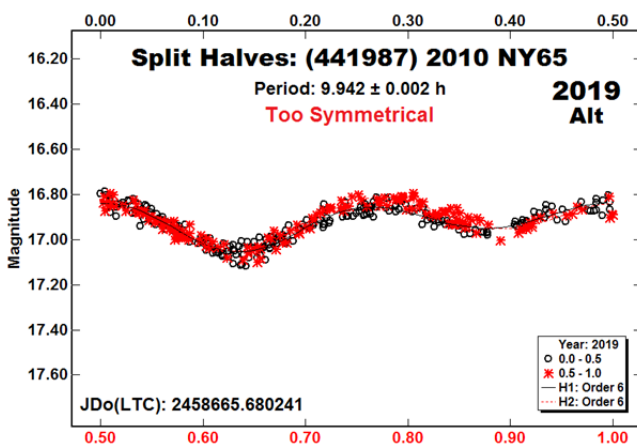
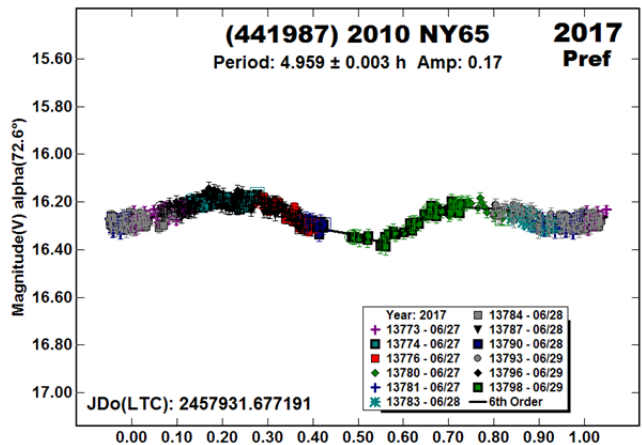
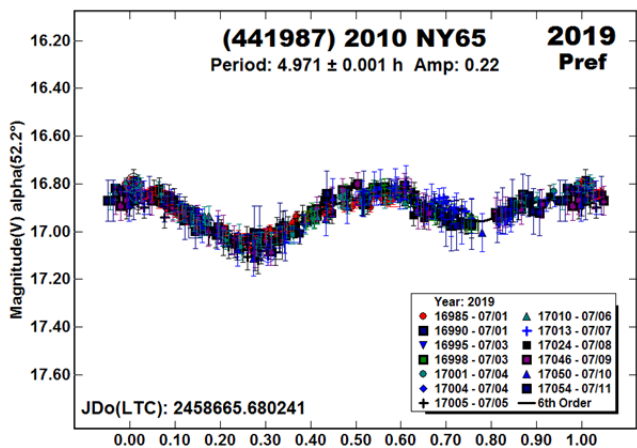
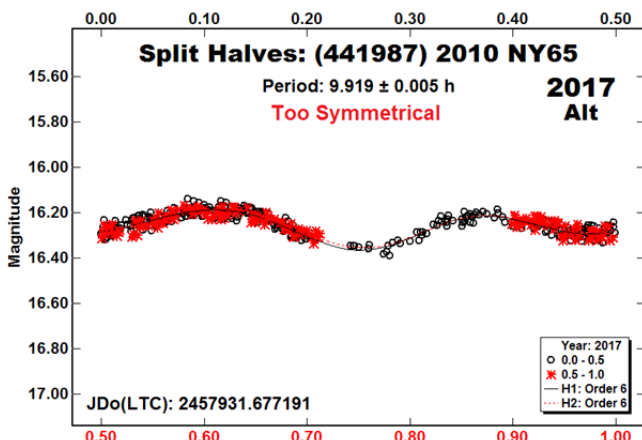
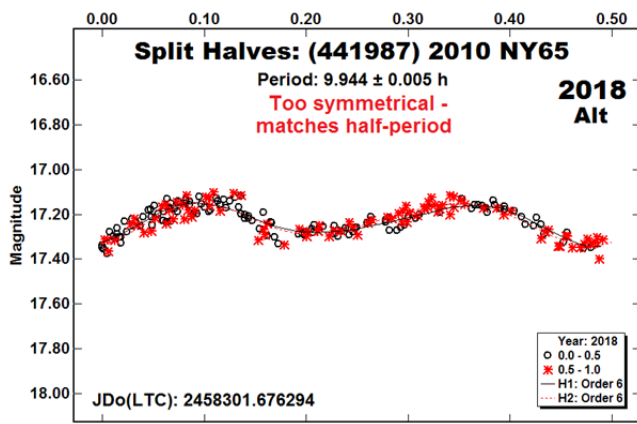
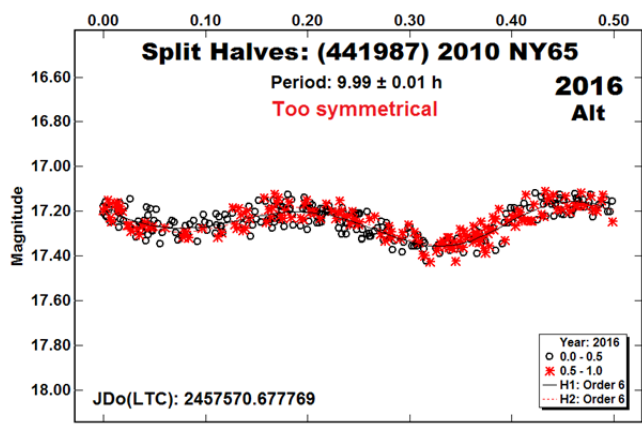
The period spectrum for our 2020 observations favors the 4.9-hour solution as an *alternate* solution, the dominant solution being 9.953 h. Once again, we redid the analysis on previous data sets.



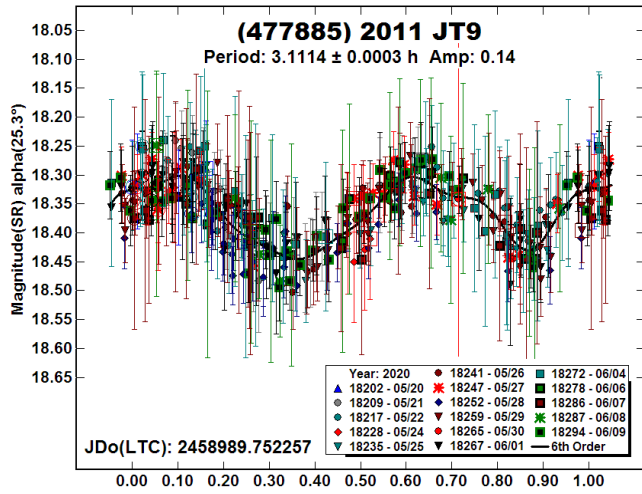
We have adopted a period of  $P = 4.794$  h for this work, which closely matches our original results because the previous data sets produce lightcurves forced to near 9.9 h that are too symmetrical about their two halves. This is an indication that the half period is possible and, in many cases, more likely.

The results of our re-analysis of the earlier data sets are shown below without comment.

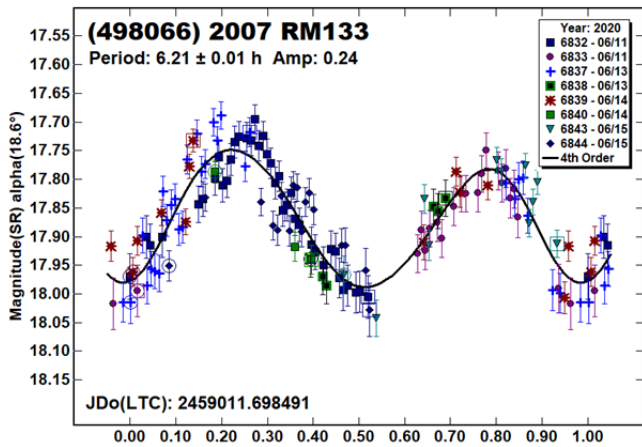
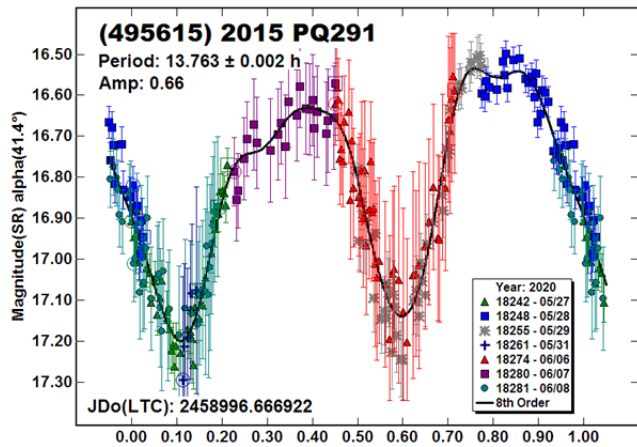




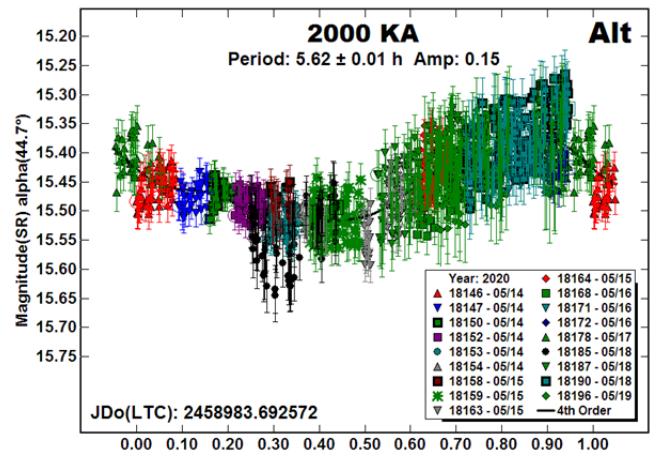
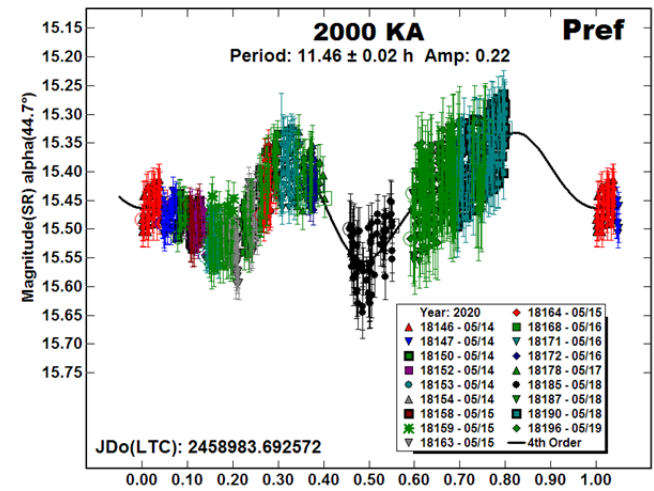
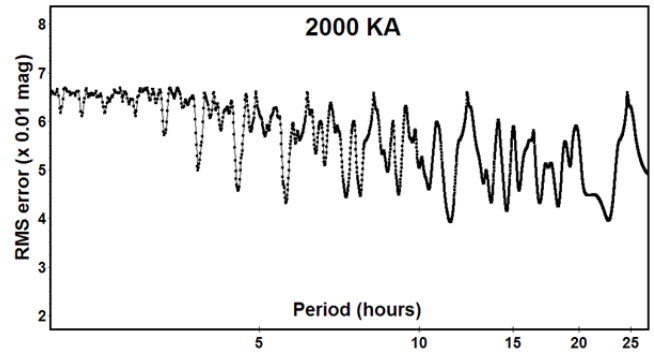
(477885) 2011 JT9. Pravec et al. (2020web) reported a period of 3.325 h based on observations towards the end of 2020 June. Our observations about a month earlier led to a slightly shorter period.



(495615) 2015 PQ291. (498066) 2007 RM133. There were no previous entries in the LCDB for these two NEAs. 2015 PQ29 has an estimated diameter of 850 m. 2007 RM133 has an effective diameter of about 700 m. Despite the gap in the lightcurve for 2007 RM133, the solution is reasonably but not completely secure given the amplitude and phase angle (Harris et al., 2014).

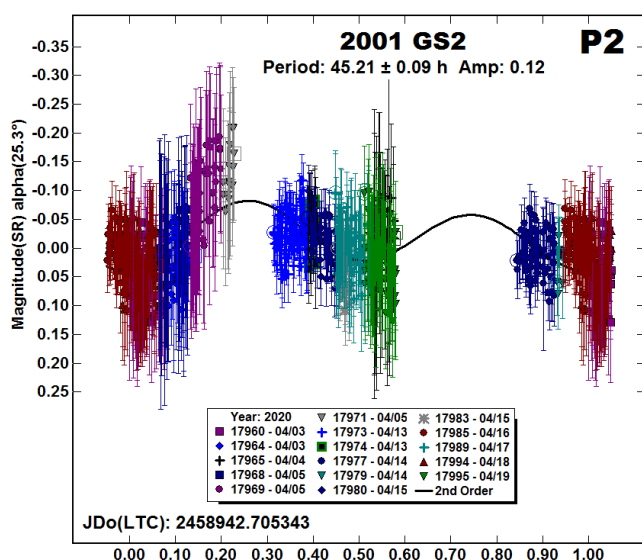
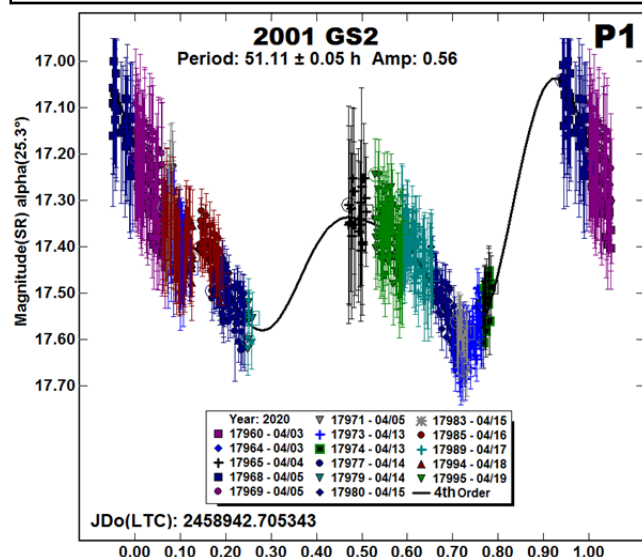
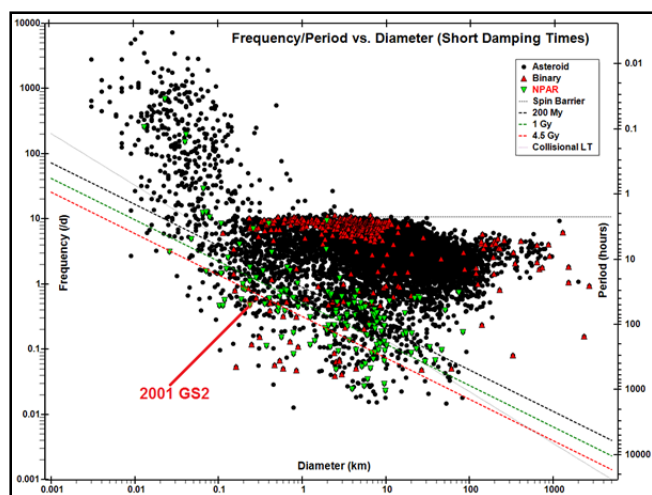


2000 KA. Pravec et al. (2020web) found a period of 5.690 h. Our result is about double that: 11.46 h. The fit to the longer period could be a *fit by exclusion* (minimized overlapping data points) but when the data are forced to the half-period, the divergence from 0.8 to 1.0 rotation phase places doubt on that solution.



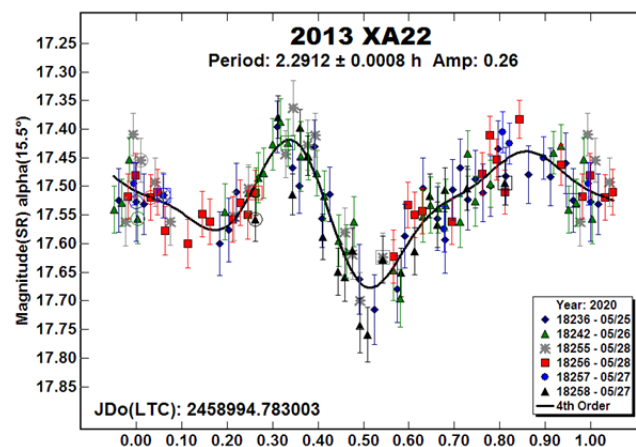
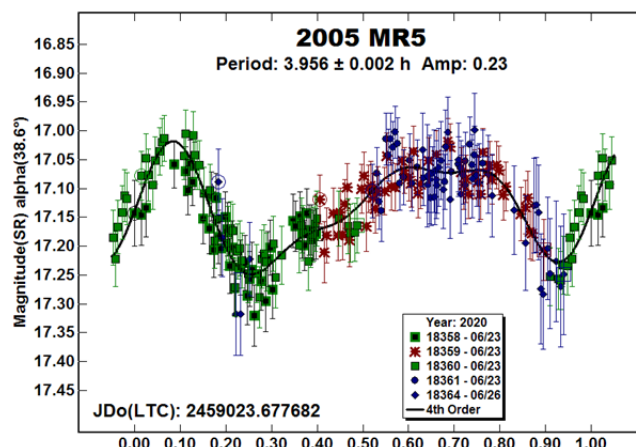
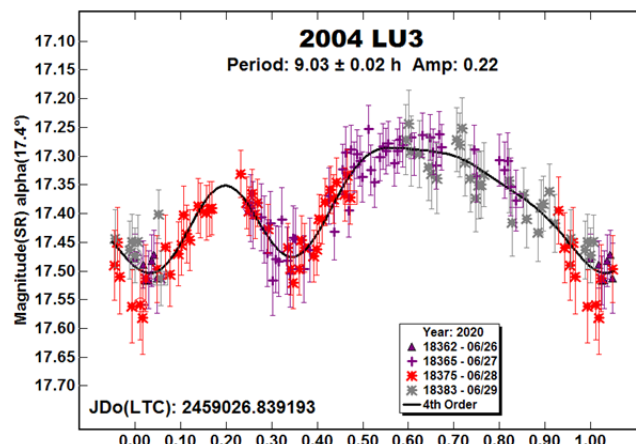
2001 GS2. Even the longer damping time for this NEA to go from tumbling to single-axis rotation is much greater than the age of the Solar System (Pravec et al., 2014; 2005). This neglects, however, the collisional life time (CLT) for this asteroid, which lies well below the CLT line in the frequency-diameter plot from the LCDB.

Since *MPO Canopus* does not properly handle tumbling asteroids, the plots represent the dominant periods found by the program. They may or may not be the true periods of rotation and precession.



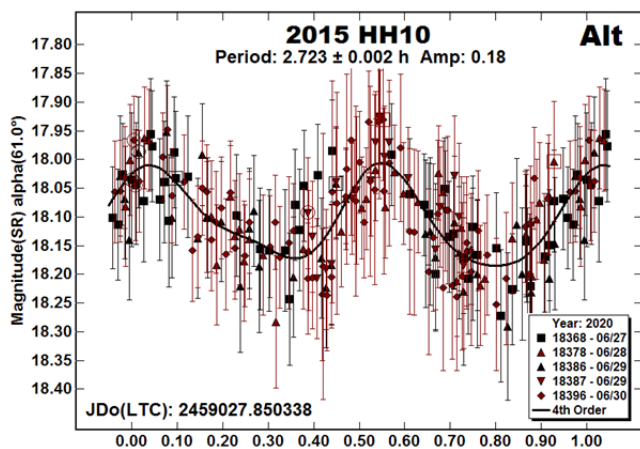
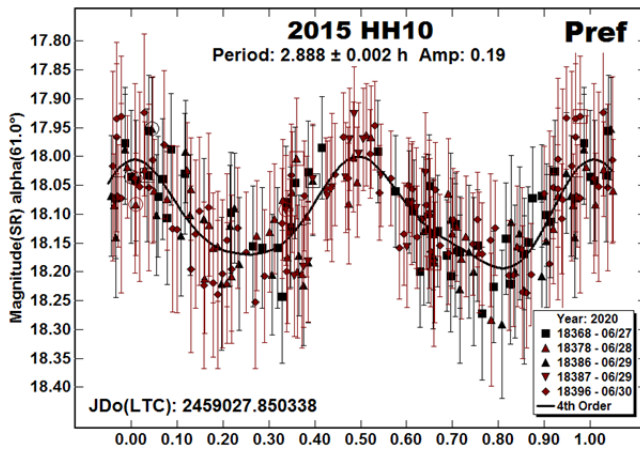
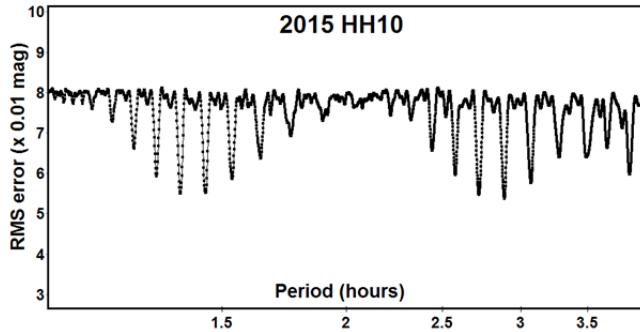
2004 LU3, 2005 MR5, 2013 XA22. There were no previous entries in the LCDB for 2004 LU3, a 600 m NEA with an unusually-shaped lightcurve. The shape, however, seems to be accurate since the period spectrum shows no other solution with a similarly low RMS.

There were also no previous entries for 2005 MR5 and 2013 XA22. The estimated diameter for 2005 MR5 is 250 m and its period of 3.956 h is considered secure. Likewise, the period for the 80-m 2013 XA22 is considered unambiguous.

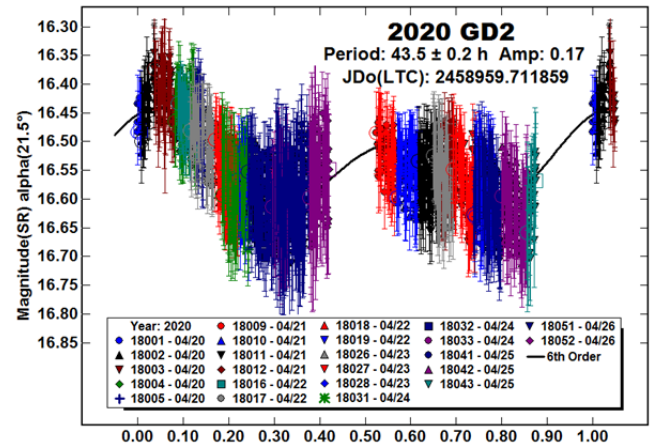


2015 HH10. The period spectrum shows several, nearly equal solutions in two distinct groups. Those near 1.4 h represent the half-periods of the two periods adopted for this paper. The adopted solution is 2.888 h but the one at 2.723 h, which equates to one-half more rotations over 24 hours, can be said to be equally possible.

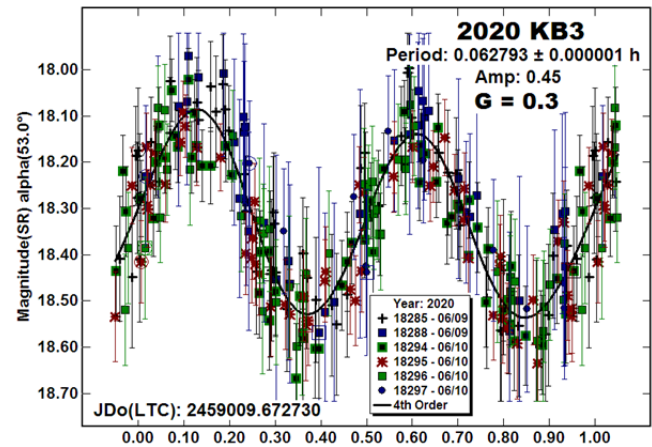
It's interesting to note that the period spectrum slightly favors the half-period for 2.723 h. Given the noisy data, it's hard to say if one of the two 2-h solutions is a *fit by exclusion*, i.e., it minimizes the RMS error by minimizing overlapping data points.



2020 GD2, 2020 KB3. There were no previous entries in the LCDB for either NEA. 2020 GD2 has an estimated diameter of 250 m.



2020 KB3 has a period of only 226 seconds. Its estimated diameter is 33 m.



Acknowledgements

Funding for observations at CS3 and work on the asteroid lightcurve database (Warner et al., 2009) and ALCDEF database (*alcdef.org*) are supported by NASA grant 80NSSC18K0851.

The authors gratefully acknowledge Shoemaker NEO Grants from the Planetary Society (2007, 2013). These were used to purchase some of the telescopes and CCD cameras used in this research.

This work includes data from the Asteroid Terrestrial-impact Last Alert System (ATLAS) project. ATLAS is primarily funded to search for near earth asteroids through NASA grants NN12AR55G, 80NSSC18K0284, and 80NSSC18K1575; byproducts of the NEO search include images and catalogs from the survey area. The ATLAS science products have been made possible through the contributions of the University of Hawaii Institute for Astronomy, the Queen's University Belfast, the Space Telescope Science Institute, and the South African Astronomical Observatory.

Number	Name	2020 mm/dd	Phase	L <sub>PAB</sub>	B <sub>PAB</sub>	Period(h)	P.E.	Amp	A.E.
1685	Toro	06/15-06/27	47.5, 52.3	317	6	10.1871	0.0004	1.07	0.02
6569	Ondaatje	05/18-05/27	46.3, 44.8	276	28	5.295 <sup>A</sup> 5.956	0.001 0.001	0.92	0.02
8014	1990 MF	06/15-07/05	30.7, 67.4	246	8	50.09	0.08	0.20	0.02
52768	1998 OR2	04/05-04/14	74.3, 77.5	158	8	4.1114	0.0002	0.27	0.03
66251	1999 GJ2	04/18-05/03	*7.9, 9.4	216	7	50.9	0.1	0.14	0.03
85184	1991 JG1	05/15-05/20	*26.7, 35.6	207	17	24.19	0.02	0.65	0.05
85989	1999 JD6	06/18-06/23	51.6, 53.4	313	15	7.665	0.003	1.39	0.05
86667	2000 FO10	05/02-05/19	13.7, 48.6	210	13	53.88	0.01	1.30	0.03
136874	1998 FH74	05/16-05/24	15.7, 17.0	242	23	28.55 <sup>A</sup> 14.29	0.03 0.02	0.23	0.03
137064	1998 WP5	04/12-04/17	18.1, 11.7	208	11	13.777	0.005	0.66	0.02
137199	1999 KX4	05/20-05/22	57.8, 56.3	225	39	2.7697	0.0008	0.17	0.02
159929	2005 UK	05/21-05/26	60.7, 63.3	195	11	33.4 <sup>A</sup> 38.3 <sup>A</sup> 66.3	0.2 0.2 0.5	0.48	0.05
175189	2005 EC224	04/03-04/17	11.1, 4.8	207	4	3.758	0.002	0.15	0.02
331471	1984 QY1	05/29-06/08	40.2, 27.4	258	29	45.81 <sup>T</sup> 37.8	0.08 0.1	0.38	0.05
349063	2006 XA	06/11-06/14	28.9, 26.2	287	8	2.436	0.002	0.23	0.03
373428	1999 TC5	04/03-04/05	2.7, 5.5	194	3	3.45	0.01	0.21	0.05
382503	2001 RE8	06/28-07/01	20.6, 23.0	281	14	61.1	0.5	0.67	0.05
441987	2010 NY65	06/27-07/01	75.0, 54.5	254	25	4.974 <sup>A</sup> 9.953	0.003 0.004	0.32	0.04
477885	2011 JT9	05/20-06/09	25.3, 26.1	251	27	3.1114	0.0003	0.14	0.02
495615	2015 PQ291	05/27-06/08	41.5, 50.1	217	8	13.763	0.002	0.66	0.05
498066	2007 RM133	06/11-06/15	18.6, 16.4	269	11	6.21	0.01	0.24	0.05
	2000 KA	05/14-05/19	42.8, 10.5	234	12	11.46 <sup>A</sup> 5.62	0.02 0.01	0.22	0.03
	2001 GS2	04/03-04/19	*25.2, 10.2	205	2	51.15 <sup>T</sup> 45.21	0.05 0.09	0.54	0.05
	2004 LU3	06/26-06/29	17.4, 19.3	266	10	9.03	0.02	0.22	0.03
	2005 MR5	06/23-06/26	38.9, 45.4	267	25	3.956	0.002	0.23	0.03
	2013 XA22	05/25-05/28	15.6, 21.9	238	6	2.2912	0.0008	0.26	0.03
	2015 HH10	06/27-06/30	60.9, 66.2	323	14	2.888 <sup>A</sup> 2.723	0.002 0.002	0.19	0.04
	2020 GD2	04/21-04/26	17.1, 8.5	209	4	43.5	0.2	0.17	0.03
	2020 KB3	06/09-06/10	52.7, 48.5	235	11	0.062793	0.000001	0.45	0.05

Table II. Observing circumstances. <sup>A</sup>Alternate period in ambiguous solution. <sup>T</sup>Second period in a suspected tumbler. The phase angle ( $\alpha$ ) is given at the start and end of each date range. If there is an asterisk before the first phase value, the phase angle reached a maximum or minimum during the period. L<sub>PAB</sub> and B<sub>PAB</sub> are, respectively the average phase angle bisector longitude and latitude (see Harris et al., 1984).

## References

References from web sites should be considered transitory, unless from an agency with a long lifetime expectancy. Sites run by private individuals, even if on an institutional web site, do not necessarily fall into this category.

ALCDEF (2020). Asteroid Lightcurve Data Exchange Format web site. <http://alcdef.org>

AstDys-2 (2020). Asteroids - Dynamic Site web location. <https://newton.spacedys.com/astdys2/>

Betzler, A.S.; Novaes, A.B. (2009). "Photometric Observations of 1998 OR2, 1999 AQ10, and 2008 TC3." *Minor Planet Bull.* **36**, 145-147.

Binzel, R.P.; DeMeo, F.E.; Turtelboom, E.V.; Bus, S.J.; Tokunaga, A.; Burbine, T.H.; Lantz, C.; Polishook, D.; Carry, B.; Morbidelli, A.; Birlan, M.; Vernazza, P.; Burt, B.J.; Moskovitz, N.; Slivan, S.M.; Thomas, C.A.; Rivkin, A.S.; Hicks, M.D.; Dunn, T.; Reddy, V.; Sanchez, J.A.; Granvik, M.; Kohout, T. (2019). "Compositional distributions and evolutionary processes for the near-Earth object population: Results from the MIT-Hawaii Near-Earth Object Spectroscopic Survey (MITHNEOS)." *Icarus* **324**, 41-76.

CSS (2020). Catalina Sky Survey web site. <https://catalina.lpl.arizona.edu/>

Đurech, J.; Vokrouhlický, D.; Pravec, P.; Hanuš, J.; Farnocchia, D.; Krugly, Y.N.; Inasaridze, R.Y.; Ayvazian, V.R.; Fatka, P.; Chiorny, V.G.; Gaftonyuk, N.; Galád, A.; Groom, R.; Hornoch, K.; Kučáková, H.; Kušnirák, P.; Lehký, M.; Kvaratskhelia, O.I.; Masi, G.; Molotov, I.E. Oey, J.; Pollock, J.T.; Shevchenko, V.G.; Vraštil, J.; Warner, B.D. (2018). "YORP and Yarkovsky effects in asteroids (1685) Toro, (2100) Ra-Shalom, (3103) Eger, and (161989) Cacus." *Astron. Astrophys.* **609**, A86.

- Harris, A.W.; Young, J.W.; Scaltriti, F.; Zappala, V. (1984). "Lightcurves and phase relations of the asteroids 82 Alkmene and 444 Gypsis." *Icarus* **57**, 251-258.
- Harris, A.W.; Pravec, P.; Galad, A.; Skiff, B.A.; Warner, B.D.; Vilagi, J.; Gajdos, S.; Carbognani, A.; Hornoch, K.; Kusnirak, P.; Cooney, W.R.; Gross, J.; Terrell, D.; Higgins, D.; Bowell, E.; Koehn, B.W. (2014). "On the maximum amplitude of harmonics on an asteroid lightcurve." *Icarus* **235**, 55-59.
- Higgins, D. (2008). "Asteroid Lightcurve Analysis at Hunters Hill Observatory and Collaborating Stations: April 2007 - June 2007." *Minor Planet Bull.* **35**, 30-32.
- Kaasalainen, M.; Torppa, J. (2001). "Optimization Methods for Asteroid Lightcurve Inversion. I. Shape Determination." *Icarus* **153**, 24-36.
- Kaasalainen, M.; Torppa, J.; Muinonen, K. (2001). "Optimization Methods for Asteroid Lightcurve Inversion. II. The Complete Inverse Problem." *Icarus* **153**, 37-51.
- Koehn, B.W.; Bowell, E.L.G.; Skiff, B.A.; Sanborn, J.J.; McLelland, K.P.; Pravec, P.; Warner, B.D. (2014). "Lowell Observatory Near-Earth Asteroid Photometric Survey (NEAPS) - 2009 January through 2009 June." *Minor Planet Bull.* **41**, 286-300.
- MPC (2020). Minor Planet Center. MPCOrb elements file. <https://minorplanetcenter.net/iau/MPCORB.html>
- Polishook, D. (2012). "Lightcurves and Spin Periods of Near-Earth Asteroids, The Wise Observatory, 2005 – 2010." *Minor Planet Bull.* **39**, 187-192.
- Polishook, D.; Brosch, N. (2008). "Photometry of Aten asteroids – More than a handful of binaries." *Icarus* **194**, 111-124.
- Pravec, P.; Sarounova, L.; Wolf, M. (1996). "Lightcurves of 7 Near-Earth Asteroids." *Icarus* **124**, 471-482.
- Pravec, P.; Wolf, M.; Sarounova, L. (1999web, 2005web, 2020web). <http://www.asu.cas.cz/~ppravec/neo.htm>
- Pravec, P.; Harris, A.W.; Scheirich, P.; Kušnirák, P.; Šarounová, L.; Hergenrother, C.W.; Mottola, S.; Hicks, M.D.; Masi, G.; Krugly, Y.N.; Shevchenko, V.G.; Nolan, M.C.; Howell, E.S.; Kaasalainen, M.; Galád, A.; Brown, P.; Degraff, D.R.; Lambert, J. V.; Cooney, W.R.; Foglia, S. (2005). "Tumbling asteroids." *Icarus* **173**, 108-131.
- Pravec, P.; Scheirich, P.; Durech, J.; Pollock, J.; Kusnirak, P.; Hornoch, K.; Galad, A.; Vokrouhlicky, D.; Harris, A.W.; Jehin, E.; Manfroid, J.; Opitom, C.; Gillon, M.; Colas, F.; Oey, J.; Vrástil, J.; Reichart, D.; Ivarsen, K.; Haislip, J.; LaCluyze, A. (2014). "The tumbling state of (99942) Apophis." *Icarus* **233**, 48-60.
- Radar Team (2020). "Asteroid Visiting Earth's Neighborhood Brings its own Face Mask." <https://www.ucf.edu/news/asteroid-visiting-earths-neighborhood-brings-its-own-face-mask/>
- Rubincam, D.P. (2000). "Relative Spin-up and Spin-down of Small Asteroids." *Icarus* **148**, 2-11.
- Tonry, J.L.; Denneau, L.; Flewelling, H.; Heinze, A.N.; Onken, C.A.; Smartt, S.J.; Stalder, B.; Weiland, H.J.; Wolf, C. (2018). "The ATLAS All-Sky Stellar Reference Catalog." *Ap. J.* **867**, A105.
- Warner, B.D. (2013a). "Asteroid Lightcurve Analysis at the Palmer Divide Observatory: 2012 June – September." *Minor Planet Bull.* **40**, 26-29.
- Warner, B.D. (2013b). "Asteroid Lightcurve Analysis at the Palmer Divide Observatory: 2013 January – March." *Minor Planet Bull.* **40**, 137-145.
- Warner, B.D. (2014). "Near-Earth Asteroid Lightcurve Analysis at CS3-Palmer Divide Station: 2014 March-June." *Minor Planet Bull.* **41**, 213-224.
- Warner, B.D. (2016). "Near-Earth Asteroid Lightcurve Analysis at CS3-Palmer Divide Station: 2016 April-July." *Minor Planet Bull.* **43**, 311-319.
- Warner, B.D. (2017). "Near-Earth Asteroid Lightcurve at CS3-Palmer Divide Station: 2017 April thru June." *Minor Planet Bull.* **44**, 335-344.
- Warner, B.D.; Harris, A.W.; Pravec, P. (2009). "The Asteroid Lightcurve Database." *Icarus* **202**, 134-146. Updated 2020 June. <http://www.minorplanet.info/lightcurvedatabase.html>
- Warner, B.D.; Stephens, R.D. (2019). "Near-Earth Asteroid Lightcurve Analysis at the Center for Solar System Studies: 2018 July-September." *Minor Planet Bull.* **46**, 27-40.
- Warner, B.D.; Stephens, R.D. (2020). "Near-Earth Asteroid Lightcurve Analysis at the Center for Solar System Studies: 2019 September - 2020 January." *Minor Planet Bull.* **47**, 105-120.
- Waszczak, A.; Chang, C.-K.; Ofek, E.O.; Laher, R.; Masci, F.; Levitan, D.; Surace, J.; Cheng, Y.-C.; Ip, W.-H.; Kinoshita, D.; Helou, G.; Prince, T.A.; Kulkarni, S. (2015). "Asteroid Light Curves from the Palomar Transient Factory Survey: Rotation Periods and Phase Functions from Sparse Photometry." *Astron. J.* **150**, A75.
- Zappala, V.; Cellini, A.; Barucci, A.M.; Fulchignoni, M.; Lupishko, D.E. (1990). "An analysis of the amplitude-phase relationship among asteroids." *Astron. Astrophys.* **231**, 548-560.

**BINARY ASTEROIDS AT  
THE CENTER FOR SOLAR SYSTEM STUDIES**

Brian D. Warner  
Center for Solar System Studies / MoreData!  
446 Sycamore Ave.  
Eaton, CO 80615 USA  
brian@MinorPlanetObserver.com

Robert D. Stephens  
Center for Solar System Studies / MoreData!  
Rancho Cucamonga, CA 91730

Alan W. Harris  
MoreData!  
La Cañada, CA 91011

(Received: 2020 April 6 Revised: 2020 August 9)

We report on the discovery at the Center for Solar System Studies of four confirmed binary asteroids: 1656 Suomi, (85275) 1994 LY, (85628) 1998 KV2, and (539940) 2017 HW1 along with the suspected candidate (184990) 2006 KE89.

CCD photometric observations at the Center for Solar System Studies in 2020 April to July of four near-Earth and one Hungaria asteroid led to finding four confirmed binaries and one strong candidate. Table I lists the telescopes and CCD cameras that were combined to make the observations.

All the cameras use CCD chips from the KAF blue-enhanced family and so have essentially the same response. The pixel scales ranged from 1.24-1.60 arcsec/pixel.

Telescopes	Cameras
0.30-m $f/6.3$ Schmidt-Cass	FLI Microline 1001E
0.35-m $f/9.1$ Schmidt-Cass	FLI Proline 1001E
0.40-m $f/10$ Schmidt-Cass	SBIG STL-1001E
0.40-m $f/10$ Schmidt-Cass	
0.50-m $f/8.1$ Ritchey-Chrétien	

Table I. List of available telescopes and CCD cameras at CS3. The exact combination for each telescope/camera pair can vary due to maintenance or specific needs.

All lightcurve observations were unfiltered since a clear filter can cause a 0.1-0.3 mag loss. The exposure duration varied depending on the asteroid's brightness and sky motion. Guiding on a field star sometimes resulted in a trailed image for the asteroid.

Measurements were made using *MPO Canopus*. The Comp Star Selector utility in *MPO Canopus* found up to five comparison stars of near solar-color for differential photometry. Comp star magnitudes were taken from ATLAS catalog (Tonry et al., 2018), which has Sloan *griz* magnitudes that were derived from the GAIA and Pan-STARR catalogs, among others, and are the "native" magnitudes of the catalog.

To reduce the number of times and amount of resetting nightly zero points, we use the ATLAS  $r'$  (SR) magnitudes. Those adjustments are mostly  $\leq 0.03$  mag. The occasions where larger corrections were required may have been related in part to using unfiltered observations, poor centroiding of the reference stars, and not correcting for second-order extinction terms.

The Y-axis of the primary lightcurves gives ATLAS SR "sky" (catalog) magnitudes. The values on the Y-axis of the secondary

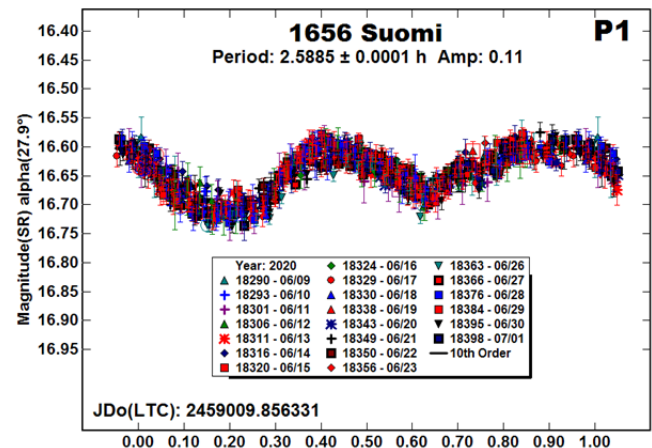
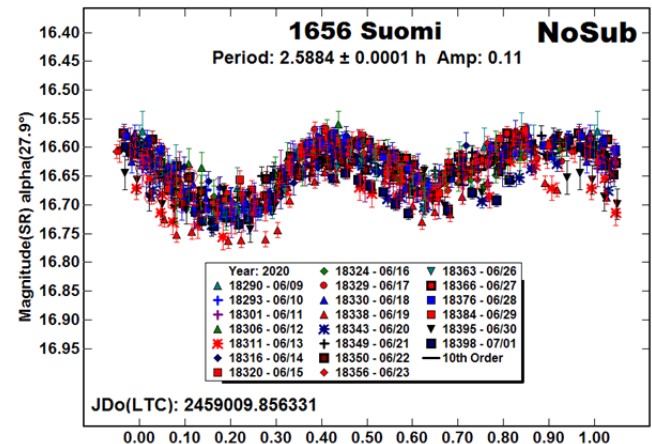
lightcurves are usually differential magnitudes with 0.0 corresponding to the average magnitude of the primary curve.

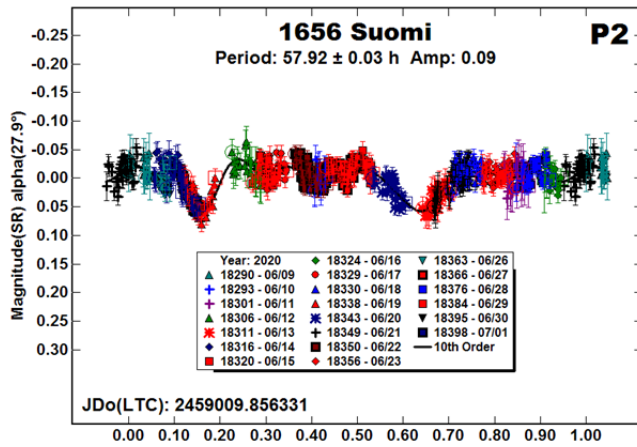
During period analysis, the magnitudes were normalized to the comparison stars used in the earliest session and to the phase angle given in parentheses using  $G = 0.15$ . The X-axis shows rotational phase from  $-0.05$  to  $1.05$ . If the plot includes the amplitude, e.g., "Amp: 0.65", this is the amplitude of the Fourier model curve and *not necessarily the adopted amplitude for the lightcurve*.

Our initial search for previous results started with the asteroid lightcurve database (LCDB; Warner et al., 2009) found on-line at <http://www.minorplanet.info/lightcurvedatabase.html>. Readers are strongly encouraged to obtain, when possible, the original references listed in the LCDB. From here on, we'll use only "LCDB" to reference the paper by Warner et al. (2009).

**1656 Suomi.** Stephens (2004) observed this Hungaria in 2004 and found a period of 2.59 h. There were no indications of a satellite. Subsequent observations by Brinsfield (2008) and Warner (2012; 2014a; 2017) also produced negative results. On the other hand, observations by Warner (2016a) in 2015 hinted at a second period of 12.60 h, but no obvious mutual events (occultations/eclipses) due to a satellite were noted.

The observations in 2020 almost immediately showed what appeared to be attenuations (deviations from a single period lightcurve) but they were seen only occasionally. This suggested a long secondary period.

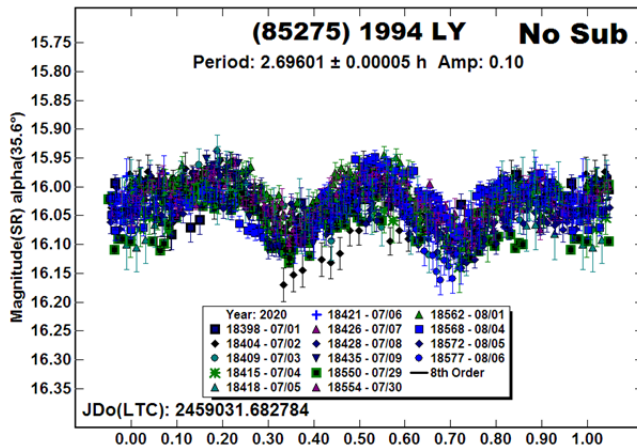




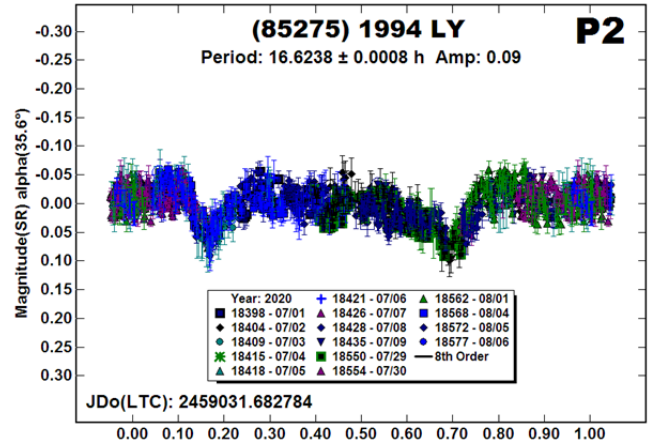
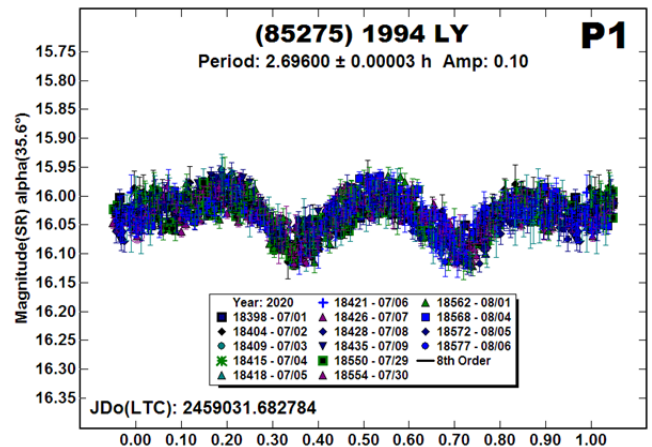
After following the asteroid for more than a month, mutual events were confirmed. The coverage of each event is not complete but it is sufficient to confirm an orbital period of 57.92 h. Based on the 0.07 mag events, the estimated ratio of the effective secondary-to-primary diameters is  $D_s/D_p \geq 0.26 \pm 0.02$ . A CBET (Central Bureau Electronic Telegram) submission was made in early 2020 July to the Central Bureau for Astronomical Telegrams (CBAT).

The long period suggests an orbit of about six primary radii. At 28° phase angle, the image and the shadow are well separated. Depending on geometry, this could lead to double events at the primary and secondary events or missing one of the two entirely. The narrower event (duration about 7 h) is probably a single (eclipse or transit) event while the broader event (duration about 12 h) is perhaps an eclipse combined with a transit or occultation event.

(85275) 1994 LY. Based on an extensive data set, Pravec et al. (2007web, private communications) reported a period of 2.6962 h and a suspected secondary period 48.5 h. Brinsfield (2008) reported a period of 2.6960 h based on data obtained at about the same time as Pravec et al. but did not indicate seeing mutual events or attenuations.

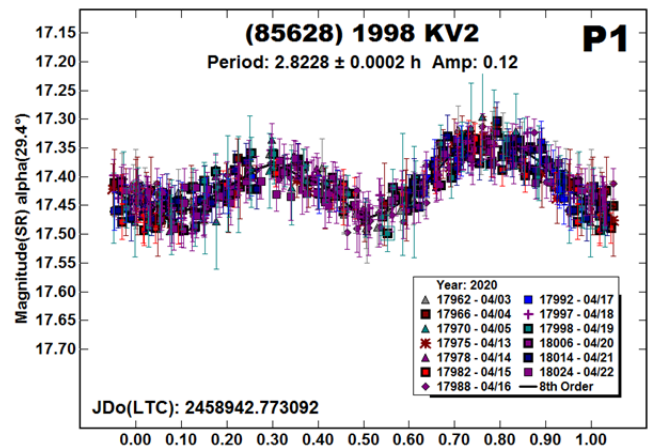


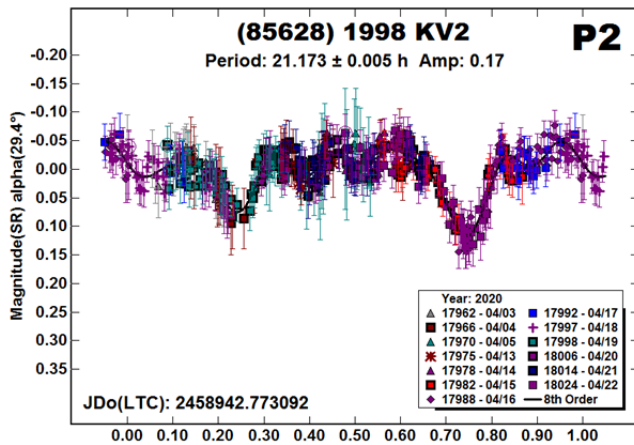
Our observations were made between 2020 July 1-9 showed obvious attenuations early on. Despite the secondary period being close to commensurate with an Earth day, we were able to get full coverage of the satellite's lightcurve. Analysis by Petr Pravec (private communications) confirmed that our data set supported a second period of about 16.6 h. Additional data from July 29 – Aug 6 confirmed and refined the results. The event depths range from 0.06-0.08 mag, which leads to an estimated  $D_s/D_p \geq 0.24 \pm 0.02$ .



(85628) 1998 KV2. Warner (2014b) first observed this 1-km NEA in 2014 April, finding a primary period of 2.819 h but no signs of attenuations in the lightcurve. Follow-up observations in 2016 February to May (Warner 2016b; 2016c) were also negative for indications of a satellite. The 2018 June observations (Warner, 2018) led to a period of 2.999 h and a suspected secondary period of 13.28 h.

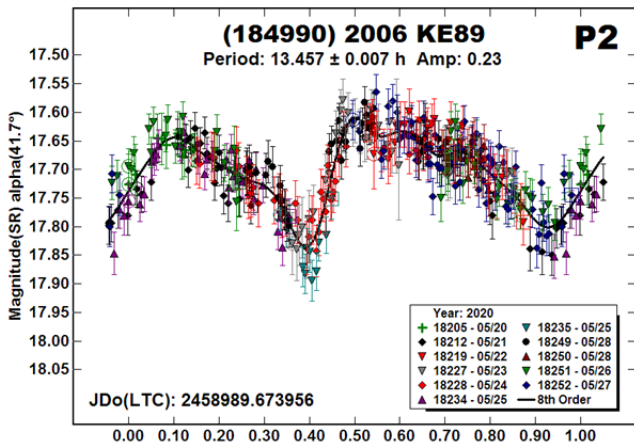
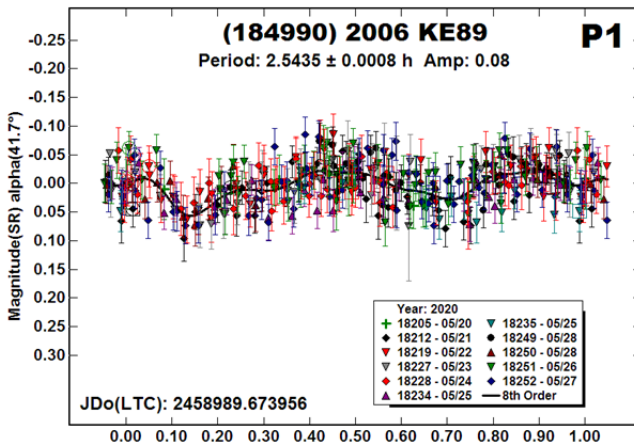
Conclusive evidence of a satellite was found with the 2020 April observations, with the data leading to an orbital period of 21.173 h and mutual events ranging from 0.08-0.13 mag that give  $D_s/D_p \geq 0.28 \pm 0.02$ .





Pravec et al. (2020web) independently discovered the satellite but did not have complete coverage of the satellite lightcurve. They used our orbital period to derive  $P_1 = 2.8229 \pm 0.0004$  h. The discovery was announced in CBET 4757.

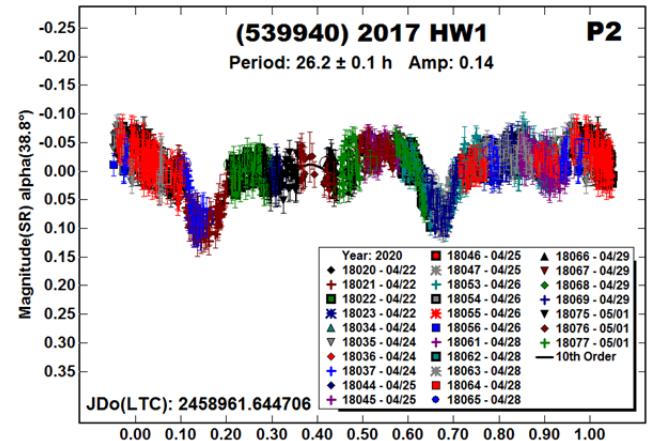
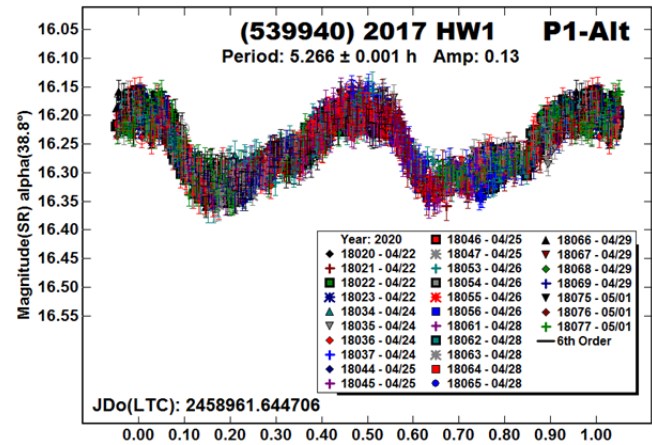
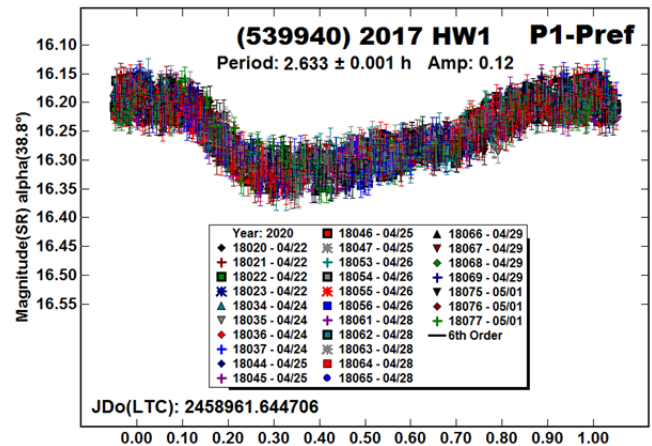
(184990) 2006 KE89. Behrend (2006web) reported a period of 5.187 h based on observations from mid-June 2006. Skiff et al. (2019b) found a low-quality result of 5.16 h. Our observations in 2020 May led to a proposed primary period of 2.5435 h, or half that given by Behrend and Skiff. A secondary period of 13.457 h was also found.



Both periods are in the expected range for a small binary asteroid but the shape of the  $P_2$  lightcurve is puzzling. One interpretation is a very elongated satellite that *may* be producing mutual events on the order of 0.07-0.11 mag. If so, then this gives  $D_s/D_p \geq 0.26 \pm 0.02$ .

It's interesting to note that a good part of the incomplete Behrend (2006web) lightcurve bears some resemblance to the  $P_2$  lightcurve given here. The next follow-up opportunity is in mid-2021 ( $V \sim 18.4$ ,  $\delta = 18^\circ$ )

(539940) 2017 HW1. Pravec et al. (2020web) observed this NEA in 2020 February and April and found a primary period of 2.6346 h. They also reported a suspected secondary period of 15.69 h but did not get conclusive evidence of a satellite.



Number	Name	2020 mm/dd	Phase	L <sub>PAB</sub>	B <sub>PAB</sub>	Period(h)	P.E.	Amp	A.E.	Grp/Dr
1656	Suomi	06/09-07/01	28.0, 24.9	319	24	2.5885 57.92	0.0001 0.03	0.11 0.07	0.01 0.01	H 0.26
85275	1994 LY	07/01-08/06	35.5, 46.1	283	23	2.69600 16.6238	0.00003 0.0008	0.10 0.08	0.01 0.01	NEA 0.23
85628	1998 KV2	04/03-04/22	29.4, 15.1	216	16	2.8228 21.173	0.0002 0.005	0.12 0.17	0.02 0.02	NEA 0.28
184990	2006 KE89	05/20-05/28	*41.8, 46.2	242	44	2.5435 13.457	0.0009 0.007	0.08 0.23	0.02 0.03	NEA 0.26
539940	2017 HW1	04/22-05/01	38.6, 24.4	207	18	2.633 26.2	0.001 0.1	0.12 0.14	0.02 0.02	NEA 0.31

Table II. Observing circumstances. The second line gives the orbital period of the satellite and maximum depth of the mutual events. The phase angle ( $\alpha$ ) is given at the start and end of each date range. If there is an asterisk before the first phase value, the phase angle reached a maximum or minimum during the period. L<sub>PAB</sub> and B<sub>PAB</sub> are, respectively the average phase angle bisector longitude and latitude (see Harris et al., 1984). For the Grp/Dr column, the first line gives the group/family based on Warner et al. (2009). H: Hungaria. The second line gives the ratio of the minimum effective secondary/primary diameters (Ds/Dp).

Our observations toward the end of 2020 April confirmed mutual events and led to a primary period of 2.633 h. A period of 5.266 h cannot be formally excluded but it does not fit with the general trend of other binary asteroids of similar size and orbital periods. The orbital period was found to be  $26.2 \pm 0.1$  h with mutual events ranging from 0.09 to 0.12 mag. This indicates  $Ds/Dp \geq 0.31 \pm 0.03$ . The discovery announcement appeared in CBET 4771.

#### Acknowledgements

Funding for observations at CS3 and work on the asteroid lightcurve database (Warner et al., 2009) and ALCDEF database (*alcdef.org*) are supported by NASA grant 80NSSC18K0851. The authors gratefully acknowledge Shoemaker NEO Grants from the Planetary Society (2007, 2013). These were used to purchase some of the telescopes and CCD cameras used in this research. This work includes data from the Asteroid Terrestrial-impact Last Alert System (ATLAS) project. ATLAS is primarily funded to search for near earth asteroids through NASA grants NN12AR55G, 80NSSC18K0284, and 80NSSC18K1575; byproducts of the NEO search include images and catalogs from the survey area. The ATLAS science products have been made possible through the contributions of the University of Hawaii Institute for Astronomy, the Queen's University Belfast, the Space Telescope Science Institute, and the South African Astronomical Observatory.

#### References

References from web sites should be considered transitory, unless from an agency with a long lifetime expectancy. Sites run by private individuals, even if on an institutional web site, do not necessarily fall into this category.

Behrend, R. (2006web). Observatoire de Geneve web site. [http://obswww.unige.ch/~behrend/page\\_cou.html](http://obswww.unige.ch/~behrend/page_cou.html)

Brinsfield, J.W. (2008). "The Rotation Periods of 1465 Autonoma, 1656 Suomi, 4483 Petofi, 4853 Marielukac, and (85275) 1994 LY." *Minor Planet Bull.* **35**, 23-24.

Harris, A.W.; Young, J.W.; Scaltriti, F.; Zappala, V. (1984). "Lightcurves and phase relations of the asteroids 82 Alkmene and 444 Gypsis." *Icarus* **57**, 251-258.

Pravec, P.; Wolf, M.; Sarounova, L. (2007web, 2020web). <http://www.asu.cas.cz/~ppravec/neo.htm>

Skiff, B.A.; McLelland, K.P.; Sanborn, J.; Pravec, P.; Koehn, B.W. (2019). "Lowell Observatory Near-Earth Asteroid Photometric Survey (NEAPS): Paper 4." *Minor Planet Bull.* **46**, 458-503.

Stephens, R.D. (2004). "Photometry of 1196 Sheba, 1341 Edmee, 1656 Suomi, 2577 Litva, and 2612 Kathryn." *Minor Planet Bull.* **31**, 95-97.

Tonry, J.L.; Denneau, L.; Flewelling, H.; Heinze, A.N.; Onken, C.A.; Smartt, S.J.; Stalder, B.; Weiland, H.J.; Wolf, C. (2018). "The ATLAS All-Sky Stellar Reference Catalog." *Ap. J.* **867**, A105.

Warner, B.D. (2012). "Asteroid Lightcurve Analysis at the Palmer Divide Observatory: 2012 March – June." *Minor Planet Bull.* **39**, 245-252.

Warner, B.D. (2014a). "Asteroid Lightcurve Analysis at CS3-Palmer Divide Station: 2014 January-March." *Minor Planet Bull.* **41**, 144-155.

Warner, B.D. (2014b). "Near-Earth Asteroid Lightcurve Analysis at CS3-Palmer Divide Station: 2014 March-June." *Minor Planet Bull.* **41**, 213-224.

Warner, B.D. (2016a). "Asteroid Lightcurve Analysis at CS3-Palmer Divide Station: 2015 June-September." *Minor Planet Bull.* **43**, 57-65.

Warner, B.D. (2016b). "Near-Earth Asteroid Lightcurve Analysis at CS3-Palmer Divide Station: 2016 January-April." *Minor Planet Bull.* **43**, 240-250.

Warner, B.D. (2016c). "Near-Earth Asteroid Lightcurve Analysis at CS3-Palmer Divide Station: 2016 April-July." *Minor Planet Bull.* **43**, 311-319.

Warner, B.D. (2017). "Asteroid Lightcurve Analysis at CS3-Palmer Divide Station: 2017 April thru June." *Minor Planet Bull.* **44**, 289-294.

Warner, B.D. (2018). "Near-Earth Asteroid Lightcurve Analysis at CS3-Palmer Divide Station: 2018 April-June." *Minor Planet Bull.* **45**, 366-379.

Warner, B.D.; Harris, A.W.; Pravec, P. (2009). "The Asteroid Lightcurve Database." *Icarus* **202**, 134-146. Updated 2020 June. <http://www.minorplanet.info/lightcurvedatabase.html>

**LIGHTCURVE ANALYSIS OF HILDA ASTEROIDS  
AT THE CENTER FOR SOLAR SYSTEM STUDIES:  
1529 OTERMA AND 17428 CHARLEROI**

Brian D. Warner  
Center for Solar System Studies / MoreData!  
446 Sycamore Ave.  
Eaton, CO 80615 USA  
brian@MinorPlanetObserver.com

Robert D. Stephens  
Center for Solar System Studies / MoreData!  
Rancho Cucamonga, CA

(Received: 2020 July 13)

New CCD photometric observations of 1529 Oterma were made in 2020 May, leading to a preferred period of 14.317 h. This differs from one of our earlier results by an almost exact 8:5 ratio. The data for 17428 Charleroi from 2020 allowed both 4.8 and 6.0 h periods, which are nearly an exact 5:4 ratio. A review of data from 2016 found an alternate period of 4.793 h but could not formally exclude a solution near 5.99 h, which was the only period possible from the 2017 data. Both cases suggest that rotational aliasing is at play and so make it difficult to find a secure solution.

CCD photometric observations of Hilda asteroids are made at the Center for Solar System Studies (CS3) as part of an ongoing study of this family/group that is located between the outer main-belt and Jupiter Trojans in a 3:2 orbital resonance with Jupiter. The goal is to determine the spin rate statistics of the Hildas and to find pole and shape models when possible. We also look to examine the degree of influence that the YORP (Yarkovsky–O’Keefe–Radzievskii–Paddack) effect (Rubincam, 2000) has on distant objects and to compare the spin rate distribution against the Jupiter Trojans, which can provide evidence that the Hildas are more “comet-like” than main-belt asteroids.

Telescopes	Cameras
0.30-m f/6.3 Schmidt-Cass	FLI Microline 1001E
0.35-m f/9.1 Schmidt-Cass	FLI Proline 1001E
0.35-m f/11 Schmidt-Cass	SBIG STL-1001E
0.40-m f/10 Schmidt-Cass	
0.50-m f/8.1 Ritchey-Chrétien	

Table I. List of available telescopes and CCD cameras at CS3. The exact combination for each telescope/camera pair can vary due to maintenance or specific needs.

Table I lists the telescopes and CCD cameras that are combined to make observations. Up to nine telescopes can be used for the campaign, although seven is more common. All the cameras use CCD chips from the KAF blue-enhanced family and so have essentially the same response. The pixel scales ranged from 1.24–1.60 arcsec/pixel. All lightcurve observations were unfiltered since a clear filter can result in a 0.1–0.3 magnitude loss. The exposures varied depending on the asteroid’s brightness.

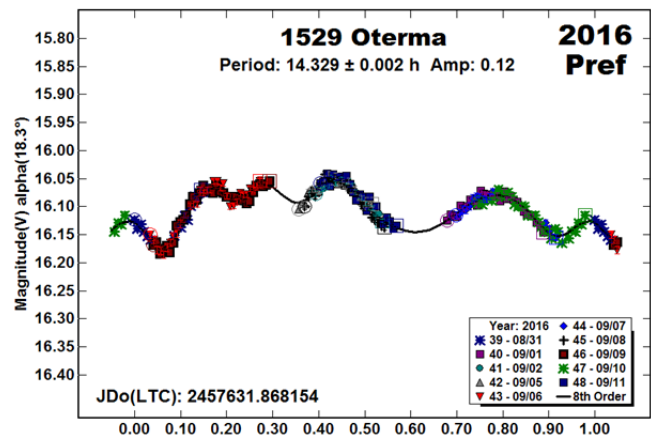
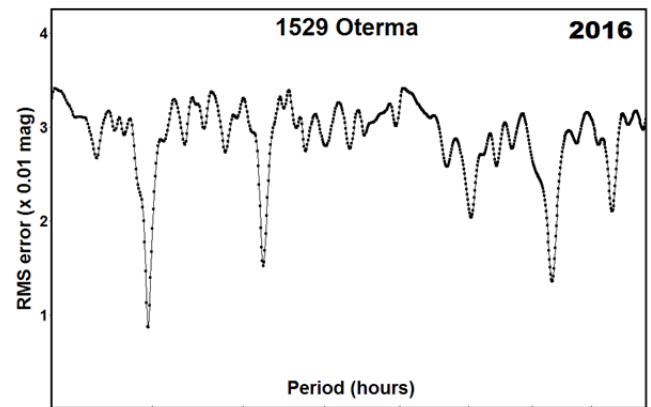
To reduce the number of times and amounts of adjusting nightly zero points, we use the ATLAS catalog  $r$  (SR) magnitudes (Tonry et al., 2018). Those adjustments are usually  $\leq \pm 0.03$  mag. The rare greater corrections may have been related in part to using unfiltered observations, poor centroiding of the reference stars, and not correcting for second-order extinction.

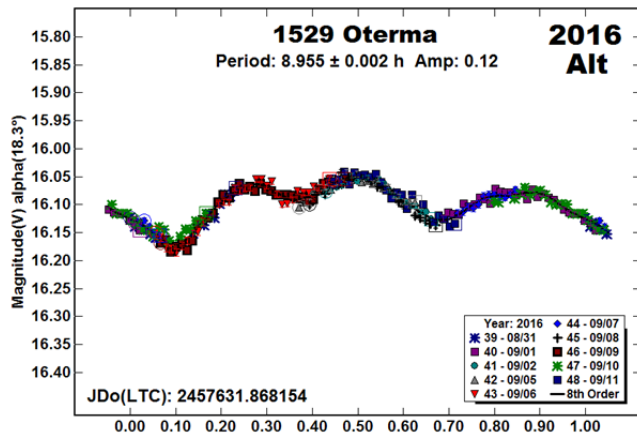
The Y-axis values are ATLAS SR “sky” (catalog) magnitudes. During period analysis, the magnitudes were normalized to the comparison stars used in the earliest session and to the phase angle given in parentheses using  $G = 0.15$ . The X-axis shows rotational phase from  $-0.05$  to  $1.05$ . If the plot includes the amplitude, e.g., “Amp: 0.65”, this is the amplitude of the Fourier model curve and *not necessarily the adopted amplitude for the lightcurve*.

Our initial search for previous results started with the asteroid lightcurve database (LCDB; Warner et al., 2009) found on-line at <http://www.minorplanet.info/lightcurvedatabase.html>. Readers are strongly encouraged to obtain, when possible, the original references listed in the LCDB. From here on, we’ll use only “LCDB” to reference the paper by Warner et al. (2009).

**1529 Oterma.** Finding the rotational period for this 6-km Hilda served as a good example of having to deal with *rotational aliasing*, which is when the true number of rotations over the span of the dataset is uncertain. To demonstrate the problem, we present analysis of our datasets from two previous apparitions as well as the most recent one obtained in 2020.

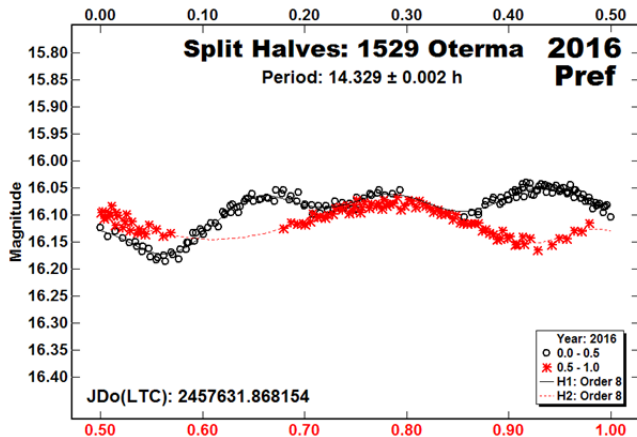
For historical background, Dahlgren et al. (1998) reported a period of 15.75 h based on observations from 1994 Jan 21 – Feb 3. Their bimodal lightcurve had an amplitude of 0.18 mag but covered rotation phase 0.2–0.5 only once and the Feb 3 observations deviated from the phased lightcurve. This indicated that their solution may not have been fully secure.





We first observed Oterma in 2016 (Warner et al., 2017b) and found a period of 8.95 h, which the period spectrum clearly favors. The second-most likely solution near 14.3 h would eventually be what we consider the correct answer. Note that 8<sup>th</sup>-order Fourier fits were required to have the Fourier model curve closely follow the data.

Looking at the two lightcurves from 2016, the “Alt” solution at 8.955 h would seem the obvious choice. The lightcurve at 14.329 h is incomplete and would often be considered a *fit by exclusion*, i.e., when the Fourier analysis finds a local RMS minimum by minimizing the number of overlapping data points. This is the interpretation we took when adopting a period of 8.955 h.



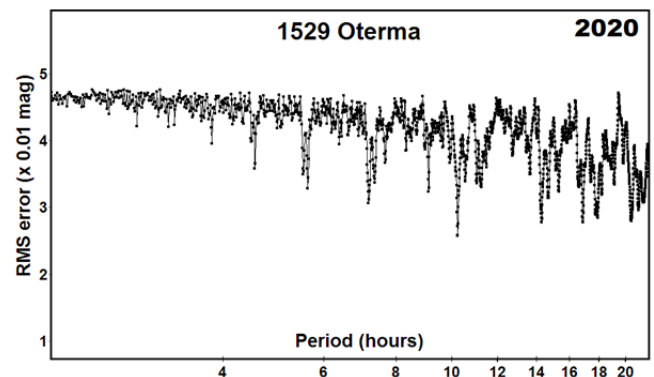
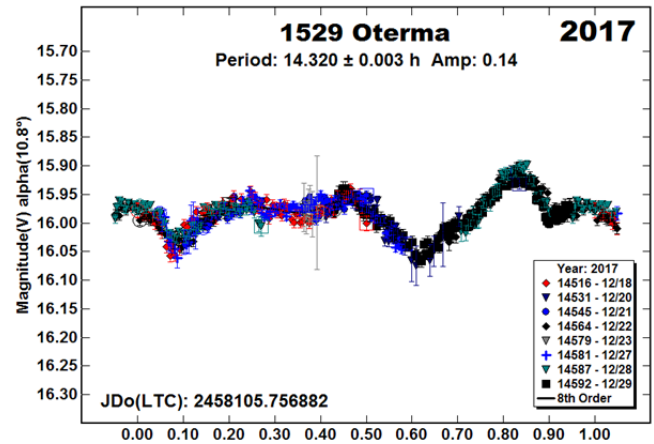
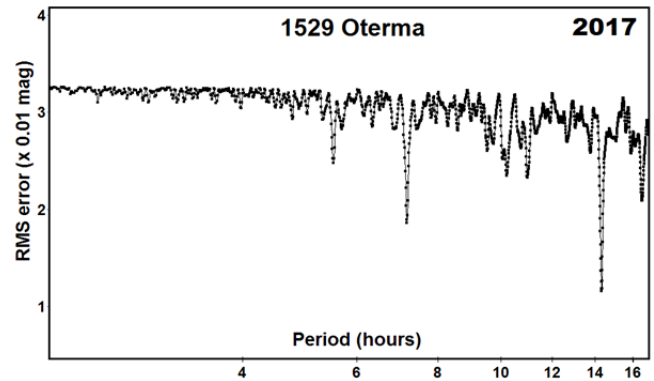
However, when taking another look at the 2016 dataset as part of our analysis of the 2020 dataset, we used a split-halves plot. This plot superimposes the second half of a lightcurve for a given period over the first half (see Harris et al., 2014). If the two halves are nearly symmetrical, especially if within the noise of the data, and the amplitude is  $A < \sim 0.20$  mag, the half-period should be given careful consideration. It’s clear that the two halves of the 2016 solution for 14.329 h are not symmetrical and so that period, despite the apparent certitude based on the shorter period lightcurve, should be the preferred solution.

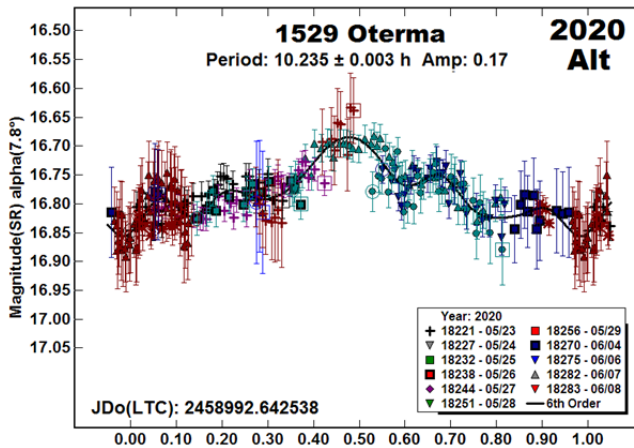
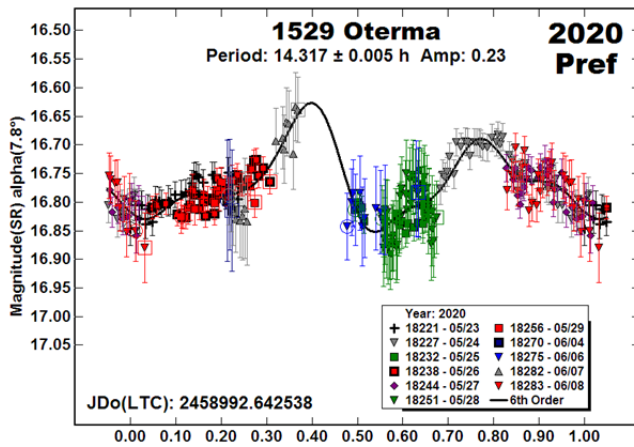
This is where *rotational aliasing* comes to the fore but, in this case, it is more complicated than usual to reach the final result when the two periods differ by an almost exact ratio of 8:5. If a lightcurve at any period is close to symmetrical, then when doing a period search, it’s often difficult to be sure if data from one session is being matched to the proper half of the lightcurve.

If a simple shift of 0.5 rotation phase of one of the halves would closely match the underlying half, then either the original or the half-period are possible and the period ratio will be such that dividing the two numbers has a fractional value of 0.0 or 0.5. It is not so simple if the fractional value is something else, such as a fractional value of 0.6 for the 8:5 period ratio. It may be helpful to note that one half of the lightcurve is trimodal and the other bimodal, though this will not always be the case.

We again observed the asteroid in 2017 December (Warner et al., 2018) and the data led to a period of 14.321 h, which was very close to the period of 14.298 h found by Ditteon et al. (2018). At that time, we re-examined the data from 2016 and found an alternate period of 14.329 h.

Re-analysis of the 2017 data for this work modified the period slightly to 14.320 h. It was obvious that a split-halves plot was not required to resolve an ambiguity; this was supported by the failed attempts to find a period close to 9 h that not even significant zero-point adjustments could overcome.





Moving to 2020, our observations from May 23 – June 8 led to a somewhat noisy dataset that contained only short runs (~3.5 h) that would cover about one-quarter of the 14.3-h period. The resulting period spectrum does not support the 9-hour solution, shows 14.3 h to be a secondary choice, and prefers 10.235 h.

Here, the periods of 10.235 h and 14.320 h are an almost exact 7:5 ratio or, as discussed above, one where the fractional value of dividing the two numbers is not 0.0 or 0.5 and so a simple shift of one half will not necessarily match the other half.

None of the previous datasets supported a period near 10.2 h. However, we recall the oft-cited phrase, “Absence of proof is not proof of absence,” meaning that, *based on the 2020 data alone*, one cannot completely ignore the 10.2-hour result and so it needed to be reported, even if it is unlikely when considering the other datasets. More data are needed to exclude a period of 10.2 h formally once and for all. In the meantime, for this work it was ruled out because of its very low probability.

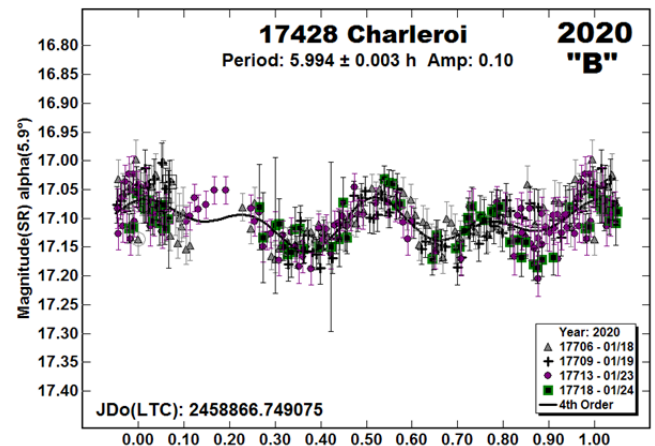
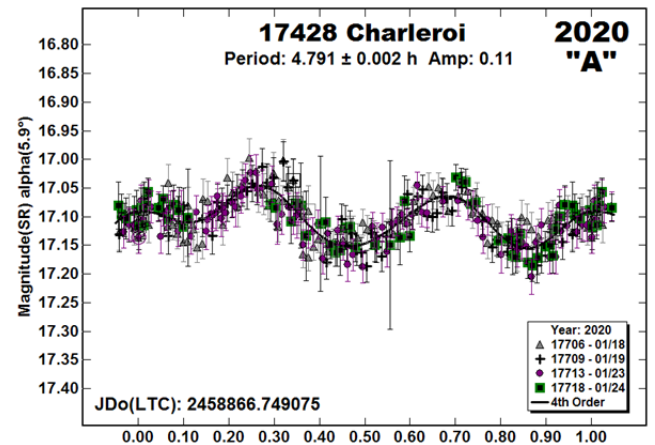
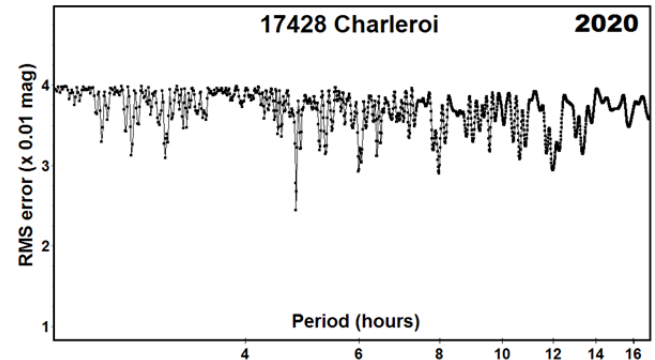
The low amplitudes in the 2016 and 2017 apparitions allowed for lightcurves that were monomodal or tri- and higher modal, not just bimodal (Harris et al., 2014). We adopted 14.317 h for the 2020 dataset since the minimums and maximums were about properly spaced for the bimodal lightcurve that was assumed because of the larger amplitude but despite the lack of full coverage.

Overall, we adopt the period of 14.320 h derived from the 2017 dataset, which had high-quality and, most important, provided an unambiguous solution that was closely supported by the other datasets. Even so, this asteroid needs more study to remove all reasonable doubts about its rotation period.

17428 Charleroi. Our results from earlier apparitions are the only ones listed in the LCDB. In Warner et al. (2017a) we reported a period of 5.990 h. In Warner et al. (2018) a similar period of 6.034 h was found. Our 2020 January observations *initially* led to a period of 5.335 h. That significant difference prompted a return to the earlier datasets to compare and contrast their results with those based on the latest dataset. The end result would be to bring the 2020 result into line with the others *and* introduce the possibility of *rotational aliasing*.

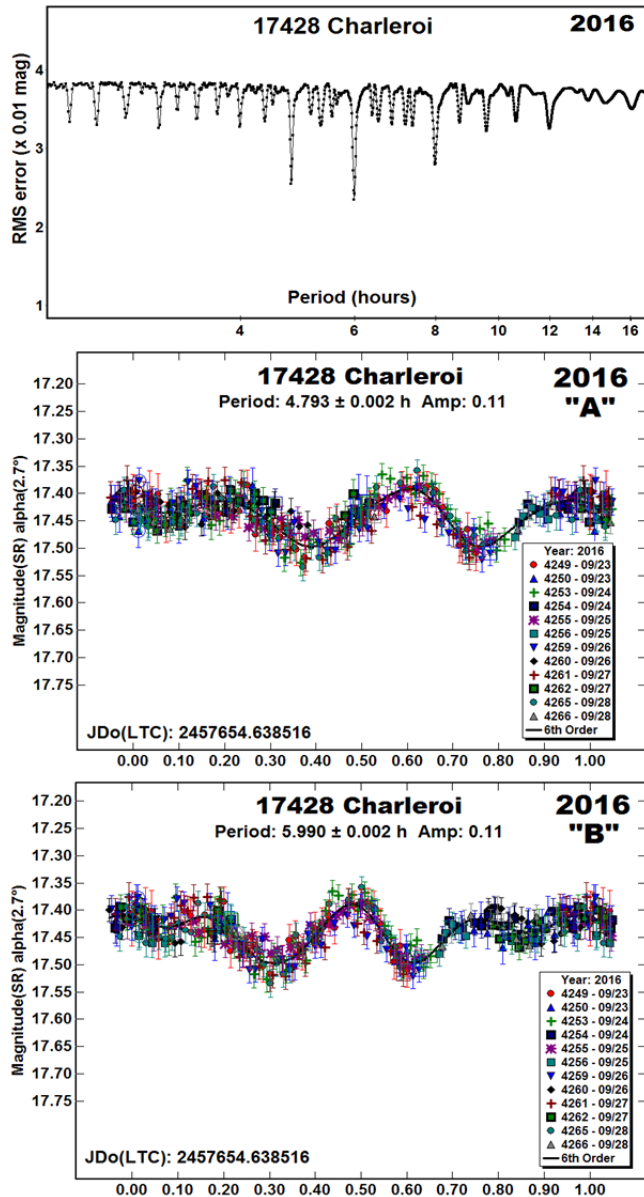
For the 2016 and 2017 datasets, the comparison star magnitudes were changed from another catalog to ATLAS (Tonry et al., 2018) SR (Sloan  $r'$ ) magnitudes so that we would have greater confidence in the night-to-night zero points.

The considerations of *rotation aliasing* for 1529 Oterma are the same here and will not be repeated in detail; only a brief summary for the analysis for each apparition will be given.



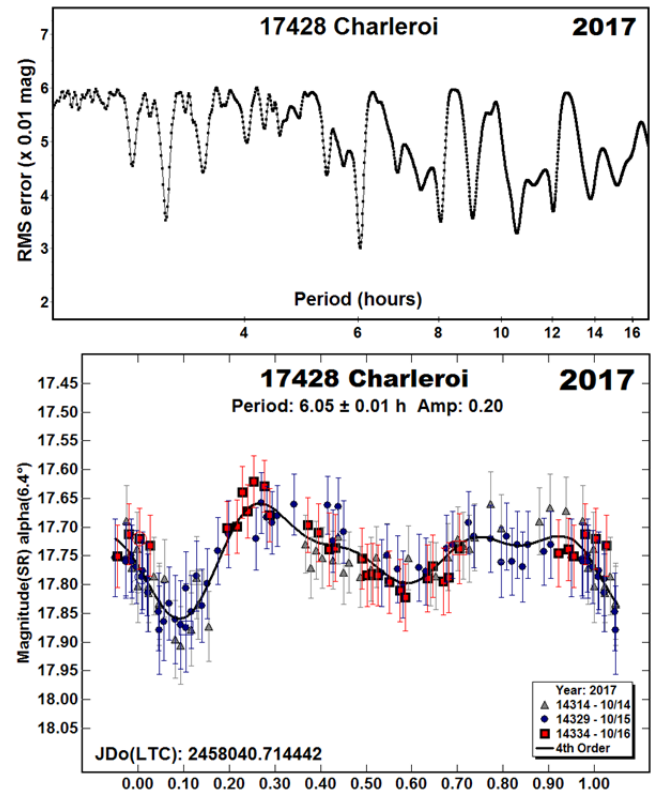
After going through re-analysis, the 2020 period spectrum no longer favored the 5.3-hour period; in fact, it's barely noticeable. Instead, a period of 5.994 h (2020 "B") was strongly favored. However, this produced an unusually-shaped lightcurve with gaps in coverage, raising the possibility of a *fit by exclusion*. A more "normal" lightcurve was found at a period of 4.791 h, or nearly an exact 5:4 ratio between the two periods.

The period spectrum from 2016 September dataset still favors 5.990 h (2016 "B") but a solution of 4.793 h (2016 "A") is a nearly-equal possibility. The lightcurve for the longer period has more complete coverage but the shape of the two is very similar: there is no obvious choice for which period is the correct solution.



The dataset from 2017 October was sparse, covered only three days, and was noisy. It would seem the least likely to resolve the ambiguities but a period near 6 h was the only possibility. A fit to 4.8 h was not worth recording, let alone considering.

A similar argument to the one used for 1529 Oterma applies here when choosing a period to adopt for this work, i.e., to adopt a period that is supported by all datasets despite the hard-to-resolve ambiguities that appear in some datasets. Our preference is the 5.990 h derived from the 2017 dataset since it is based on the densest dataset and provides complete coverage of the lightcurve.



It should go without saying that data from at least one other station at a much different longitude might have resolved any ambiguities. Such collaborations are encouraged, if possible.

Acknowledgements

Funding for observations at CS3 and work on the asteroid lightcurve database (Warner et al., 2009) and ALCDEF database (*alcdef.org*) are supported by NASA grant 80NSSC18K0851. This work includes data from the Asteroid Terrestrial-impact Last Alert System (ATLAS) project. ATLAS is primarily funded to search for near earth asteroids through NASA grants NN12AR55G, 80NSSC18K0284, and 80NSSC18K1575; byproducts of the NEO search include images and catalogs from the survey area. The ATLAS science products have been made possible through the contributions of the University of Hawaii Institute for Astronomy, the Queen's University Belfast, the Space Telescope Science Institute, and the South African Astronomical Observatory. The authors gratefully acknowledge Shoemaker NEO Grants from the Planetary Society (2007, 2013). These were used to purchase some of the telescopes and CCD cameras used in this research.

Number	Name	20yy/mm/dd	Phase	L <sub>PAB</sub>	B <sub>PAB</sub>	Period(h)	P.E.	Amp	A.E.
1529	Oterma	16/08/31-10/03	18.3, 14.8	55	-8	14.329 <sup>A</sup> 8.955	0.002 0.002	0.12 0.12	0.01 0.01
1529	Oterma	17/12/18-12/29	10.8, 8.3	127	4	14.320	0.002	0.13	0.01
1529	Oterma	20/05/23-06/08	7.8, 10.1	207	9	14.317 <sup>A</sup> 10.235	0.005 0.003	0.23 0.17	0.03 0.03
17428	Charleroi	16/09/23-09/28	*2.7, 2.5	4	9	5.990 <sup>A</sup> 4.793	0.002 0.002	0.11 0.11	0.01 0.01
17428	Charleroi	17/10/14-10/16	6.4, 6.0	47	5	6.05	0.01	0.20	0.02
17428	Charleroi	20/01/15-01/24	6.6, 4.5	186	-5	5.994 <sup>A</sup> 4.791	0.003 0.002	0.10 0.11	0.02 0.02

Table II. Observing circumstances. <sup>A</sup>Alternate period. The phase angle ( $\alpha$ ) is given at the start and end of each date range. L<sub>PAB</sub> and B<sub>PAB</sub> are the average phase angle bisector longitude and latitude (see Harris *et al.*, 1984).

#### References

- Dahlgren, M.; Lahulla, J.F.; Lagerkvist, C.-I.; Lagerros, J.; Mottola, S.; Erikson, A.; Gonano-Beurer, M.; Di Martino, M. (1998). "A Study of Hilda Asteroids. V. Lightcurves of 47 Hilda Asteroids." *Icarus* **133**, 247-285.
- Ditteon, R.; Adam, A.; Doyel, M.; Gibson, J.; Lee, S.; Linville, D.; Michalik, D.; Turner, R.; Washburn, K. (2018). "Lightcurve Analysis of Minor Planets Observed at the Oakley Southern Sky Observatory: 2016 October - 2017 March." *Minor Planet Bull.* **45**, 13-16.
- Harris, A.W.; Young, J.W.; Scaltriti, F.; Zappala, V. (1984). "Lightcurves and phase relations of the asteroids 82 Alkmene and 444 Gyptis." *Icarus* **57**, 251-258.
- Harris, A.W.; Pravec, P.; Galad, A.; Skiff, B.A.; Warner, B.D.; Vilagi, J.; Gajdos, S.; Carbognani, A.; Hornoch, K.; Kusnirak, P.; Cooney, W.R.; Gross, J.; Terrell, D.; Higgins, D.; Bowell, E.; Koehn, B.W. (2014). "On the maximum amplitude of harmonics on an asteroid lightcurve." *Icarus* **235**, 55-59.
- Rubincam, D.P. (2000). "Relative Spin-up and Spin-down of Small Asteroids." *Icarus* **148**, 2-11.
- Tonry, J.L.; Denneau, L.; Flewelling, H.; Heinze, A.N.; Onken, C.A.; Smartt, S.J.; Stalder, B.; Weiland, H.J.; Wolf, C. (2018). "The ATLAS All-Sky Stellar Reference Catalog." *Astrophys. J.* **867**, A105.
- Warner, B.D.; Harris, A.W.; Pravec, P. (2009). "The Asteroid Lightcurve Database." *Icarus* **202**, 134-146. Updated 2020 June. <http://www.minorplanet.info/lightcurvedatabase.html>
- Warner, B.D.; Stephens, R.D.; Coley, D.R. (2017a). "Lightcurve Analysis of Hilda Asteroids at the Center for Solar System Studies: 2016 June-September." *Minor Planet Bull.* **44**, 36-41.
- Warner, B.D.; Stephens, R.D.; Coley, D.R. (2017b). "Lightcurve Analysis of Hilda Asteroids at the Center for Solar System Studies: 2016 September-December." *Minor Planet Bull.* **44**, 130-137.
- Warner, B.D.; Stephens, R.D.; Coley, D.R. (2018). "Lightcurve Analysis of Hilda Asteroids at the Center for Solar System Studies: 2017 October-December." *Minor Planet Bull.* **45**, 147-161.

## PHOTOMETRIC OBSERVATIONS OF TWENTY-SEVEN MINOR PLANETS

Tom Polakis  
 Command Module Observatory  
 121 W. Alameda Dr.  
 Tempe, AZ 85282  
 tpolakis@cox.net

(Received: 2020 June 29 Revised: 2020 Aug 18)

Phased lightcurves and synodic rotation periods for 26 main-belt asteroids are presented, based on CCD observations made from 2020 March through 2020 June. A raw lightcurve is included for one asteroid for which no period solution was found. All the data have been submitted to the ALCDEF database.

CCD photometric observations of 27 main-belt asteroids were performed at Command Module Observatory (MPC V02) in Tempe, AZ. Images were taken using a 0.32-m f/6.7 Modified Dall-Kirkham telescope, SBIG STXL-6303 CCD camera, and a 'clear' glass filter. Exposure time for all the images was 2 minutes. The image scale after 2×2 binning was 1.76 arcsec/pixel. Table I shows the observing circumstances and results. All of the images for these 27 asteroids were obtained between 2020 March and 2020 June.

Images were calibrated using a dozen bias, dark, and flat frames. Flat-field images were made using an electroluminescent panel. Image calibration and alignment was performed using *MaxIm DL* software.

The data reduction and period analysis were done using *MPO Canopus* (Warner, 2017). The 45'×30' field of the CCD typically enables the use of the same field center for three consecutive nights. In these fields, the asteroid and three to five comparison stars were measured. Comparison stars were selected with colors within the range of  $0.5 < B-V < 0.95$  to correspond with color ranges of asteroids. In order to reduce the internal scatter in the data, the brightest stars of appropriate color that had peak ADU counts below the range where chip response becomes nonlinear were selected. *MPO Canopus* plots instrumental vs. catalog magnitudes for solar-colored stars, which is useful for selecting comp stars of suitable color and brightness.

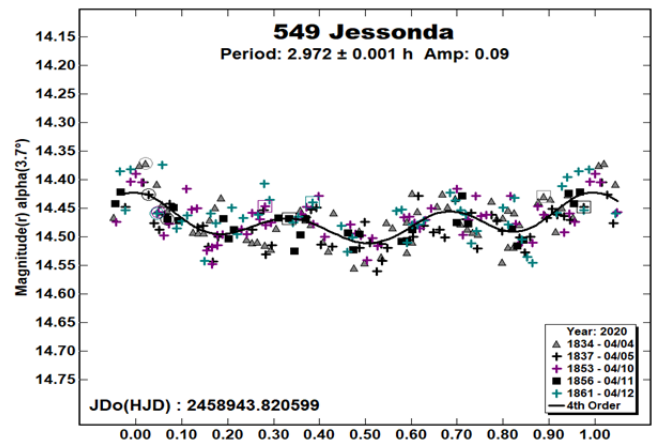
Since the sensitivity of the KAF-6303 chip peaks in the red, the clear-filtered images were reduced to Sloan  $r'$  to minimize error with respect to a color term. Comparison star magnitudes were obtained from the ATLAS catalog (Tonry et al., 2018), which is incorporated directly into *MPO Canopus*. The ATLAS catalog derives Sloan  $griz$  magnitudes using a number of available catalogs. The consistency of the ATLAS comp star magnitudes and color-indices allowed the separate nightly runs to be linked often with no zero-point offset required or shifts of only a few hundredths of a magnitude in a series.

A 9-pixel (16 arcsec) diameter measuring aperture was used for asteroids and comp stars. It was typically necessary to employ star subtraction to remove contamination by field stars. For the asteroids described here, I note the RMS scatter on the phased lightcurves, which gives an indication of the overall data quality including errors from the calibration of the frames, measurement

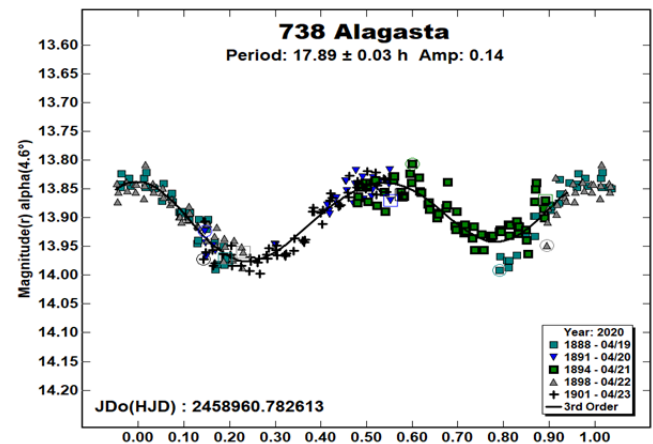
of the comp stars, the asteroid itself, and the period-fit. Period determination was done using the *MPO Canopus* Fourier-type FALC fitting method (cf. Harris et al., 1989). Phased lightcurves show the maximum at phase zero. Magnitudes in these plots are apparent and scaled by *MPO Canopus* to the first night.

Most asteroids were selected from the CALL website (Warner, 2011a) using the criteria of magnitude greater than 15.5 and quality of results, U, less than 2+. In this set of observations, 1 of the 27 asteroids had no previous period analysis, 1 had  $U = 1$ , and 24 had  $U = 2$ . The Asteroid Lightcurve Database (LCDB; Warner et al., 2009) was consulted to locate previously published results. All the new data for these asteroids can be found in the ALCDEF database.

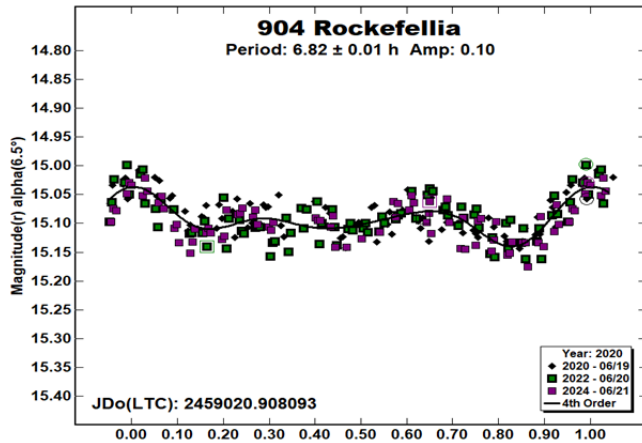
**549 JESSONDA.** Max Wolf discovered this asteroid in a highly eccentric orbit from Heidelberg in 1904. Three previous analyses produced similar periods: Behrend (2005),  $2.9709 \pm 0.0002$  h; Warner (2011b),  $2.971 \pm 0.001$  h; and Stephens (2015),  $2.962 \pm 0.002$  h. A total of 233 images were taken in five nights, resulting in a trimodal lightcurve with a synodic period of  $2.972 \pm 0.002$  h, agreeing with previous assessments. The amplitude is 0.09 mag, with an RMS error of 0.029 mag.



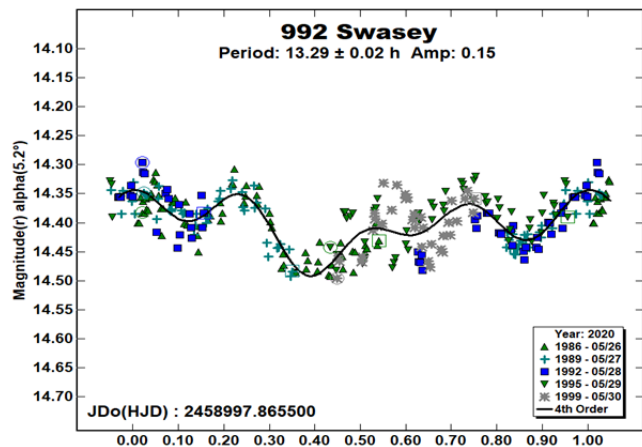
**738 ALAGASTA** was discovered at Heidelberg in 1913 by Franz Kaiser. Sada et al. (2005) published a period of  $17.83 \pm 0.04$  h, and Garceran et al. (2016) obtained  $18.86 \pm 0.01$  h. During five nights, 264 images were used to compute a period of  $17.89 \pm 0.03$  h, agreeing with Sada et al.'s value. The lightcurve has an amplitude of 0.14 mag, and an RMS error of 0.019 mag.



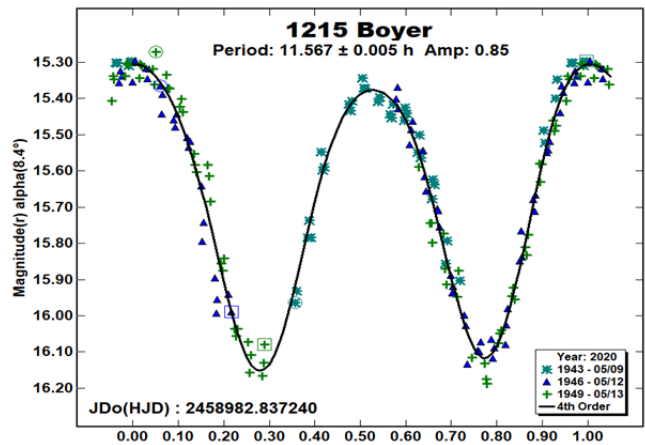
**904 Rockefeller.** This outer main-belt asteroid is another of Max Wolf's discoveries at Heidelberg. Many disagreeing periods are found in the LCDB. They include Fauvaud and Fauvaud (2013), with  $5.82 \pm 0.01$  h, Behrend (2004), who computed  $12.72 \pm 0.05$  h, and Polakis (2018) who calculated  $5.826 \pm 0.004$  h. Additionally, Polakis (2019) observed the asteroid on 13 nights around the 2019 opposition, and was unable to resolve a period. The 2020 opposition proved to be more favorable, and three nights and 239 data points were sufficient to produce a period solution of  $6.820 \pm 0.010$  h. The amplitude of the lightcurve is 0.10 mag, with an RMS error on the fit of 0.024 mag.



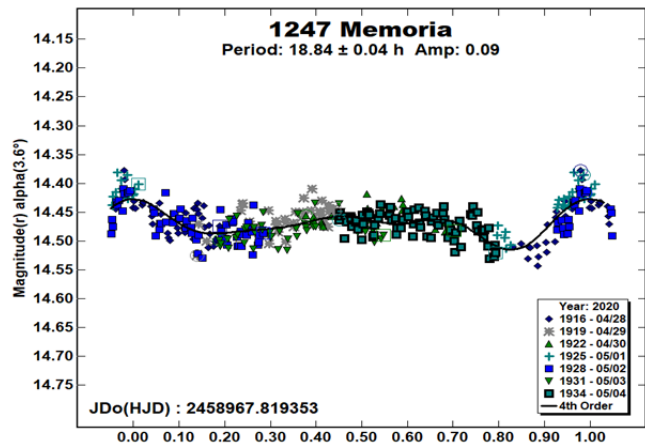
**992 Swasey.** Otto Struve discovered this Eos-family minor planet in 1922 from Williams Bay. Behrend (2004) computed a synodic period of  $13.308 \pm 0.003$  h, while Pál et al. (2020) published nearly double this value:  $26.3193 \pm 0.0005$  h. A total of 289 data points from five nights yielded a period of  $11.564 \pm 0.006$  h. The period spectrum did not show signals at either of the previous solutions. The amplitude is 0.15 mag, with an RMS error on the fit of 0.029 mag.



**1215 Boyer** is a Eunomia-family object with an inclination of  $16^\circ$ . Its discovery was made by Alfred Schmitt at Algiers in 1932. Kim et al. (2014) published a period of  $10.36 \pm 0.05$  h. During three nights, 169 images were sufficient to compute an unambiguous period of  $11.567 \pm 0.005$  h, which disagrees with Kim's value. The amplitude is  $0.85 \pm 0.046$  mag.



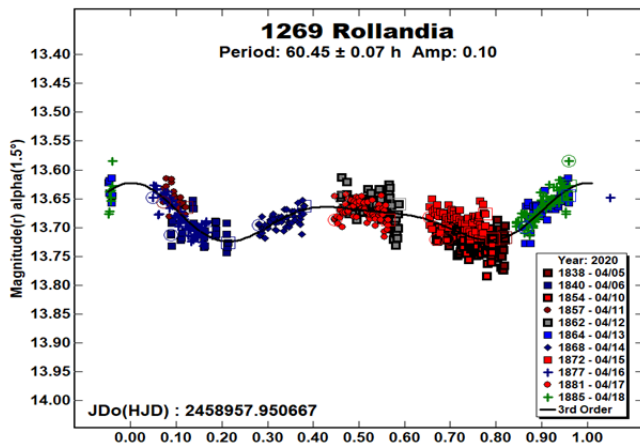
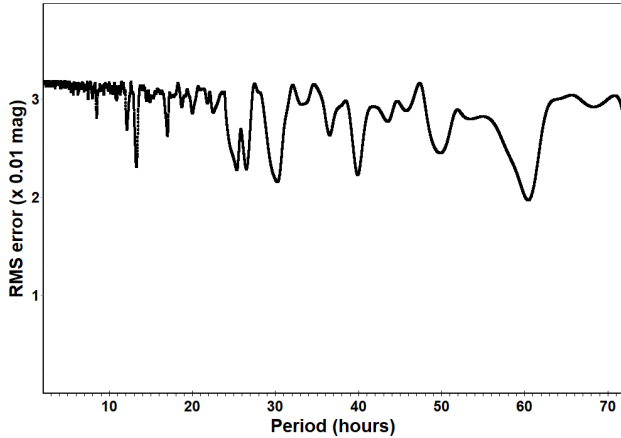
**1247 Memoria** is a Themis-family asteroid that came to a favorable opposition in 2020. It was discovered at Uccle in 1932 by Paul-Auguste-Ernest Laugier. The only period in the LCDB is that of Behrend (2019), who computed  $18.79 \pm 0.02$  h. In a seven-night interval, 351 images were gathered, producing a solution of  $18.840 \pm 0.040$  h, in agreement with Behrend. The amplitude of the lightcurve is  $0.09 \pm 0.021$  mag.



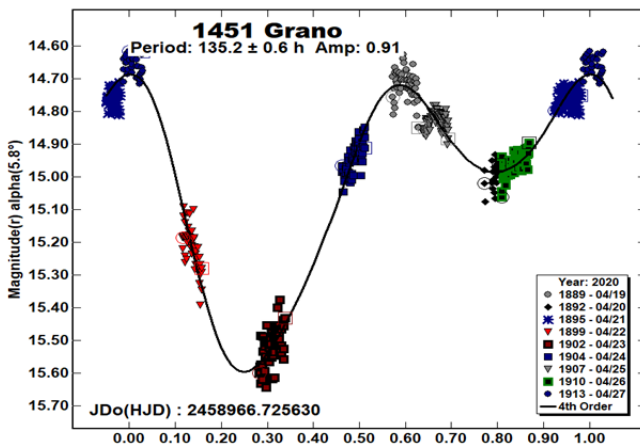
**1269 Rollandia** is a Hilda-family minor planet, discovered by Grigory Neujmin in 1930 at Simeis. Determining a rotation period has been problematic, with multiple authors yielding no clear solution. This is a partial list of unique periods that have been published in the past decade: Fauvaud and Fauvaud (2013),  $15.32 \pm 0.03$  h; Warner and Stephens (2017),  $19.98 \pm 0.02$  h; Polakis (2019),  $28.277 \pm 0.017$  h; and Warner and Stephens (2019);  $17.12 \pm 0.02$  h.

In an attempt to resolve the problem, the asteroid was observed at V02 on 11 nights, during which 698 images were obtained. The period spectrum shows multiple troughs, with the best bimodal solution landing at  $60.45 \pm 0.07$  h, which is yet another unique solution. The amplitude is 0.10 mag, with an RMS fit error of 0.025 mag.

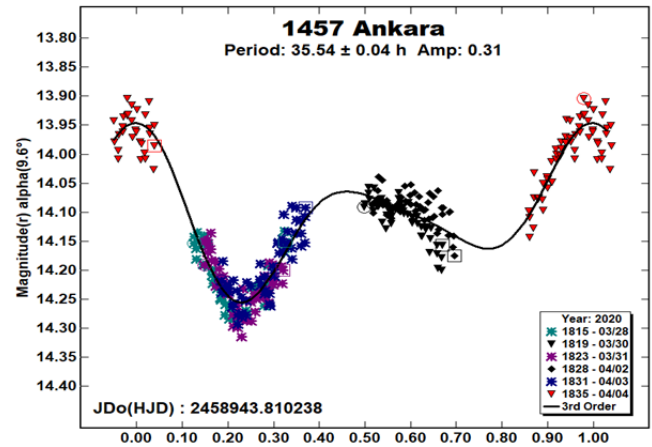
Period Spectrum: 1269 Rollandia



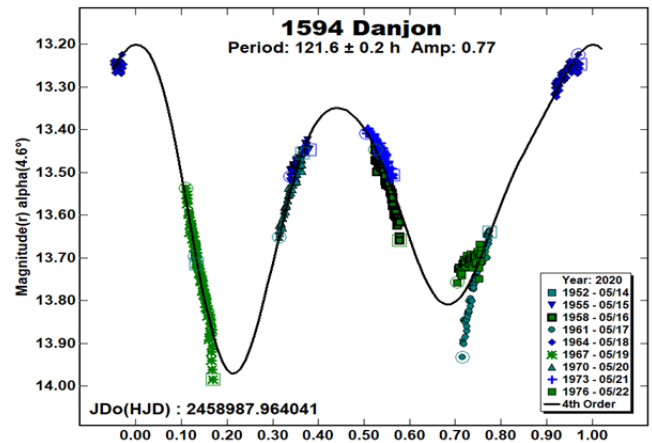
1451 Grano belongs to the Flora family. It was discovered at Turku in 1938 by Yrjö Väisälä. Behrend (2007) ascertained a period of  $5.109 \pm 0.004$  h, while Stephens (2010), observing for a longer interval, found a period of  $138 \pm 0.05$  h. The longer period appears to be better supported, as 485 data points over nine nights produced a synodic period of  $135.2 \pm 0.6$  h, with a large amplitude of  $0.91 \pm 0.043$  mag.



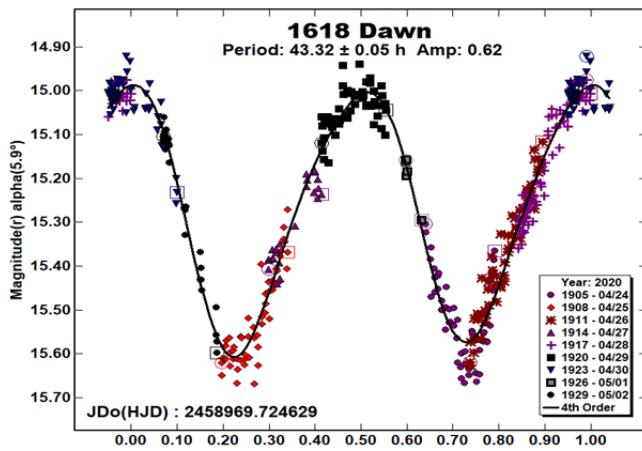
1457 Ankara was discovered at Heidelberg by Karl Reinmuth in 1937. The only period in the LCDB is that of Behrend (2004), who computed  $31.8 \pm 0.6$  h. During six nights, 317 images were used to ascertain a synodic period of  $35.54 \pm 0.05$  h. The amplitude is 0.31 mag, with an RMS error on the fit of 0.026 mag.



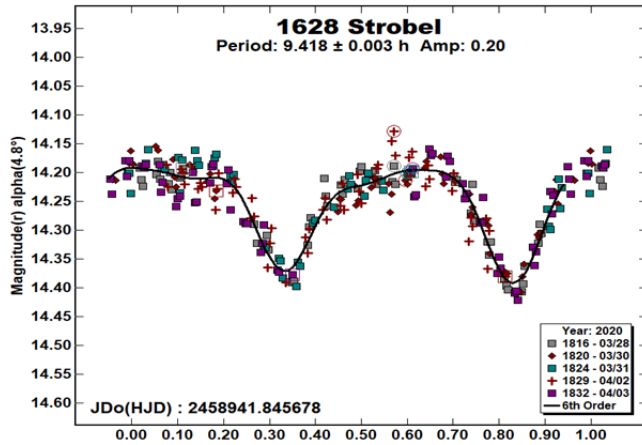
1594 Danjon is an inner-belt object with a high eccentricity of 0.20. Its discovery was made by Louis Boyer at Algiers in 1949. It is named after André-Louis Danjon, who created the familiar Danjon scale to gage the brightness of Earthshine. Behrend (2006) shows a period of  $>12$  h. During nine nights, 462 images were taken. The resulting period is  $121.6 \pm 0.2$  h, with an amplitude of  $0.77 \pm 0.032$  mag. The asteroid was followed for only  $1\frac{1}{2}$  rotations, and the trailing points away from the Fourier fit may indicate tumbling.



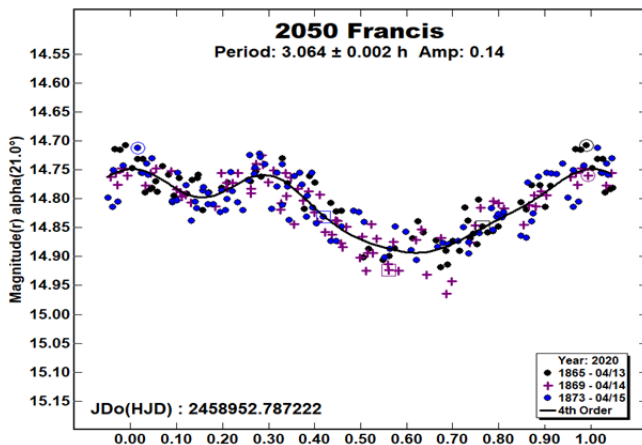
1618 Dawn is a member of the Karin family, which all share a similar orbit as 832 Karin. Five agreeing solutions appear in the LCDB. Slivan (2008) published a period of  $43.19 \pm 0.05$  h, Hanuš et al. (2013) calculated  $43.219 \pm 0.005$  h, and Waszczak et al. (2015) computed  $43.242 \pm 0.2574$  h. A total of 413 data points was gathered over nine nights to produce a period solution of  $43.64 \pm 0.04$  h, agreeing with previous assessments. The amplitude is 0.61 mag, with an RMS error of 0.043 mag.



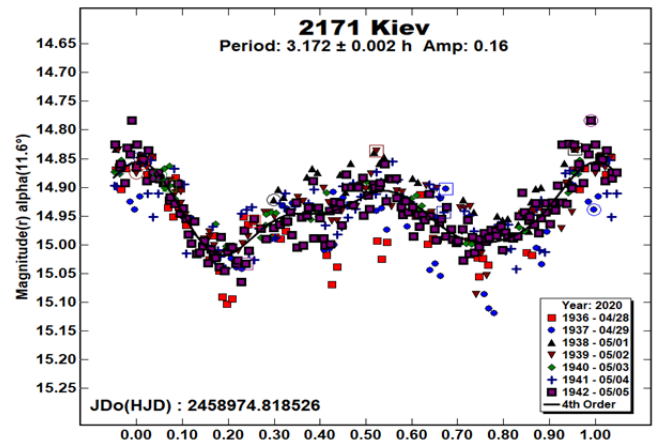
**1628 Strobel.** is another of Karl Reinmuth's discoveries, working from Heidelberg in 1923. Binzel (1987) produced a period solution of 11.80 h, and Behrend (2005) obtained  $9.52 \pm 0.01$  h. More recently, Pál et al. (2020) published a period of  $9.4244 \pm 0.0005$  h. During five nights, 279 images were gathered to compute a similar rotation period of  $9.418 \pm 0.003$  h. The amplitude is 0.20 mag, with an RMS error of 0.024 mag.



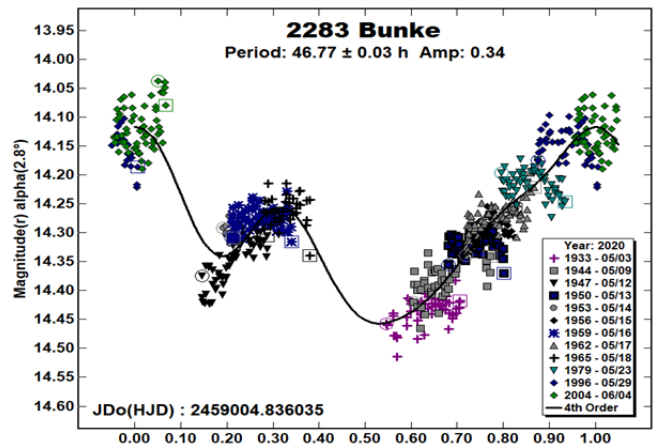
**2050 Francis.** Elanor Helin found this Phocaea-family asteroid in 1974 at Palomar. Franco et al. (2013) calculated a rotation period of  $3.069 \pm 0.001$  h, and Behrend (2020) obtained nearly double this period, with  $6.136 \pm 0.001$  h. After three nights, 234 images were obtained. The resulting bimodal solution is a period of  $3.064 \pm 0.002$  h. The amplitude of the lightcurve is  $0.14 \pm 0.027$  mag.



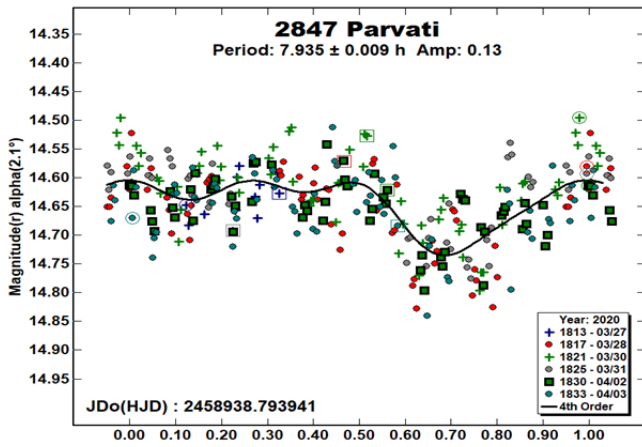
**2171 Kiev** is a Flora-family object in an eccentric orbit. It was discovered by Tamara Smirnova at Nauchnyj in 1973. No period solutions appear in the LCDB. Despite its short period, seven nights and 461 images were required to derive an acceptable solution of  $3.172 \pm 0.002$  h. The RMS error of the fit of  $0.036$  mag is significant relative to the amplitude of 0.16 mag.



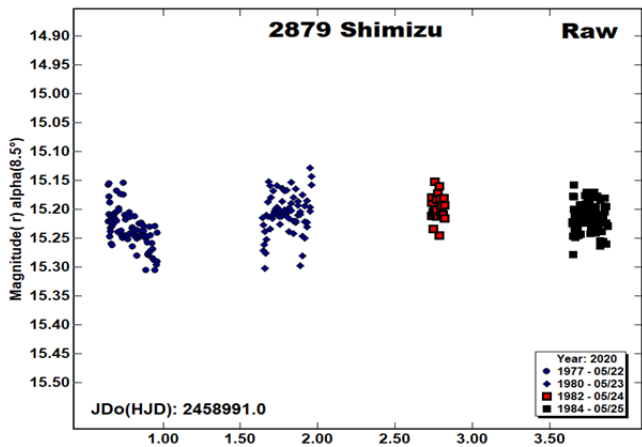
**2283 Bunke.** Irina Zhuravleva discovered this minor planet in 1974, working at Nauchnyj. Menke (2005) found a period of  $3.96 \pm 0.01$  h, and Kryszczyńska et al. (2012) published a period of  $4.3 \pm 0.1$  h. After 12 nights, data points were used to compute a rotation period of  $46.77 \pm 0.03$  h, disagreeing with past assessments. The amplitude of the lightcurve is  $0.34 \pm 0.04$  mag. The lightcurve is incomplete owing to commensurability with two earth rotations.



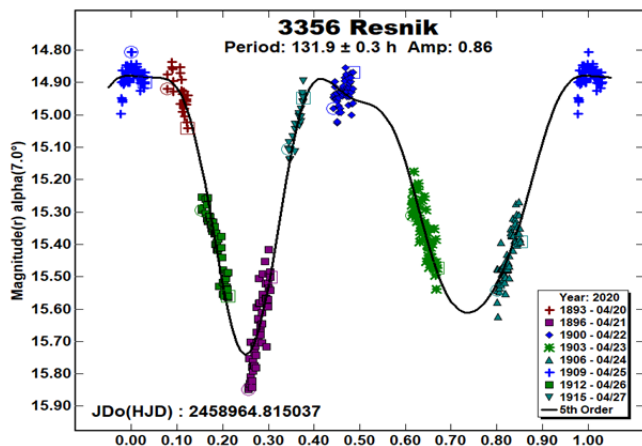
**2847 Parvati** was discovered at Lowell Observatory in Flagstaff in 1959. Two solutions in the LCDB are by Behrend (2018),  $22.757 \pm 0.002$  h; and Mas et al. (2018),  $2.640 \pm 0.003$  h. A total of 289 data points collected in six nights were taken. The resulting period solution is  $7.935 \pm 0.009$  h, disagreeing with both previous values. The amplitude is 0.13 mag, with a significant RMS error of 0.051 mag.



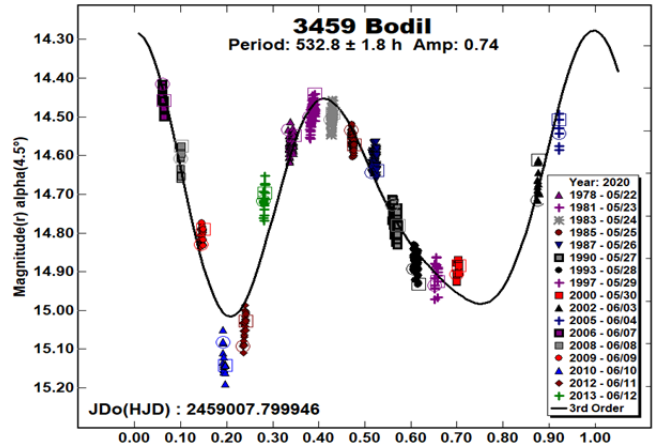
2879 Shimizu was discovered at Heidelberg in 1932 by Karl Reinmuth. Behrend (2006) gives a period of  $18.72 \pm 0.05$  h, while Pál et al. (2020) shows a result of  $55.3718 \pm 0.0005$  h. After reducing data from four nights with 249 data points, it became apparent that a period solution would not be achievable during this apparition. The raw lightcurve is presented.



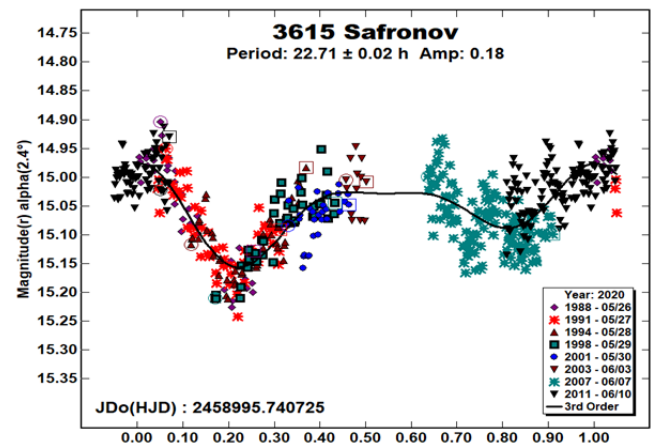
3356 Resnik was discovered in 1984 at Flagstaff by Edward Bowell, who named it after STS-51-L crew member Judith Resnik. The only period solution in the LCDB is that of Higgins (2008), who shows  $>32$  h. A total of 387 images were taken during nine nights, revealing it to be a slow rotator, with a synodic period of  $131.9 \pm 0.3$  h, and an amplitude of  $0.86 \pm 0.049$  mag.



3459 Bodil is a Flora-family minor planet in an eccentric orbit. It was discovered by Poul Jensen in 1986 from Brorfelde. The only period solution in the LCDB is that of Erasmus et al. (2020), who published  $52.572 \pm 0.231$  h. It was observed around its favorable opposition on 17 nights, during which 536 images were taken. The slow rotator has a synodic period of  $532.9 \pm 1.8$  h, with an amplitude of  $0.74 \pm 0.053$  mag.



3615 Safronov. Observing at Flagstaff in 1983, Edward Bowell found this Themis-family asteroid. The only period in the LCDB belongs to Chang et al. (2014), who shows  $>16$  h. A total of 499 images taken during eight nights were used to secure a rotation period of  $22.71 \pm 0.02$  h. The amplitude is 0.18 mag, with an RMS error on the fit of 0.042 mag.

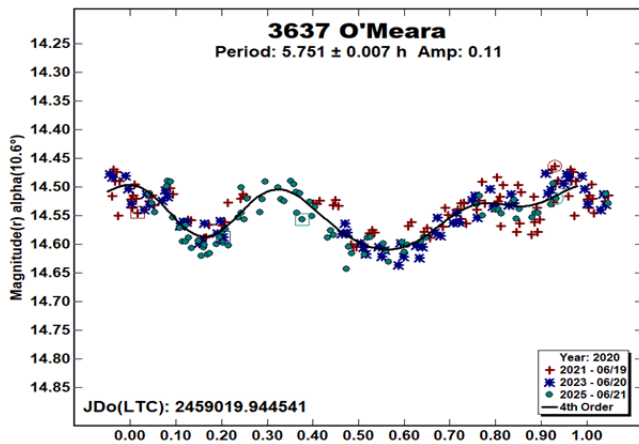


3637 O'Meara is a minor planet in the Eunomia family. The discovery was made at Flagstaff in 1984 by Brian Skiff, who named it after the prolific amateur astronomer and author Steven O'Meara. Aznar Macias (2017) published a rotation period of  $4.118 \pm 0.25$  h, and Pál et al. (2020) computed  $5.77146 \pm 0.00005$  h. Aznar Macias' analysis, based on his dense dataset taken over a range of 24 days, suggested that the object may be a binary asteroid.

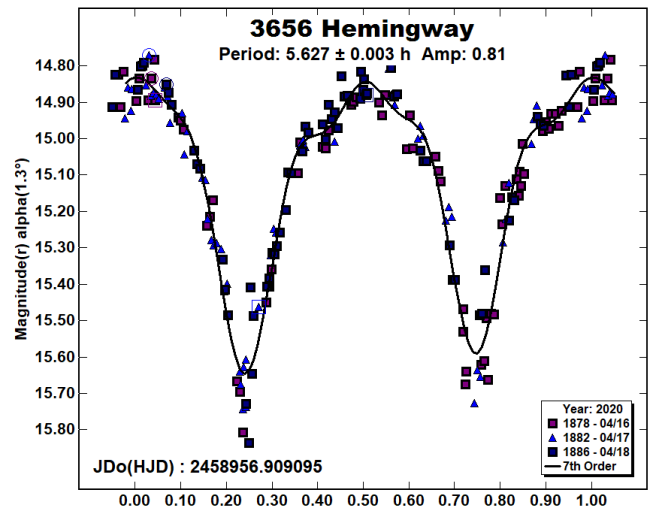
During three nights, 213 images were taken, yielding a period of  $5.751 \pm 0.007$  h, agreeing with Pál's value. The amplitude of the lightcurve is  $0.11 \pm 0.023$  mag. While this dataset used less images and covered only three nights, the period spectrum and resulting lightcurve do not support the binary nature suggested by Aznar Macias.

Number	Name	2020/mm/dd	Phase	L <sub>PAB</sub>	B <sub>PAB</sub>	Period(h)	P.E.	Amp	A.E.	Grp
549	Jessonda	04/04-04/12	3.7, 6.8	189	-5	2.972	0.001	0.09	0.03	MB-M
738	Alagasta	04/19-04/23	4.6, 3.2	220	4	17.89	0.03	0.14	0.02	MB-O
904	Rockefellia	06/19-06/21	6.5, 6.4	271	18	6.820	0.010	0.10	0.02	MB-O
992	Swasey	05/26-05/30	5.2, 6.6	235	6	13.29	0.02	0.15	0.03	EOS
1215	Boyer	05/03-05/13	8.0, 8.9	223	20	11.567	0.005	0.85	0.05	EUN
1247	Memoria	04/28-05/04	3.6, 1.4	227	2	18.840	0.040	0.09	0.02	THM
1269	Rollandia	04/05-04/18	*1.5, 3.2	199	3	60.45	0.07	0.10	0.03	HIL
1451	Grano	04/19-04/27	5.8, 3.6	217	5	135.2	0.60	0.91	0.04	FLOR
1457	Ankara	03/28-04/04	9.6, 12.5	170	-7	35.54	0.05	0.31	0.03	MB-M
1594	Danjon	05/14-05/22	*4.6, 1.7	240	2	121.6	0.2	0.77	0.03	MB-I
1618	Dawn	04/24-05/02	5.9, 8.9	201	4	43.64	0.04	0.61	0.04	KAR
1628	Strobel	03/28-04/03	4.8, 7.2	176	-1	9.418	0.003	0.20	0.02	MB-O
2050	Francis	04/13-04/15	21.0, 21.0	202	31	3.064	0.002	0.14	0.03	PHO
2171	Kiev	04/28-05/05	11.6, 8.5	234	9	3.172	0.002	0.16	0.04	FLOR
2283	Bunke	05/03-06/04	2.8, 16.9	224	5	46.77	0.03	0.34	0.04	FLOR
2847	Parvati	03/27-04/03	2.1, 5.2	186	-3	7.935	0.009	0.13	0.05	FLOR
2879	Shimizu	05/22-05/25	8.5, 9.3	231	14	--	--	--	--	MB-O
3356	Resnik	04/19-04/27	7.5, 4.2	219	6	131.9	0.3	0.86	0.05	FLOR
3459	Bodil	05/22-06/12	*4.7, 9.6	247	4	532.9	1.8	0.74	0.05	FLOR
3615	Safronov	05/26-06/10	2.4, 8.2	241	3	22.71	0.02	0.18	0.04	THM
3637	O'Meara	06/19-06/21	10.6, 10.5	273	18	5.751	0.007	0.11	0.02	EUN
3656	Hemingway	04/16-04/18	1.3, 0.8	208	-1	5.627	0.003	0.81	0.06	MB-I
4041	Miyamotoyohko	05/19-05/21	7.4, 7.9	225	11	5.142	0.004	0.23	0.03	EOS
4353	Onizaki	05/09-05/13	4.7, 5.9	226	7	4.429	0.001	0.36	0.03	MB-I
4570	Runcorn	04/04-04/18	11.4, 18.6	178	-2	233.4	0.5	1.35	0.08	FLOR
7910	Aleksola	05/14-05/18	6.2, 5.4	239	7	6.440	0.008	0.17	0.03	MB-I
15710	Bocklin	05/19-05/21	6.6, 6.4	240	9	7.516	0.004	0.77	0.04	FLOR

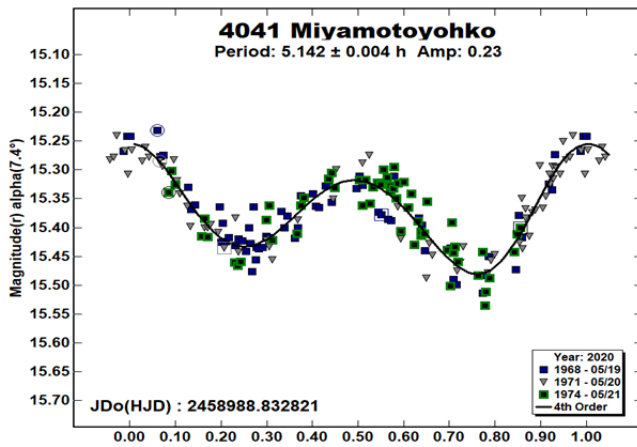
Table I. Observing circumstances and results. The phase angle is given for the first and last date. If preceded by an asterisk, the phase angle reached an extrema during the period. L<sub>PAB</sub> and B<sub>PAB</sub> are the approximate phase angle bisector longitude/latitude at mid-date range (see Harris et al., 1984). Grp is the asteroid family/group (Warner et al., 2009).



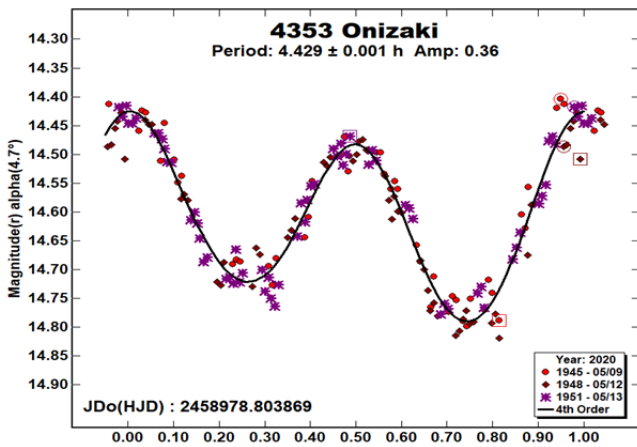
3656 Hemingway was discovered by Lyudmila Chernykh at Nauchnyj in 1978. Two similar periods appear in the LCDB: Waszczak et al. (2015),  $5.626 \pm 0.052$  h and Durech et al. (2018),  $5.63027 \pm 0.00002$  h. During three consecutive nights, 190 data points were sufficient to ascertain a rotation period of  $5.627 \pm 0.003$  h, in agreement with previously published values. The lightcurve has an amplitude of  $0.81 \pm 0.062$  mag.



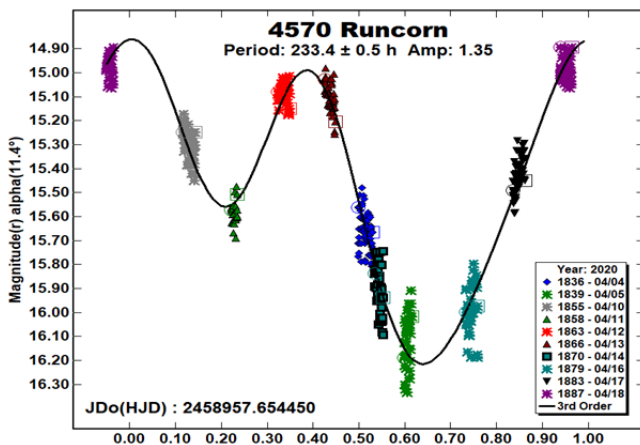
4041 Miyamotoyohko was discovered by Takuo Kojima at Chiyoda in 1988. Behrend (2015) shows a period of  $7.694 \pm 0.001$  h. During three nights in 2020 May, 187 images were collected, and a synodic period of  $5.142 \pm 0.004$  h was computed, disagreeing with Behrend's result. The lightcurve's amplitude is 0.23 mag, with an RMS error on the fit of 0.027 mag.



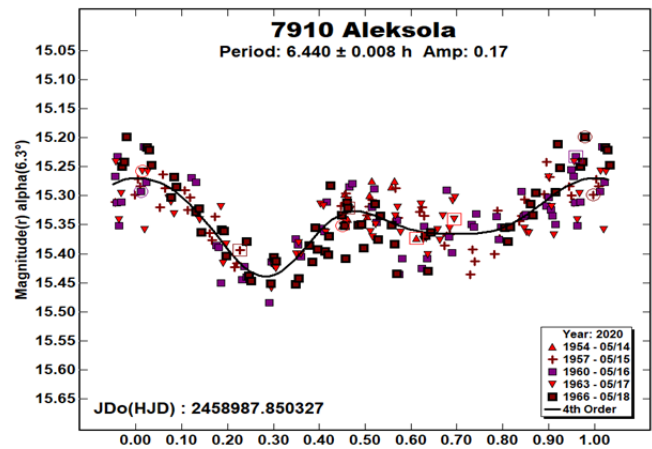
4353 Onizaki was discovered by Mizuno and Furuta at Kani in 1989. Waszczak et al. (2015) computed a period of  $4.429 \pm 0.0273$  h, and Pravec et al. (2020) calculated  $4.4296 \pm 0.0002$  h. A total of 165 images were used to acquire a rotation period of  $4.429 \pm 0.001$  h, agreeing with previous values. The amplitude is  $0.36 \pm 0.028$  mag.



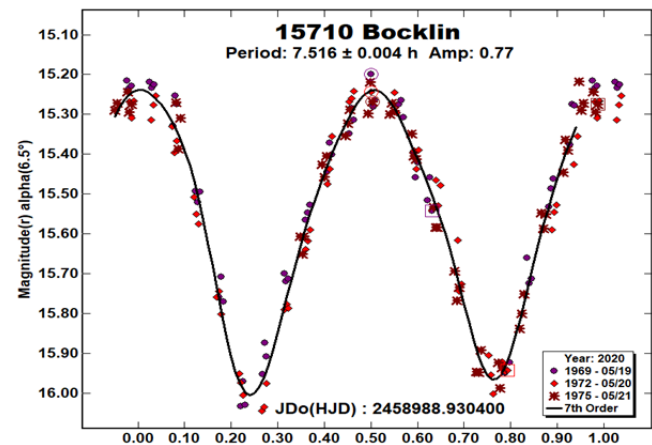
4570 Runcorn is a Flora-family asteroid discovered by Edward Bowell in 1985 from Flagstaff. Hanuš et al. (2016) published a period of  $20.1514 \pm 0.0005$  h. This slow rotator required ten nights and 451 images to obtain a period solution of  $233.4 \pm 0.5$  h, disagreeing with that of Hanuš. The amplitude is  $1.35 \pm 0.077$  mag. Signal-to-noise ratio became a concern around its minimum magnitude of  $r' \sim 16$ , which is typically beyond the practical range of this telescope and sky conditions.



7910 Aleksola was discovered by Nikolai Chernykh from Crimea in 1976. Pál et al. (2020) published a period of  $6.41852 \pm 0.00005$  h. During five nights, 219 images were obtained. They produced a period solution of  $6.440 \pm 0.008$  h, agreeing with Pál's value. The lightcurve has an amplitude of  $0.17 \pm 0.034$  mag.



15710 Bocklin. This Flora-family minor planet was found by Freimut Borngen at Tautenburg in 1989. Durech et al. (2018) shows a period of  $7.52272 \pm 0.00002$  h, and Erasmus et al. (2020) published  $7.521 \pm 0.005$  h. During three nights, 160 images were gathered, and used to compute a synodic period of  $7.516 \pm 0.004$  h, agreeing with previous assessments. The lightcurve has an amplitude of 0.77 mag, with an RMS error on the fit of 0.042 mag.



#### Acknowledgements

The author would like to express his gratitude to Brian Skiff for his indispensable mentoring in data acquisition and reduction. Thanks also go out to Brian Warner for support of his *MPO Canopus* software package.

#### References

Aznar Macias, A. (2017). "3637 O'Meara: New Binary Candidate." *Minor Planet Bull.* **44**, 59-60.

Behrend, R. (2004, 2005, 2006, 2007, 2015, 2018, 2019, 2020). Observatoire de Geneve web site.

[http://obswww.unige.ch/~behrend/page\\_cou.html](http://obswww.unige.ch/~behrend/page_cou.html)

- Binzel, R.P. (1987). "A photoelectric survey of 130 asteroids." *Icarus* **72**, 135-208.
- Chang, C.-K.; Ip, W.-H.; Lin, H.-W.; Cheng, Y.-C.; Ngeow, C.-C.; Yang, T.-C.; Waszczak, A.; Kulkarni, S.R.; Levitan, D.; Sesar, B. (2014). "313 New Asteroid Rotation Periods from Palomar Transient Factory Observations." *Astrophys. J.* **788**, A17.
- Durech, J.; Hanuš, J.; Ali-Lagoa, V. (2018). "Asteroid models reconstructed from the Lowell Photometric Database and WISE data." *Astron. Astrophys.* **617**, A57.
- Erasmus, N.; Navarro-Meza, S.; McNeill, A.; Trilling, D.E.; Sickafoose, A.; Denneau, L.; Flewelling, H.; Heinze, A.; Tonry, J.L. (2020). "Investigating Taxonomic Diversity within Asteroid Families through ATLAS Dual-band Photometry." *Ap. J. Suppl. Ser.* **247**, A13.
- Fauvaud, S.; Fauvaud, M. (2013). "Photometry of Minor Planets. I. Rotation Periods from Lightcurve Analysis for Seven Main-belt Asteroids." *Minor Planet Bull.* **40**, 224-229.
- Franco, L.; Tomassini, A.; Scardella, M. (2013). "Rotational Period of Asteroid Francis." *Minor Planet Bull.* **40**, 197.
- Garceran, A.C.; Aznar, A.; Mansego, E.A.; Rodriguez, P.B.; de Haro, J.L.; Silva, A.F.; Silva, G.F.; Martinez, V.M.; Chiner, O.R. (2016). "Nineteen Asteroids Lightcurves at Asteroids Observers (OBAS) - MPPD: 2015 April - September." *Minor Planet Bull.* **43**, 92-97.
- Hanuš, J.; Brož, M.; Durech, J.; Warner, B.D.; Brinsfield, J.; Durkee, R.; Higgins, D.; Koff, R.A.; Oey, J.; Pilcher, F.; Stephens, R.; Strabla, L.P.; Ullisse, Q.; Girelli, R. (2013). "An anisotropic distribution of spin vectors in asteroid families." *Astron. Astrophys.* **559**, A134.
- Hanuš, J.; Durech, J.; Oszkiewicz, D.A.; Behrend, R.; Carry, B.; and 164 authors (2016). "New and updated convex shape models of asteroids based on optical data from a large collaboration network." *Astron. Astrophys.* **586**, A108.
- Harris, A.W.; Young, J.W.; Scaltriti, F.; Zappala, V. (1984). "Lightcurves and phase relations of the asteroids 82 Alkmene and 444 Gypsis." *Icarus* **57**, 251-258.
- Harris, A.W.; Young, J.W.; Bowell, E.; Martin, L.J.; Millis, R.L.; Poutanen, M.; Scaltriti, F.; Zappala, V.; Schober, H.J.; Debehogne, H.; Zeigler, K.W. (1989). "Photoelectric Observations of Asteroids 3, 24, 60, 261, and 863." *Icarus* **77**, 171-186.
- Higgins, D. (2008). "Asteroid Lightcurve Analysis at Hunters Hill Observatory and Collaborating Stations: April 2007 - June 2007." *Minor Planet Bull.* **35**, 30-32.
- Kim, M.-J.; Choi, Y.-J.; Moon, H.-K.; Byun, Y.-I.; Brosch, N.; Kaplan, M.; Kaynar, S.; Uysal, O.; Guzel, E.; Behrend, R.; Yoon, J.-N.; Mottola, S.; Hellmich, S.; Hinse, T.C.; Eker, Z.; Park, J.-H. (2014). "Rotational Properties of the Maria Asteroid Family." *Astron. J.* **147**, A56.
- Kryszczynska, A.; Colas, F.; Polinska, M.; Hirsch, R.; Ivanova, V.; Apostolovska, G.; Bilkina, B.; Velichko, F.P.; Kwiatkowski, T.; Kankiewicz, P. and 20 coauthors. (2012). "Do Slivan states exist in the Flora family? I. Photometric survey of the Flora region." *Astron. Astrophys.* **546**, A72.
- Mas, V.; Fornas, G.; Lozano, J.; Rodrigo, O.; Fornas, A.; Carreño, A.; Arce, E.; Brines, P.; Herrero, D. (2018). "Twenty-one Asteroid Lightcurves at Asteroids Observers (OBAS) - MPPD: Nov 2016 - May 2017." *Minor Planet Bull.* **45**, 76-82.
- Menke, J. (2005). "Lightcurves and periods for asteroids 471 Papagena, 675 Ludmilla, 1016 Anitra, 1127 Mimi, 1165 Imprinetta, 1171 Rustahawelia, and 2283 Bunke." *Minor Planet Bull.* **32**, 64-66.
- Pál, A.; Szakáts, R.; Kiss, C.; Bódi, A.; Bognár, Z.; Kalup, C.; Kiss, L.L.; Marton, G.; Molnár, L.; Plachy, E.; Sárneczky, K.; Szabó, G.M.; Szabó, R. (2020). "Solar System Objects Observed with TESS—First Data Release: Bright Main-belt and Trojan Asteroids from the Southern Survey." *Ap. J. Suppl. Ser.*, in press; arXiv:2001.05822v1.
- Polakis, T. (2018). "Lightcurve Analysis for Eleven Main-belt Asteroids." *Minor Planet Bull.* **45**, 199-203.
- Polakis, T. (2019). "Lightcurves of Twelve Main-Belt Minor Planets." *Minor Planet Bull.* **46**, 287-292.
- Pravec, P.; Wolf, M.; Sarounova, L. (2020). Ondrejov Asteroid Photometry Project. <http://www.asu.cas.cz/~ppravec/neo.htm>
- Sada, P.V.; Canizales, E.D.; Armada, E.M. (2005). "CCD photometry of asteroids 651 Antikleia, 738 Alagasta, and 2151 Hadwiger using a remote commercial telescope." *Minor Planet Bull.* **32**, 73-75.
- Slivan, S.M.; Binzel, R.P.; Boroumand, S.C.; Pan, M.W.; Simpson, C.M.; Tanabe, J.T.; Villastrigo, R.M.; Yen, L.L.; Ditteon, R.P.; Pray, D.P.; Stephens, R.D. (2008). "Rotation rates in the Koronis family, complete to  $H \approx 11.2$ ." *Icarus* **195**, 226-276.
- Stephens, R.D. (2010). "Asteroids Observed from GMARS and Santana Observatories: 2010 April - June." *Minor Planet Bull.* **37**, 159-161.
- Stephens, R.D. (2015). "Asteroids Observed from CS3: 2014 October - December." *Minor Planet Bull.* **42**, 104-106.
- Tonry, J.L.; Denneau, L.; Flewelling, H.; Heinze, A.N.; Onken, C.A.; Smartt, S.J.; Stalder, B.; Weiland, H.J.; Wolf, C. (2018). "The ATLAS All-Sky Stellar Reference Catalog." *Astrophys. J.* **867**, A105.
- Warner, B.D.; Harris, A.W.; Pravec, P. (2009). "The Asteroid Lightcurve Database." *Icarus* **202**, 134-146. Updated 2020 June. <http://www.minorplanet.info/lightcurvedatabase.html>
- Warner, B.D. (2011a). Collaborative Asteroid Lightcurve Link website. <http://www.minorplanet.info/call.html>
- Warner, B.D. (2011b). "Upon Further Review: VI. An Examination of Previous Lightcurve Analysis from the Palmer Divide Observatory." *Minor Planet Bull.* **38**, 96-101.
- Warner, B.D. (2017). *MPO Canopus* software. <http://bdwpublishing.com>
- Warner, B.D.; Stephens, R.D. (2017). "Lightcurve Analysis of Hilda Asteroids at the Center for Solar System Studies: 2016 June-September." *Minor Planet Bull.* **44**, 36-41.
- Warner, B.D.; Stephens, R.D. (2019). "Lightcurve Analysis of Hilda Asteroids at the Center for Solar System Studies: 2019 April-June." *Minor Planet Bull.* **46**, 406-412.
- Waszczak, A.; Chang, C.-K.; Ofek, E.O.; Laher, R.; Masci, F.; Levitan, D.; Surace, J.; Cheng, Y.-C.; Ip, W.-H.; Kinoshita, D.; Helou, G.; Prince, T.A.; Kulkarni, S. (2015). "Asteroid Light Curves from the Palomar Transient Factory Survey: Rotation Periods and Phase Functions from Sparse Photometry." *Astron. J.* **150**, A75.

## A SEARCH FOR MUTUAL ECLIPSE EVENTS OF THE ASYNCHRONOUS BINARY ASTEROID 1016 ANITRA

Kim Lang  
Klokkeholm Observatory  
Blomstervaenget 15, DK-9320 Klokkeholm  
DENMARK  
kim\_lang@kila-astro.dk

(Received: 2020 July 15 Revised: 2020 August 22)

Asteroid 1016 Anitra was observed extensively between 2020 March 13 and April 24. Mutual eclipse events were searched for but none were observed. Data are analyzed in two sub sets. The March subset found two bimodal lightcurves with periods and amplitudes of  $P_1 = 5.9292 \pm 0.0002$  h,  $A_1 = 0.30$  mag and  $P_2 = 2.6092 \pm 0.0002$  h,  $A_2 = 0.11$  mag. The April subset found  $P_1 = 5.9281 \pm 0.0002$  h,  $A_1 = 0.34$  mag and  $P_2 = 2.6091 \pm 0.0001$  h,  $A_2 = 0.11$  mag.

Numerous photometric investigations have been made of 1016 Anitra: Alkema (2013; 5.929 hours), Kryszyńska et al. (2012; 5.9288 h), Menke (2005; 5.930 h), Pray et al. (2006; 5.928 h), Schmidt (2016; 5.9301 h), and KlingleSmith III et al. (2017; 5.9295 h). Amplitudes ranged from 0.28 to 0.50 mag. Pilcher et al. (2016), of which this author was a coauthor, demonstrated that the lightcurves of Anitra are two strictly additive components of periods  $P_1 = 5.92951$  h,  $A_1 = 0.30$  mag and  $P_2 = 2.069143$  h,  $A_2 = 0.10$  mag. Petr Pravec demonstrated in Pilcher et al. (2016) that there is no signal in the linear combinations of the two frequencies, which might indicate that the asteroid is “tumbling”, *i.e.*, in non-principal axis rotation (NPAR). Thus, Anitra is likely an asynchronous binary. The orbital period of asynchronous binary asteroids is expected to be long (tens of hours) and the chances for observing mutual eclipse events are slim. These mutual eclipse events are deemed necessary to prove the binary nature of a suspected asynchronous binary. Benishek, also a coauthor of Pilcher et al. (2016), had observations of possible mutual eclipse events but unfortunately none of the other observers had data that could confirm these observations.

All observations reported here are made without filters and unbinned. Exposure times were 100 or 150 s. A 0.35-m Newtonian f/4.5 telescope was used with a Moravian G2-3200 camera and Wynne-Riccardi coma corrector. The mount was a friction drive model Mesu-200, a German equatorial type. The camera was thermoelectrical cooled to  $-30$  °C and all images were unfiltered and calibrated with a master dark of same exposure length as the science frames and a master flat using *Astro Art 7.0*. During calibration the time-series was not aligned to avoid interpolation of pixel intensities prior to analysis which was done with *MPO Canopus v.10.8.1.1* (Warner, 2019). The Comp Star Selector utility in *MPO Canopus* found up to five comparison stars of near solar-color in (V-R) for differential photometry.

Catalog magnitudes were taken from the ATLAS catalog (Tonry et al., 2018). Adjustments of the nightly zero points are small and usually less than  $\pm 0.03$  when using the ATLAS catalog. Period analysis is done with *MPO Canopus 10.8*, which implements the FALC algorithm by Harris (Harris et al., 1989). The same algorithm is used in an iterative fashion, as in the case of Anitra, there is more than one period.

The apparition of 1016 Anitra (opposition on 2020-03-05.6) was anticipated with aspiration of detecting mutual eclipse events. From March 13<sup>th</sup> to April 24<sup>th</sup> some 2382 exposures with 76.8 hours of open shutter time were accumulated. The observatory of this author is located at latitude 57° North so from the end of twilight to airmass of 2 no single lightcurve was longer than 3.8 h. The final analysis consists of two sets of phased plots one for each rotational period  $P_1$  and  $P_2$ . Figures 1 and 2 are for the March subset and Figures 3 and 4 are for the April subset. A residual plot after subtraction of both periods is shown in Figure 5 for the April subset demonstrates that there is no trace of mutual eclipse events detected above the noise level of 15 and 16 millimagnitudes respectively. A residual plot for the March subset is equally disappointing and the reader is spared the view.

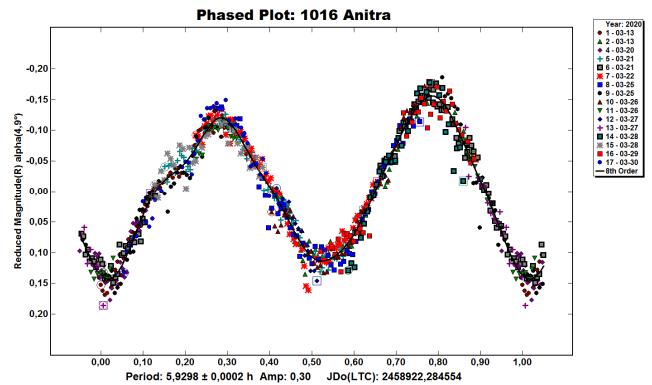


Figure 1. Lightcurve of primary period ( $P_1$ ) for the interval 2020 Mar 13 to 30. Phase angle between  $4.90^\circ$  and  $12.6^\circ$ .

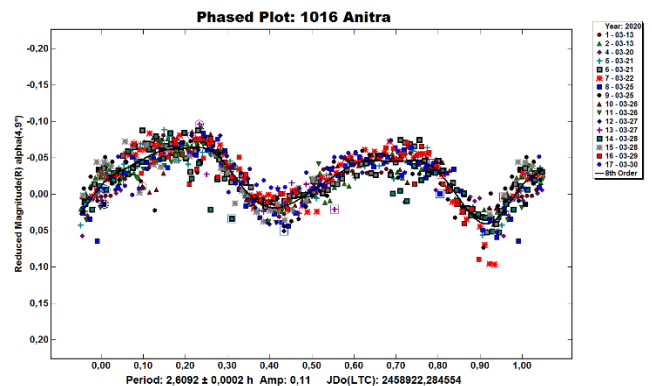


Figure 2. Lightcurve of secondary period ( $P_2$ ) for the interval 2020 March 13 to 30.

Number	Name	2020 mm/dd	Phase	$L_{PAB}$	$B_{PAB}$	Period(h)	P.E.	Amp	A.E.	Grp
1016	Anitra	2020 03/13-03/30	4.90,12.6	165	3	5.9298	0.0002	0.30	0.02	MB-M
						2.6092	0.0002	0.11	0.02	
1016	Anitra	2020 04/09-04/24	16.6,21.4	168	1	5.9281	0.0002	0.34	0.02	
						2.6091	0.0001	0.11	0.02	

Table I. Observing circumstances and results. The phase angle is given for the first and last date. If preceded by an asterisk, the phase angle reached an extrema during the period.  $L_{PAB}$  and  $B_{PAB}$  are the approximate phase angle bisector longitude/latitude at mid-date range (see Harris et al., 1984). Grp is the asteroid family/group (Warner et al., 2009).

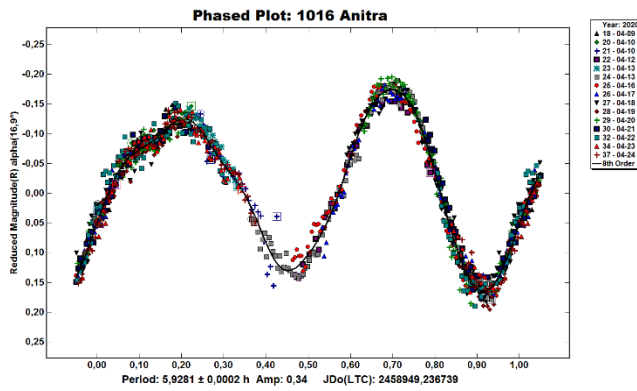


Figure 3. Lightcurve of primary period (P1) for the interval 2020 April 9 to 24. Phase angle between 16.6° and 21.4°.

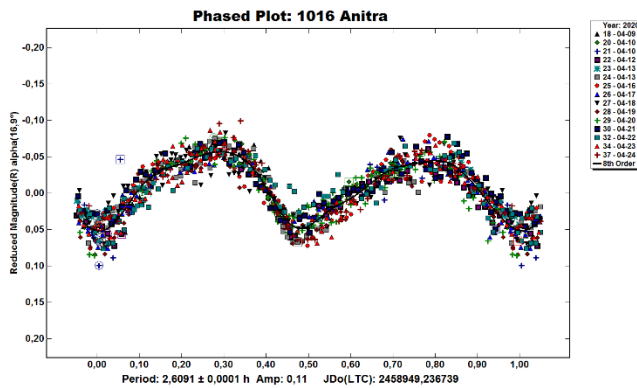


Figure 4. Lightcurve of secondary period (P2) for the interval 2020 April 9 to 24.

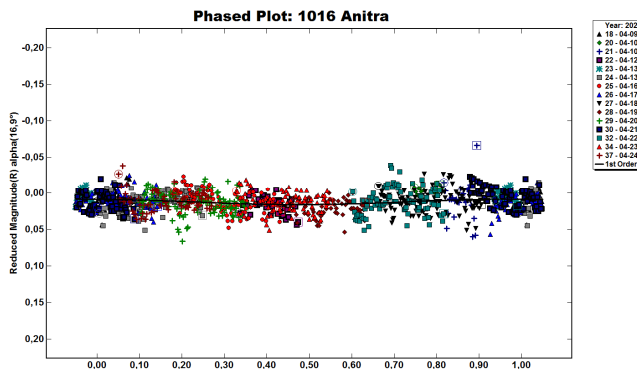


Figure 5. Residual plot after subtracting both periods P1 and P2 from the lightcurves for the interval 2020 April 9 to 24. An interval from 9 h to 100 h was searched with only 1 harmonic term.

#### Acknowledgements

This work includes data from the Asteroid Terrestrial-impact Last Alert System (ATLAS) project. ATLAS is primarily funded to search for near earth asteroids through NASA grants NN12AR55G, 80NSSC18K0284, and 80NSSC18K1575; byproducts of the NEO search include images and catalogs from the survey area. The ATLAS science products have been made possible through the contributions of the University of Hawaii Institute for Astronomy, the Queen's University Belfast, the Space Telescope Science Institute, and the South African Astronomical Observatory.

#### References

- Alkema, M.S. (2013). "Asteroid Lightcurve Analysis at Elephant Head Observatory: 2012 November - 2013 April." *Minor Planet Bull.* **40**, 133-137.
- Harris, A.W.; Young, J.W.; Scaltriti, F.; Zappala, V. (1984). "Lightcurves and phase relations of the asteroids 82 Alkmene and 444 Gyptis." *Icarus* **57**, 251-258.
- Harris, A.W.; Young, J.W.; Bowell, E.; Martin, L.J.; Millis, R.L.; Poutanen, M.; Scaltriti, F.; Zappala, V.; Schober, H.J.; Debehogne, H.; Zeigler, K.W. (1989). "Photoelectric Observations of Asteroids 3, 24, 60, 261, and 863." *Icarus* **77**, 171-186.
- Klinglesmith III, D.A.; Hendrickx, S.; Kimber, C. (2017). "Asteroids observed from Estcorn Observatory." *Minor Planet Bull.* **44**, 345-348.
- Kryszczyńska, A.; Colas, F.; Polińska, M.; Hirsch, R.; Ivanova, V.; Apostolovska, G.; Bilkina, B.; Velichko, F.P.; Kwiatkowski, T.; Kankiewicz, P.; Vachier, F.; Umlenski, V.; Michałowski, T.; Marciniak, A.; Maury, A.; Kamiński, K.; Fagas, M.; Dimitrov, W.; Borczyk, W.; Sobkowiak, K. (2012). "Do Slivan states exist in the Flora family? I. Photometric survey of the Flora region." *Astron. Astrophys.* **546**, A72.
- Menke, J.L. (2005). "Lightcurves and Periods for Asteroids 471 Papagena, 675 Ludmilla, 1016 Anitra, 1127 Mimi, 1165 Imprinetta, 1171 Rusthawelia, and 2283 Burke." *Minor Planet Bull.* **32**, 64-66.
- Pilcher, F.; Benishek, V.; Jacobsen, J.; Kristensen, L.H.; Lang, K.; Larsen, F.R.; Odden, C.; Pravec, P. (2016). "Minor Planet 1016 Anitra: A Likely Asynchronous Binary." *Minor Planet Bull.* **43**, 274-277.
- Pray, D.P.; Galad, A.; Gajdos, S.; Vilagi, J.; Cooney, W.; Gross, J.; Terrel, D.; Higgins, D.; Husarik, M.; Kusnirak, P. (2006). "Lightcurve Analysis of Asteroids 53, 698, 1016, 1523, 1950, 4608, 5080, 6170, 7760, 8213, 11271, 14257, 15350 and 17509." *Minor Planet Bull.* **33**, 92-95.
- Schmidt, R. (2016). "NIR Minor Planet Photometry from Burleith Observatory, 2015." *Minor Planet Bulletin* **43**, 129-131.
- Tonry, J.L.; Denneau, L.; Flewelling, H.; Heinze, A.N.; Onken, C.A.; Smartt, S.J.; Stalder, B.; Weiland, H.J.; Wolf, C. (2018). "The ATLAS All-Sky Stellar Reference Catalog." *Astrophys. J.* **867**, A105.
- Warner, B.D.; Harris, A.W.; Pravec, P. (2009). "The Asteroid Lightcurve Database." *Icarus* **202**, 134-146. Updated 2020 March. <http://www.minorplanet.info/lightcurvedatabase.html>
- Warner, B.D. (2019). MPO Canopus software. <http://bdwpublishing.com>

## A NEW PHOTOMETRIC WORKFLOW AND LIGHTCURVES OF FIFTEEN ASTEROIDS

Eric V. Dose  
3167 San Mateo Blvd NE #329  
Albuquerque, NM 87110  
mp@ericdose.com

(Received: 2020 Jun 28)

A new data reduction workflow makes intense use of the recent ATLAS refcat2 catalog, with the intent of using every eligible comparison star available in the sky field of view. By applying this workflow to CCD observations made late 2019 and early 2020, we generated lightcurves and synodic rotation periods, also presented here, for fifteen asteroids of various families.

A new photometric reduction workflow is described which attempts to use all eligible comparison stars in an image's field of view. Lightcurves, synodic periods, and amplitudes are given for fifteen asteroids.

ATLAS refcat2 (Tonry et al 2018) as used in this work is a comprehensive catalog of Gaia astrometry and all-sky photometry in several passbands, each data point cross-calibrated across several advanced, recent photometric catalogs. The workflow was largely implemented by python automation scripts written by the author (Dose, 2020).

### New Photometric Reduction Workflow

The new workflow begins by collecting all ATLAS catalog stars (typically ca. 200-800) within an image's field of view, and then screening them for appropriate magnitude, magnitude uncertainty, color index, lack of nearby interfering sources, and for catalog-stated non-variability and photometric quality. Each image will begin with typically 40-150 of these screened comparison "comp" star candidates. By visual inspection of numerous diagnostic plots, one then removes those comp stars with erratic photometric behavior, trending magnitudes, and the like, typically yielding 40-120 accepted comp stars for the session. Given that the ATLAS catalog is >99% complete to magnitude 16, this workflow benefits from including effectively all eligible comp stars offered by the sky.

The low-level aperture photometry engine applied here is adapted from the author's variable star observing programs (Dose, 2019), including a split-annulus sky-flux measuring algorithm adept at nullifying the effect of most cosmic rays and nearby light sources not visually detected.

Instrumental magnitudes for all accepted comp stars in all of a session's images are then submitted as dependent variable to mixed-model regression (Gelman and Hill, 2006) as implemented by the python package statsmodels. Extracted parameters include zero-point, parabolic vignetting, and, optionally, extinction, linear magnitude drift with time, and even transform. The mixed model is then applied in reverse to all asteroid instrumental magnitudes to give the final best estimates of catalog-basis, top-of-atmosphere asteroid magnitudes in Sloan r passband; these best magnitudes are already transformed and corrected for sky extinction. Modest image-to-image random fluctuations ("cirrus effect") are also accounted for and plotted as facilitated by mixed-model statistics.

A sequence of adjustments, mixed-model regression, diagnostic plotting, and asteroid magnitude extraction is iterated; adjustments include restricting comp star color and magnitude ranges to better match the target asteroid, as well as excluding outlier comp stars, outlier comp star observations, and/or entire images. Iterations continue until convergence; typically 2-4 iterations are needed. It is usually profitable to set uniform ranges to comp star magnitude and color ranges among all sessions of a campaign (all nightly sessions in one apparition for one asteroid), to minimize night-to-night artifacts arising solely from unnecessary variation in comp star selection.

This process directly yields best estimates of asteroid magnitude on catalog basis, that is, the session's lightcurve. These final, catalog-basis asteroid magnitudes are imported directly into *MPO Canopus* software (Warner, 2018b) for Fourier analysis. In *MPO Canopus*, magnitudes are adjusted for distances and for phase-angle dependence with an *H-G* model, using  $G = 0.15$  unless otherwise specified.

By taking full advantage of the large number and high quality of ATLAS comp stars, the author finds that sessions of a given campaign match in reduced absolute magnitudes, that is, they seldom need any night-to-night magnitude offsets at all. In *MPO Canopus* terms, the DeltaComp values are zero for almost all sessions for the asteroids reported here. Exceptions occur for phase angles below about  $1^\circ$ , where the *H-G* correction model may miss intense opposition effects (e.g., from asteroid surface crystals with internal right angles). This limitation of the *H-G* model will result in inaccurate phase-angle corrections near zero phase even were one's measured magnitudes perfectly correct. That aside, and if the zero-adjustment findings hold up, the ability for a given asteroid to match many nights of photometry without arbitrary magnitude adjustments will prove especially helpful for studying asteroids with long periods. For wide phase-angle ranges, amplitude dependence on phase angle should probably be included as well (Zappalá et al., 1990).

The present workflow automatically generates ALCDEF-compliant files. All lightcurve data herein have been submitted to the ALCDEF database.

### Lightcurves from the New Workflow

Fifteen asteroids were observed from Deep Sky West observatory (IAU V28) in northern New Mexico. Images were acquired with a 0.35-m SCT reduced to  $f/7.7$ , an SBIG STXL-6303E camera without binning and cooled to  $-35^\circ\text{C}$  fitted with a Clear filter (Astrodon), on a PlaneWave L-500 direct-drive mount. The equipment is operated remotely via *ACP* software (DC-3 Dreams), running plan text files generated for each night by the author's python scripts (Dose, 2020). Most sessions were interleaved by cycling between the positions of 2-4 asteroids (and/or unrelated long-period variable stars for separate studies), as facilitated by the mount's rapid slews. Exposures longer than 120 seconds were autoguided. Time basis was standardized by *Meinberg* NTP service and monitor (Meinberg, 2020) against 4-6 remote NTP servers, continuously to within 2-10 milliseconds.

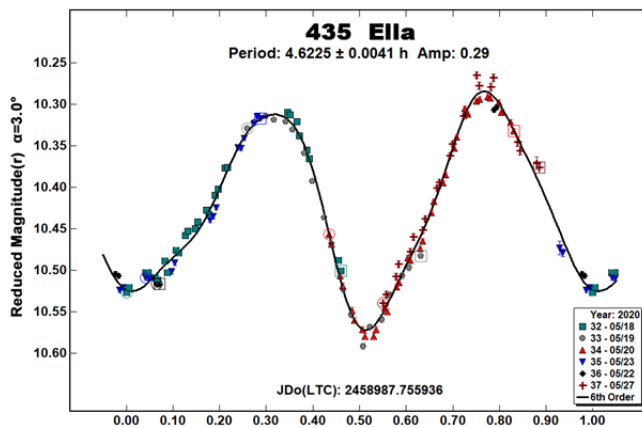
FITS images were plate-solved by *PinPoint* (DC-3 Dreams) and calibrated using temperature-matched, median-averaged dark images and recent flat images of a flux-adjustable flat panel. Every photometric image was visually inspected, and any images with poor tracking or with other light sources expected to overlap the target asteroid were simply excluded. Accepted photometry-ready images were submitted to the workflow presented above, producing the lightcurves presented here.

Number	Name	yyyy mm/dd	Phase	$L_{PAB}$	$B_{PAB}$	Period(h)	P.E.	Amp	A.E.	Grp
435	Ella	2020 05/18-05/27	*3.5, 1.2	244	-2	4.622	0.004	0.29	0.02	NYSA
768	Struveana	2019 10/21-11/17	*6.7, 6.7	40	0	10.744	0.006	0.32	0.02	MB-O
1074	Beljawska	2019 11/04-11/10	17.8, 15.9	86	1	6.286	0.002	0.31	0.02	THM
1130	Skuld	2019 10/27-11/03	*1.11, 3.27	35	0	4.808	0.001	0.26	0.02	FLOR
1592	Mathieu	2020 05/18-06/20	*9.4, 17.6	241	12	28.528	0.010	0.16	0.02	MB-O
2415	Ganesa	2020 05/19-06/25	3.0, 16.9	233	2	6.894	0.001	0.23	0.02	MB-M
3151	Talbot	2020 05/15-05/26	*6.6, 7.3	239	12	19.444	0.007	0.50	0.02	MB-O
3683	Baumann	2020 05/20-06/22	*7.6, 8.6	253	10	7.888	0.001	0.22	0.02	MB-O
3800	Karayusuf	2020 05/13-05/20	20.5, 19.0	236	19	2.232	0.001	0.14	0.02	MC
5534	1941 UN	2019 10/17-11/05	9.4, 19.4	10	2	14.402	0.004	0.17	0.02	MB-O
7910	Aleksola	2020 06/08-06/20	12.6, 18.1	242	9	6.416	0.002	0.20	0.02	MB-I
11190	Jennibell	2019 10/31-11/03	1.3, 3.1	35	0	3.429	0.003	0.32	0.04	FLOR
14923	1994 TU3	2019 10/27-10/31	6.9, 5.2	41	-5	2.653	0.001	0.13	0.02	PHO
39197	2000 XA	2019 10/23-10/31	*3.9, 4.1	32	-3	5.221	0.001	0.65	0.02	H
42196	2001 DE21	2019 10/29	1.9	32	-3	7.480	0.160	0.27	0.02	EOS

Table 1. Observing circumstances and results. The phase angle is given for the first and last date. If preceded by an asterisk, the phase angle reached an extrema during the period.  $L_{PAB}$  and  $B_{PAB}$  are the approximate phase angle bisector longitude/latitude at mid-date range (see Harris et al., 1984). Grp is the asteroid family/group (Warner et al., 2009).

**435 Ella.** This well-studied Nysa-family asteroid was found to have a synodic period of 4.6225 h, in agreement with published periods of 4.623 h (Barucci et al., 1992), 4.624 h (Piiironen et al., 1998), 4.6233 h (Behrend, 2006), 4.64 h (Chang et al., 2016), and 4.621 h (Lang et al., 2018).

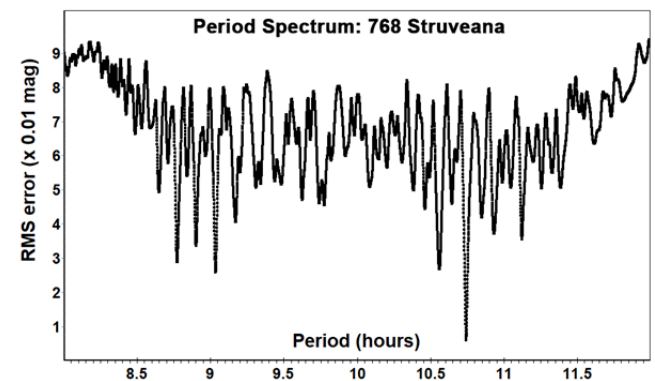
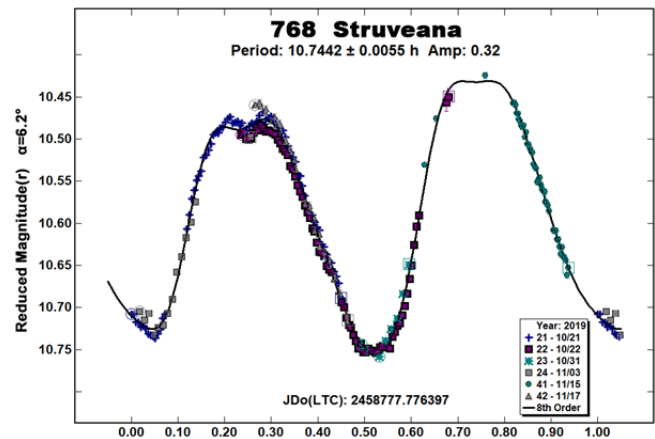
ATLAS comparison stars were abundant; in the new photometric workflow described above, comp stars for this asteroid averaged 57 in number, with every night employing at least 36. Fourier fit and phased plot used magnitudes obtained directly from the mixed-model regression, that is, without night-to-night magnitude adjustments beyond standard distance reductions and  $H-G$  corrections. RMS error is 10 millimagnitudes.



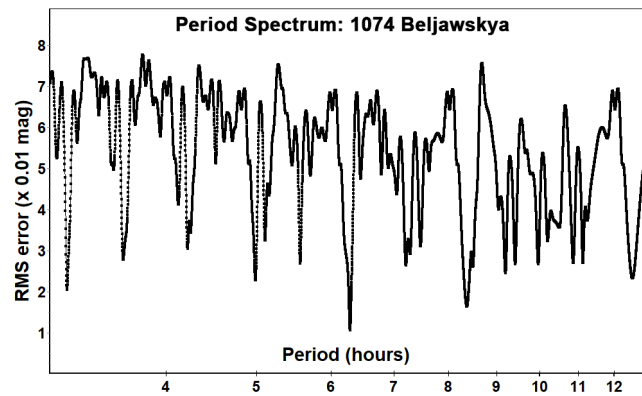
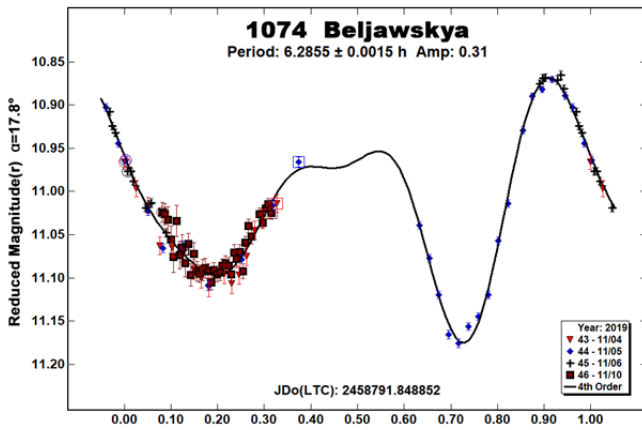
**768 Struveana.** For this outer main-belt asteroid, the LCDB lists two previous period determinations: 8.802 h (Gil-Hutton and Cañada, 2003) and 8.76 h (Behrend, 2007), with uncertainty code of 2+. However, the present data's deeper coverage, high amplitude to RMS-error ratio, and period spectrum all clearly favor a different synodic period of 10.7442 h. We note that our bimodal period differs from previous periods by one half-period per 24 hours. RMS error is 8 millimagnitudes.

The Fourier fit benefited from magnitude adjustments to two nights with very low phase angles: +0.040 magnitudes for Oct 31 (phase angle  $\alpha = 1.47^\circ$ ) and +0.110 for Nov 3 ( $\alpha = 0.29^\circ$ ). The other four nights with larger phase angles needed no such adjustment. As the two adjustments were limited to very low phase angles, were negative in magnitude (indicating brightening and thus requiring positive corrections), and were monotonic in scale with phase angle, they indicate a large opposition effect for which standard  $H-G$  corrections fail to account.

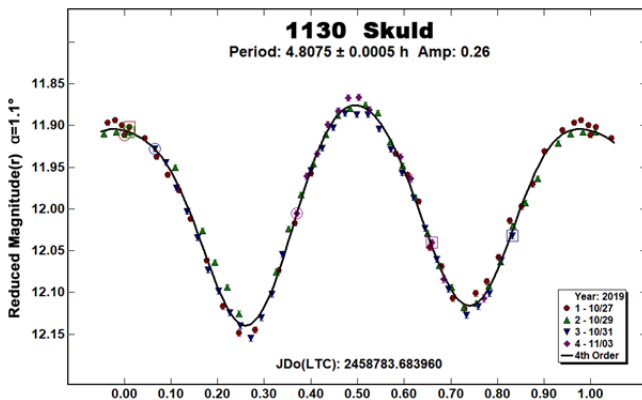
Trial corrections with  $G$  values other than the MPC standard of  $G = 0.15$  did not reduce need for extra nightly adjustments of data taken at very low phase angles. The phased plot does suggest some increase in amplitude with phase angle (Zappalá et al., 1990).



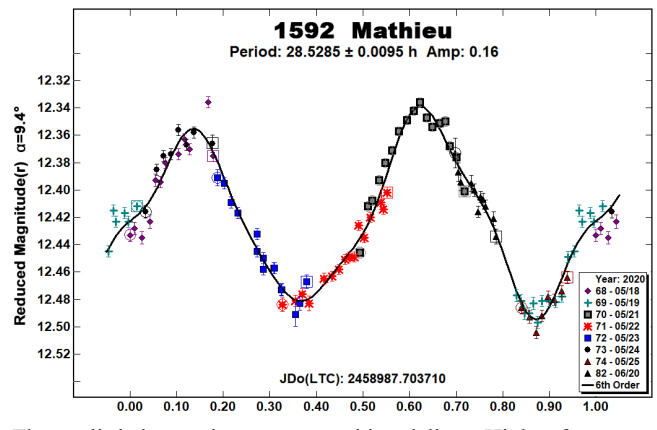
**1074 Beljawska.** This very early lightcurve effort of the author's for this Themis asteroid suffered imperfect phase sampling, but even so it captured both of its brightness minima and yielded a provisional bimodal synodic rotation period of 6.2855 h, matching one known published survey period of 6.285 h (Waszczak et al., 2015). On average, 48 ATLAS comp stars were applied to each image; no night-to-night magnitude adjustments were needed. RMS error is 10 millimagnitudes.



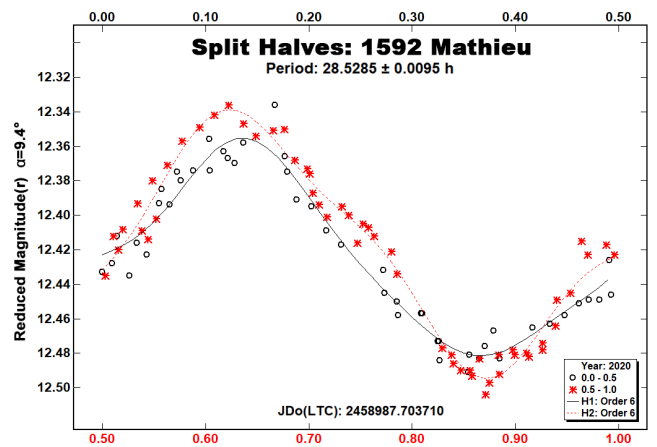
**1130 Skuld.** This well-studied Flora asteroid was found to have synodic rotation period of 4.8075 h, matching published periods of 4.75 h (Behrend, 2004), 4.807 h (Buchheim, 2010), 4.810 h (Robinson, 2011), 4.8079 h (Kryszczynska et al., 2012), 4.8096 h (Behrend, 2017), and 4.8058 h (Behrend, 2019). Nightly magnitude adjustments were made for two nights at very low phase angles: +0.010 for Oct 27 ( $\alpha = 1.11^\circ$ ), and +0.060 for Oct 29 ( $\alpha = 0.19^\circ$ ), almost certainly arising from opposition effects inadequately accounted for by  $H-G$  correction. RMS error is 8 millimagitudes.



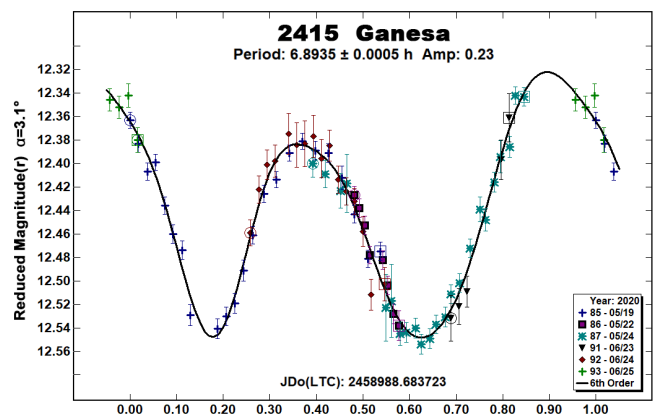
**1592 Mathieu.** This Flora asteroid was observed over eight nights spanning a month. Its synodic period is clearly bimodal and of duration 28.5285 h, consistent with a published monomodal period of 14.23 h (Warner, 2006) and a survey estimate of 28.4821 h (Durech et al., 2016). No nightly magnitude adjustments were made; RMS error is 9 millimagitudes.



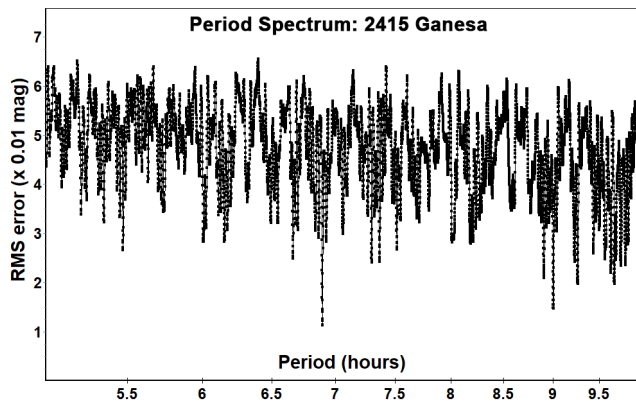
The split-halves plot supports bimodality. Higher-frequency structure in the lightcurve, evident even at this low amplitude, suggests that this asteroid's shape model might profitably be revisited.



**2415 Ganesa.** This middle main-belt asteroid has an apparent synodic period of 6.8935 h. Applying a  $G$  value of 0.09 rather than the default 0.15 value markedly improved the Fourier fit. No nightly magnitude adjustments were made; RMS error is 11 millimagitudes.

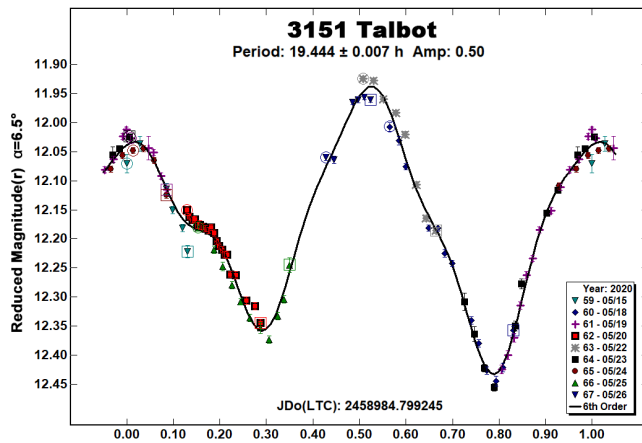


Our rotation period result differs from one published result of 8.0 h (Sarneczky et al., 1999) and from a survey finding (marked ambiguous in LCDB) of 2.67 h (Chang et al., 2016), notably close to 1/3 of the Sarneczky result. The earlier 8.0-h period does not appear in the present period spectrum: it is notably an alias of the present result by a half-cycle per 24 hours.

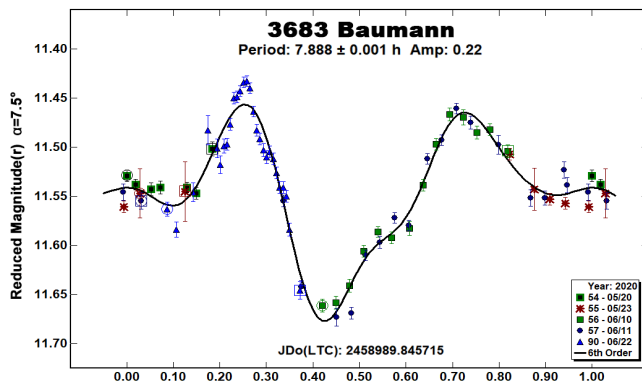


3151 Talbot. This outer main-belt asteroid was found to have a synodic rotation period of 19.444 h, in good agreement with published period of 19.49 h (Ferrero, 2011) and a survey estimate of 19.499 h (Pál et al., 2020). No nightly magnitude adjustments were made; RMS error is 16 millimagnitudes.

This is the first lightcurve reported near its phase angle bisector latitude of 12°, so with the PAB latitude range filled in and the newly secure period, this asteroid may merit new shape modeling.

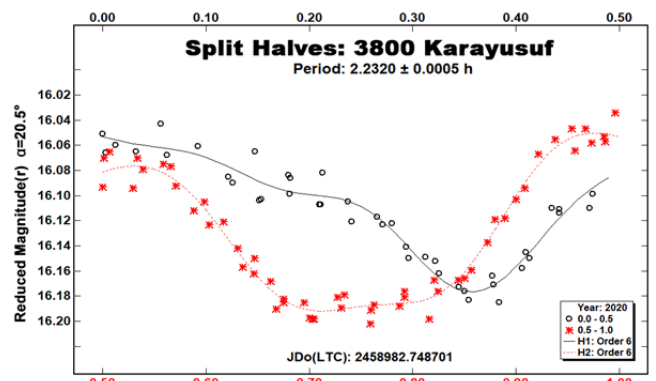
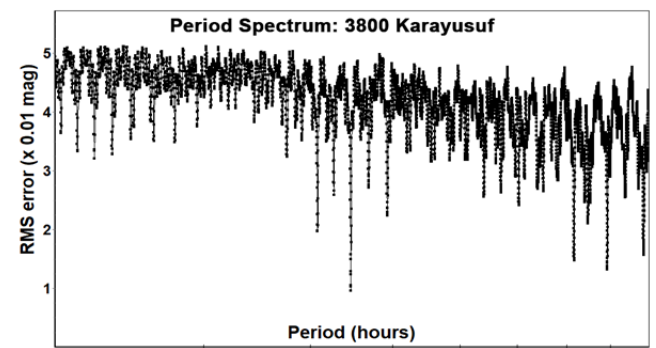
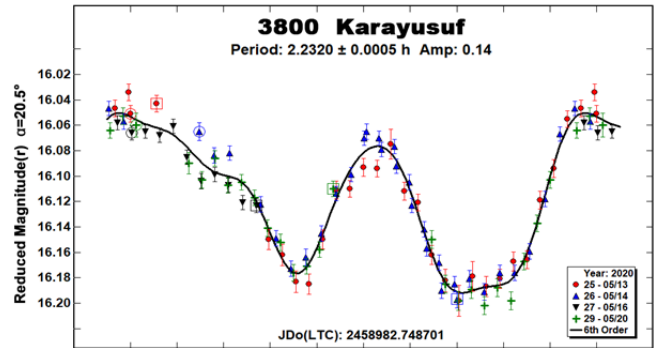


3683 Baumann. This outer main-belt asteroid was found during its favorable 2020 opposition to have a bimodal synodic period of 7.888 h, or half of a previously reported period of 15.758 h derived from sparse photometry (Waszczak et al., 2015).



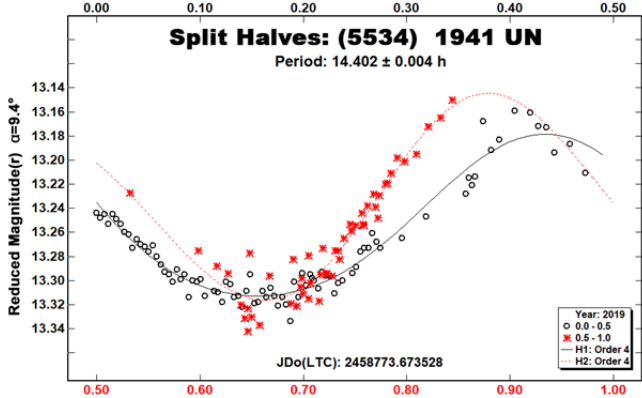
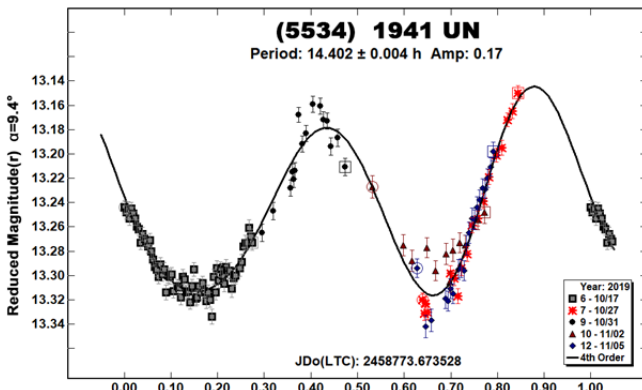
No nightly adjustments were made; RMS error is 15 millimagnitudes. The data suggest somewhat higher amplitude at the higher phase angle of June 22 (Zappalá et al., 1990).

3800 Karayusuf. This rapidly rotating and well-studied Mars-crosser was found to have synodic rotation period of 2.232 h, in excellent agreement with published periods of 2.2319 h (Warner, 2008), 2.232 h (Warner, 2010), 2.221 h (Warner 2014), 2.2318 h (Franco et al., 2018), 2.232 h (Klinglesmith and Erin, 2018), 2.2319 h (Skiff, 2018), and 2.2328 h (Warner 2018a). No nightly magnitude adjustments were made; RMS error is 10 millimagnitudes. Period-search and split-phase plots support a bimodal lightcurve over unimodal or higher-mode interpretations.

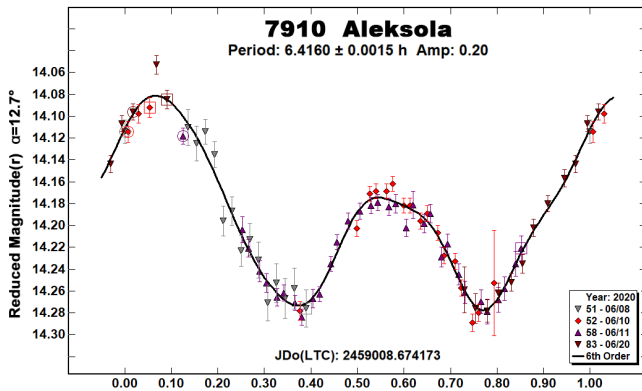


We saw no evidence of 3800 Karayusuf's being binary, though these observations were brief.

(5534) 1941 UN. Photometry on outer main-belt asteroid strongly indicates a synodic rotation period of 14.402 h. The LCDB lists one previous period of 4.10 h (LCDB-Zeigler). Neither that period nor any period less than 14.4 h gave a credible Fourier fit to the current five nights of photometric data, not even a “fit by exclusion” to the admittedly uneven phase coverage of this early effort. No nightly magnitude adjustments were made; RMS error is 11 millimagnitudes. The two halves of the phased lightcurve plot might appear similar, but a split-halves plot confirms a bimodal interpretation.

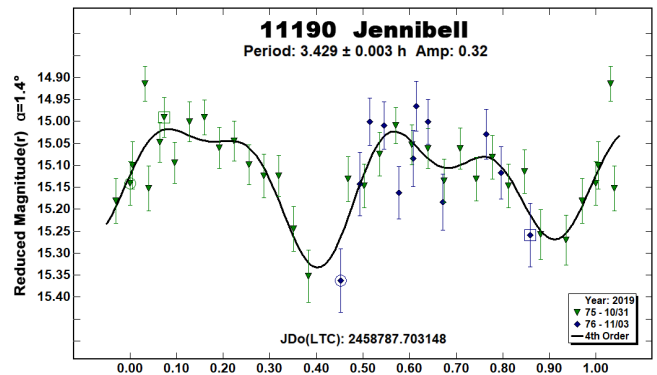


7910 Aleksola. The lightcurve for this inner main-belt asteroid during its favorable 2020 apparition is decidedly bimodal, with the two brightening events differing in scale by a factor of two.



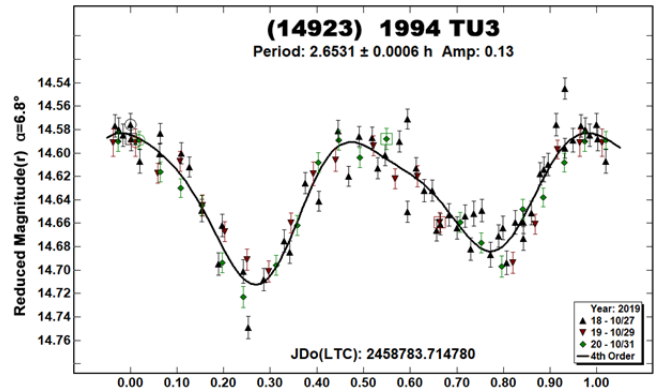
The current lightcurve requires a synodic period of 6.4160 h; the only previous period found was a survey-derived period of 6.41852 h (Pál et al., 2020) but marked as ambiguous in the LCDB. Adjusting the *G* value from the standard 0.15 to 0.40 markedly improved the Fourier fit without nightly magnitude adjustments; RMS error is 10 millimagnitudes.

11190 Jennibell. This Flora-family asteroid was located as a very faint signal in two nights of images targeting (1130) Skuld. The lightcurve appears bimodal with synodic period 3.428 h. RMS error to a 4<sup>th</sup> order Fourier fit is 63 millimagnitudes, but its short period affords complete phase coverage, and both bimodal brightness minima were clearly located. The author found no previous reports of rotational period for this asteroid.

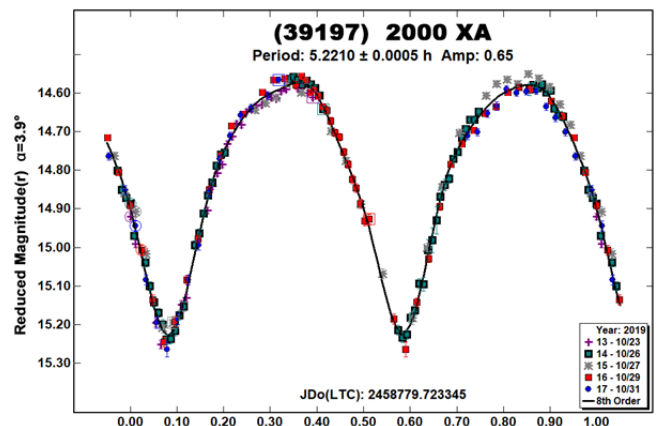


(14923) 1994 TU3. This Phocaea asteroid was found to have a bimodal synodic rotation period of 2.6531 h, with low amplitude of 0.13 magnitudes (Sloan *r*). No nightly magnitude adjustments were made; RMS error is 17 millimagnitudes.

The present result differs strikingly from published periods of 30 h (Behrend, 2001) and 7.3 h (Warner, 2009). The current photometric data do not allow for a proper test of the 30 h period, but no period between 6 and 10 hours gave a credible Fourier fit to the present data obtained over three nights.



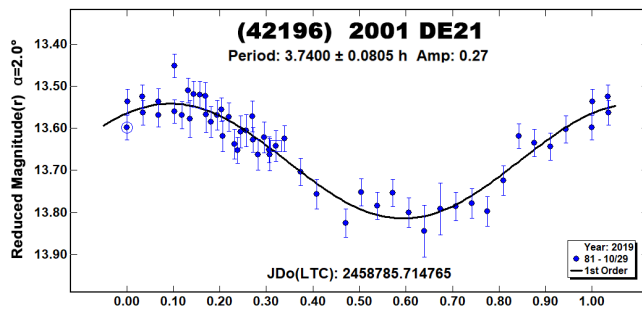
(39197) 2000 XA. This Hungaria asteroid was observed during its favorable 2019 opposition. The synodic rotation period was found to be 5.2210 h, agreeing with published periods of 5.221 h (Waszczak et al., 2015) and 5.2238 h (Benishek, 2020). RMS error is 18 millimagnitudes.



The fundamental period appears well established; at this large amplitude, the bimodal interpretation is almost certainly correct (Harris et al., 2014). The next opposition mid-2021 will be a magnitude fainter and satisfactory only for the Southern Hemisphere.

**(42196) 2001 DE21.** This Eos asteroid was located as a faint signal in one night of images targeting (39197) 2000 XA. The synodic fundamental was measured as 3.74 h, suggesting a bimodal synodic period of 7.48 h. The author found no previously published period. RMS error is 34 millimagnitudes.

The 4.9-hour observing session covered the fundamental but not the bimodal period, so while the fundamental period appears secure, later observations will be needed to confirm the modality. The next favorable opposition occurs 2024 October.



#### Acknowledgements

The author thanks the authors of the ATLAS paper (Tonry et al, 2018) for their generous and helpfully detailed description of the ATLAS refcat2 release catalog and joins them in acknowledging the very many contributors to and supporters of that catalog effort, as listed near the end of their paper.

Planning and processing software for this project was written in the python language, whose interpreter is provided without cost by the Python Foundation. This project's computations also made extensive use of several supporting packages also provided without cost, notably the pandas, ephem, matplotlib, requests, and statsmodels packages; the author thanks the package authors as well for their significant effort and offerings without which this work would have been infeasible.

#### References

- Barucci, M.A.; di Martino, M.; Fulchignoni, M. (1992). "Rotational Properties of Small Asteroids: Photoelectric Observations." *Astron. J.*, **103**, 1679-1686.
- Behrend, R. (2001, 2004, 2006, 2007, 2017, 2019). Observatoire de Geneve web site. [http://obswww.unige.ch/~behrend/page\\_cou.html](http://obswww.unige.ch/~behrend/page_cou.html)
- Benishek, V. (2020). "Photometry of 39 asteroids at Sopot Astronomical Observatory: 2019 September – 2020 March." *Minor Planet Bulletin* **47**, 231-241.
- Buchheim, R.K. (2010). "Lightcurve and Phase Curve of 1130 Skuld." *Minor Planet Bulletin* **37**, 41-42.
- Chang, C.-K.; Lin, H.-W.; Ip, W.-H.; Prince, T.A.; Kulkarni, S.R.; Levitan, D.; Laher, R.; Surace, J. (2016). "Large Super-fast Rotator Hunting Using the Intermediate Palomar Transient Factory." *Astrophys J. Suppl. Ser.*, **227**, id 20.

Dose, E. (2019). Code repository "photrix", version tag 2.0.1, <https://github.com/edose/photrix>

Dose, E. (2020). Code repository "mpc", version tag 0.1beta, <https://github.com/edose/mpc>

Đurech, J.; Hanuš, J.; Oszkiewiecz, D.; Vanco, R. (2016). "Asteroid models from the Lowell photometric database." *Astron. Astrophys.* **587**, A48.

Ferrero, A. (2011). "Lightcurve Determination of 3151 Talbot and 4666 Dietz." *Minor Planet Bulletin* **38**, 223-224.

Franco, L.; Bacci, P.; Maestriperieri, M.; Carotta, G.; Carotta, M.; Mesti, L.; Fragai, M. (2018). "Lightcurve for 3800 Karayusuf." *Minor Planet Bulletin* **45**, 403.

Gelman, A.; Hill, J. (2006). *Data Analysis Using Regression and Multilevel/Hierarchical Models*. Cambridge University Press, New York.

Gil-Hutton, R.; Cañada, M. (2003). "Photometry of Fourteen Main Belt Asteroids." *Rev. Mex. Astronomia Astrofisica* **39**, 69-76.

Harris, A.W.; Young, J.W.; Scaltriti, F.; Zappala, V. (1984). "Lightcurves and phase relations of the asteroids 82 Alkmene and 444 Gyptis." *Icarus* **57**, 251-258.

Harris, A.W.; Pravec, P.; Galad, A.; Skiff, B.A.; Warner, B.D.; Vilagi, J.; Gajdos, S.; Carbognani, A.; Hornoch, K.; Kusnirak, P.; Cooney, W.R.; Gross, J.; Terrell, D.; Higgins, D.; Bowell, E.; Koehn, B.W. (2014). "On the maximum amplitude of harmonics on an asteroid lightcurve." *Icarus* **235**, 55-59.

Klinglesmith, D.A.; Erin, A.L. (2018). "Three asteroids from ETSCORN: 461 Saskia, 3800 Karayusuf, and (42701) 1998 MD13." *Minor Planet Bulletin* **45**, 397-398.

Kryszczyńska, A.; Colas, F.; Polinska, M.; Hirsch, R.; Ivanova, V.; Apostolovska, G.; Bilkina, B.; Velichko, F.P.; Kwiatkowski, T.; Kankiewicz, P. and 20 coauthors. (2012). "Do Slivan states exist in the Flora family? I. Photometric survey of the Flora region." *Astron. Astrophys.* **546**, A72.

Lang, K.; Jacobsen, J.; Kristensen, L.H. (2018). "Rotational Periods of Asteroids 184 Dejopeja, 435 Ella, and 5049 Sherlock." *Minor Planet Bulletin* **45**, 197-198.

LCDB-Zeigler, record found under "Zeigler unpublished", via <http://www.minorplanet.info/PHP/lcdbsummaryquery.php>

Meinberg (2020). *NTP and Monitor* software. <https://www.meinbergglobal.com/english/sw/ntp.htm>

Pál, A.; Szakáts, R.; Kiss, C.; Bódi, A.; Bognár, Z.; Kalup, C.; Kiss, L.L.; Marton, G.; Molnár, L.; Plachy, E.; Sárneczky, K.; Szabó, G.M.; Szabó, R. (2020). "Solar System Objects Observed with TESS - First Data Release: Bright Main-belt and Trojan Asteroids from the Southern Survey." *Astrophys. J. Suppl.* **247**, 26.

Piironen, J.; Lagerkvist, C.-I.; Erikson, A.; Oja, T.; Magnusson, P.; Festin, L.; Nathues, A.; Gaul, M.; Velichko, F. (1998). "Physical Studies of Asteroids XXXII. Rotation periods and UBVRI-colours for selected asteroids." *Astron. Astrophys. Suppl. Ser.* **128**, 525-540.

Robinson, L. (2011). Asteroid Lightcurves from Sunflower Observatory 739. <http://btboar.tripod.com/lightcurves/>

Sarnecky, K.; Szabó, Gy.; Kiss, L.L. (1999). "CCD observations of 11 faint asteroids." *Astron. Astrophys. Suppl. Ser.* **137**, 363-368.

Skiff, B. (2018). Submission posting on CALL web site, found at: <http://www.minorplanet.info/call.html>

Tonry, J.L.; Denneau, L.; Flewelling, H.; Heinze, A.N.; Onken, C.A.; Smartt, S.J.; Stalder, B.; Weiland, H.J.; Wolf, C. (2018). "The ATLAS All-Sky Stellar Reference Catalog." *Astrophys. J.* **867**, A105.

Warner, B.D. (2006). "Asteroid Lightcurve Analysis at the Palmer Divide Observatory – March-June 2006." *Minor Planet Bulletin* **33**, 85-88.

Warner, B.D. (2008). "Asteroid Lightcurve Analysis at the Palmer Divide Observatory: February-May 2008." *Minor Planet Bulletin* **35**, 163-166.

Warner, B.D. (2009). "Asteroid Lightcurve Analysis at the Palmer Divide Observatory: 2008 May-September." *Minor Planet Bulletin* **36**, 7-13.

Warner, B.D.; Harris, A.W.; Pravec, P. (2009). "The asteroid lightcurve database." *Icarus*, **202**, 134-146. Updated 2020 June. <http://www.minorplanet.info/lightcurvedatabase.html>

Warner, B.D. (2010). "Asteroid Lightcurve Analysis at the Palmer Divide Observatory: 2010 March-June." *Minor Planet Bulletin* **37** 161-165.

Warner, B.D. (2014). "Asteroid Lightcurve Analysis at CS3-Palmer Divide Station: 2014 January-March." *Minor Planet Bulletin* **41**, 144-155.

Warner, B.D. (2018a). "Asteroid Lightcurve Analysis at CS3-Palmer Divide Station: 2018 April-June." *Minor Planet Bulletin* **45**, 380-386.

Warner, B.D. (2018b). *MPO Canopus* Software, version 10.7.12.9, BDW Publishing. <http://www.bdwpublishing.com>

Waszczak, A.; Chang, C.-K.; Ofek, E.O.; Laher, R.; Masci, F.; Levitan, D.; Surace, J.; Cheng, Y.-C.; Ip, W.-H.; Kinoshita, D.; Helou, G.; Prince, T.A.; Kulkarni, S. (2015). "Asteroid Light Curves from the Palomar Transient Factory Survey: Rotation Periods and Phase Functions from Sparse Photometry." *Astron. J.* **150**, A75.

See specific asteroid lightcurve data via: <http://vizier.u-strasbg.fr/viz-bin/VizieR-3?-source=J/AJ/150/75/table4>

Zappalá, V.; Cellini, A.; Barucci, A.M.; Fulchignoni, M.; Lupishko, D.E. (1990). "An analysis of the amplitude-phase relationship among asteroids." *Astron. Astrophys.* **231**, 548-560.

## LIGHTCURVE PHOTOMETRY OPPORTUNITIES: 2020 OCTOBER-DECEMBER

Brian D. Warner  
Center for Solar System Studies / MoreData!  
446 Sycamore Ave.  
Eaton, CO 80615 USA  
[brian@MinorPlanetObserver.com](mailto:brian@MinorPlanetObserver.com)

Alan W. Harris  
MoreData!  
La Cañada, CA 91011-3364 USA

Josef Ďurech  
Astronomical Institute  
Charles University  
18000 Prague, CZECH REPUBLIC  
[durech@sirrah.troja.mff.cuni.cz](mailto:durech@sirrah.troja.mff.cuni.cz)

Lance A.M. Benner  
Jet Propulsion Laboratory  
Pasadena, CA 91109-8099 USA  
[lance.benner@jpl.nasa.gov](mailto:lance.benner@jpl.nasa.gov)

We present lists of asteroid photometry opportunities for objects reaching a favorable apparition and have no or poorly-defined lightcurve parameters. Additional data on these objects will help with shape and spin axis modeling using lightcurve inversion. We also include lists of objects that will or might be radar targets. Lightcurves for these objects can help constrain pole solutions and/or remove rotation period ambiguities that might come from using radar data alone.

We present several lists of asteroids that are prime targets for photometry during the period 2020 October-December.

In the first three sets of tables, "Dec" is the declination and "U" is the quality code of the lightcurve. See the latest asteroid lightcurve data base (LCDB from here on; Warner et al., 2009a) documentation for an explanation of the U code:

<http://www.minorplanet.info/lightcurvedatabase.html>

The ephemeris generator on the CALL web site allows you to create custom lists for objects reaching  $V \leq 18.0$  during any month in the current year and up to five years in the future, e.g., limiting the results by magnitude and declination, family, and more.

[http://www.minorplanet.info/PHP/call\\_OppLCDBQuery.php](http://www.minorplanet.info/PHP/call_OppLCDBQuery.php)

We refer you to past articles, e.g., Warner et al. (2009b) for more detailed discussions about the individual lists and points of advice regarding observations for objects in each list.

Once you've obtained and analyzed your data, it's important to publish your results. Papers appearing in the *Minor Planet Bulletin* are indexed in the Astrophysical Data System (ADS) and so can be referenced by others in subsequent papers. It's also important to make the data available at least on a personal website or upon request. We urge you to consider submitting your raw data to the ALCDEF database. This can be accessed for uploading and downloading data at

<http://www.alcdef.org>

Containing almost 3.7 million observations for 14952 objects (2020 March 30), this makes the site one of the larger publicly available sources for raw asteroid time-series lightcurve data.

Now that many backyard astronomers and small colleges have access to larger telescopes, we have expanded the photometry opportunities and spin axis lists to include asteroids reaching  $V = 15.5$  and brighter (sometimes 15.0 when the list has too many potential targets).

### Lightcurve/Photometry Opportunities

Objects with  $U = 3-$  or 3 are excluded from this list since they will likely appear in the list for shape and spin axis modeling. Those asteroids rated  $U = 1$  should be given higher priority over those rated  $U = 2$  or  $2+$ , but not necessarily over those with no period. On the other hand, *do not overlook asteroids with  $U = 2/2+$  on the assumption that the period is sufficiently established.* Regardless, do not let the existing period influence your analysis since even highly-rated result have been proven wrong at times. Note that the lightcurve amplitude in the tables could be more or less than what's given. Use the listing only as a guide.

An entry in bold italics is a near-Earth asteroid (NEA).

Number	Name	Brightest			LCDB Data			U
		Date	Mag	Dec	Period	Amp	U	
2534	Houzeau	10 02.9	14.6	+3	53.237	0.22	2	
3989	Odin	10 03.2	15.0	+9				
2252	CERGA	10 03.7	15.4	+6				
1024	Hale	10 04.3	13.7	-16	16.	0.10	1+	
2819	Ensor	10 05.0	14.1	+4				
1654	Bojeva	10 05.4	14.3	+1	10.5559	0.27	2	
842	Kerstin	10 05.9	14.5	+8				
21182	1994 EC2	10 09.0	14.5	+9				
8556	Jana	10 09.4	14.7	-4				
2300	Stebbins	10 10.8	15.0	+6				
1526	Mikkeli	10 12.3	14.9	+15		0.51		
6014	Chribrenmark	10 15.0	14.9	+8				
1935	Lucerna	10 16.1	14.8	+8				
1498	Lahti	10 16.6	15.0	+27	58.	0.8	1+	
570	Kythera	10 16.8	12.7	+10	8.12	0.12-0.20	2	
30717	1937 UD	10 17.8	14.7	+6				
2913	Horta	10 18.6	14.6	+7				
8651	Alineraynal	10 19.8	15.0	+15		0.32		
859	Bouzareah	10 27.6	13.5	+12	23.2	0.13	2-	
4103	Chahine	10 28.4	13.7	+29		0.35		
2976	Lautaro	10 31.2	14.6	+11	17.41	0.12	2-	
1351	Uzbekistania	11 05.1	14.1	+23	73.9	0.34-0.34	2	
1578	Kirkwood	11 09.7	14.3	+16	12.518	0.05-0.22	2	
1042	Amazone	11 18.8	14.1	+22	540.	0.10-0.25	2	
21242	1995 WZ41	11 18.8	14.2	+20				
137311	1999 TX9	11 18.9	14.6	+30		0.46		
3398	Stattmayer	11 20.1	15.0	+12	8.28	0.13	2+	
2191	Uppsala	11 21.5	14.8	+22				
838	Seraphina	11 22.2	13.4	+20	15.67	0.07-0.30	2	
2312	Duboshin	11 22.6	14.5	+20	50.78	0.15	2+	
2263	Shaanxi	11 22.7	14.9	+22	41.7	0.36	2-	
12193	1979 EL	11 24.0	14.9	+7	7.5766	0.35-0.41	2+	
748	Simeisa	11 25.4	13.4	+22	11.919	0.22-0.36	2	
7288	1991 FE1	11 27.1	14.8	+27	4.89	0.47	2	
8823	1987 WS3	11 29.4	14.4	+20				
1934	Jeffers	11 29.8	14.0	+4				
<b>153201 2000 WQ107</b>		<b>12 01.1 13.2 +25</b>						
4493	Naitomitsu	12 04.2	15.0	+25	5.04	0.07	1+	
2950	Rousseau	12 14.0	14.1	+14	18.228	0.30	2	
1213	Algeria	12 22.1	15.0	+24	>16.	0.19	2	
8532	1992 YW3	12 24.2	14.9	+25	>30.	0.35	2	
931	Whittemora	12 26.3	12.4	+18	19.199	0.15-0.25	2+	

### Low Phase Angle Opportunities

The Low Phase Angle list includes asteroids that reach very low phase angles. The " $\alpha$ " column is the minimum solar phase angle for the asteroid. Getting accurate, calibrated measurements (usually V band) at or very near the day of opposition can provide important information for those studying the "opposition effect."

Use the on-line query form for the LCDB to get more details about a specific asteroid.

[http://www.minorplanet.info/PHP/call\\_OppLCDBQuery.php](http://www.minorplanet.info/PHP/call_OppLCDBQuery.php)

You will have the best chance of success working objects with low amplitude and periods that allow covering at least half a cycle every night. Objects with large amplitudes and/or long periods are much more difficult for phase angle studies since, for proper analysis, the data must be reduced to the average magnitude of the asteroid for each night. This reduction requires that you determine the period and the amplitude of the lightcurve; for long period objects that can be difficult. Refer to Harris et al. (1989) for the details of the analysis procedure.

As an aside, some use the maximum light to find the phase slope parameter ( $G$ ). However, this can produce significantly different values for both  $H$  and  $G$  versus when using average light, which is the method used for values listed by the Minor Planet Center.

The International Astronomical Union (IAU) has adopted a new system, H-G<sub>12</sub>, introduced by Muinonen et al. (2010). It will be some years before H-G<sub>12</sub> becomes widely used. Furthermore, it still needs refinement. That can be done mostly by having data for more asteroids, but only if at very low and moderate phase angles. We strongly encourage obtaining data every degree between 0° to 7°, the non-linear part of the curve that is due to the opposition effect. At angles  $\alpha > 7^\circ$ , well-calibrated data every 2° or so out to about 25-30°, if possible, should be sufficient. Coverage beyond about 50° is not generally helpful since the H-G system is best defined with data from 0-30°.

Num	Name	Date	$\alpha$	V	Dec	Period	Amp	U	
3280	Gretry	09 04.6	0.84	14.5	-05	10.56	0.35-0.51	3-	
573	Recha	09 06.3	0.18	12.8	-06	7.166	0.20-0.34	3	
805	Hormuthia	09 06.7	0.37	13.3	-05	9.510	0.05	3-	
147	Protogeneia	09 10.9	0.93	12.8	-02	7.853	0.25-0.28	3	
586	Thekla	09 14.1	0.64	13.5	-02	13.670	0.24-0.30	3	
399	Persephone	09 17.6	0.90	13.5	+01	9.136	0.40	3	
434	Hungaria	09 19.1	0.56	12.3	-02	26.521	0.51-0.75	3	
616	Elly	09 24.3	0.95	13.9	+03	5.297	0.34-0.44	3	
91	Aegina	09 24.6	0.26	11.8	+00	6.025	0.12-0.27	3	
1692	Subbotina	09 25.2	0.48	14.3	+02	9.246	0.30	3	
1576	Fabiola	09 27.9	0.17	14.5	+02	6.889	0.2	-0.26	3-
2534	Houzeau	10 02.9	0.19	14.5	+03	53.237	0.22	2	
2819	Ensor	10 05.1	0.22	14.1	+04				
331	Etheridgea	10 05.8	0.55	13.1	+04	25.315	0.12-0.13	3	
644	Cosima	10 08.0	0.86	13.4	+04	7.556	0.20-0.28	3	
518	Halawe	10 10.5	0.71	13.0	+08	14.310	0.50-0.55	3	
1114	Lorraine	10 12.9	0.44	13.8	+07	20.71	0.15	3-	
1059	Mussorgskia	10 15.0	0.17	14.0	+08	5.636	0.2	-0.21	3
570	Kythera	10 16.8	0.31	12.8	+10	8.120	0.12-0.20	2	
158	Koronis	10 17.1	0.55	12.8	+11	14.218	0.28-0.43	3	
189	Phthia	10 18.2	0.16	11.9	+09	22.346	0.18-0.28	3	
439	Ohio	10 18.7	0.71	13.9	+08	37.46	0.20-0.24	3	
326	Tamara	10 22.7	0.89	12.3	+09	14.445	0.10-0.27	3	
180	Garumna	10 22.8	0.49	13.7	+13	23.866	0.27-0.6	3	
67	Asia	10 24.6	0.74	10.7	+10	15.853	0.22-0.26	3	
953	Painleva	10 26.4	0.31	13.6	+12	7.389	0.05-0.05	2-	
859	Bouzareah	10 27.5	0.23	13.5	+12	23.2	0.13	2-	
401	Ottilia	10 29.8	0.09	13.6	+14	6.049	0.11-0.24	3	
761	Brendelia	11 02.5	0.36	14.5	+16	57.96	0.25	2+	
499	Venusia	11 03.2	0.54	13.8	+17	13.48	0.33-0.36	3	
268	Adorea	11 07.9	0.96	13.0	+13	7.80	0.15-0.20	3	
1150	Achaia	11 09.4	0.92	14.0	+15	60.99	0.72	3	
1578	Kirkwood	11 09.6	0.21	14.3	+16	12.518	0.05-0.22	2	
82	Alkmene	11 10.6	0.68	11.6	+19	12.999	0.18-0.54	3	
215	Oenone	11 13.0	0.42	12.9	+19	27.937	0.1	-0.20	3
379	Huenna	11 13.9	0.79	12.5	+16	14.141	0.07-0.12	3	
528	Rezia	11 14.2	0.26	13.7	+19	7.337	0.36-0.39	3	
235	Carolina	11 16.8	0.88	13.0	+16	17.610	0.25-0.38	3	
21242	1995 WZ41	11 18.8	0.26	14.2	+20				
1042	Amazone	11 18.9	0.78	14.1	+22	540.	0.10-0.25	2	
266	Aline	11 19.0	0.18	11.5	+19	13.018	0.05-0.10	3	
157	Dejanira	11 21.2	0.54	13.3	+19	15.825	0.33-0.52	3	
1810	Epimetheus	11 21.4	0.97	14.5	+22	28.61	0.04	2	
838	Seraphina	11 22.2	0.13	13.4	+20	15.67	0.07-0.30	2	
367	Amicitia	11 24.7	0.89	12.8	+19	5.055	0.25-0.90	3	

Num	Name	Date	$\alpha$	V	Dec	Period	Amp	U
748	Simeisa	11 25.4	0.38	13.4	+22	11.919	0.22-0.36	2
8823	1987 WS3	11 29.5	0.97	14.3	+20			
2215	Sichuan	11 30.1	0.51	13.6	+21	3.975	0.38-0.39	3
178	Belisana	12 01.2	0.38	12.5	+23	12.323	0.08-0.18	3
2617	Jiangxi	12 06.0	0.13	13.0	+23	11.77430	0.28-0.57	3
2112	Ulyanov	12 07.9	0.70	13.9	+21	3.041	0.32-0.36	3
171	Ophelia	12 09.3	0.49	12.3	+21	6.665	0.14-0.46	3
4729	Mikhailmil'	12 09.4	0.31	14.1	+22	17.74	0.36	2-
243	Ida	12 09.8	0.58	13.5	+24	4.634	0.45-0.86	3
2233	Kuznetsov	12 10.0	0.56	14.4	+22	5.031	0.23-0.25	3
423	Diotima	12 11.6	0.93	11.6	+26	4.775	0.05-0.20	3
940	Kordula	12 13.8	0.72	14.1	+26	15.57	0.36	3
2831	Stevin	12 14.2	0.13	14.5	+23			
1348	Michel	12 15.0	0.34	13.8	+22	8.095	0.43-0.47	3
2536	Kozyrev	12 17.6	0.71	14.5	+25	7.196	0.26-0.52	3
792	Metcalfia	12 22.8	0.67	13.0	+22	9.17	0.15-0.76	3
1137	Raissa	12 26.6	0.84	13.5	+25	142.79	0.56-0.56	3-
440	Theodora	12 27.2	0.46	13.1	+24	4.828	0.43-0.72	3
774	Armor	12 29.5	0.99	13.8	+20	25.107	0.11-0.34	2

### Shape/Spin Modeling Opportunities

Those doing work for modeling should contact Josef Ďurech at the email address above. If looking to add lightcurves for objects with existing models, visit the Database of Asteroid Models from Inversion Techniques (DAMIT) web site

<https://astro.troja.mff.cuni.cz/projects/damit/>

Additional lightcurves could lead to the asteroid being added to or improving one in DAMIT, thus increasing the total number of asteroids with spin axis and shape models.

Included in the list below are objects that:

1. Are rated U = 3- or 3 in the LCDB.
2. Do not have reported pole in the LCDB Summary table.
3. Have at least three entries in the Details table of the LCDB where the lightcurve is rated U  $\geq$  2.

The caveat for condition #3 is that no check was made to see if the lightcurves are from the same apparition or if the phase angle bisector longitudes differ significantly from the upcoming apparition. The last check is often not possible because the LCDB does not list the approximate date of observations for all details records. Including that information is an on-going project.

Favorable apparitions are in bold text. NEAs are in italics.

Num	Name	Brightest			LCDB Data		U
		Date	Mag	Dec	Period	Amp	
<b>8256</b>	<b>Shenzhen</b>	<b>10 03.5</b>	<b>14.9</b>	<b>-4</b>	<b>3.395</b>	<b>0.30-0.32</b>	<b>3</b>
2189	Zaragoza	10 04.7	15.1	-17	4.9281	0.17-0.91	3
<b>6265</b>	<b>1985 TW3</b>	<b>10 06.1</b>	<b>14.8</b>	<b>+1</b>	<b>2.7093</b>	<b>0.26-0.36</b>	<b>3</b>
754	Malabar	10 06.5	13.4	-3	11.74	0.19-0.38	3
1590	Tsiolkovskaja	10 06.7	14.1	+9	6.731	0.10-0.4	3
<b>713</b>	<b>Luscinia</b>	<b>10 07.5</b>	<b>12.8</b>	<b>+11</b>	<b>9.9143</b>	<b>0.09-0.40</b>	<b>3</b>
1115	Sabauda	10 08.4	14.5	-12	6.718	0.16-0.27	3
<b>4132</b>	<b>Bartok</b>	<b>10 09.3</b>	<b>13.9</b>	<b>-12</b>	<b>3.297</b>	<b>0.32-0.44</b>	<b>3</b>
194	Prokne	10 11.6	10.7	-11	15.679	0.08-0.27	3
<b>102</b>	<b>Miriam</b>	<b>10 12.3</b>	<b>11.0</b>	<b>+9</b>	<b>23.613</b>	<b>0.04-0.14</b>	<b>3</b>
1171	Rusthawelia	10 12.3	13.2	+3	10.98	0.26-0.31	3
<b>2346</b>	<b>Lilio</b>	<b>10 17.3</b>	<b>14.3</b>	<b>+16</b>	<b>3.031</b>	<b>0.20-0.31</b>	<b>3</b>
657	Gunlod	10 17.6	15.3	+24	15.6652	0.19-0.20	3
326	Tamara	10 22.5	12.3	+9	14.445	0.10-0.27	3
67	Asia	10 24.4	10.7	+10	15.853	0.22-0.26	3
618	Elfriede	10 29.1	12.9	-9	14.791	0.11-0.17	3
255	Oppavia	11 02.2	14.2	+21	19.499	0.14-0.16	3
<b>635</b>	<b>Vundtia</b>	<b>11 02.7</b>	<b>13.2</b>	<b>+5</b>	<b>11.79</b>	<b>0.15-0.27</b>	<b>3</b>
<b>2074</b>	<b>Shoemaker</b>	<b>11 03.1</b>	<b>15.2</b>	<b>-5</b>	<b>2.5328</b>	<b>0.06-0.13</b>	<b>3</b>
<b>1520</b>	<b>Imatra</b>	<b>11 06.6</b>	<b>14.4</b>	<b>+27</b>	<b>18.635</b>	<b>0.27-0.35</b>	<b>3-</b>
3028	Zhangguoxi	11 07.6	15.0	+9	4.826	0.12-0.25	3
252	Clementina	11 09.8	13.9	+11	10.864	0.32-0.44	3
<b>3155</b>	<b>Lee</b>	<b>11 10.3</b>	<b>14.5</b>	<b>+22</b>	<b>8.31</b>	<b>0.22-0.4</b>	<b>3</b>
373	Melusina	11 11.0	13.3	+35	12.97	0.20-0.25	3
1453	Fennia	11 12.3	15.0	+52	4.4121	0.10-0.20	3
206	Hersilia	11 13.7	12.2	+12	11.122	0.13-0.20	3

Num	Name	Brightest			LCDB Data		U
		Date	Mag	Dec	Period	Amp	
1777	Gehrels	11 14.0	14.9	+23	2.8355	0.21-0.27	3
<b>177</b>	<b>Irma</b>	<b>11 15.0</b>	<b>11.8</b>	<b>+21</b>	<b>13.856</b>	<b>0.24-0.37</b>	<b>3</b>
235	Carolina	11 16.8	13.0	+16	17.61	0.25-0.38	3
<b>1313</b>	<b>Berna</b>	<b>11 18.2</b>	<b>14.2</b>	<b>+39</b>	<b>25.46</b>	<b>0.20-0.58</b>	<b>3</b>
<b>266</b>	<b>Aline</b>	<b>11 19.0</b>	<b>11.4</b>	<b>+19</b>	<b>13.018</b>	<b>0.05-0.10</b>	<b>3</b>
1342	Brabantia	11 25.7	15.0	+51	4.1754	0.17-0.21	3
<b>305</b>	<b>Gordonia</b>	<b>11 26.7</b>	<b>12.1</b>	<b>+17</b>	<b>12.893</b>	<b>0.10-0.23</b>	<b>3</b>
975	Perseverantia	11 27.0	14.1	+23	7.267	0.17-0.23	3
348	May	11 27.3	13.2	+15	7.3812	0.14-0.16	3
232	Russia	11 28.2	14.3	+12	21.905	0.14-0.31	3
53435	1999 VM40	11 28.7	15.0	+43	5.189	0.19-0.38	3
143	Adria	11 30.8	13.4	+38	22.005	0.07-0.10	3
<b>9069</b>	<b>Hovland</b>	<b>12 01.2</b>	<b>14.9</b>	<b>+21</b>	<b>4.217</b>	<b>0.08-0.11</b>	<b>3</b>
74	Galatea	12 04.2	11.5	+17	17.268	0.08-0.16	3
483	Seppina	12 08.0	13.6	-3	12.727	0.14-0.29	3
275	Sapientia	12 09.0	12.6	+17	14.931	0.05-0.12	3-
2448	Sholokhov	12 10.1	15.2	+1	10.059	0.21-0.63	3
26471	Tracybecker	12 12.1	15.2	+29	2.6868	0.18-0.24	3
522	Helga	12 12.5	13.9	+20	8.129	0.13-0.31	3
298	Baptistina	12 20.1	13.6	+35	16.23	0.10-0.25	3
333	Badenia	12 20.5	13.4	+29	9.862	0.20-0.33	3
533	Sara	12 21.2	14.0	+14	11.654	0.19-0.30	3
156	Xanthippe	12 23.6	12.9	+16	22.37	0.10-0.12	3
<b>971</b>	<b>Alsatia</b>	<b>12 26.7</b>	<b>12.5</b>	<b>+29</b>	<b>9.614</b>	<b>0.17-0.29</b>	<b>3</b>
1069	Planckia	12 27.7	13.8	+9	8.665	0.14-0.42	3
<b>3712</b>	<b>Kraft</b>	<b>12 28.5</b>	<b>14.2</b>	<b>+40</b>	<b>9.341</b>	<b>0.27-1.20</b>	<b>3</b>

### Radar-Optical Opportunities

Past radar targets:

<http://echo.jpl.nasa.gov/~lance/radar.nea.periods.html>

Arecibo available targets:

<http://www.naic.edu/~pradar>

<http://www.naic.edu/~pradar/ephemfuture.txt>

Goldstone available targets:

[http://echo.jpl.nasa.gov/asteroids/goldstone\\_asteroid\\_schedule.html](http://echo.jpl.nasa.gov/asteroids/goldstone_asteroid_schedule.html)

These are based on *known* targets at the time the list was prepared. It is very common for newly discovered objects to move up the list and become radar targets on short notice. We recommend that you keep up with the latest discoveries the Minor Planet Center observing tools.

In particular, monitor NEAs and be flexible with your observing program. In some cases, you may have only 1-3 days when the asteroid is within reach of your equipment. Be sure to keep in touch with the radar team (through Benner's email or their Facebook or Twitter accounts) if you get data. The team may not always be observing the target but your initial results may change their plans. In all cases, your efforts are greatly appreciated.

Use the ephemerides below as a guide to your best chances for observing, but remember that photometry may be possible before and/or after the ephemerides given below. Note that *geocentric* positions are given. Use these web sites to generate updated and *topocentric* positions:

MPC: <http://www.minorplanetcenter.net/iau/MPEph/MPEph.html>

JPL: <http://ssd.jpl.nasa.gov/?horizons>

In the ephemerides below, ED and SD are, respectively, the Earth and Sun distances (AU), V is the estimated Johnson V magnitude, and  $\alpha$  is the phase angle. SE and ME are the great circle distances (in degrees) of the Sun and Moon from the asteroid. MP is the lunar phase and GB is the galactic latitude. "PHA" indicates that the object is a "potentially hazardous asteroid", meaning that at some (long distant) time, its orbit might take it very close to Earth.

About YORP Acceleration

Many, if not all, of the targets in this section are near-Earth asteroids. These objects are particularly sensitive to YORP acceleration. YORP (Yarkovsky–O’Keefe–Radzievskii–Paddack) is the asymmetric thermal re-radiation of sunlight that can cause an asteroid’s rotation period to increase or decrease. High precision lightcurves at multiple apparitions can be used to model the asteroid’s *sidereal* rotation period and see if it’s changing.

It usually takes four apparitions to have sufficient data to determine if the asteroid rotation rate is changing under the influence of YORP. This is why observing an asteroid that already has a well-known period remains a valuable use of telescope time. It is even more so when considering the BYORP (binary-YORP) effect among binary asteroids that has stabilized the spin so that acceleration of the primary body is not the same as if it would be if there were no satellite.

To help focus efforts in YORP detection, Table I gives a quick summary of this quarter’s radar-optical targets. The family or group for the asteroid is given under the number name. Also, under the name will be additional flags such as “PHA” for Potentially Hazardous Asteroid, NPAR for a tumbler, and/or “BIN” to indicate the asteroid is a binary (or multiple) system. “BIN?” means that the asteroid is a suspected but not confirmed binary. The period is in hours and, in the case of binary, for the primary. The Amp column gives the known range of lightcurve amplitudes. The App columns gives the number of different apparitions at which a lightcurve period was reported while the Last column gives the year for the last reported period. The R SNR column indicates the estimated radar SNR using the tool at

<http://www.naic.edu/~eriverav/scripts/index.php>

The SNRs were calculated using the current MPCORB absolute magnitude (H), a period of 4 hours (2 hours if  $D \leq 200$  m) if it’s not known, and the approximate minimum Earth distance during the current quarter. These are estimates only and assume that the radars are fully functional.

If the SNR value is in bold text, the object was found on the radar planning pages listed above. Otherwise, the planning tool at

[http://www.minorplanet.info/PHP/call\\_OppLCDBQuery.php](http://www.minorplanet.info/PHP/call_OppLCDBQuery.php)

was used to find known NEAs that were  $V < 18.0$  during the quarter. An object is usually placed on the list only if the estimated Arecibo SNR  $> 10$  when using the SNR calculator mentioned above.

It’s rarely the case, especially when shape/spin axis modeling, that there are too many observations. Remember that the best set for modeling includes data not just from multiple apparitions but from as wide a range of phase angles during each apparition as well.

For potential radar targets “A” is Arecibo; “G” is Goldstone.

Asteroid	Period	Amp	App	Last	R SNR
<b>(302830) 2003 FB</b> NEA	-	-	-	-	<b>10 A</b>
(5645) 1990 SP NEA	30.39	0.70	1	2002	55 A 20 G
<b>(511808) 2015 FH120</b> NEA	-	-	-	-	-
<b>(159402) 1999 AP10</b> NEA	<b>7.908</b>	<b>0.36</b>	<b>1</b>	<b>2009</b>	<b>525 A</b> <b>175 G</b>

Asteroid	Period	Amp	App	Last	R SNR
(474179) 1999 VS6 NEA	16.91	0.51	1	2017	15 A
<b>(380929) 2006 HU30</b> NEA	<b>49.0</b>	<b>0.17</b>	<b>1</b>	<b>2013</b>	<b>30 A</b> <b>10 G</b>
2015 WN1 NEA	-	-	-	-	100 A
2017 WJ16 NEA	-	-	-	-	??
162173 Ryugu NEA	7.627	0.10 0.16	2	2012	35 A
<b>(153201) 2000 WO107</b> NEA	-	-	-	-	<b>1800 A</b> <b>600 G</b>
<b>(7753) 1988 XB</b> NEA	-	-	-	-	<b>150 A</b> <b>50 G</b>
<b>(482505) 2012 TQ78</b> NEA	-	-	-	-	<b>10 A</b>
<b>(501647) 2014 SD224</b> NEA	-	-	-	-	<b>210 A</b> <b>70 G</b>

Table I. Summary of radar-optical opportunities for the current quarter. Period and amplitude data are from the asteroid lightcurve database (LCDB; Warner et al., 2009a). SNR values are estimates that are affected by radar power output along with rotation period, size, and distance. They are given for relative comparisons among the objects in the list.

**(302830) 2003 FB (H = 18.8)**

There are no entries in the LCDB for this NEA. The estimated diameter when assuming an albedo of 0.2 (Warner et al., 2009a) is about 500 meters. This makes it less likely that the period will be  $P < 2$  hours. Note that the observing window is very short and starts in late September.

DATE	RA	Dec	ED	SD	V	$\alpha$	SE	ME	MP	GB
09/25	04 44.0	-30 44	0.21	1.08	17.8	61.9	107	116	+0.60	-40
09/27	04 59.9	-30 12	0.20	1.07	17.7	64.5	105	104	+0.79	-36
09/29	05 17.7	-29 25	0.18	1.06	17.6	67.5	103	93	+0.92	-32
10/01	05 37.5	-28 20	0.17	1.04	17.5	70.9	100	82	+0.99	-28
10/03	05 59.5	-26 51	0.16	1.03	17.5	74.7	96	72	+0.99	-23
10/05	06 23.8	-24 55	0.15	1.02	17.5	79.0	93	63	-0.91	-17
10/07	06 50.2	-22 26	0.14	1.00	17.5	83.8	88	55	-0.78	-10

**(5645) 1990 SP (H = 17.1)**

The estimated diameter is 1.1 km. The sole entry in the LCDB is from Pravec et al. (2005), who reported a period of 30.39 h and amplitude of 0.7 mag. It is also a likely tumbler with the second period undetermined. Southern observers will have the advantage during the short window that is open the first ten days of October.

DATE	RA	Dec	ED	SD	V	$\alpha$	SE	ME	MP	GB
10/01	05 15.6	-18 00	0.20	1.07	16.0	63.4	106	77	+0.99	-29
10/02	05 23.6	-17 37	0.19	1.07	15.9	64.7	105	70	-1.00	-27
10/03	05 32.0	-17 11	0.19	1.06	15.9	66.0	104	64	-0.99	-25
10/04	05 40.7	-16 43	0.18	1.06	15.9	67.5	103	58	-0.96	-23
10/05	05 49.9	-16 11	0.18	1.05	15.9	69.0	102	52	-0.91	-21
10/06	05 59.5	-15 35	0.17	1.04	15.8	70.6	100	47	-0.85	-18
10/07	06 09.4	-14 56	0.17	1.04	15.8	72.2	99	43	-0.78	-16
10/08	06 19.9	-14 13	0.16	1.03	15.8	74.0	97	40	-0.70	-13
10/09	06 30.7	-13 26	0.16	1.03	15.8	75.8	95	38	-0.60	-11
10/10	06 41.9	-12 35	0.16	1.02	15.8	77.8	93	38	-0.50	-8

**(511808) 2015 FH120 (H = 18.6)**

There is no lightcurve entry in the LCDB for this 600 meter NEA.

DATE	RA	Dec	ED	SD	V	$\alpha$	SE	ME	MP	GB
10/01	02 51.3	-45 29	0.23	1.14	17.5	48.0	122	54	+0.99	-60
10/03	03 03.3	-47 38	0.22	1.12	17.4	51.0	119	56	-0.99	-57
10/05	03 17.7	-49 54	0.20	1.11	17.4	54.4	116	64	-0.91	-54
10/07	03 35.5	-52 17	0.19	1.09	17.3	58.1	113	74	-0.78	-51
10/09	03 57.7	-54 43	0.18	1.07	17.2	62.3	109	85	-0.60	-47
10/11	04 25.7	-57 06	0.17	1.05	17.2	66.9	104	93	-0.40	-42
10/13	05 01.1	-59 13	0.16	1.04	17.2	72.1	99	97	-0.20	-37
10/15	05 45.3	-60 47	0.15	1.02	17.2	77.8	94	96	+0.05	-31
10/17	06 37.6	-61 22	0.14	1.00	17.3	84.0	88	92	-0.00	-25
10/19	07 34.3	-60 33	0.14	0.99	17.5	90.6	82	89	+0.07	-18

**(159402) 1999 AP10 (H = 16.1)**

Franco et al. (2010) first reported a period 7.9 h. This was confirmed during the same apparition (2009) by Hasegawa et al. (2018). Given the near Earth-day commensurability, it's good that the 1.8 km NEA will be observable for several months. Still, a coordinated campaign with observers well separated in longitude will make for quicker results.

DATE	RA	Dec	ED	SD	V	$\alpha$	SE	ME	MP	GB
10/01	22 38.1	+02 18	0.12	1.11	12.9	24.8	152	22	+0.99	-46
10/11	22 24.7	+22 56	0.09	1.07	12.6	38.6	138	123	-0.40	-29
10/21	22 06.8	+54 06	0.08	1.04	12.8	56.9	119	96	+0.24	-1
10/31	21 01.3	+82 14	0.10	1.02	13.5	69.5	105	80	+1.00	+23
11/10	10 58.2	+79 32	0.12	1.02	14.1	71.4	102	66	-0.35	+36
11/20	10 21.7	+69 25	0.16	1.04	14.5	66.6	105	130	+0.28	+42
11/30	10 01.2	+62 59	0.19	1.07	14.7	58.7	112	72	+1.00	+45
12/10	09 39.6	+58 24	0.22	1.12	14.9	49.3	121	71	-0.28	+44
12/20	09 14.6	+54 36	0.26	1.17	15.0	39.1	131	136	+0.31	+42
12/30	08 48.5	+50 51	0.30	1.23	15.2	29.1	142	37	+1.00	+39

**(474179) 1999 VS6 (H = 19.0)**

Warner (2017) found a period of 16.9 h based on observations obtained in 2017. The estimated diameter is about 500 meters. Those able to observe at high declinations will have a decided advantage and opportunity.

DATE	RA	Dec	ED	SD	V	$\alpha$	SE	ME	MP	GB
10/20	04 08.4	+10 12	0.19	1.15	17.0	31.1	143	166	+0.15	-29
10/23	04 01.2	+16 35	0.17	1.14	16.6	27.5	148	128	+0.45	-27
10/26	03 50.8	+24 26	0.15	1.13	16.3	24.7	152	90	+0.74	-23
10/29	03 35.7	+33 44	0.14	1.12	16.1	24.2	152	55	+0.94	-18
11/01	03 13.2	+44 03	0.13	1.11	16.1	27.7	149	32	-1.00	-12
11/04	02 38.8	+54 22	0.13	1.10	16.2	34.6	141	43	-0.90	-5
11/07	01 45.2	+63 14	0.14	1.09	16.5	42.9	132	70	-0.66	+1
11/10	00 25.6	+69 13	0.15	1.08	16.9	50.8	123	95	-0.35	+6
11/13	22 49.8	+71 30	0.16	1.07	17.2	57.6	115	108	-0.07	+11
11/16	21 26.3	+70 48	0.18	1.06	17.6	63.1	108	105	+0.01	+14

**(380929) 2006 HU30 (H = 19.6)**

The estimated diameter for this NEA is about 350 meters. Warner (2014) reported a period of 49 h. Here's another case when a coordinated campaign of observers is warranted and recommended.

DATE	RA	Dec	ED	SD	V	$\alpha$	SE	ME	MP	GB
10/15	06 50.5	-65 33	0.17	1.00	18.7	85.0	85	90	-0.05	-25
10/19	05 24.5	-61 05	0.14	1.02	18.1	75.8	96	99	+0.07	-34
10/23	04 08.0	-51 18	0.13	1.05	17.4	62.9	111	91	+0.45	-46
10/27	03 11.4	-36 26	0.12	1.07	16.9	46.6	128	60	+0.82	-59
10/31	02 32.5	-19 39	0.12	1.10	16.5	30.3	146	29	+1.00	-66
11/04	02 06.0	-04 55	0.14	1.12	16.5	19.1	158	53	-0.90	-62
11/08	01 47.7	+06 08	0.17	1.15	16.9	16.4	161	102	-0.56	-54
11/12	01 35.1	+13 56	0.20	1.17	17.4	19.2	157	156	-0.15	-48
11/16	01 26.4	+19 26	0.23	1.20	17.9	22.9	152	141	+0.01	-43
11/20	01 20.8	+23 24	0.27	1.23	18.4	26.0	147	86	+0.28	-39

**2015 WN1 (H = 26.5)**

The estimated diameter is only 15 meters, which is why the asteroid remains faint despite an Earth distance of only 0.01 au. The asteroid's sky motion and the possibility of being a super-fast rotator call for short exposures at the start (see Pravec et al., 2000). Access to a 1-meter scope or larger is recommended.

DATE	RA	Dec	ED	SD	V	$\alpha$	SE	ME	MP	GB
11/12	21 25.0	-12 18	0.01	0.99	19.5	89.3	90	135	-0.15	-40
11/13	23 28.6	-01 26	0.01	0.99	18.4	57.9	122	152	-0.07	-58
11/14	01 06.8	+07 46	0.01	1.00	18.2	33.0	147	163	-0.02	-55
11/15	02 05.6	+12 34	0.02	1.00	18.4	18.9	161	163	+0.00	-46
11/16	02 40.5	+14 59	0.02	1.01	18.7	11.2	169	157	+0.01	-40
11/17	03 02.6	+16 19	0.03	1.01	19.0	6.8	173	148	+0.05	-36

**2017 WJ16 (H = 24.3)**

There are no entries for this NEA in the LCDB. The estimated diameter is only 40 meters, making it another candidate for being a super-fast rotator ( $P \ll 2$  h). As pointed out by Pravec et al., (2000), exposures must be kept to no longer than  $0.187 \times P$  to avoid "rotational smearing," which can lead to too small a lightcurve amplitude or, worse, completely hide any rotational indicators.

DATE	RA	Dec	ED	SD	V	$\alpha$	SE	ME	MP	GB
11/18	08 21.3	+07 41	0.02	1.00	18.2	69.2	110	146	+0.11	+23
11/20	07 50.5	+17 58	0.02	1.00	17.4	57.5	122	171	+0.28	+21
11/22	06 56.2	+32 37	0.01	1.00	16.6	42.4	137	134	+0.48	+15
11/24	05 17.1	+47 59	0.01	1.00	16.2	31.1	149	92	+0.68	+6
11/26	02 59.0	+54 37	0.01	1.00	16.5	35.5	144	57	+0.84	-4
11/28	01 12.8	+52 22	0.02	1.00	17.3	46.0	133	44	+0.95	-10
11/30	00 14.1	+48 01	0.02	1.00	18.0	54.8	124	55	+1.00	-14
12/02	23 41.3	+44 15	0.03	1.00	18.6	61.5	117	75	-0.97	-17

**162173 Ryugu (H = 19.3)**

Ryugu is the target of the Hayabusa 2 sample return mission. It visited the asteroid in mid-2018 and, if all goes well, should land on Earth in December of this year. The rotation period is 7.63 h (e.g., Muller et al., 2017).

DATE	RA	Dec	ED	SD	V	$\alpha$	SE	ME	MP	GB
10/01	23 38.2	+34 58	0.19	1.17	17.3	28.7	146	41	+0.99	-26
10/11	23 15.9	+34 11	0.17	1.13	17.0	32.1	143	108	-0.40	-25
10/21	22 55.4	+31 22	0.14	1.10	16.9	38.7	136	93	+0.24	-25
10/31	22 41.5	+26 44	0.13	1.07	16.8	47.3	127	51	+1.00	-28
11/10	22 35.9	+20 38	0.11	1.05	16.7	57.0	118	145	-0.35	-32
11/20	22 38.9	+13 03	0.10	1.02	16.7	67.2	107	50	+0.28	-39
11/30	22 49.9	+03 34	0.09	1.00	16.7	78.0	97	79	+1.00	-48
12/10	23 08.2	-09 01	0.07	0.98	16.7	89.2	87	150	-0.28	-60

**(153201) 2000 WO107 (H = 19.3)**

There is no lightcurve entry in the LCDB for this 400-m NEA. As fate often provides, the asteroid is at its brightest when close in the sky to a nearly full moon. Even so, the very large swing in phase angles make it a good target for finding the H and G values.

DATE	RA	Dec	ED	SD	V	$\alpha$	SE	ME	MP	GB
11/27	11 36.6	-04 03	0.04	0.97	16.5	108.8	69	146	+0.90	+54
11/29	09 02.5	+13 09	0.03	1.00	13.9	65.7	113	82	+0.98	+35
12/01	05 43.6	+24 47	0.04	1.02	13.2	16.7	163	10	-1.00	-1
12/03	04 13.7	+24 39	0.06	1.05	13.8	5.7	174	35	-0.93	-19
12/05	03 35.9	+23 34	0.09	1.07	15.0	14.9	164	68	-0.80	-26
12/07	03 16.4	+22 47	0.12	1.09	15.8	20.4	157	99	-0.61	-29
12/09	03 04.8	+22 13	0.15	1.12	16.5	24.0	153	129	-0.39	-31
12/11	02 57.3	+21 50	0.18	1.14	17.0	26.6	149	159	-0.18	-32
12/13	02 52.3	+21 33	0.20	1.16	17.4	28.7	146	167	-0.04	-33
12/15	02 48.9	+21 20	0.23	1.18	17.8	30.4	143	138	+0.00	-34

**(7753) 1988 XB (H = 18.6)**

Most NEAs are in the S taxonomic complex. However, this 575 m asteroid is type Cb (Binzel et al., 2019), meaning it is particularly dark (low albedo). This is another good chance to find the H and G values.

DATE	RA	Dec	ED	SD	V	$\alpha$	SE	ME	MP	GB
11/25	10 09.3	+05 49	0.07	0.99	15.7	85.4	91	146	+0.76	+46
11/30	08 45.0	+17 03	0.08	1.03	15.3	57.1	119	65	+1.00	+33
12/05	07 44.8	+23 09	0.10	1.07	15.3	37.3	139	12	-0.80	+22
12/10	07 03.6	+26 11	0.13	1.11	15.5	23.3	154	90	-0.28	+14
12/15	06 35.0	+27 41	0.17	1.14	15.7	13.1	165	169	+0.00	+9
12/20	06 14.8	+28 25	0.20	1.18	15.9	5.9	173	117	+0.31	+5
12/25	06 00.5	+28 44	0.24	1.22	16.4	5.0	174	54	+0.77	+3
12/30	05 50.5	+28 51	0.28	1.26	17.0	9.2	168	10	+1.00	+1
01/04	05 43.7	+28 50	0.33	1.30	17.5	13.5	162	76	-0.76	+0

**(482505) 2012 TQ78 (H = 19.5)**

There are no entries in the LCDB for this 375-m NEA. The rotation period will *likely* be  $P > 2$  h, but assume nothing.

DATE	RA	Dec	ED	SD	V	$\alpha$	SE	ME	MP	GB
11/10	05 42.6	+26 53	0.28	1.22	18.5	30.3	142	70	-0.35	-2
11/15	05 48.2	+30 48	0.24	1.19	18.0	28.7	145	141	+0.00	+1
11/20	05 54.1	+36 08	0.20	1.16	17.6	27.8	147	146	+0.28	+5
11/25	06 01.4	+43 34	0.17	1.13	17.1	28.8	146	88	+0.76	+10
11/30	06 12.8	+54 01	0.14	1.10	16.8	33.8	142	42	+1.00	+16
12/05	06 40.1	+68 20	0.12	1.07	16.7	44.4	131	49	-0.80	+24
12/10	10 10.4	+83 57	0.11	1.03	16.9	60.3	114	87	-0.28	+32
12/15	16 35.7	+71 50	0.11	1.00	17.4	78.3	96	97	+0.00	+36

**(501647) 2014 SD224 (H = 22.3)**

The estimated size is 100 m, which makes NEA a potential super-fast rotator. Use as short exposures as possible to start and then adjust for a higher SNR (longer exposures) as able and needed.

DATE	RA	Dec	ED	SD	V	$\alpha$	SE	ME	MP	GB
12/10	06 49.1	+46 40	0.10	1.07	18.6	28.6	149	93	-0.28	+19
12/12	06 45.5	+48 24	0.08	1.06	18.3	28.5	149	120	-0.10	+19
12/14	06 40.0	+50 36	0.07	1.05	18.0	28.9	149	144	-0.01	+19
12/16	06 31.0	+53 31	0.06	1.04	17.6	30.2	148	151	+0.02	+19
12/18	06 15.3	+57 32	0.05	1.03	17.2	33.0	145	134	+0.14	+18
12/20	05 43.0	+63 19	0.04	1.01	16.8	38.4	140	110	+0.31	+17
12/22	04 12.9	+71 01	0.03	1.00	16.5	48.7	130	85	+0.51	+14
12/24	23 55.4	+70 55	0.02	0.99	16.5	67.8	111	67	+0.69	+9
12/26	21 18.0	+46 52	0.02	0.98	17.3	97.7	81	77	+0.85	-2

## References

- Binzel, R.P.; DeMeo, F.E.; Turtelboom, E.V.; Bus, S.J.; Tokunaga, A.; Burbine, T.H.; Lantz, C.; Polishook, D.; Carry, B.; Morbidelli, A.; Birlan, M.; Vernazza, P.; Burt, B.J.; Moskovitz, N.; Slivan, S.M.; Thomas, C.A.; Rivkin, A.S.; Hicks, M.D.; Dunn, T.; Reddy, V.; Sanchez, J.A.; Granvik, M.; Kohout, T. (2019). "Compositional distributions and evolutionary processes for the near-Earth object population: Results from the MIT-Hawaii Near-Earth Object Spectroscopic Survey (MITHNEOS)." *Icarus* **324**, 41-76.
- Franco, L.; Carbognani, A.; Wiggins, P.; Koehn, B.W.; Schmidt, R. (2010). "Collaborative Lightcurve Photometry of Near-Earth Asteroid (159402) 1999 AP10." *Minor Planet Bull.* **37**, 83-85.
- Harris, A.W.; Young, J.W.; Contreiras, L.; Dockweiler, T.; Belkora, L.; Salo, H.; Harris, W.D.; Bowell, E.; Poutanen, M.; Binzel, R.P.; Tholen, D.J.; Wang, S. (1989). "Phase relations of high albedo asteroids: The unusual opposition brightening of 44 Nysa and 64 Angelina." *Icarus* **81**, 365-374.
- Hasegawa, S.; Kuroda, D.; Kitazato, K.; Kasuga, T.; Sekiguchi, T.; Takato, N.; Aoki, K.; Arai, A.; and 36 co-authors. (2018). "Physical properties of near-Earth asteroids with a low delta-v: Survey of target candidates for the Hayabusa2 mission." *Pub. Astron. Soc. Japan* **70**, A114.
- Muironen, K.; Belskaya, I.N.; Cellino, A.; Delbò, M.; Levasseur-Regourd, A.-C.; Penttilä, A.; Tedesco, E.F. (2010). "A three-parameter magnitude phase function for asteroids." *Icarus* **209**, 542-555.
- Muller, T.G.; Durech, J.; Ishiguro, M.; Mueller, M.; Kruhler, T.; Yang, H.; Kim, M.-J.; O'Rourke, L.; Usui, F.; Kiss, C.; Altieri, B.; Carry, B.; Choi, Y.-J.; Delbo, M.; Emery, J.P.; Greiner, J.; Hasegawa, S.; Hora, J.L.; Knust, F.; Kuroda, D.; Osip, D.; Rau, A.; Rivkin, A.; Schady, P.; Thomas-Osip, J.; Trilling, D.; Urakawa, S.; Vilenius, E.; Weissman, P.; Zeidler, P. (2017). "Hayabusa-2 mission target asteroid 162173 Ryugu (1999 JU3): Searching for the object's spin-axis orientation." *Astron. Astrophys.* **599**, A103.
- Pravec, P.; Hergenrother, C.; Whiteley, R.; Sarounova, L.; Kusnirak, P. (2000). "Fast Rotating Asteroids 1999 TY2, 1999 SF10, and 1998 WB2." *Icarus* **147**, 477-486.
- Pravec, P.; Harris, A.W.; Scheirich, P.; Kušnirák, P.; Šarounová, L.; Hergenrother, C.W.; Mottola, S.; Hicks, M.D.; Masi, G.; Krugly, Y.N.; Shevchenko, V.G.; Nolan, M.C.; Howell, E.S.; Kaasalainen, M.; Galád, A.; Brown, P.; Degraff, D.R.; Lambert, J.V.; Cooney, W.R.; Foglia, S. (2005). "Tumbling asteroids." *Icarus* **173**, 108-131.
- Warner, B.D.; Harris, A.W.; Pravec, P. (2009a). "The asteroid lightcurve database." *Icarus* **202**, 134-146.
- Warner, B.D.; Harris, A.W.; Pravec, P.; Durech, J.; Benner, L.A.M. (2009b). "Lightcurve Photometry Opportunities: 2009 October-December." *Minor Planet Bulletin* **36**, 188-190.
- Warner, B.D. (2014). "Near-Earth Asteroid Lightcurve Analysis at CS3-Palmer Divide Station: 2013 September-December." *Minor Planet Bull.* **41**, 113-124.
- Warner, B.D. (2017). "Near-Earth Asteroid Lightcurve at CS3-Palmer Divide Station: 2017 April thru June." *Minor Planet Bull.* **44**, 335-344.

## ROTATIONAL PERIOD AND LIGHTCURVE OF 7910 ALEKSOLA

Alfonso Noschese  
AstroCampania Associazione  
Osservatorio Elianto (K68), Pontecagnano (SA) Italy  
a.noschese@astrocampania.it

Nello Ruocco  
AstroCampania Associazione, Naples, Italy  
Osservatorio Astronomico Nastro Verde (C82), Sorrento (Na)  
Italy

Antonio Vecchione  
AstroCampania Associazione, Naples, Italy

(Received: 2020 July 15 Revised: 2020 August 11)

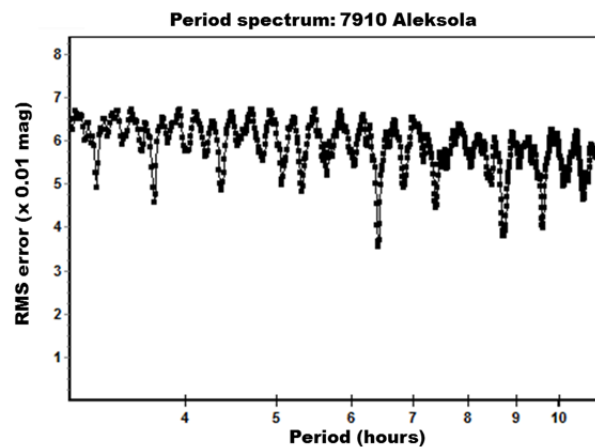
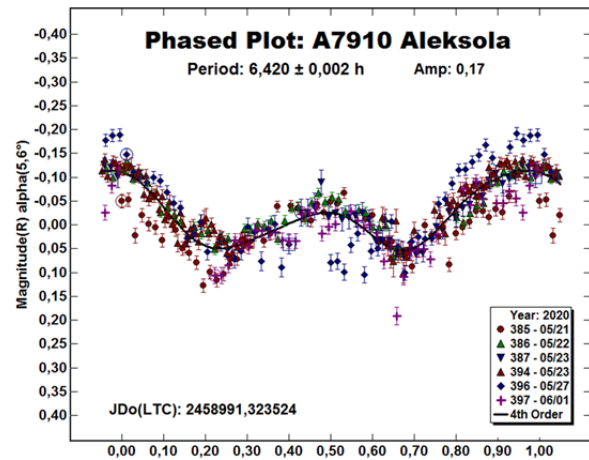
The lightcurve and rotation period determination for 7910 Aleksola are reported. The results are:  $P = 6.420 \pm 0.002$  h and  $A = 0.17$  mag.

The aim of this research is to find the rotational period and lightcurve of main-belt asteroid 7910 Aleksola. CCD photometric observations of 7910 Aleksola were carried out by means of Elianto observatory located in the south of Italy (Pontecagnano) using a 0.3-m Newton telescope operating at  $f/4$  equipped with a Moravian KAF1603 ME CCD camera (1536×1024 array of 9-micron pixels) with a clear filter. A session of the measurements was also carried out at ‘Nastro Verde’ observatory located at Sorrento (Naples), Italy by means of a 0.35-m Schmidt-Cassegrain telescope operating at  $f/6.3$  using a SBIG ST-10 XME CCD camera with 2148×1472 array of 6.8-micron pixels with a clear filter.

All images were astrometrically aligned, dark and flat-field corrected using *Maxim DL* software. *MPO Canopus* (Warner, 2017) was used to measure the magnitudes, perform Fourier analysis, and produce the final lightcurve. In particular, data were reduced in *MPO Canopus* using differential photometry. Night-to-night zero-point calibration was accomplished by selecting up to five comparison stars with near-solar colors using the “comp star selector” feature. To analyze the data points ATLAS star catalog (Tonry et al., 2018) was used for determining the comparison star magnitudes. The “StarBGone” routine within *MPO Canopus* was used to subtract stars that occasionally merged with the asteroid during the observations. *MPO Canopus* was also used for rotation period analysis. The software employs a FALC Fourier analysis algorithm developed by Harris (Harris et al., 1989).

7910 Aleksola was discovered at Nauchnyj on 1976 April 01 by N. S. Chernykh. It is a main-belt asteroid with a semi-major axis of 2.248 AU, orbital period of 3.4 years, eccentricity of 0.138 and inclination of 8.363 deg. This five-kilometer-asteroid has an absolute magnitude of 13.6 and a geometric albedo of 0.20 (JPL, 2020). CCD photometric observations were performed between 2020 May 22 and 2020 June 1. Six observation sessions were produced for lightcurve analysis to collect 342 data points and adopting an exposure time ranging between 120 s and 360 s.

Our data analysis gave a period of  $6.420 \pm 0.002$  h accompanied by an amplitude of 0.17 mag. The period found is in excellent agreement with a recently report (Páll, 2020). The amplitude found in our case is larger if compared with the one ( $0.13 \pm 0.03$ ) measured by the same authors while is closer to that reported ( $0.18 \pm 0.01$ ) on the web by Pravec (Pravec, 2020).



### References

- Harris, A.W.; Young, J.W.; Scaltriti, F.; Zappala, V. (1984). “Lightcurves and phase relations of the asteroids 82 Alkmene and 444 Gyptis.” *Icarus* 57, 251-258.
- Harris, A.W.; Young, J.W.; Bowell, E.; Martin, L.J.; Millis, R.L.; Poutanen, M.; Scaltriti, F.; Zappala, V.; Schober, H.J.; Debehogne, H.; Zeigler, K.W. (1989). “Photoelectric Observations of Asteroids 3, 24, 60, 261, and 863.” *Icarus* 77, 171-186.
- JPL (2020). Small-Body Database Browser.  
<https://ssd.jpl.nasa.gov/sbdb.cgi>

Number	Name	20yy mm/dd	Pts	Phase	L <sub>PAB</sub>	B <sub>PAB</sub>	Period(h)	P.E.	Amp	A.E.	Grp
7910	Aleksola	20/05/22-20/06/01	342	5.58-9.71	239.9	8.1	6.420	0.02	0.20	0.01	MB

Table I. Observing circumstances and results. The phase angle is given for the first and last date. L<sub>PAB</sub> and B<sub>PAB</sub> are the approximate phase angle bisector longitude and latitude at mid-date range (Harris *et al.*, 1984). Grp is the asteroid family/group (Warner *et al.*, 2009).

Páll, A.; Szakáts, R.; Kiss, C.; Bódi, A.; Bognár, Z.; Kalup, C.; Kiss, L.L.; Marton, G.; Molnár, L.; Plachy, E.; Sármeczky, K.; Szabó, G.M.; Szabó, R. (2020). "Solar System Objects Observed with TESS - First Data Release: Bright Main-belt and Trojan Asteroids from the Southern Survey." *Astrophysical Journal Supplement Series* **247**, 26-34.

Pravec, P. (2020). Ondrejov Asteroid Photometry Project. Summary of prepublished data.  
<http://www.asu.cas.cz/~ppravec/newres.txt>

Tonry, J.L.; Denneau, L.; Flewelling, H.; Heinze, A.N.; Onken, C.A.; Smartt, S.J.; Stalder, B.; Weiland, H.J.; Wolf, C. (2018). "The ATLAS all-sky stellar reference catalog." *Astrophys. J.* **867**, 105.

Warner, B.D.; Harris, A.W.; Pravec, P. (2009). "The Asteroid Lightcurve Database." *Icarus* **202**, 134-146. Updated 2020 March.  
<http://www.minorplanet.info/lightcurvedatabase.html>

Warner, B.D. (2017). MPO Software, MPO Canopus version 10.7.11.1. Bdw Publishing. <http://minorplanetobserver.com>

## ASTEROID PHOTOMETRY AND LIGHTCURVE ANALYSIS AT GORA'S OBSERVATORIES – PART II.

Lic. Milagros Colazo

Facultad de Matemática, Astronomía y Física,  
Universidad Nacional de Córdoba, ARGENTINA  
Grupo de Observadores de Rotaciones de Asteroides (GORA)  
<https://aoacm.com.ar/gora/index.php>  
milirita.colazovinovo@gmail.com

César Fornari, Marcos Santucho, Aldo Mottino, Carlos Colazo,  
Raúl Melia, Néstor Suarez, Nicolás Vasconi, Daniela Arias,  
Ariel Stechina, Damián Scotta, José García,  
Claudio Pittari, Guillermo Ferrero  
Grupo de Observadores de Rotaciones de Asteroides,  
ARGENTINA

Estación Astrofísica Bosque Alegre (MPC 821)  
Bosque Alegre, Córdoba, ARGENTINA

Observatorio Astronómico Córdoba (MPC 822)  
Córdoba Capital, Córdoba, ARGENTINA

Observatorio Astronómico El Gato Gris (MPC 119)  
Tanti, Córdoba, ARGENTINA

Observatorio Galileo Galilei (MPC X31)  
Oro Verde, Entre Ríos, ARGENTINA

Observatorio Antares (MPC X39)  
Pilar, Buenos Aires, ARGENTINA

Observatorio de Aldo Mottino (OAM)  
Rosario, Santa Fe, ARGENTINA

Observatorio de Ariel Stechina (OAS)  
Reconquista, Santa Fe, ARGENTINA

Observatorio de Damián Scotta (ODS)  
San Carlos Centro, Santa Fe, ARGENTINA

Observatorio Punto Azul (OPA)  
Villa María, Córdoba, ARGENTINA

Observatorio de Raúl Melia (RMG)  
Gálvez, Santa Fe, ARGENTINA

Grupo de Astrometría y Fotometría (GAF)  
Córdoba Capital, Córdoba, ARGENTINA

(Received: 2020 May 22)

Synodic rotation periods and amplitudes are reported for 414 Liriope, 949 Hel, 952 Caia, and 1145 Robelmonte.

In this work, we present periods and amplitudes of lightcurves for 414 Liriope, 949 Hel, 952 Caia, and 1145 Robelmonte. These results are the product of a collaborative work by GORA (Grupo de Observadores de Rotaciones de Asteroides). In a recent publication (Colazo et al., 2020), we limited our observations to asteroids with well-defined periods, as part of a preliminary learning. Now, we have focused the study on more complex objectives, which allowed us to provide novel data of scientific relevance. The observatories and equipment used are listed in Table 1.

Observatory	Telescope	Camera
Estación Astrofísica Bosque Alegre	Newtonian telescope (D=1540mm; f=4.9)	CCD APOGEE Alta U9
Observatorio Astronómico Córdoba	Celestron SCT (D=355mm; f=11.0)	CCD SBIG ST7 + F.R.
Observatorio El Gato Gris	Celestron SCT (D=355mm; f=10.6)	CCD SBIG STF8300M
Observatorio Galileo Galilei	Third Planet Optics RC (D=405mm; f=8.0)	CCD SBIG STF8300M
Observatorio Antares	Newtonian telescope (D=200mm; f=5.0)	CCD QHY9 Mono
Observatorio de Aldo Mottino	Newtonian telescope (D=250mm; f=4.7)	CCD SBIG STF8300M
Observatorio de Ariel Stechina	Newtonian telescope (D=254mm; f=4.7)	CCD SBIG STF402
Observatorio de Damián Scotta	Newtonian telescope (D=300mm; f=4.0)	CCD Atik3141
Observatorio Punto Azul	Newtonian telescope (D=254mm; f=5.0)	CCD QHY6 Mono
Observatorio de Raúl Melia	Celestron-Byers SCT (D=200mm; f=10.0)	CCD Meade DSI Pro II

Table I. List of observatories and equipment.

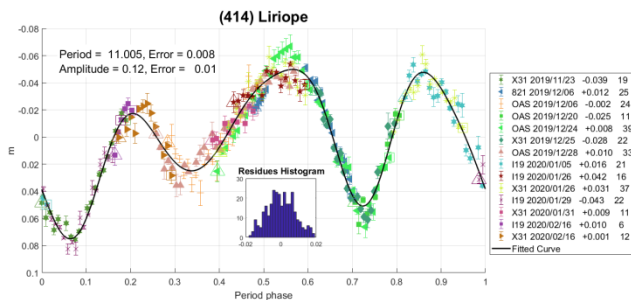
Image acquisition was performed without filters and with exposure times of a few minutes. All images used were corrected with dark frames and, in some cases, bias and flat-field frames were also used. Differential photometry measurements were performed using *FotoDif* software and for the analysis we employed *Periodos* software (Mazzone, 2012).

Below, we present the results for each asteroid under study. The lightcurve figures contain the estimated period and amplitude, a 95% confidence interval regarding the period estimate, RMS of the fitting, estimated amplitude and amplitude error, Julian date corresponding to 0° rotation phase, and the number of data points. In the reference boxes, the columns represent, respectively, the marker, observatory MPC code or – failing that – the GORA internal code, session date, session off-set, and number of data points (Mazzone et al., 2014).

Targets were selected based on three criteria: those asteroids with magnitudes accessible to the equipment of all participants; those with favorable observation conditions from Argentina i.e. with negative declinations  $\delta$ ; and objects with few periods reported in the literature and/or with Lightcurve Database (LCDB, Warner et al., 2009) quality codes (U) of less than 3.

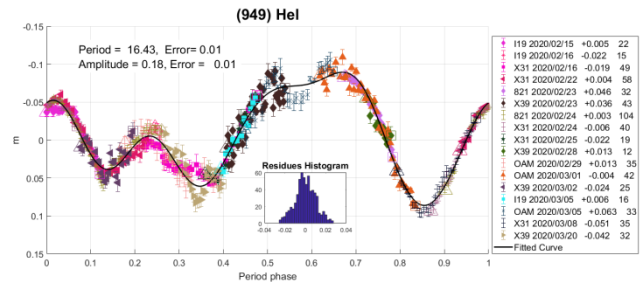
**414 Liriope.** This asteroid is classified as a C-type asteroid in Tholen taxonomy and has an estimated diameter of  $88.760 \pm 2.169$  km (Mainzer et al., 2016). It was discovered on 1896 January 16 by Charlois. The last period and amplitude reported in the literature were from Waszczak et al. (2015). Those were  $7.3397 \pm 0.0056$  h and 0.11 mag.

Our observations were made between 2019 November 22 and 2020 February 15. After several observations were completed, we realized that there were no good fits to the published periods. We decided to continue accumulating observations until a more confident period solution became evident. We found a period  $11.005 \pm 0.008$  h and lightcurve amplitude of  $0.12 \pm 0.01$  mag.



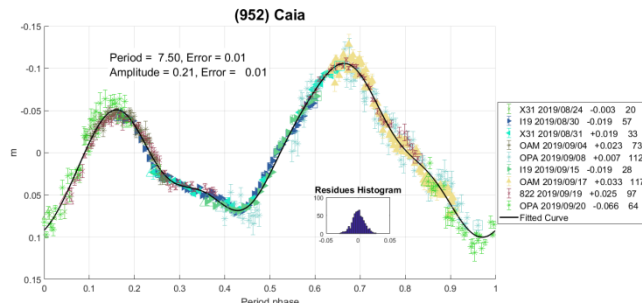
**949 Hel.** This asteroid was discovered in 1921 by Maximilian Franz Wolf from the Heidelberg-Königstuhl Observatory, Germany. It has an estimated diameter of  $63.494 \pm 0.743$  km (Mainzer et al., 2016). The periods previously reported were  $10.862 \pm 0.007$  h and  $10.85 \pm 0.05$  h (Behrend 2001; 2004) with amplitudes of  $0.12 \pm 0.01$  and  $0.14 \pm 0.02$  mag, respectively.

Our calculated period was  $16.43 \pm 0.01$  h with a lightcurve amplitude of  $0.18 \pm 0.01$  mag. It is interesting to note that Brines et al. (2017) reported a period of  $8.215 \pm 0.01$  h, about half the period that we have reported in this paper.



**952 Caia.** This asteroid was discovered on 1916 October 27 by Neujmin. Mainzer et al. (2016) found an estimated diameter of  $88.692 \pm 0.422$  km. We observed this asteroid from 2019 August 24 to September 20, inspired by the discrepancy in the information found in the literature.

While a short period of around 3.7 h was reported by Behrend (2004; 2009) and Aznar Macias et al. (2018), periods of around 7.5 h were reported by Harris (1978;  $7.50 \pm 0.01$  h) and Stanzel and Schober (1980; 7.51 h). For the Behrend and Aznar Macias et al. results, the U values were below 3. Our observations resulted in a period of  $7.50 \pm 0.01$  h with amplitude of  $0.21 \pm 0.01$  mag. These better agree with the longer periods reported by Harris (1978) and by Stanzel and Schober (1980).

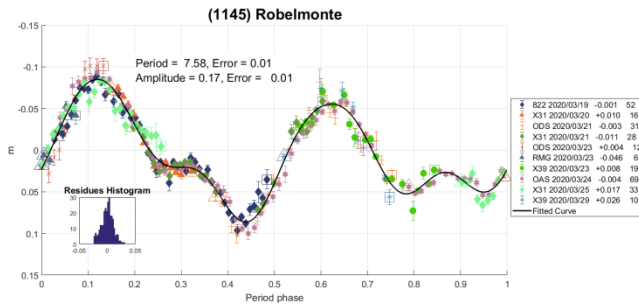


Number	Name	20yy/mm/dd	Phase	$L_{PAB}$	$B_{PAB}$	Period(h)	P.E.	Amp	A.E.	Grp
414	Liriopé	19/11/22-20/02/15	4.0, 17.0	75	-5	11.005	0.008	0.12	0.01	MB-O
949	Hel	20/02/15-03/20	17.9, 7.1	189	-9	16.43	0.01	0.18	0.01	MB-O
952	Caia	19/06/24-09/20	*22.0, 11.4	331	-10	7.50	0.01	0.21	0.01	MB-O
1145	Robelmonte	20/03/19-03/29	10.8, 6.2	198	-4	7.58	0.01	0.17	0.01	V

Table II. Observing circumstances and results. The phase angle is given for the first and last date. If preceded by an asterisk, the phase angle reached an extrema during the period.  $L_{PAB}$  and  $B_{PAB}$  are the approximate phase angle bisector longitude/latitude at mid-date range (see Harris et al., 1984). Grp is the asteroid family/group (Warner et al., 2009). MB-O: outer main-belt. V: Vestoid.

1145 Robelmonte. This asteroid belongs to the Vesta family and has an estimated diameter of  $22.822 \pm 0.348$  km (Mainzer et al., 2016). It was discovered on 1929 February 3 by Delporte.

The last reported period was of  $7.5822 \pm 0.0027$  h with a lightcurve amplitude of 0.13 mag (Waszczak et al., 2015). Gattrelle (2012) reported a period of  $9.01 \pm 0.01$  h while Mansego et al., (2016) found a period of  $8.002 \pm 0.002$  h. Our observations resulted in a period of  $7.58 \pm 0.01$  h with amplitude of  $0.17 \pm 0.01$  mag, which is in concordance with the results obtained by Waszczak et al. (2015).



#### Acknowledgements

We want to thank Julio Castellano as we used his *FotoDif* program for preliminary analysis and to Fernando Mazzone for his *Periodos* program that was used in final analyses. This research has made use of the Small Bodies Data Ferret (<http://sbn.psi.edu/ferret/>), supported by the NASA Planetary System. This research has made use of data and/or services provided by the International Astronomical Union's Minor Planet Center.

#### References

- Aznar Macias, A.; Cornea, R.; Suciú, O. (2018). "Photometric Analysis and Physical Parameters for Six Mars-crossing and Ten Main-belt Asteroids from APT Observatory Group: 2017 April-September." *Minor Planet Bull.* **45**, 92-96.
- Behrend, R. (2001, 2004, 2009). Observatoire de Genève web site. [http://obswww.unige.ch/~behrend/page\\_cou.html](http://obswww.unige.ch/~behrend/page_cou.html)
- Brines, P.; Lozano, J.; Rodrigo, O.; Fornas, A.; Herrero, D.; Mas, V.; Fornas, G.; Carreño, A.; Arce, E. (2017). "Sixteen Asteroids Lightcurves at Asteroids Observers (OBAS) – MPPD: 2016 June–November." *Minor Planet Bull.* **44**, 145–149.
- Colazo, M.; Fornari, C.; Santucho, M.; Mottino, A.; Colazo, C.; Melia, R.; Vasconi, N.; Arias, D.; Pittari, C.; Suarez, N.; Pulver, E.; Ferrero, G.; Chapman, A.; Girardini, C.; Rodríguez, E.; Amilibia, G.; Anzola, M.; Tornatore, M.; Nolte, R.; Morero, S. (2020). "Asteroid Photometry and Lightcurve Analysis at GORA's Observatories." *Minor Planet Bull.* **47**, 188-191.
- Gattrelle, G.M. (2012). "Lightcurve Results for Eleven Asteroids." *Minor Planet Bull.* **39**, 40–46.
- Harris, A.W. (1978). UNPUBLISHED.
- Harris, A.W.; Young, J.W.; Scaltriti, F.; Zappala, V. (1984). "Lightcurves and phase relations of the asteroids 82 Alkmene and 444 Gyptis." *Icarus* **57**, 251-258.
- Mainzer, A.K.; Bauer, J.M.; Cutri, R.M.; Grav, T.; Kramer, E.A.; Masiero, J.R.; Nugent, C.R.; Sonnett, S.M.; Stevenson, R.A.; Wright, E.L. (2016). "NEOWISE Diameters and Albedos V1.0." NASA Planetary Data System. EAR-A-COMPIL-5-NEOWISEDIAM-V1.0.
- Mansego, E.A.; Rodriguez, P.B.; de Haro, J.L.; Chiner, O.R.; Silva, A.F.; Porta, D.H.; Martinez, V.M.; Silva, G.F.; Garcerán, A.C. (2016). "Eighteen Asteroids Lightcurves at Asteroides Observers (OBAS) – MPPD: 2016 March–May." *Minor Planet Bull.* **43**, 332–336.
- Mazzone, F.D. (2012). *Periodos* software, version 1.0. <http://www.astrosurf.com/salvador/Programas.html>
- Mazzone, F.; Colazo, C.; Mina, F.; Melia, R.; Spagnotto, J.; Bernal, A. (2014). "Collaborative asteroid photometry and lightcurve analysis at observatories OAEGG, OAC, EABA AND OAS." *Minor Planet Bull.* **41**, 17-18.
- Stanzel, R.; Schober, H.J. (1980). "The asteroids 118 Peitho and 952 CAIA - Rotation periods and lightcurves from photoelectric observations." *Astron. Astrophys. Suppl. Ser.* **39**, 3-5.
- Warner, B.D.; Harris, A.W.; Pravec, P. (2009). "The Asteroid Lightcurve Database." *Icarus* **202**, 134-146. Updated 2020 June. <http://www.minorplanet.info/lightcurvedatabase.html>
- Waszczak, A.; Chang, C.-K.; Ofeck, E.O.; Laher, F.; Masci, F.; Levitan, D.; Surace, J.; Cheng, Y.; Ip, W.; Kinoshita, D.; Helou, G.; Prince, T.A.; Kulkarni, S. (2015). "Asteroid Light Curves from the Palomar Transient Factory Survey: Rotation Periods and Phase Functions from Sparse Photometry." *Astron. J.* **150**, A75.

## THE 2019 MEXICAN ASTEROID PHOTOMETRY CAMPAIGN

L. Olguín, J.C. Saucedo, P. Loera-González, M.E. Contreras  
 Departamento de Investigación en Física  
 Universidad de Sonora  
 Hermosillo, Sonora, México  
 lorenzo.olguin@unison.mx

J.R. Valdés, J. Guichard, R. López-González,  
 J. Michimani-García, G. Cerdán-Hernández  
 Instituto Nacional de Astrofísica Óptica y Electrónica  
 Tonantzintla, Puebla, México

W. J. Schuster  
 Instituto de Astronomía-Ensenada  
 Universidad Nacional Autónoma de México  
 Ensenada, B.C., México

P. Valdés-Sada  
 Departamento de Física y Matemáticas  
 Universidad de Monterrey  
 San Pedro Garza García, N.L., México

R. Núñez-López  
 Departamento de Física, Matemáticas e Ingeniería, URN  
 Universidad de Sonora  
 Caborca, Sonora, México

S. A. Ayala-Gómez  
 Facultad de Ciencias Físico-Matemáticas  
 Universidad Autónoma de Nuevo León  
 Monterrey, N.L., México

(Received: 2020 July 8 Revised: 2020 July 18)

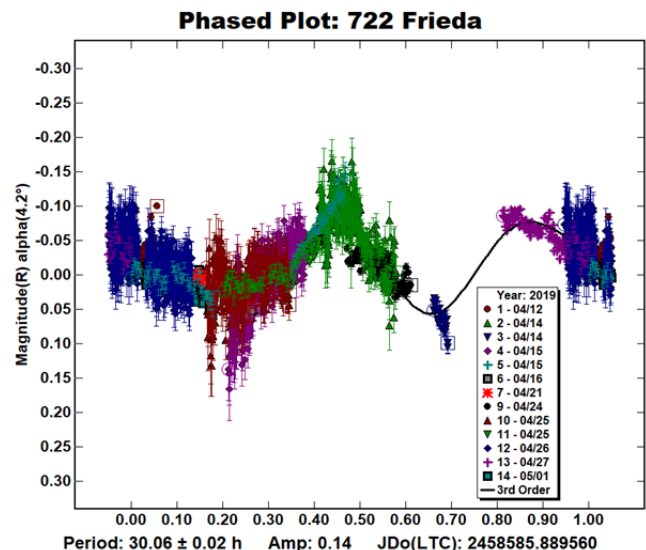
We present photometric optical lightcurves and derived rotation periods for a sample of five asteroids: 722 Frieda ( $30.06 \pm 0.02$  h), 1239 Queteleta ( $10.278 \pm 0.003$  h), 2162 Anhui ( $8.101 \pm 0.001$  h), 4148 McCartney ( $20.756 \pm 0.0006$  h), and 4408 Zlata Koruna ( $4.392 \pm 0.001$  h). These observations were carried out at the Observatorio Astronómico Nacional at Sierra San Pedro Mártir (OAN-SPM), Baja California, Mexico, the Carl Sagan Observatory (OCS) of the Universidad de Sonora, México, and at the INAOE Tonantzintla Observatory (TONA), Puebla, México.

During the first half of 2019, we have obtained photometric data of five asteroids: 722 Frieda, 1239 Queteleta, 2162 Anhui, 4148 McCartney, and 4408 Zlata Koruna as part of the Mexican Asteroid Photometry Campaign (CMFA in Spanish). Our observations were carried out at three observatories: the Observatorio Astronómico Nacional at San Pedro Mártir (OAN-SPM), Baja California, Mexico; the Carl Sagan Observatory (OCS) of the Universidad de Sonora, Mexico; and the INAOE Tonantzintla Observatory (TONA), in Tonantzintla, Puebla, México. Observations at the OAN-SPM were carried out with the 0.84-m  $f/15$  Ritchey-Chretien telescope and a 2048×2048 pix<sup>2</sup> E2V-4240 cryogenic CCD, operating at a temperature of -110 °C. Images were generally binned 2×2 with a final field of view of 9×9 arcmin<sup>2</sup>. The equipment used at the OCS was a 3056×3056-12 μm Apogee Alta F9000 CCD camera mounted on a Meade LX-200GPS 0.41-m  $f/10$  telescope. Images were trimmed to a subframe of 2000×2000 pixels and were generally 3×3 binned, yielding a final plate scale of 1.8 arcsec/pix and an effective

20×20 arcmin<sup>2</sup> FOV. Observations at TONA were made with a 0.77-m Schmidt Camera (TSC) equipped with a 3352×2532 pixel SBIG STF-8300 camera. Images were 2×2 binned with a final plate scale of 1.04 arcsec/pixel. Data reduction was made with *IRAF* or *MaximDL* following standard procedures to correct for bias, dark current and flat-field effects. Photometry and lightcurve analysis were made using the *MPO Canopus* (V.9.5.0.14, Warner, 2017) software package, which allowed us to obtain a synodic period for each object.

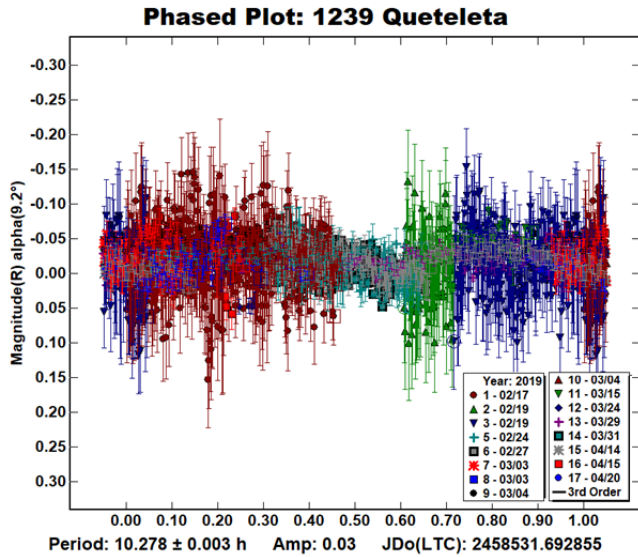
722 Frieda is a main-belt asteroid. It was discovered in 1911 by J. Palisa (Jet Propulsion Laboratory, Small-Body Database; Schmadel, 2003). The most recent values for its diameter, absolute magnitude  $H$ , and albedo are 10.51 km, 12.3, and 0.23, respectively. These data are reported at the Asteroid Lightcurve Database (LCDB) by Nugent et al. (2015). A synodic period value of  $131.1 \pm 0.2$  h is reported by Polakis and Skiff (2019).

We have observed 722 Frieda during a total of 16 nights: eight nights at the OAN-SPM (2019 Apr 12-18, and Apr 21), three nights at the TONA observatory (2019 Apr 9, 14, and 15), and five nights at the OCS (2019 Apr 23-25, 27, and May 1<sup>st</sup>). Three nights were rejected based on their low data quality or photometric issues, and finally 13 nights and 2217 data points were used to derive a lightcurve. We obtained a period of  $30.06 \pm 0.02$  h with an amplitude of  $0.14 \pm 0.05$  mag. Our estimated synodic period is much lower than the previous value. However, due to the large data scatter and incomplete phase coverage in our data, the reason for this disagreement is not clear.

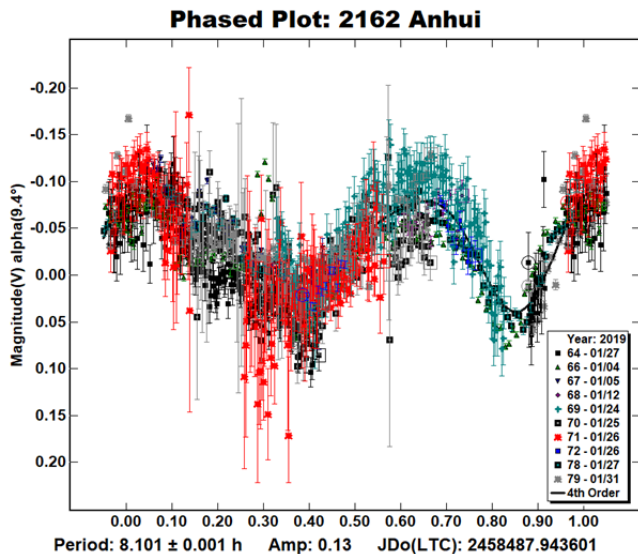


1239 Queteleta is a main-belt asteroid discovered in 1932 by E. Delporte (JPL Small-Body Database; Schmadel, 2003). It has an absolute magnitude of  $H = 12.4$  (JPL Small-Body Database) with an albedo and a diameter of 0.051 and 18.681 km, respectively, reported by Masiero et al. (2011). Regarding its rotation period value, after a search of the Asteroid Lightcurve Database and the literature, no previously reported value was found. We observed this object for 17 nights: seven nights at TONA (2019 Feb 17, 19, 20, 24, 27, Mar 3, 4), six nights at the OCS (2019 Mar 3, 4, 15, 24, 29, 31), and four nights at the OAN-SPM (2019 Apr 14, 15, 18 and 20). Two nights were discarded due to low photometric data quality. Our derived lightcurve is rather flat, with only small features which are of the order of the observational data dispersion. Thus, we may conclude that Queteleta is a quite round

asteroid. Despite its possible round shape, we have attempted to estimate its rotation period using 2110 data points, obtaining a value of  $10.278 \pm 0.003$  h with a peak-to-peak amplitude of  $0.03 \pm 0.03$  mag. We are aware that this value might be not completely reliable, given the high data noise of some of our observations, but we consider it is a good first approximation.

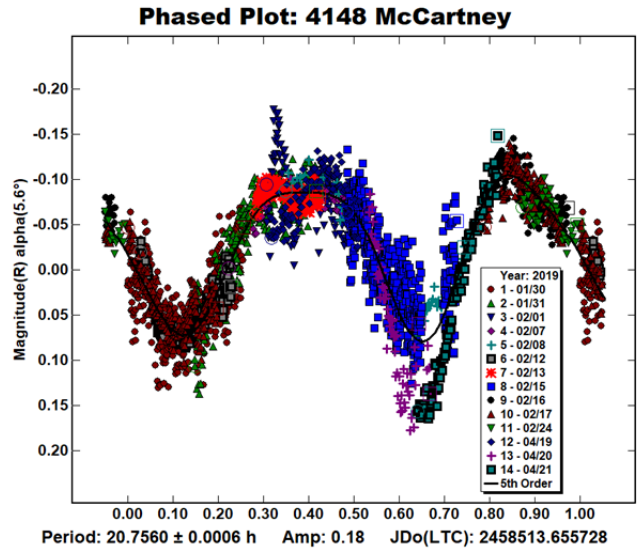


2162 Anhui This object is a main-belt asteroid discovered at the Purple Mountain Observatory (JPL Small-Body Database; Schmadel, 2003) in 1966. Its absolute magnitude  $H = 12.82 \pm 0.25$  is reported by Veres et al. (2015) while its reported diameter and albedo are  $7.494 \pm 0.148$  km, and  $0.1988 \pm 0.0324$  (Masiero et al., 2011). Berhend et al. (2018) and Pravec et al. (2018) reported very similar rotation period values of  $8.106 \pm 0.001$  h, and  $8.1048 \pm 0.0005$  h, respectively. We have carried out observations during 11 nights: six at the OCS (2019 Jan 4, 5, 12, 26, 27, 31), and five at the TONA Observatory (2019 Jan 24, 25, 26, 27, 30). One night was discarded based on its low quality. We obtained a lightcurve with a total of 1258 data points and derived a rotation period of  $8.101 \pm 0.001$  h with an amplitude of  $0.13 \pm 0.04$  mag. We can see that our period value is consistent with the two previously reported values.

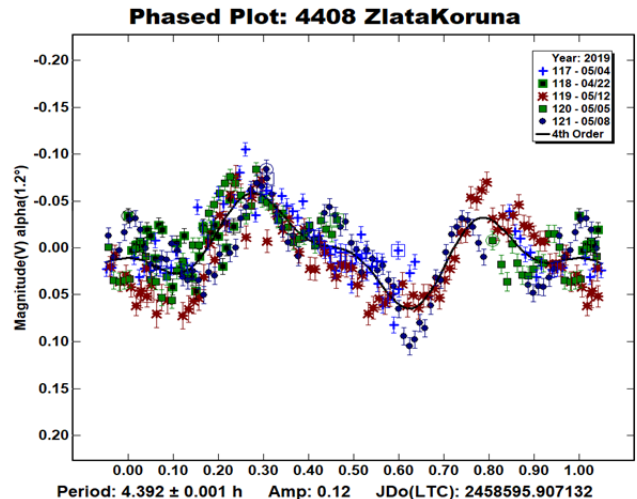


4148 McCartney is a main-belt asteroid. It was discovered in 1983 by E. Bowell at Flagstaff Observatory (JPL Small-Body Database; Schmadel, 2003). It has an absolute magnitude of  $H=12.86 \pm 0.44$  (Veres et al., 2015). An albedo of  $0.2795 \pm 0.0573$  and a diameter of  $7.610 \pm 0.066$  km are reported by Masiero et al. (2011). This object has two reported period values, namely,  $20.737 \pm 0.002$  h (Pravec et al., 2019) and  $20.748 \pm 0.003$  h (Odden et al., 2019).

We have observed this object during 17 nights distributed as follow: four at the TONA Observatory (2019 Jan 30, 31, and Feb 1, 15), five at OCS (2019 Feb 7, 8, 24, 28, and Mar 20), and eight at OAN-SPM (2019 Feb 12, 13, 16, 17, 18, Apr 19, 20, and 21). Of all these, three nights were discarded due to their low quality. With these data we have derived a rotation period of  $20.7560 \pm 0.0006$  h with an amplitude of  $0.18 \pm 0.03$  mag, which is consistent with the previously reported values. A total of 2690 data points were used to build the lightcurve.



4408 Zlata Koruna is a main-belt asteroid discovered by A. Mrkos in 1988 that has an absolute magnitude of  $H = 12.9$  (JPL Small-Body Database; Schmadel, 2003). To the best of our knowledge, there are no reported periods for this object. We have collected data for this object during 5 nights: one at the OAN-SPM (2019 Apr 22), and four at the OCS (2019 May 4, 5, 8, and 12), giving a total of 323 points. Based on our observations we have estimated a period of  $4.392 \pm 0.001$  h with an amplitude of  $0.12 \pm 0.04$  mag.



Number	Name	yyyy mm/dd	Phase	L <sub>PAB</sub>	B <sub>PAB</sub>	Period(h)	P.E.	Amp	A.E.	Grp
722	Frieda	2019 04/09-05/01	6.1, 7.0	208	+2	30.06	0.02	0.14	0.05	MB
1239	Queteleta	2019 02/17-04/20	9.3, 19.4	166	+2	10.278	0.003	0.03	0.03	MB
2162	Anhui	2019 01/04-01/31	4.7, 11.4	111	-1	8.101	0.001	0.13	0.04	MB
4148	McCartney	2019 01/30-04/21	5.7, 28.5	144	0	20.756	0.0006	0.18	0.03	MB
4408	Zlata Koruna	2019 04/22-05/12	5.6, 5.5	221	0	4.392	0.001	0.12	0.04	MB

Table I. Observing circumstances and results. The phase angle is given for the first and last date. If preceded by an asterisk, the phase angle reached an extrema during the period. L<sub>PAB</sub> and B<sub>PAB</sub> are the approximate phase angle bisector longitude/latitude at mid-date range (see Harris et al., 1984). Grp is the asteroid family/group (Warner et al., 2009).

#### Acknowledgements

MEC acknowledges support from CONACyT Fellowship C-841/2018. LO, PLG and JCS acknowledge UNISON project USO315003483. This work was partially based upon observations acquired at the Observatorio Astronómico Nacional in the Sierra San Pedro Mártir, Baja California, México. We would like to thank the Departamento de Agricultura y Ganadería of the Universidad de Sonora for hosting the OCS observatory and for their valuable support.

This research has made use of data and/or services provided by the International Astronomical Union's Minor Planet Center, NASA JPL HORIZONS and Small-Body Databases, The Asteroid Light Curve Database (LCDB) and The Collaborative Asteroid Lightcurve Link (CALL). IRAF was originally distributed by the National Optical Astronomy Observatory, which is operated by the Association of Universities for Research in Astronomy (AURA) under a cooperative agreement with the National Science Foundation.

#### References

- Behrend, R. (2018). Observatoire de Geneve web site. [http://obswww.unige.ch/~behrend/page\\_cou.html](http://obswww.unige.ch/~behrend/page_cou.html)
- Harris, A.W.; Young, J.W.; Scaltriti, F.; Zappala, V. (1984). "Lightcurves and phase relations of the asteroids 82 Alkeme and 444 Gyptis." *Icarus* **57**, 251-258.
- Masiero, J.R.; Mainzer, A.K.; Grav, T.; Bauer, J.M.; Cutri, R.M.; Dailey, J.; Eisenhardt, P.R.M.; McMillan, R.S.; Spahr, T.B.; Skrutski, M.F.; Tholen, D.; Walker, R.G.; Wright, E.L.; DeBaun, E.; Elsbury, D.; Gautier IV, T.; Gomillion, S.; Wilkins, A. (2011). "Main Belt Asteroids with WISE/NEOWISE. I. Preliminary Albedos and Diameters." *Ap. J.* **741**, 68.
- Nugent, C.R.; Mainzer, A.; Masiero, J.; Bauer, J.; Cutri, R.M.; Grav, T.; Kramer, E.; Sonnett, S.; Stevenson, R.; Wright, E.L. (2015). "NEOWISE Reactivation Mission Year One: Preliminary Asteroid Diameters and Albedos." *Ap. J.* **814**, 117.
- Odden, C.; Zachary, A.; Beckwith, R.; Chandran, R.; El Alam, Z.; Glover, E.; Kacergis, J.; Lazaro-Carrasco, I.; Solomon, H.; Wang, J.; Klinglesmith, D.; Goodwrench, Z.; Pilcher, F. (2019). "Lightcurve and Period Determination for asteroid 4148 McCartney." *Minor Planet Bull.* **46**, 293-294.
- Polakis, T.; Skiff, B. (2019). "Photometric Observations of Seventeen Minor Planets." *Minor Planet Bull.* **46**, 400-406.
- Pravec, P.; Wolf, M.; Sarounova, L. (2018, 2019). Ondrejov Asteroid Photometry Project website. <http://www.asu.cas.cz/~ppravec/neo.htm>
- Schmadel, L.D. (2003). *Dictionary of Minor Planet Names*, pp. 73, 102, 118, 414, 543. Springer, New York.
- Veres, P.; Jedicke, R.; Fitzsimmons, A.; Denneau, L.; Granvik, M.; Bolin, B.; Chastel, S.; Wainscoat, R.; Burgett, W.; Chambers, K.C.; Flewelling, H.; Kaiser, N.; Magnier, E.A.; Morgan, J.S.; Price, P.A.; Tonry, J.L.; Waters, C. (2015). "Absolute magnitudes and slope parameters for 250,000 asteroids observed by Pan-STARRS PS1 - Preliminary results." *Icarus* **261**, 34-47.
- Warner, B.D.; Harris, A.W.; Pravec, P. (2009). "The Asteroid Lightcurve Database." *Icarus* **202**, 134-146. Updated 2019 Dec. <http://www.minorplanet.info/lightcurvedatabase.html>
- Warner, B.D. (2017). MPO Canopus software. <http://bdwpublishing.com>

**MEASURED LIGHTCURVES AND ROTATIONAL PERIODS OF 1132 HOLLANDIA AND 1184 GAEA**

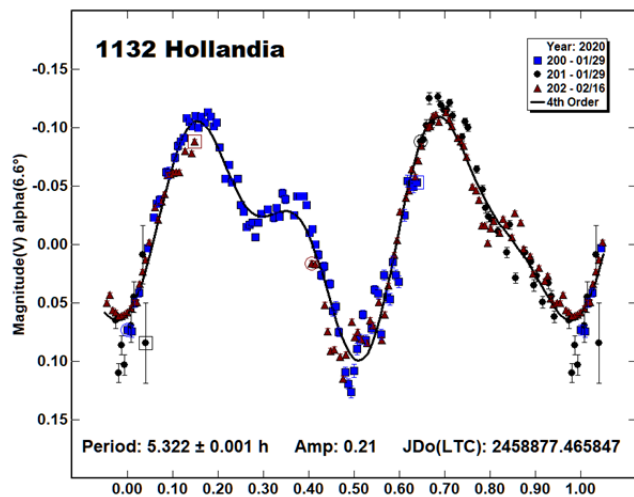
Michael Fauerbach  
 Florida Gulf Coast University  
 and SARA Observatories  
 10501 FGCU Blvd.  
 Ft. Myers, FL 33965-6565  
 mfauerba@fgcu.edu

(Received: 2020 June 27 Revised: 2020 August 9)

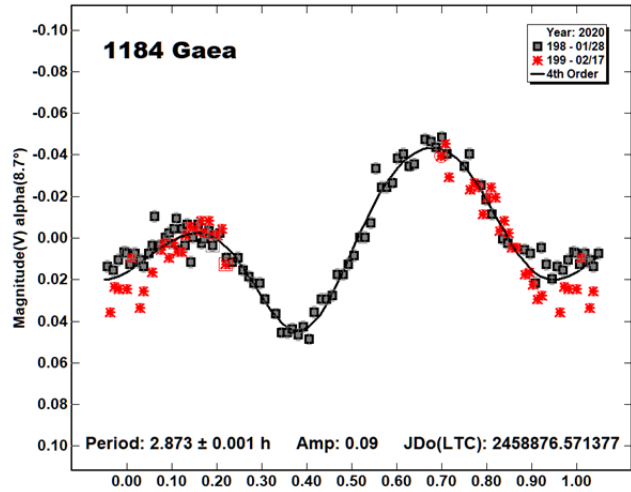
Photometric observations of 1132 Hollandia and 1184 Gaea were obtained on three nights 2020 January 27 to 2020 February 16. The following rotational periods were determined: 1132 Hollandia  $5.322 \pm 0.001$  h; 1184 Gaea  $2.873 \pm 0.001$  h.

Photometric observations obtained with the Southeastern Association for Research in Astronomy (SARA) consortium 1m Jacobus Kapteyn Telescope at the Observatorio del Roque de los Muchachos on the Spanish island of La Palma are presented. The telescope is coupled with an Andor iKon-L series CCD. A detailed description of the instrumentation and setup can be found in Keel et al. (2017). The data were calibrated using MaximDL and photometric analysis was performed using MPO Canopus (Warner, 2017). Due to limited time the target asteroids were selected from a list of previously observed asteroids by FGCU’s Asteroid Research Group. This will enable us to perform shape modeling via lightcurve inversion in the future.

**1132 Hollandia.** This main-belt asteroid was observed during two nights for 5.5 h and 4 h respectively. Our analysis yields a rotational period of  $5.322 \pm 0.001$  h with an amplitude of 0.21 mag. This is in excellent agreement with previous publications by Sauppe et al. (2007, 5.326 h) and Clark (2015, 5.360 h), as well as our previous result (Fauerbach and Brown, 2018, 5.312 h).



**1184 Gaea.** FGCU’s Asteroid Research Group had observed 1184 Gaea in 2017 (Fauerbach and Brown, 2018) and 2018 (Fauerbach and Fauerbach, 2019) and derived periods of 2.871 h and 2.873 h respectively. Observations at the Oakley Southern Sky Observatory (Ditteon and Trent, 2018) derived a period of  $2.8735 \pm 0.0005$  h. Behrend (2011) reported a period of  $2.94 \pm 0.06$  h, which cannot be reproduced by our data. The current observations lead to a period of  $2.873 \pm 0.001$  h with an amplitude of 0.09 mag in excellent agreement with previous measurements.



References

Behrend, R. (2011). Observatoire de Geneve web site. [http://obswww.unige.ch/~behrend/page\\_cou.html](http://obswww.unige.ch/~behrend/page_cou.html)

Clark, M. (2015). “Asteroid Photometry from the Preston Gott Observatory.” *Minor Planet Bulletin* **42**, 15-20.

Ditteon, R.; Trent, L. (2018). “Lightcurve Analysis of Minor Planets Observed at the Oakley Southern Sky Observatory: 2017 June-July.” *Minor Planet Bulletin* **45**, 328-329.

Fauerbach, M.; Brown, A. (2018). “Lightcurve Analysis of Minor Planets 1132 Hollandia, 1184 Gaea, 1322 Copernicus, 1551 Argelander, and 3230 Vampirov.” *Minor Planet Bulletin* **45**, 240-241.

Fauerbach, M.; Fauerbach, M. (2019). “Lightcurve Analysis of Asteroids 131 Vala, 1184 Gaea, 7145 Linxexu and 26355 Grueber.” *Minor Planet Bulletin* **46**, 236-237.

Harris, A.W.; Young, J.W.; Scaltriti, F.; Zappala, V. (1984). “Lightcurves and phase relations of the asteroids 82 Alkmene and 444 Gyptis.” *Icarus* **57**, 251-258.

Number	Name	yyyy mm/dd	Phase	L <sub>PAB</sub>	B <sub>PAB</sub>	Period(h)	P.E.	Amp	A.E.	Grp
1132	Hollandia	2020 01/29,02/16	6.3,2.8	145	7.9	5.322	0.001	0.21	0.02	MB-M
1184	Gaea	2020 01/28,02/17	8.7,2.8	147	7.2	2.873	0.001	0.09	0.01	MB-M

Table I. Observing circumstances and results. The phase angle is given for the first and last date. If preceded by an asterisk, the phase angle reached an extrema during the period. L<sub>PAB</sub> and B<sub>PAB</sub> are the approximate phase angle bisector longitude/latitude at mid-date range (see Harris et al., 1984). Grp is the asteroid family/group (Warner et al., 2009).

Keel, W.C.; Oswalt, T.; Mack, P.; Henson, G.; Hillwig, T.; Batcheldor, D.; Berrington, R.; De Pree, C.; Hartmann, D.; Leake, M.; Licandro, J.; Murphy, B.; Webb, J.; Wood, M.A. (2017). "The Remote Observatories of the Southeastern Association for Research in Astronomy (SARA)." *Publications of the Astronomical Society of the Pacific* 129:015002 (12pp). <http://iopscience.iop.org/article/10.1088/1538-3873/129/971/015002/pdf>

Sauppe, J.; Torno, S.; Lemke-Oliver, R.; Ditteon, R. (2007). "Asteroid Lightcurve Analysis at the Oakley Observatory - March/April 2007." *Minor Planet Bulletin* 34, 119-122.

Warner, B.D.; Harris, A.W.; Pravec, P. (2009). "The Asteroid Lightcurve Database." *Icarus* 202, 134-146. Updated 2017 Nov. <http://www.minorplanet.info/lightcurvedatabase.html>

Warner, B.D. (2017). MPO Canopus software version 10.7.10.0. <http://www.bdwpublishing.com>

## LIGHTCURVES AND ROTATION PERIODS OF 50 VIRGINIA, 57 MNEMOSYNE, 58 CONCORDIA, 59 ELPIS, 78 DIANA, AND 529 PREZIOSA

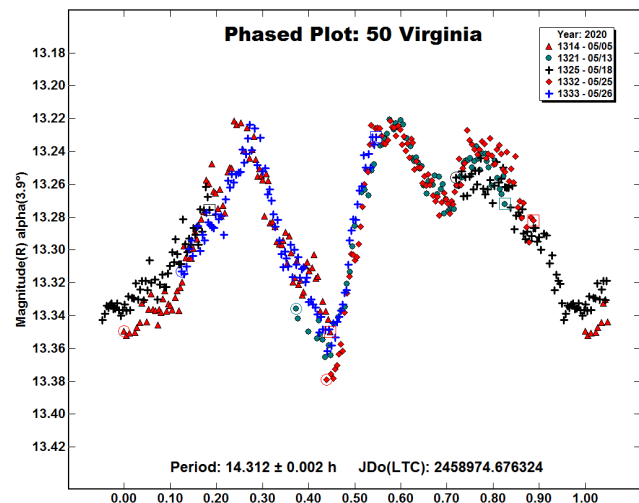
Frederick Pilcher  
Organ Mesa Observatory (G50)  
4438 Organ Mesa Loop  
Las Cruces, NM 88011 USA  
fpilcher35@gmail.com

(Received: 2020 June 23)

Synodic rotation periods and amplitudes were found for  
50 Virginia:  $14.312 \pm 0.002$  h,  $0.14 \pm 0.01$  mag;  
57 Mnemosyne:  $25.281 \pm 0.002$  h,  $0.10 \pm 0.01$  mag;  
58 Concordia:  $9.899 \pm 0.001$  h,  $0.10 \pm 0.01$  mag;  
59 Elpis:  $13.672 \pm 0.001$  h,  $0.16 \pm 0.01$  mag; 78 Diana:  
 $7.2929 \pm 0.0001$  h,  $0.06 \pm 0.01$  mag; 529 Preziosa:  
 $25.943 \pm 0.001$  h,  $0.30 \pm 0.02$  mag.

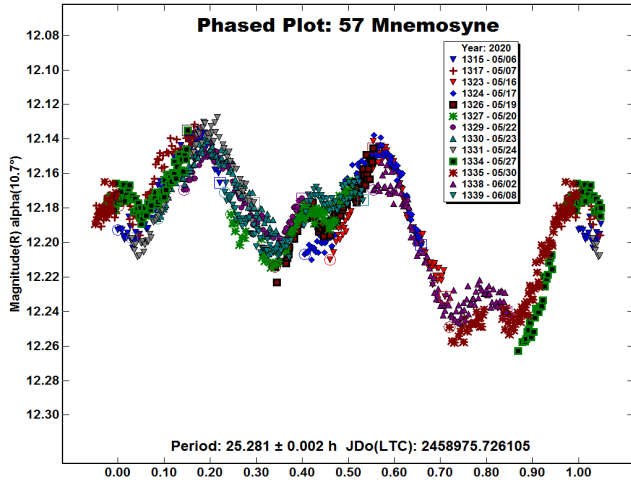
Observations to produce the results reported in this paper were made at the Organ Mesa Observatory with a Meade 35-cm LX200 GPS Schmidt-Cassegrain, SBIG STL-1001E CCD, and 60-second unguided exposures. For the bright targets 59 Elpis and 78 Diana, exposures were through the R filter. For all other targets, exposures were through the clear filter. Image measurement and lightcurve construction were with *MPO Canopus* software with all calibration star magnitudes from the CMC15 catalog reduced to the Cousins R band. To reduce the number of data points on the lightcurves and make them easier to read, data points have been binned in sets of 3 with a maximum time difference of 5 minutes.

50 Virginia. The lightcurve data base (LCDB, Warner et al., 2009; updated 2020 March) lists a period of 14.315 h based on several secure  $U = 3$  published periods within 0.005 h of this value. New observations on five nights from 2020 May 5-26 provide a good fit to a lightcurve with a period of  $14.312 \pm 0.001$  h, amplitude  $0.14 \pm 0.01$  mag. This period is consistent with many previously published periods.

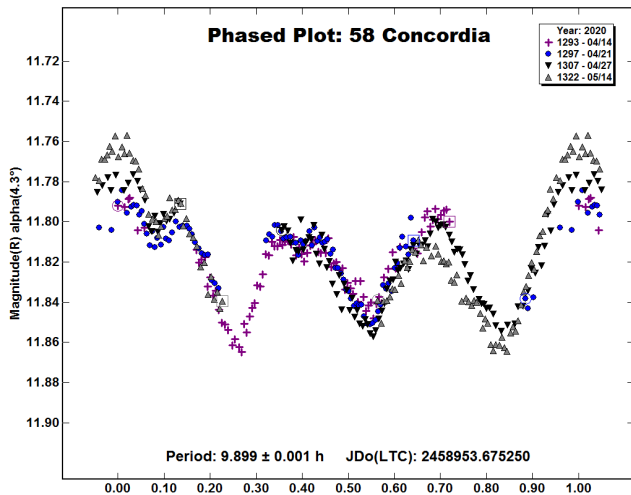


57 Mnemosyne. Earlier published periods are by Harris et al. (1992), 12.463 h; Ditteon and Hawkins (2007), 12.66 h; and Behrend (2016), 12.92 h. This author (Pilcher, 2019b) was unable to fit a lightcurve to a period near 12.5 h and found a synodic period of 25.324 h with one maximum and minimum per cycle

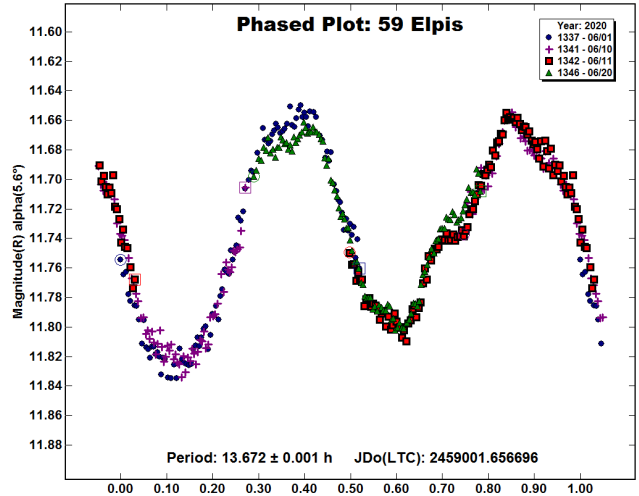
near celestial longitude 197 deg. New observations on 13 nights from 2020 May 6 to June 8, near celestial longitude 258 deg, confirm the longer period with a good fit to an irregular lightcurve with synodic period  $25.281 \pm 0.002$  h, amplitude  $0.10 \pm 0.01$  mag. The difference between the two synodic periods is 0.043 h, or 0.16%, which is much larger than the formal error of either. At celestial longitudes differing by 61 deg, a synodic period difference of 0.16% is not unrealistic. The results from 2019 and 2020 should be considered compatible, and their difference should be helpful toward future lightcurve inversion (LI) modeling.



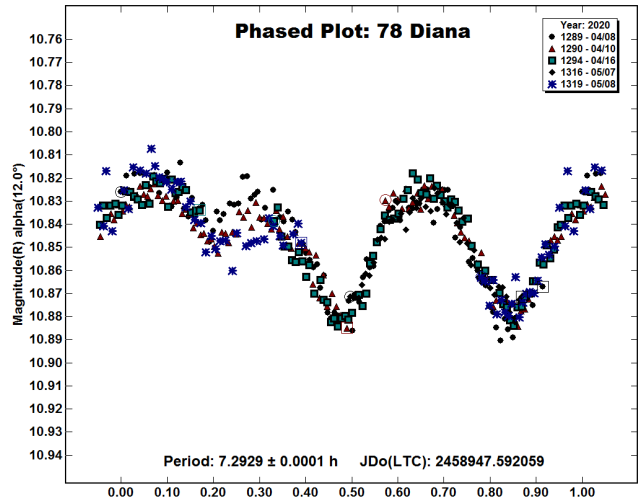
**58 Concordia.** Previously published periods are by Gil-Hutton (1993), >16 h; Wang (2002), 9.89 h; Behrend (2006), 9.9 h; Behrend (2010), 9.905 h; Behrend (2011), 9.904 h; Stephens (2006), 9.895 h; Pilcher (2016), 9.895 h; and Pilcher (2019a), 9.895 h. New observations on four nights from 2020 Apr. 14 to May 14 provide a good fit to an irregular lightcurve with period  $9.899 \pm 0.001$  h, amplitude  $0.10 \pm 0.01$  mag. A 9.899-hour period is consistent with most of the previously published values.



**59 Elpis.** The lightcurve data base (LCDB, Warner et al., 2009; updated 2020 March) lists a period of 13.671 h and is rated U = 3, secure, based on seven previously published periods within 0.02 h of this value. New observations on four nights from 2020 June 1-20 provide a good fit to a lightcurve with period  $13.672 \pm 0.001$  h, amplitude  $0.16 \pm 0.01$  mag. This period is consistent with many previously published periods.



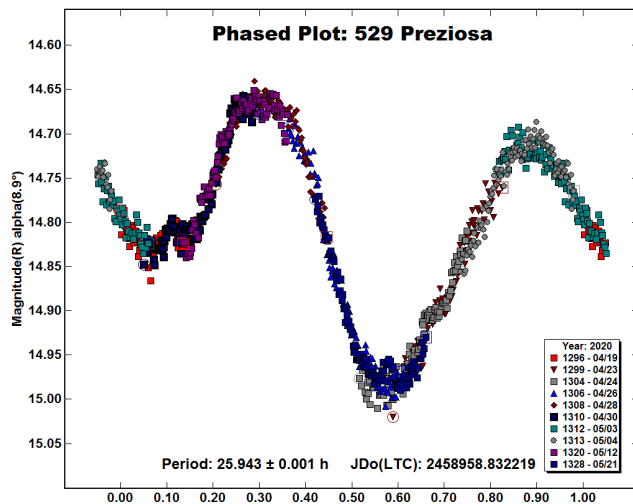
**78 Diana.** Previously published periods are by Taylor et al. (1976), 8 h; Harris and Young (1989), 7.225 h; Licchelli (2006), 7.300 h; Fleenor (2007), 7.346 h; and Benishek and Protitch-Benishek (2008), 7.2991 h. New observations on five nights from 2020 Apr 8 to May 8 provide a good fit to a lightcurve with period  $7.2929 \pm 0.0001$  h, amplitude 0.06 ± 0.01 mag with 3 unequal maxima and minima per rotational cycle. A period of 7.2929 h is consistent with all of the previously published periods.



Number	Name	2020/mm/dd	Phase	L <sub>PAB</sub>	B <sub>PAB</sub>	Period(h)	P.E	Amp	A.E.
50	Virginia	05/05-05/26	*3.9, 4.5	234	3	14.312	0.002	0.14	0.01
57	Mnemosyne	05/06-06/08	10.7, 5.3	258	15	25.281	0.002	0.10	0.01
58	Concordia	04/14-05/14	*4.3, 10.2	212	5	9.899	0.001	0.10	0.01
59	Elpis	06/01-06/20	*5.6, 6.5	258	11	13.672	0.001	0.10	0.01
78	Diana	04/08-05/08	12.0, 21.6	179	-6	7.2929	0.0001	0.06	0.01
529	Preziosa	04/19-05/21	*8.9, 2.1	235	3	25.943	0.001	0.30	0.02

Table I. Observing circumstances and results. The phase angle is given for the first and last date; if preceded by an asterisk, the phase angle reached a minimum or maximum during the period. L<sub>PAB</sub> and B<sub>PAB</sub> are the approximate phase angle bisector longitude and latitude at mid-date range (see Harris *et al.*, 1984).

**529 Preziosa.** The only previously published period is by Binzel (1987) who, on the basis of a sparse lightcurve, obtained a period of 27 h. New observations on ten nights from 2020 Apr 19 to May 21 provide a good fit to a period of  $25.943 \pm 0.001$  h, amplitude  $0.30 \pm 0.02$  mag.



#### References

- Behrend, R. (2006, 2010, 2011, 2016). Observatoire de Geneve web site. [http://obswww.unige.ch/~behrend/page\\_cou.html](http://obswww.unige.ch/~behrend/page_cou.html)
- Benishek, V.; Protitch-Benishek, V. (2008). "CCD photometry of seven asteroids at the Belgrade Astronomical Observatory." *Minor Planet Bull.* **35**, 28-30.
- Binzel, R.P. (1987). "A photoelectric survey of 130 asteroids." *Icarus* **72**, 135-208.
- Ditteon, R.; Hawkins, S. (2007). "Asteroid lightcurve analysis at the Oakley Observatory – November 2006." *Minor Planet Bull.* **34**, 59-64.
- Fleener, M.L. (2007). "Asteroid lightcurve analysis from Volunteer Observatory December 2006 to April 2007." *Minor Planet Bull.* **34**, 66-67.
- Gil-Hutton, R. (1993). "Photoelectric photometry of asteroids 58 Concordia, 122 Gerda, 326 Tamara, and 441 Bathilde." *Rev. Mexicana Astron. Astrof.* **25**, 75-77.
- Harris, A.W.; Young, J.W.; Scaltriti, F.; Zappala, V. (1984). "Lightcurves and phase relations of the asteroids 82 Alkmene and 444 Gyptis." *Icarus* **57**, 251-258.
- Harris, A.W.; Young, J.W.; Dockweiler, T.; Gibson, J.; Poutanen, M.; Bowell, E. (1992). "Asteroid lightcurve observations from 1981." *Icarus* **95**, 115-147.
- Harris, A.W.; Young, J.W. (1989). "Asteroid lightcurve observations from 1979-1981." *Icarus* **81**, 314-364.
- Licchelli, D. (2006). "Lightcurve analysis of asteroids 78, 126, 522, 565, 714, 1459, 6974." *Minor Planet Bull.* **33**, 11-13.
- Pilcher, F. (2016). "Rotation period determinations for 50 Virginia, 58 Concordia, 307 Nike, and 339 Dorothea." *Minor Planet Bull.* **43**, 304-306.
- Pilcher, F. (2019a). "Rotation period determinations for 58 Concordia, 384 Burdigala, 464 Megaira, 488 Kreusa, and 491 Carina." *Minor Planet Bull.* **46**, 360-363.
- Pilcher, F. (2019b). "New lightcurves of 50 Virginia, 57 Mnemosyne, 59 Elpis, 444 Gyptis, and 997 Priska." *Minor Planet Bull.* **46**, 445-448.
- Stephens, R.D. (2006). "Asteroid lightcurve photometry from Santana and GMARS observatories – winter and spring 2006." *Minor Planet Bull.* **33**, 100-101.
- Taylor, R.C.; Gehrels, T.; Capen, R.C. (1976). "Minor planets and related objects XXI. Photometry of eight asteroids." *Astron. J.* **81**, 778-786.
- Wang, X.-B. (2002). "CCD photometry of asteroids (58) Concordia, (360) Carlova, and (405) Thia." *Earth, Moon, and Planets* **91**, 25-30.
- Warner, B.D.; Harris, A.W.; Pravec, P. (2009). "The Asteroid Lightcurve Database." *Icarus* **202**, 134-146. Updated 2020 March. <http://www.minorplanet.info/lightcurvedatabase.html>

## DETERMINING THE ROTATIONAL PERIODS AND LIGHTCURVES OF THREE MAIN-BELT ASTEROIDS

Roberto Bonamico  
BSA Osservatorio (K76)  
Strada Collarelle 53  
12038 Savigliano, Cuneo, ITALY  
info@osservatorioastronomicobsa.it  
website: <http://www.osservatorioastronomicobsa.it>

(Received: 2020 July 14)

CCD photometric observations of three main-belt asteroids were made from 2020 March to May. We report the results of lightcurve analysis for 1784 Benguella:  $P = 41.035 \pm 0.008$  h,  $A = 0.87$  mag; 4582 Hank:  $P = 6.446 \pm 0.001$  h,  $A = 0.58$  mag; and 5947 Bonnie:  $P = 13.414 \pm 0.003$  h,  $A = 0.10$  mag.

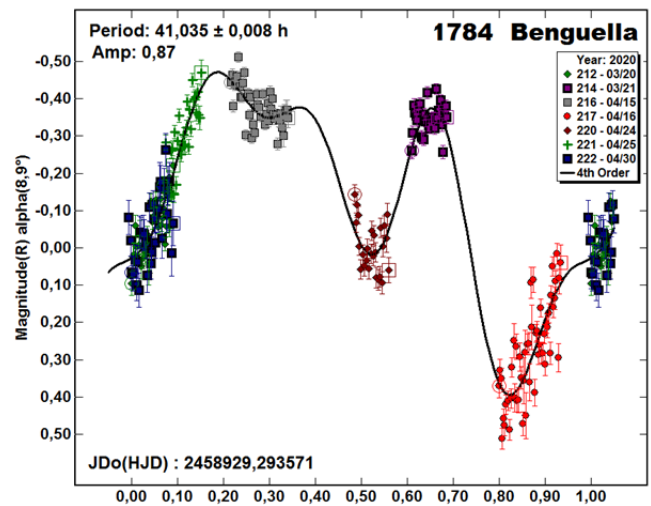
During the period from 2020 March to May, the Astronomical Observatory BSA studied the rotation period of three asteroids in the main belt. These asteroids were chosen from the website at <http://minorplanet.info/call.html>.

Observations were made with a Marcon 0.30-m  $f/5$  Newtonian telescope with an Atik 314L+ CCD camera using a Sony ICX285AL sensor (1360×1024, 6.5-microns). The observatory used *MaximDL* (<http://diffractionlimited.com/product/maxim-dl/>) for camera control, *The Sky 6 Pro* (<http://www.bisque.com>) for mount control, and *Voyager* (<http://software.starkeeper.it>) to automate the entire observatory.

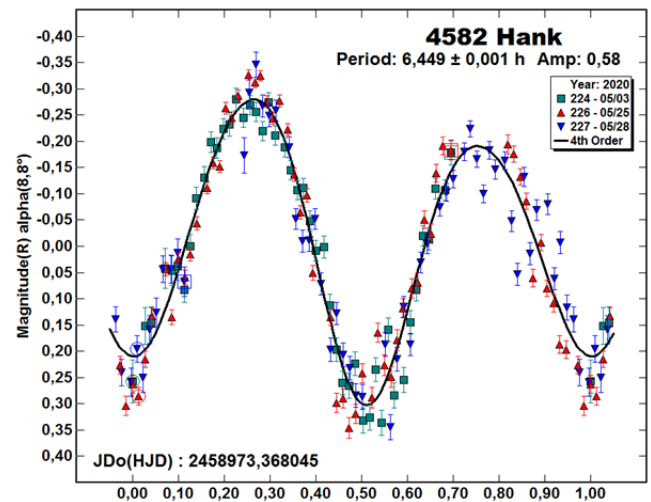
All photometric reductions were done with *MPO Canopus* v10.7.12.9 (<http://bdwpublishing.com>). Precise night-to-night zero-point calibration was obtained using the Comparison Star Selector utility in *MPO Canopus*. Whenever possible, five solar-colored comparison stars from the MPOSC3 catalog supplied with *MPO Canopus* were used.

**1784 Benguella.** In the spring of 2020, the particularly difficult weather conditions did not facilitate photometric research.

The seven observational nights scattered for over a month were not enough to precisely complete the calculation of the rotation period of this asteroid. The decreasing magnitude eventually reached the limit of the instrument and observations were stopped. The data analysis led to  $P = 41.035 \pm 0.008$  h and lightcurve amplitude  $A = 0.87$  mag. Future observations are encouraged to get better results.



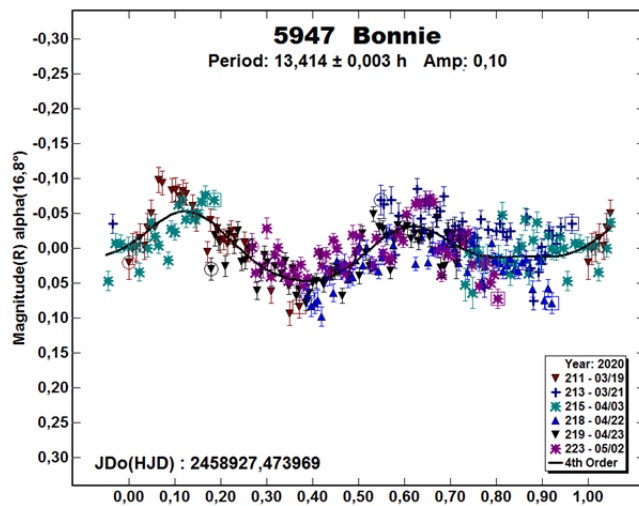
**4582 Hank.** Due to the short period and large amplitude ( $P = 6.446 \pm 0.001$  h,  $A = 0.58$  mag), three observation nights were enough to calculate the rotation period precisely.



**5947 Bonnie.** Six observational evenings took place on this asteroid. The bright magnitude, which gradually increased during the observation period, compensated for the small lightcurve amplitude, allowing the result of  $P = 13.414 \pm 0.003$  h and  $A = 0.10$  mag. Given the good number of hours available for each observational night, no further investigations were made.

Number	Name	yyyy mm/dd	Phase	$L_{PAB}$	$B_{PAB}$	Period(h)	P.E.	Amp	A.E.	Grp
1784	Benguella	2020 03/20-04/30	8.5, 22.0	163.1	22.0	41.035	0.008	0.87	0.03	MB
4582	Hank	2020 05/03-05/27	8.9, 11.9	228.2	14.9	6.446	0.001	0.58	0.01	MB
5947	Bonnie	2020 03/18-04/23	17.0, 10.0	209.1	18.7	13.414	0.003	0.10	0.01	MB

Table I. Observing circumstances and results. The phase angle is given for the first and last date. If preceded by an asterisk, the phase angle reached an extrema during the period.  $L_{PAB}$  and  $B_{PAB}$  are the approximate phase angle bisector longitude/latitude at mid-date range (see Harris et al., 1984). Grp is the asteroid family/group (Warner et al., 2009).



## References

Harris, A.W.; Young, J.W.; Scaltriti, F.; Zappala, V. (1984). "Lightcurves and phase relations of the asteroids 82 Alkmene and 444 Gyptis." *Icarus* **57**, 251-258.

Warner, B.D.; Harris, A.W.; Pravec, P. (2009). "The Asteroid Lightcurve Database." *Icarus* **202**, 134-146. Updated 2020 Feb. <http://www.minorplanet.info/lightcurvedatabase.html>

Warner, B.D. (2019). MPO Software. *MPO Canopus* v 10.7.12.9 <http://bdwpublishing.com>

## LIGHTCURVE BASED ROTATIONAL PERIOD DETERMINATION FOR ASTEROIDS 1579 HERRICK AND 2171 KIEV

Pablo Loera-González, Lorenzo Olguín & Julio Saucedo-Morales  
Departamento de Investigación en Física  
Universidad de Sonora  
Hermosillo, Sonora, México  
pabloloerag@gmail.com

Ramona Nuñez-López  
Departamento de Física, Matemáticas e Ingeniería  
Universidad de Sonora, Unidad Regional Norte  
Caborca, Sonora, México

(Received: 2020 July 11 Revised: 2020 August 22)

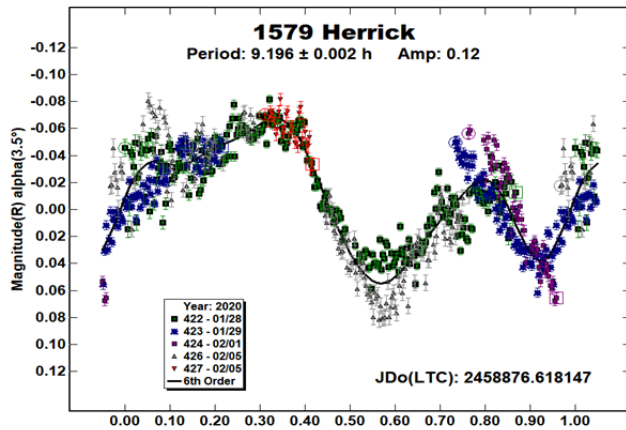
We present results for rotational period determination using lightcurves for two asteroids observed during the first half of 2020. For 1579 Herrick we obtained  $P = 9.196 \pm 0.002$  h and amplitude  $A = 0.12 \pm 0.03$  mag, for 2171 Kiev we obtained  $P = 3.1714 \pm 0.0002$  h and amplitude  $A = 0.14 \pm 0.08$  mag. We also found evidence for the presence of a secondary period  $P_2 = 23.38 \pm 0.03$  h.

The Mexican Asteroid Photometry Campaign (CMFA in Spanish) began in 2015 as an effort to study asteroids and to establish a collaborative network among researchers from different Mexican institutions (Sada et al., 2016) and has been regularly reporting results on asteroid period determination. As part of the results for 2020 we present lightcurves and periods for two asteroids. Images were taken during January, February, April and May 2020 using the observatory's 16" SCT telescope and SBIG-10XME CCD camera. No filters were used to attain the highest possible S/N ratio. The images were reduced using bias, dark and flat images following standard procedures and the photometric analysis was made with *MPO Canopus* (Warner, 2017). Data on asteroid visibility and information on previous results, was obtained from *The Asteroid Lightcurve Database* (Warner et al., 2009) and the *JPL Small-Body Database* website.

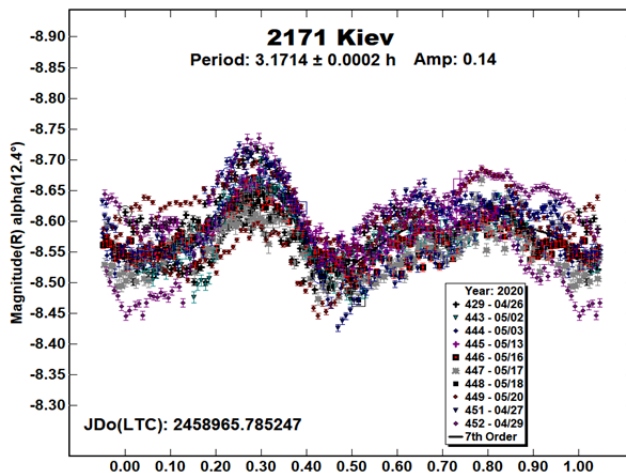
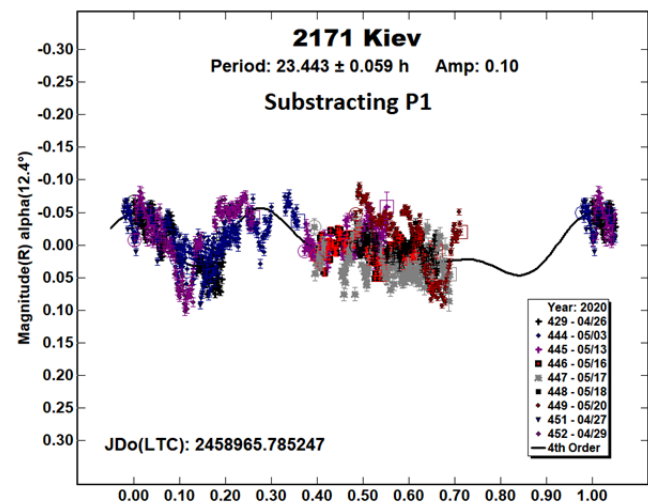
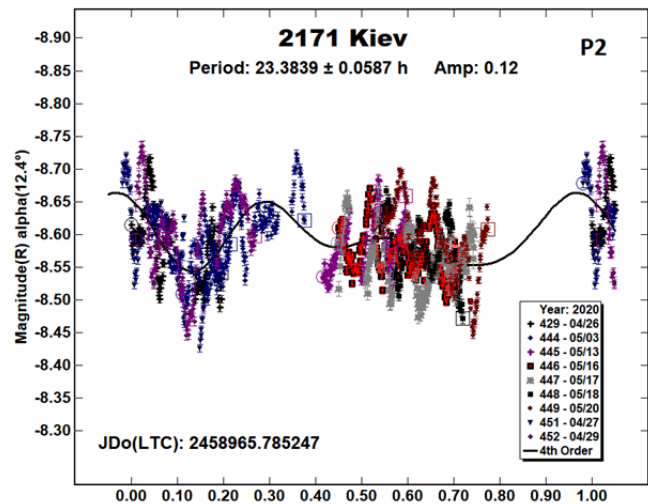
**1579 Herrick.** Initially named 1948 SB, this body was discovered on 1948 Sept 30 by S. Arend at Uccle and subsequently named in honor of Samuel Herrick (1911-1974) who is well-known for his contributions to celestial mechanics and astrodynamics (Schmadel, 2003). This asteroid was observed at the Universidad de Sonora Observatory on 2020 Jan 28, 29 and Feb 1 and 5, collecting over 21 h of data. Exposure time was set to a 100 s; data from Feb 5 was split into two sessions due to guiding problems. With the total of 603 points, a Fourier fit was obtained with order 6 resulting in a period  $P = 9.196 \pm 0.002$  h and amplitude  $A = 0.12 \pm 0.03$  mag. At the time of writing no other results for period or amplitude were found for this asteroid.

Number	Name	yyyy mm/dd	Phase	$L_{PAB}$	$B_{PAB}$	Period(h)	P.E.	Amp	A.E.	Grp
1579	Herrick	2020 01/28-02/05	*3.5, 3.8	130.0	-8.7	9.196	0.002	0.12	0.03	MB-O
2171	Kiev	2020 04/26-05/20	*12.6, 6.3	234.2	8.7	3.1714	0.0002	0.14	0.08	MB

Table I. Observing circumstances and results. The phase angle is given for the first and last date. If preceded by an asterisk, the phase angle reached an extrema during the period.  $L_{PAB}$  and  $B_{PAB}$  are the approximate phase angle bisector longitude/latitude at mid-date range (see Harris et al., 1984). Grp is the asteroid family/group (Warner et al., 2009).



**2171 Kiev.** This main-belt object was discovered 1973 August 28 by T.M Smirnova at Nauchnyj and originally designated 1973 QD1 (Schamdel, 2003). Ten nights were used to collect 54 h 22 m of data: Apr 26, 27, 29 and May 2, 3, 13, 16, 17, 18 and 20. Exposure times for the images were 90 and 100 s to adjust for magnitude variation. Initially a 6<sup>th</sup> order Fourier fit was made and after exploration of multiple options a 7<sup>th</sup> order fit was selected as it adjusted better to the data without a change in the resulting period which was  $P = 3.1714 \pm 0.0002$  h with an amplitude  $A = 0.14 \pm 0.08$  mag. Dispersion in our data is evident on the first observing nights and although it reduces considerably close to opposition it is still high. Variation in magnitude during maxima and minima from different dates led us to consider searching for a second period. A search with *MPO Canopus' Dual period search* was carried out revealing a tentative result for such a second period of  $P2 = 23.38 \pm 0.05$  h. These results for the rotational period and amplitude coincide within errors with those of Romeuf et al (2020), who found  $P = 3.1716 \pm 0.0002$  h and  $A = 0.11$  mag. They consider that this is a primary period in a binary system with a second orbital period of  $22.96 \pm 0.01$  h. Romeuf et al. consider their result as tentative. We recommend further study with data spanning at least two months of daily observations to further refine this result. For clarity we have included the curve folded by P2 after subtracting the P1 variation from the lightcurve.



#### References

Harris, A.W.; Young, J.W.; Scaltriti, F.; Zappala, V. (1984). "Lightcurves and phase relations of the asteroids 82 Alkeme and 444 Gytis." *Icarus* **57**, 251-258.

JPL Small-Body Database (accessed 2020 July 3).

<https://ssd.jpl.nasa.gov/sbdb.cgi#top>

Sada, P.V.; Navarro-Meza, S.; Reyes-Ruiz, M.; Olguín, L.; Saucedo, J.C.; Loera-González, P. (2016). "Results of the 2015 Mexican Asteroid Photometry Campaign." *Minor Planet Bull.* **43**, 154-156.

Schamdel, L.D. (2003). *Dictionary of Minor Planet Names*. pp 168. Springer, New York.

Romeuf, D.; Augustin, D.; Behrend, R.; Benishek, V.; Pravec, P.; Christmann, B.; Michelet, J.; Montaignut, R.; Barbotin, E.; Sogorb, P.; Durkee, R.; Manzini, F.; Sold, F. (2020). <https://obswww.unige.ch/~behrend/page4cou.html> & [http://www.david-romeuf.fr/Publications/Pro/CBET/CBET\\_4794\\_2171-Kiev.pdf](http://www.david-romeuf.fr/Publications/Pro/CBET/CBET_4794_2171-Kiev.pdf)

Warner, B.D. (2017). *MPO Canopus software*. <http://bdwpublishing.com>

Warner, B.D.; Harris, A.W.; Pravec, P. (2009). "The Asteroid Lightcurve Database." *Icarus* **202**, 134-146. Updated 2020 June. <http://www.minorplanet.info/lightcurvedatabase.html>

## CALL FOR OBSERVATIONS OF THE ACTIVE CENTAUR 29P/SCHWASSMANN-WACHMANN

Maria Womack

Florida Space Institute and Department of Physics  
University of Central Florida, Orlando, FL USA  
mariawomack@gmail.com

Gal Sarid

SETI Institute  
Mountain View, CA USA

Walter Harris and Kacper Wierzechos  
Lunar and Planetary Laboratory  
University of Arizona, Tucson, AZ

Laura Woodney

California State University San Bernardino  
San Bernardino, CA USA

(Received: 2020 July 14 Revised: 2020 July 23)

29P/Schwassmann-Wachmann is the most famous resident of the Centaur-JFC (Jupiter Family Comet) “gateway” region just beyond Jupiter. It may eventually become the brightest JFC in human history (Sarid et al., 2019). Its nucleus has exhibited a dust coma for more than 90 years, and it undergoes explosive outbursts several times a year. It is a strong candidate for a future space mission, and long-term dedicated and coordinated surveys from amateur and professional astronomers are needed to characterize the near-nucleus region and monitor material produced during outbursting events and quiescent outgassing activity. Through long-term monitoring we also seek to constrain the nucleus’ rotation period and spin pole orientation. We request multi-wavelength, multi-modality observations, including visible lightcurves, photometry, broadband filter imaging, astrometry, spectroscopy, interferometry and occultations. This article provides suggested observing dates, guidance about useful observations, predictions for a minimum visual magnitude, and a link to an observing campaign planning website. Interested observers are also welcome to contact the first author.

Key observations of Centaurs (objects orbiting primarily between Jupiter and Neptune) will allow us to better understand ongoing evolutionary processes in relatively pristine icy bodies. These objects transition from cryogenic storage in the Kuiper Belt region to active lifetimes as Jupiter-Family comets (JFCs). Approximately 10% of known Centaurs show episodic periods of cometary-like activity (Jewitt, 2009) and 29P/Schwassmann-Wachmann (hereafter 29P/SW1) is the most famous for exhibiting continuous activity that is likely related to its current orbit in the Gateway region (Sarid et al., 2019). Due to its importance to understanding icy planetesimals and solar system formation and evolution, 29P/SW1 was recently the target for two proposed NASA Discovery missions (Harris et al., 2019; Singer et al., 2019), and it is likely to be a candidate in future proposals.

Comet 29P/SW1 was the first small body discovered to have an orbit entirely beyond Jupiter. For many decades it has been the most distant object to show comet activity. Later discoveries of the population of objects in the giant planet and trans-Neptunian regions have shown it to be a Centaur. It is the most active icy body in the solar system and regularly exhibits a coma with

apparent magnitudes of  $m_v \sim 16$ -17, superimposed with major outbursts of 1 - 4 magnitudes several times a year, and nearly continuous smaller outbursts of 0.5 - 1.0 magnitudes (Miles et al., 2016; Trigo-Rodríguez et al., 2010; Wierzechos and Womack, 2020). During Fall 2020, 29P/SW1 emerges from solar conjunction and will be observable from many ground-based observatories. Here we briefly describe some of the observations that will help constrain nucleus and activity models and prepare for an orbital or flyby mission.

Historical tracking with lightcurves shows that large outbursts appear preferentially on the outbound leg, moving away from perihelion (Krisandova and Svoren, 2014). 29P/SW1’s last perihelion was in 2019 March, and thus, if its behavior repeats, then we expect that the number of major outbursts to increase over the next 10 years.

Some analysis of the major outbursts using lightcurves has proposed a very long (>50 days) rotational period for 29P/SW1; however, the link between rotation and outburst is still controversial (Trigo-Rodríguez et al., 2010). Continuous and high precision lightcurves, accompanied by simultaneous broadband optical or infrared imaging (cf. Schambeau, 2018) are needed to test models of the nucleus spin period and pole orientation, as well as dust coma properties. Observers reporting visual magnitudes are strongly encouraged to also record the photometric aperture and filters used so that the data can be used for later calculations of  $Af\rho$  values for the dust coma (Womack et al., 2020).

29P/SW1’s coma has a semi-persistent jet-like feature, which is evident in dust, and possibly CO gas, emission at a 20 - 30 arcsec offset from the nucleus (Whipple, 1980; Gunnarsson et al., 2008; Stansberry et al., 2004; Miles et al., 2016; Womack et al., 2017; Schambeau, 2018). High angular resolution images and interferometry, especially during perigee (see Table I), would be especially useful to examine the recurrence and extent of this feature.

Infrared and mm-/submm wavelength molecular spectroscopy, including CO, the dominant outgassing volatile (Senay and Jewitt, 1994), and interferometry is also needed to characterize the nucleus’ composition and test outgassing models. Continuous long-term (>80 days) monitoring of the CO production rate, preferably with high spectral resolution ( $<0.1 \text{ km s}^{-1}$ ), is needed to document any increases in gas production that lead to dust outbursts. Recent observations show that there is not always a strong correlation with dust and CO gas outbursts (Wierzechos and Womack, 2020), and more observations will improve statistics for further analysis of these important events. Such a long-term CO survey should be accompanied by simultaneous documentation of the dust coma. Time-series monitoring of other molecular species, including CN, N<sub>2</sub><sup>+</sup>, and CO<sup>+</sup>, will also be useful to constrain models of gas coma and solar wind interaction (Ivanova et al., 2019).

Although somewhat observable at other times, the Centaur is especially well-situated in the sky for observing from many ground-based observatories at optical, infrared and mm-/submm-wavelengths during the date ranges listed in Table I.

Rings and shrouds of debris seen at the Centaurs Chariklo and Chiron raise the possibility that there may be stable structures in the inner coma of the much more active 29P/SW1. Ground-based stellar occultations at optical and infrared wavelengths are an excellent method to measure the diameter of 29P/SW1 and characterize any surrounding debris (e.g., Sickafoose et al., 2020),

and are also strongly encouraged. **29P/SW1 crosses the Milky Way plane (with Galactic latitude  $|b| < 20$  degrees) during 2021-2023, and again during 2029-2031.** The high stellar density in this region provides increased opportunities for occultation events.

Continued astrometric observations are also requested because the coma obscures the nucleus, which makes it difficult to accurately determine its position (Miles and Kretlow, 2018).

Even if 29P/SW1 dims significantly, lightcurve photometry, imaging, and spectroscopy measurements obtained during times of very low or no activity will be invaluable to constraining models of the nucleus' size, albedo, shape, and rotational state. We use equations provided by the Asteroid Size Estimator ([https://cneos.jpl.nasa.gov/tools/ast\\_size\\_est.html](https://cneos.jpl.nasa.gov/tools/ast_size_est.html)), and assume  $R_{\text{nuc}} = 32$  km for radius (Schambeau, 2018), an albedo of  $p_V = 0.04$ , and a spherical shape to predict the nucleus' absolute magnitude to be approximately  $H = 10$ . We then convert this to an apparent visual magnitude,  $m_v$ , using  $m_v = H + 5 \log D + 5 \log R$  and assume that the geocentric distance ranges from  $D = 5.0 - 7.1$  au, and that the heliocentric distance is  $R = 6$  au. We estimate that **29P/SW1's bare nucleus will be as faint as  $m_v < 17.4$  to 18.1 magnitudes**, depending on how close it is to perigee. It could be another  $\sim 0.5$  magnitude fainter if the nucleus is aspherical, has an albedo lower than 0.04, or experiences significant phase scattering.

An international observing campaign for 29P/SW1 was initiated in 2018 ([http://wirtanen.astro.umd.edu/29P/29P\\_obs.shtml](http://wirtanen.astro.umd.edu/29P/29P_obs.shtml)) by M. Womack and G. Sarid. Participation is strongly encouraged since it may help different teams coordinate observing runs, increase the chances of obtaining simultaneous measurements, thus maximizing scientific return. Additional information about the observations requested may be found on the web site. Interested observers should enter information about planned (or recent past) observations at the link. Signing up does not commit anyone to sharing their data, but we hope this will be a gathering place for researchers to see who is at the telescope and when, and perhaps lead to new collaborations. Useful repositories for data, depending on format and data type, may include this bulletin, the Minor Planet Center, International Comet Quarterly, the NASA Planetary Data System Small Bodies Node, or another resource agreed upon by the collaborators.

Solar elongation > 85 degrees (yyyy mm)	Perigee and Date (au) (yyyy mm)
2020 08 - 2021 02	4.859 in 2020 11
2021 09 - 2022 03	4.962 in 2021 12
2022 09 - 2023 03	5.078 in 2022 12
2023 10 - 2024 04	5.189 in 2024 01
2024 11 - 2025 05	5.275 in 2025 02
2025 12 - 2026 06	5.324 in 2026 03
2027 01 - 2027 07	5.324 in 2027 04
2028 01 - 2028 08	5.273 in 2028 05
2029 02 - 2029 08	5.176 in 2029 05
2030 03 - 2030 09	5.048 in 2030 06
2031 04 - 2031 10	4.915 in 2031 07

Table I. Optimal observing dates, including perigee, for the Centaur 29P/Schwassmann-Wachmann. Stellar occultations are the most favorable during 2021 – 2023 and 2029 – 2031.

#### Acknowledgements

This material is based on work by M.W. supported in part by the National Science Foundation under Grant No. AST-1945950.

#### References

- Gunnarsson, M.; Bockelée-Morvan, D.; Biver, N.; Crovisier, J.; Rickman, H. (2008). "Mapping the carbon monoxide coma of comet 29P/Schwassmann-Wachmann 1." *Astron. Astrophys.* **484**, 537-546.
- Harris, W.; Woodney, L.; Villanueva, G. (2019). "Chimera: A Mission of Discovery to the First Centaur." *EPSC-DPS* **13**, 1094H.
- Ivanova, O.; Agapitov, O.; Odstrcil, D.; Korsun, P.; Afanasiev, V.; Rosenbush, V. (2019). "Dynamics of the CO<sup>+</sup> coma of comet 29P/Schwassmann-Wachmann 1." *MNRAS* **486**, 5614-5620.
- Jewitt, D. (2009). "The Active Centaurs." *Astron. J.* **137**, 4296-4312.
- Krisandova, Z.; Svoren, J. (2014). "29P/Schwassmann-Wachmann 1 – orbital distribution of outbursts." In *Proc. of the Asteroids, Comets, Meteors Conf. 2014* (K. Muinonen et al., eds.) pp 291.
- Miles, R.; Faillace, G.A.; Mottola, S.; Raab, H.; Roche, P.; Soulier, J.-F.; Watkins, A. (2016). "Anatomy of outbursts and quiescent activity of Comet 29P/Schwassmann-Wachmann." *Icarus* **272**, 327-355.
- Miles, R.; Kretlow, M. (2018). "Studying Comets by the Stellar Occultation Method." *Journal for Occultation Astronomy* **8**, 11-13.
- Sarid, G.; Volk, K.; Steckloff, J.K.; Harris, W.; Womack, M.; Woodney, L.M. (2019). "29P/Schwassmann-Wachmann 1, A Centaur in the Gateway to the Jupiter-family Comets." *Astrophys. J. Letters* **883**, L25.
- Schambeau, C. (2018). "Analysis of Nucleus Properties of the Enigmatic Comet 29P/Schwassmann-Wachmann 1." Ph.D. dissertation, Univ. Central Florida, Orlando.
- Senay, M.C.; Jewitt, D. (1994). "Coma formation driven by carbon monoxide release from comet Schwassmann-Wachmann 1." *Nature* **371**, 229-231.
- Sickafoose, A.A.; Bosh, A.S.; Emery, J.P.; Person, M.J.; Zuluaga, C.A.; Womack, M.; Ruprecht, J.D.; Bianco, F.B.; Zangari, A.M. (2020). "Characterization of material around the centaur (2060) Chiron from a visible and near-infrared stellar occultation in 2011." *MNRAS* **491**, 3, 3643-3654.
- Singer, K.N.; Stern, S.A.; Stern, D.; Verbiscer, A.; Olkin, C. (2019). "Centaurus: Exploring Centaurs and More, Messengers from the Era of Planet Formation." *EPSC-DPS* **13**, 2025S.
- Stansberry, J.A.; Van Cleve, J.; Reach, W.T.; and 15 co-authors, (2004). "Spitzer Observations of the Dust Coma and Nucleus of 29P/Schwassmann-Wachmann 1." *Astrophys. J. Supple Seres* **154**, 463-468.
- Trigo-Rodríguez, J.M.; García-Hernández, D.A.; Sánchez, A.; Lacruz, J.; Davidsson, B.J.R.; Rodríguez, D.; Pastor, S.; de Los Reyes, J.A. (2010). "Outburst activity in comets – II. A multiband photometric monitoring of comet 29P/Schwassmann-Wachmann 1." *MNRAS* **409**, 1682-1690.

Whipple, F. (1980). "Rotation and outbursts of comet P/Schwassmann-Wachmann 1." *Astron. J.* **85**, 305-313.

Wierzchos, K.; Womack, M. (2020). "CO Gas and Dust Outbursts from Centaur 29P/Schwassmann-Wachmann." *Astron. J.* **159**, id. 136.

Womack, M.; Sarid, G.; Wierzchos, K. (2017). "CO in Distantly Active Comets." *PASP* **129**, 031001.

Womack, M.; and 23 co-authors (2020). "The visual lightcurve of comet C/1995 O1(Hale-Bopp) from 1995 – 1999." under review.

## ROTATIONAL PERIODS OF THREE MAIN-BELT ASTEROIDS

Andrea Ferrero  
Bigmuskie Observatory (B88)  
via Italo Aresca 12  
14047 Mombercelli, Asti, ITALY  
bigmuskie@outlook.com

(Received: 2020 July 14)

Here are reported the result of photometric work on three asteroids: 3222 Liller,  $P = 12.576 \pm 0.001$  h,  $A = 0.31$  mag; (8278) 1991 JJ,  $P = 75.028 \pm 0.007$  h,  $A = 1.50$  mag; and 10111 Fresnel,  $P = 7.421 \pm 0.001$  h,  $A = 0.20$  mag;

From 2020 April through June, Bigmuskie Observatory observed three main-belt asteroids to determinate their rotational periods. All three were reported on the CALL website ([http://www.minorplanet.info/PHP/call\\_OppLCDBQuery.php](http://www.minorplanet.info/PHP/call_OppLCDBQuery.php)), with no previous observations.

The setup at the Bigmuskie Observatory includes a Marcon 0.30-m  $f/8$  Ritchey-Chretien telescope coupled with a Moravian G3 01000 equipped with a KAF-1001E CCD with a pixel array of  $1024 \times 1024 \times 24$  microns. This gives a pixel scale of 2 arcsec/pix and a field of view of  $36 \times 36$  arcmin. Images were unguided and taken through a Topotec R filter. Camera and telescope control were with *Maxim DL* (<http://diffractionlimited.com/product/maxim-dl/>) and *The Sky 6 Pro* (<http://www.bisque.com>). These were controlled by *Voyager* (<http://software.starkeeper.it>) to automate the entire observatory. All photometric reductions were done with *MPO Canopus* v10.7.12.9 (<http://bdwpublishing.com>), which permits obtaining fast results and precise night-to-night zero-point calibration using the Comparison Star Selector utility.

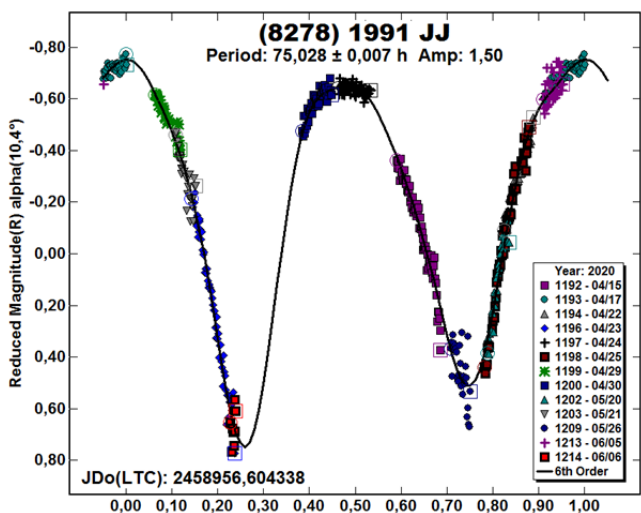
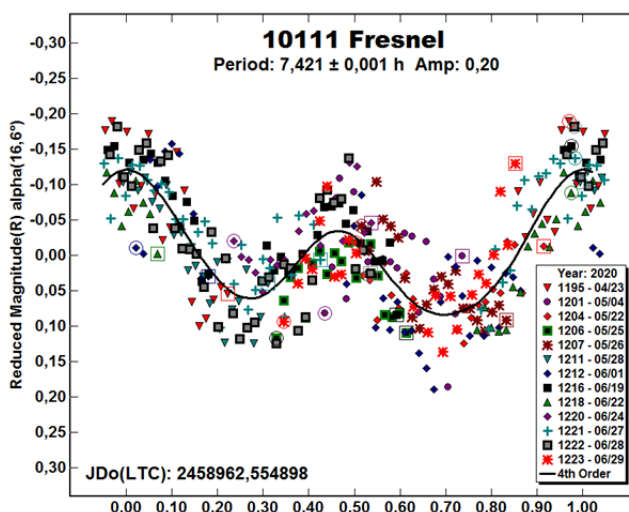
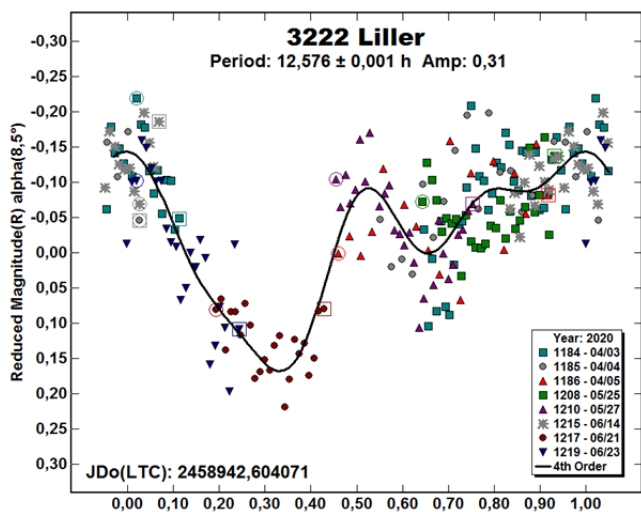
3222 Liller. Due to its period being very close to an Earth day, it took many sessions to reach the final result, which was found thanks to sessions 1217 and 1219 that aligned together into the deepest minimum of the curve. This provided a sort of "stationary landmark" and helped to find the right lightcurve. The period is  $P = 12.576 \pm 0.001$  h with an amplitude of  $A = 0.31$  mag.

(8278) 1991 JJ. This target showed a very large amplitude which helped to remove any uncertainty due to some low-quality sessions. The final period is  $P = 75.028 \pm 0.007$  h,  $A = 1.5$  mag.

10111 Fresnel. This was the most difficult target due to the low amplitude and its faint magnitude. Many periods appeared as more sessions were added, but in the end, after some shifting of zero points, the result seems to be reliable. The period is  $P = 7.421 \pm 0.001$  h and  $A = 0.20$  mag.

Number	Name	yyyy mm/dd	Phase	L <sub>PAB</sub>	B <sub>PAB</sub>	Period(h)	P.E.	Amp	A.E.	Grp
3222	Liller	2020 04/03-06/23	8.5, 18.8	208	17	12.576	0.001	0.31	0.05	MB
8278	1991 JJ	2020 04/15-06/06	10.1, 24.5	194	11	75.028	0.007	1.50	0.05	MB
10111	Fresnel	2020 04/23-06/29	16.6, 14.9	248	18	7.421	0.001	0.20	0.05	MB

Table I. Observing circumstances and results. The phase angle is given for the first and last date. If preceded by an asterisk, the phase angle reached an extrema during the period. L<sub>PAB</sub> and B<sub>PAB</sub> are the approximate phase angle bisector longitude/latitude at mid-date range (see Harris et al., 1984). Grp is the asteroid family/group (Warner et al., 2009).



References

Harris, A.W.; Young, J.W.; Scaltriti, F.; Zappala, V. (1984). "Lightcurves and phase relations of the asteroids 82 Alkmene and 444 Gytis." *Icarus* **57**, 251-258.

Warner, B.D.; Harris, A.W.; Pravec, P. (2009). "The Asteroid Lightcurve Database." *Icarus* **202**, 134-146. Updated 2020 April. <http://www.minorplanet.info/lightcurvedatabase.html>

## INDEX TO VOLUME 47

- Abrams, N.S.; Bieryla, A.; Gomez, S.; Huang, J.; Lewis, J.A.; Garrison, L.H.; Carmichael, T. "Measured Lightcurves and Rotational Periods of 3122 Florence, 3830 Trelleborg, and (131077) 2000 YH105" 3-4.
- Abrams, N.S.; Gomez, S.; Bieryla, A. "Measured Lightcurves and Rotational Periods of (16579) 1992 GO, (25660) 2000 AO88, and (37652) 1994 JS1" 168-169.
- Aimar, F.; Ghio, G. "The Rotation Periods of the Asteroids 587 Hypsipyle, 1152 Pawona, and 2937 Gibbs" 152-153.
- Benishek, V. "Asteroid Photometry at Sopot Astronomical Observatory: 2019 June-October" 75-83.
- Benishek, V. "Photometry of 39 Asteroids at Sopot Astronomical Observatory: 2019 September – 2020 March" 231-241.
- Bonamico, R. "Rotational Period of Five Asteroids" 222-223.
- Bonamico, R. "Determining the Rotational Periods and Lightcurves of Three Main-Belt Asteroids" 347-348.
- Brincat, S.M.; Hills, K.; Galdies, C. "Photometric Observations of Main-Belt Asteroid (10422) 1999 AN22" 12-13.
- Brincat, S.M.; Hills, K.; Galdies, C. "Photometric Observations of Main-Belt Asteroids 1755 Lorbach, 4857 Altgamia and (48540) 1993 TW8" 215-217.
- Carbognani, A.; Holmes, R.; Buzzi, L. "Lightcurve and Period of the NEA PHA 2019 GT3" 103-104.
- Carreño, A.; Fornas, G.; Arce, E.; Mas, V. "Twelve Main Belt Asteroids, One Near Earth and One Potentially Hazardous Asteroid Lightcurves at Asteroids Observers (OBAS) – MPPD: 2017 May-2019 Jan" 7-10.
- Casalnuovo, G.B.; Chinaglia, B. "Rotation Period Determination for Asteroid 2602 Moore" 11.
- Casalnuovo, G.B.; Chinaglia, B. "Rotation Period Determination for Asteroid 8323 Krimigis" 141.
- Casalnuovo, G.B.; Chinaglia, B. "Lightcurve Analysis for Three Main-Belt Asteroids" 186-187.
- Clark, M., "Asteroid Photometry from the Preston Grott Observatory" 163-165.
- Colazo, M.; Fornari, C.; Santucho, M.; Mottino, A.; Colazo, C.; Melia, R.; Vasconi, N.; Arias, D.; Pittari, C.; Suarez, N.; Pulver, E.; Ferrero, G.; Chapman, A.; Girardini, C.; Rodríguez, E.; Amilibia, G.; Anzola, M.; Tornatore, M.; Nolte, R.; Morero, S.; Oey, J. "Asteroid Photometry and Lightcurve Analysis at GORA's Observatories" 188-191.
- Colazo, M.; Fornari, C.; Santucho, M.; Mottino, A.; Colazo, C.; Melia, R.; Suarez, N.; Vasconi, N.; Arias, D.; Stechina, A.; Scotta, D.; García, J.; Pittari, C.; Ferrero, G. "Asteroid Photometry and Lightcurve Analysis at GORA's Observatories – Part II" 337-339.
- Díaz-Vachier, I.; Cotto-Figueros, D. "The Rotation Rates of Three Near-Earth Asteroids and a Mars-crossing Asteroid" 149-150.
- Dose, E.V. "A New Photometric Workflow and Lightcurves of Fifteen Asteroids" 324-330.
- Fauerback, M. "Measured Lightcurves and Rotational Periods of 1132 Hollandia and 1184 Gaea" 343-344.
- Fauerbach, M.; Fauerbach, M. "Photometric Observations of 2096 Vaino and 5104 Skripnichenko" 18-19.
- Ferrais, M.; Jehin, E.; Moulane, Y.; Pozuelos, F.J.; Barkaoui, K.; Benkhaldoun, Z. "Trappist-North and -South Combined Lightcurves of Near-Earth Asteroid 3122 Florence" 21-22.
- Ferrero, A. "Photometric Lightcurves of Eight Main-Belt Asteroids" 172-174.
- Ferrero, A. "Rotational Periods of Three Main-Belt Asteroids" 352-353.
- Ferrero, A.; Bonamico, R. "Rotational Period of Five Asteroids" 64-65.
- Ferrero, A.; Bonamico, R. "Lightcurves of Seven Main-belt Asteroids" 147-149.
- Franco, L.; Buchheim, R.K.; Pray, D.; Fauerback, M.; Mortari, F.; Casalnuovo, G.B.; Chinaglia, B.; Scarfi, G.; Papini, R.; Salvaggio, F. "Preliminary Spin-Shape Model for 755 Quintilla" 267-269.
- Franco, L.; Marchini, A.; Arena, C.; Casalnuovo, G.B.; Chinaglia, B.; Valvasori, A.; Bacci, P.; Maestriperieri, M.; Baj, G.; Galli, G.; Montigiani, N.; Mannucci, M. "Collaborative Asteroid Photometry for UAI: 2019 July–September" 61-63.
- Franco, L.; Marchini, A.; Scarfi, G.; Bacci, P.; Maestriperieri, M.; Di Grazia, M.; Galli, G.; Casalnuovo, G.B.; Chinaglia, B.; Baj, G.; Papini, R.; Marino, G.; Banfi, M.; Salvaggio, F.; Bacci, R.; Tinelli, L.; Mortari, F.; Foylan, M. "Collaborative Asteroid Photometry from UAI: 2019 October-December" 144-147.
- Franco, L.; Marchini, A.; Saya, L.-F.; Galli, G.; Baj, G.; Ruocco, N.; Mannucci, M.; Montigiani, N.; Tinelli, L.; Scarfi, G.; Aceti, P.; Banfi, M.; Bacci, P.; Maestriperieri, M.; Papini, R.; Salvaggio F.; Mortari, F.; Bachini, M.; Casalnuovo, G.B.; Chinaglia, B. "Collaborative Asteroid Photometry from UAI: 2020 January – March" 242-246.
- Franco, L.; Marchini, A.; Saya, L.-F.; Galli, G.; Baj, G.; Ruocco, N.; Mannucci, M.; Montigiani, N.; Tinelli, L.; Scarfi, G.; Aceti, P.; Banfi, M.; Bacci, P.; Maestriperieri, M.; Papini, R.; Salvaggio F.; Mortari, F.; Bachini, M.; Casalnuovo, G.B.; Chinaglia, B. "Corrigendum: Collaborative Asteroid Photometry from UAI: 2020 January – March" 269.
- Franco, L.; Marchini, A.; Scarfi, G.; Papini, R.; Salvaggio, F.; Baj, G.; Galli, G.; Bacci, P.; Maestriperieri, M.; Tinelli, L. "Collaborative Asteroid Photometry from UAI: 2020 April – June" 270-272.
- Franco, L.; Pilcher, F. "Spin-Shape Model for 50 Virginia" 272-274.
- Franco, L.; Pilcher, F.; Ferrero, A.; Maurice, A. "Spin-shape Model for 33 Polyhymnia" 120-122.
- Franco, L.; Pilcher, F.; Warner, B.D.; Marchini, A.; Saya, L.-F.; Maurice, A. "Spin-Shape Model for 118 Peitho" 169-171.

- Gao, X.; Tan, H. "Photometry of 2729 Urumqi at the Xingming Observatory in Urumqi City" 151.
- Groeinger, S.; Montgomery, K. "Determining the Rotational Periods and Lightcurves of Main Belt Asteroids" 174-176.
- Kluwak, T. "Rotation Period and Amplitude Determination of (18172) 2000 QL7: A Fast Rotator" 92-93.
- Lang, K. "Lightcurves of Six Asteroids from 2018 December through 2019 April" 71-73.
- Lang, K. "A Search for Mutual Eclipse Events of the Asynchronous Binary Asteroid 1016 Anitra" 322-323.
- Loera-González, P.; Olguín, L.; Saucedo-Morales, J.; Domínguez-González, R. "Lightcurve-based Period Determination for Apollo PHA (162082) 1998 HL1" 91.
- Loera-González, P.; Olguín, L.; Saucedo-Morales, J.; Núñez-López, R. "Lightcurve Based Rotational Period Determination for Asteroids 1579 Herrick and 2171 Kiev" 348-349.
- Mannucci, M.; Montigiani, N. "Rotational Period Determination for Asteroids 2460 Mitlincoln, 3070 Aitken and (11116) 1996 EK" 5-6.
- Marchini, A.; Bernardi, E.; Saya, L.F.; Papini, R.; Banfi, M.; Salvaggio, F. "Rotation Period Determination for Asteroids 3295 Murakami and 4961 Timherder" 69-70.
- Marchini, A.; Bernardi, E.; Saya, L.-F.; Papini, R.; Salvaggio, F. "Rotation Period Determination for Asteroids 4194 Sweitzer, 4421 Kayor, 4705 Secchi, (9219) 1995 WO8 and (11493) 1988 VN5" 249-252.
- Marchini, A.; Conti, M.; Vallerani, C. "Rotation Period Determination for Asteroids 992 Swasey and 3096 Bezruc" 265-267.
- Marchini, A.; Papini, R.; Banfi, M.; Salvaggio, F.; Hayes-Gehrke, M.N.; Yates, E. "Collaborative Asteroid Photometry for Asteroid 2051 Chang" 1-2.
- Noschese, A.; Mollica, M.; Catapano, A.; Vecchione, A. "Rotational Periods and Lightcurves of 2051 Chang, 3171 Wangshouguan, 8141 Nikolaev, and 10426 Charlierouse" 154-156.
- Noschese, A.; Mollica, M.; Vecchione, A. "Rotational Periods and Lightcurves of 4421 Kayor, 7118 Kuklov and (12853) 1998 FZ97" 254-255.
- Noschese, A.; Ruocco, N.; Vecchione, A. "Rotational Period and Lightcurve of 7910 Aleksola" 336-337.
- Núñez-López, R.; Loera-González, P.; Saucedo, J.C.; Olguín, L.; Contreras, M.E. "Lightcurve Based Rotational Period Determination for Asteroids 2070 Humason and 3122 Florence" 89-90.
- Odden, C.E.; Zhu, J.; Barakaiev, I.; Bilokur, M.; Colley, Z.A.; de Saint-Exupéry, M.P.; Lee, Y.; Mundra, I.R.; Nazzaro, H.A.; Nyiha, I.N.; Pedroza, A.; Prabhakar, P.S.; Taylor, A.C.; Xie, Y.; Yoon, C.S.; Yusuf, S.M.; Zhu, E.C.; Zhu, S.; Kemp, J.; Sliski, A. "Lightcurve Analysis of Asteroid 4700 Carusi" 252-253.
- Oey, J. "Lightcurve Analysis of Near-Earth Asteroids in 2017 from BMO and JBL" 136-140.
- Olguín, L.; Saucedo, J.C.; Loera-González, P.; Contreras, M.E.; Valdés, J.R.; Guichard, J.; López-González, R.; Michimani-García, J.; Cerdán-Hernández, G.; Schuster, W.J.; Valdés-Sada, P.; Núñez-López, R.; Ayala-Gómez, S.A. "The 2019 Mexican Asteroid Photometry Campaign" 340-342.
- Pilcher, F. "Lightcurves and Rotation Periods of 33 Polyhymnia, 206 Hersilia, 395 Delia, 400 Ducrosa, 900 Rosalinde, and 1066 Lobelia" 34-36.
- Pilcher, F. "Minor Planets at Unusually Favorable Elongations in 2020" 47-49.
- Pilcher, F. "Section News: Staffing Changes for The Minor Planet Bulletin" 1.
- Pilcher, F. "Call for Observations" 122.
- Pilcher, F. "Lightcurves and Rotation Periods of 10 Hygiea, 47 Aglaja, 455 Bruchsalia, 463 Lola, and 576 Emanuela" 133-135.
- Pilcher, F. "Lightcurves and Rotation Periods of 83 Beatrix, 86 Semele, 118 Peitho, 153 Hilda, 527 Euryanthe, and 549 Jessonda" 192-195.
- Pilcher, F. "General Report of Position Observations by the ALPO Minor Planets Section for the Year 2019" 217-221.
- Pilcher, F. "Section News: Retirement of MPB Producer Robert Werner" 265.
- Pilcher, F. "Lightcurves and Rotational Periods of 50 Virginia, 57 Mnemosyne, 58 Concordia, 59 Elpis, 78 Diana, and 529 Preziosa" 344-346.
- Pilcher, F.; Franco, L.; Gao, X.; Marchini, A.; Papini, R.; Tan, H. "2000 Herschel A Tumbling Asteroid" 142-143.
- Pilcher, F.; Polakis, T. "A Photometric Study of 470 Kilia" 247-248.
- Polakis, T. "Photometric Observations of Ten Minor Planets" 13-17.
- Polakis, T. "Photometric Observations of Twenty-Three Minor Planets" 94-101.
- Polakis, T. "Photometric Observations of Thirty Minor Planets" 177-186.
- Polakis, T. "Photometric Observations of Twenty-Seven Minor Planets" 314-321.
- Polakis, T.; Skiff, B. "Lightcurve Analysis of Long-period Minor Planet 2580 Smilevskia" 101-103.
- Singh, A.; Sackalovsky, C.; Sefik, Y.; Yates, E.; Moore, C.; Pagan, A.; Malwitz, A. "Lightcurve for Asteroid 4717 Kaneko" 74.
- Stephens, R.D.; Warner, B.D. "Lightcurve Analysis of L4 Trojan Asteroids at the Center for Solar System Studies: 2019 July to September" 43-47.

Stephens, R.D.; Warner, B.D. "Lightcurve Analysis of L5 Trojan Asteroids at the Center for Solar System Studies: 2020 April to June" 285-289.

Stephens, R.D.; Warner, B.D. "Main-Belt Asteroids Observed from CS3"

2019 July to September 50-60.  
2019 October to December 125-133.  
2020 January to March 224-230.  
2020 April to June 275-284.

Teer, A.; Montgomery, K. "Lightcurves and Rotational Periods of Four Main Belt Asteroids" 166-167.

Tomassini, A.; Scardella, M.; Franceschini, F.; Pierri, F. "Rotational Period Determination of Two Main Belt Asteroids: 4807 Noboru and 1435 Garlena" 20.

Warner, B.D. "Asteroid-Deepsky Appulses in 2020" 42.

Warner, B.D. "On Trying to Find Color Indices Using Only Unfiltered Observations" 214.

Warner, B.D.; Harris, A.W.; Ďurech, J.; Benner, L.A.M. "Lightcurve Photometry Opportunities"

2020 January – March 83-87.  
2020 April – June 156-161.  
2020 July – September 256-261.  
2020 October – December 330-335.

Warner, B.D.; Stephens, R.D. "Lightcurve Analysis of Hilda Asteroids at the Center for Solar System Studies"

2018 September – 2019 September 37-41.  
2019 November 123-124.  
2019 December – 2020 April 196-199.  
1529 Oterma and 17428 Charleroi 309-313.

Warner, B.D.; Stephens, R.D. "Near-Earth Asteroid Lightcurve Analysis at the Center for Solar System Studies"

2019 July – September 23-34.  
2019 September – 2020 January 105-120.  
2019 December – 2020 April 200-213.  
2020 April – June 290-304.

Warner, B.D.; Stephens, R.D.; Harris, A.W. "Binary Asteroids at the Center for Solar System Studies" 305-308.

Werner, R. "Swan Song" 265.

Williamson, B.; Sonnett, S.; Witry, J.; Chatelain, J.; Grav, T.; Reddy, V.; Lejoly C.; Kramer, E.; Mainzer, A.; Masiero, J.; Gritsevich, M.; Bauer, J. "Rotational Properties of Three Hilda Asteroids" 66-68.

Womack, M.; Sarid, G.; Harris, W.; Wierzos, K.; Woodney, L. "Call for Observations of the Active Centaur 29P/Schwassmann-Wachmann" 350-352.

## IN THIS ISSUE

This list gives those asteroids in this issue for which physical observations (excluding astrometric only) were made. This includes lightcurves, color index, and H-G determinations, etc. In some cases, no specific results are reported due to a lack of or poor-quality data. The page number is for the first page of the paper mentioning the asteroid. EP is the "go to page" value in the electronic version.

Number	Name	EP	Page	Number	Name	EP	Page
50	Virginia	8	272	3459	Bodil	50	314
50	Virginia	80	344	3615	Safronov	50	314
57	Mnemosyne	80	344	3637	O'Meara	50	314
58	Concordia	6	270	3656	Hemingway	50	314
58	Concordia	80	344	3683	Baumann	60	324
59	Elpis	80	344	3800	Karayusuf	6	270
78	Diana	80	344	3800	Karayusuf	60	324
414	Liriope	73	337	4041	Miyamotoyohko	50	314
435	Ella	60	324	4148	McCartney	76	340
529	Preziosa	80	344	4353	Onizaki	50	314
549	Jessonda	50	314	4408	Zlata Koruna	76	340
652	Jubilatrix	11	275	4570	Runcorn	50	314
722	Frieda	76	340	4582	Hank	83	347
738	Alagasta	50	314	5144	Achates	21	285
755	Quintilla	3	267	5476	1989 TO11	21	285
768	Struveana	60	324	5534	1941 UN	60	324
781	Kartvelia	6	270	5875	Kuga	11	275
904	Rockefellia	50	314	5947	Bonnie	83	347
913	Otila	6	270	6163	Reimers	11	275
949	Hel	73	337	6517	Buzzi	11	275
952	Caia	73	337	6569	Ondaatje	26	290
992	Swasey	1	265	6635	Zuber	11	275
992	Swasey	50	314	7910	Aleksola	50	314
1016	Anitra	58	322	7910	Aleksola	60	324
1025	Riema	11	275	7910	Aleksola	72	336
1074	Beljawska	60	324	8014	1990 MF	26	290
1130	Skuld	60	324	8278	1991 JJ	88	352
				10111	Fresnel	88	352
				10487	Danpeterson	11	275
				10737	Bruck	11	275
				11190	Jennibell	60	324
				12444	Prothoon	21	285
				12929	1999 TZ1	21	285
				14923	1994 TU3	60	324
				15710	Bocklin	50	314
				17428	Charleroi	45	309
				19125	1987 CH	11	275
				20037	Duke	11	275
				38635	2000 LB21	11	275
				39197	2000 XA	60	324
				42196	2001 DE21	60	324
				1132	Hollandia	79	343
				1145	Robelmonte	73	337
				1184	Gaea	79	343
				1215	Boyer	50	314
				1239	Queteleta	76	340
				1247	Memoria	50	314
				1269	Rollandia	50	314
				1303	Luthera	11	275
				1443	Ruppina	11	275
				1451	Grano	50	314
				1457	Ankara	50	314
				1529	Oterma	45	309
				1579	Herrick	84	348
				1592	Mathieu	60	324
				1594	Danjon	50	314
				1618	Dawn	50	314
				1628	Strobel	50	314
				1656	Suomi	41	305
				1667	Pels	11	275
				1685	Toro	26	290
				1784	Benguella	83	347
				2050	Francis	11	275
				2050	Francis	50	314
				2162	Anhui	76	340
				2171	Kiev	50	314
				2171	Kiev	84	348
				2283	Bunke	50	314
				2363	Cebriones	21	285
				2415	Ganesa	60	324
				2847	Parvati	50	314
				2879	Shimizu	50	314
				2893	Peiroos	21	285
				2895	Memnon	21	285
				3096	Bezruc	1	265
				3151	Talbot	60	324
				3222	Liller	88	352
				3225	Hoag	11	275
				3317	Paris	6	270
				3317	Paris	21	285
				3356	Resnik	50	314
				3451	Mentor	21	285

Number	Name	EP	Page	Number	Name	EP	Page	Number	Name	EP	Page
42609	Daubechies	11	275	175189	2005 EC224	26	290	2000	KA	26	290
52768	1998 OR2	26	290	184990	2006 KE89	41	305	2001	GS2	26	290
66251	1999 GJ2	26	290	306461	1999 LY5	11	275	2004	LU3	26	290
85184	1991 JG1	26	290	331471	1984 QY1	26	290	2005	MR5	26	290
85275	1994 LY	41	305	349063	2006 XA	26	290	2013	XA22	26	290
85628	1998 KV2	41	305	373428	1999 TC5	26	290	2015	HH10	26	290
85989	1999 JD6	26	290	382503	2001 RE8	26	290	2020	GD2	26	290
86667	2000 FO10	26	290	441987	2010 NY65	26	290	2020	KB3	26	290
136874	1998 FH74	26	290	477885	2011 JT9	26	290				
137064	1998 WP5	26	290	495615	2015 PQ291	26	290				
137199	1999 KX4	26	290	498066	2007 RM133	26	290				
159929	2005 UK	26	290	539940	2017 HW1	41	305				

**THE MINOR PLANET BULLETIN** (ISSN 1052-8091) is the quarterly journal of the Minor Planets Section of the Association of Lunar and Planetary Observers (ALPO, <http://www.alpo-astronomy.org>). Current and most recent issues of the *MPB* are available on line, free of charge from:

<http://www.minorplanet.info/MPB>

The Minor Planets Section is directed by its Coordinator, Prof. Frederick Pilcher, 4438 Organ Mesa Loop, Las Cruces, NM 88011 USA ([fpilcher35@gmail.com](mailto:fpilcher35@gmail.com)) Dr. Alan W. Harris (MoreData! Inc.; [harrisaw@colorado.edu](mailto:harrisaw@colorado.edu)), and Dr. Petr Pravec (Ondrejov Observatory; [ppravec@asu.cas.cz](mailto:ppravec@asu.cas.cz)) serve as Scientific Advisors. The Asteroid Photometry Coordinator is Brian D. Warner (Center for Solar System Studies), Palmer Divide Observatory, 447 Sycamore Ave., Eaton, CO 80615 USA ([brian@MinorPlanetObserver.com](mailto:brian@MinorPlanetObserver.com)).

*The Minor Planet Bulletin* is edited by Professor Richard P. Binzel, MIT 54-410, 77 Massachusetts Ave, Cambridge, MA 02139 USA ([rpb@mit.edu](mailto:rpb@mit.edu)). Brian D. Warner (address above) is Associate Editor, and Dr. David Polishook, Department of Earth and Planetary Sciences, Weizmann Institute of Science ([david.polishook@weizmann.ac.il](mailto:david.polishook@weizmann.ac.il)) is Assistant Editor. The *MPB* is produced by Dr. Robert A. Werner ([rawerner@polygrav.org](mailto:rawerner@polygrav.org)). The Associate Producer is Dr. Pedro A. Valdés Sada ([psada2@ix.netcom.com](mailto:psada2@ix.netcom.com)). The *MPB* is distributed by Dr. Melissa Hayes-Gehrke. Direct all subscriptions, contributions, address changes, etc. to:

Dr. Melissa Hayes-Gehrke  
UMD Astronomy Department  
1113 PSC Bldg 415  
College Park, MD 20742 USA  
([mhaysege@umd.edu](mailto:mhaysege@umd.edu))

Effective with Volume 38, the *Minor Planet Bulletin* is a limited print journal, where print subscriptions are available only to libraries and major institutions for long-term archival purposes. In addition to the free electronic download of the *MPB* noted above, electronic retrieval of all *Minor Planet Bulletin* articles (back to Volume 1, Issue Number 1) is available through the Astrophysical Data System

<http://www.adsabs.harvard.edu/>

Authors should submit their manuscripts by electronic mail ([rpb@mit.edu](mailto:rpb@mit.edu)). Author instructions and a Microsoft Word template document are available at the web page given above. All materials must arrive by the deadline for each issue. Visual photometry observations, positional observations, any type of observation not covered above, and general information requests should be sent to the Coordinator.

\* \* \* \* \*

The deadline for the next issue (48-1) is October 15, 2020. The deadline for issue 48-2 is January 15, 2021.